

Summary of FY 2001 Geosciences Research

April 2003



U.S. Department of Energy

Office of Science
Office of Basic Energy Sciences
Division of Engineering and Geosciences
Washington, D.C. 20585

Table of Contents

TABLE OF CONTENTS	I
FORWARD	XI
THE GEOSCIENCES RESEARCH PROGRAM IN THE OFFICE OF BASIC ENERGY SCIENCES	12
ARGONNE NATIONAL LABORATORY	13
Mineral-Fluid Interactions: Synchrotron Radiation Studies at the Advanced Photon Source	13
BROOKHAVEN NATIONAL LABORATORY	15
Study of the Microgeometry of Geological Materials Using Synchrotron Computed Microtomography	15
Geochemistry of Organic Sulfur in Marine Sediments	18
LAWRENCE BERKELEY NATIONAL LABORATORY	20
Computation of Seismic Wavefields in Complex Media	20
Joint Inversion for Subsurface Imaging.....	22
Center for Computational Seismology (CCS)	25
Deformation and Fracture of Poorly Consolidated Media	26
Decomposition of Scattering and Intrinsic Attenuation on Rock with Heterogeneous Multiphase Fluids Distributions	27
Unsaturated Fast Flow in Fractured Rock: Testing Film Flow and Aperture Influence	29
Prediction and Evaluation of Coupled Processes for CO ₂ Disposal in Aquifers.....	30
Colloid Transport in Unsaturated Porous Media and Rock Fractures.....	33
Integrated Isotopic Studies of Geochemical Processes	34
Clay Mineral Surface Geochemistry	36
Complexation and Precipitation Processes on Mineral Surfaces	38
Development of Isotope Techniques for Reservoir and Aquifer Characterization	40
Reactive Chemical Transport in Structured Porous Media: X-ray Microprobe and Micro-XANES Studies.....	42
LAWRENCE LIVERMORE NATIONAL LABORATORY	44
Water distribution in partially saturated porous materials.....	44
Three-dimensional analysis of seismic signatures and characterizations of fluids and fractures in anisotropic formations	46
Physical Properties of Heterogeneous Rocks Containing Fluids	47
Geophysical monitoring of carbon dioxide sequestration using electrical resistance tomography (ERT)	48
Application of Geophysical Tomographic Imagery to the Development of Subsurface Flow and Transport Models.....	50
Reactive Transport of CO ₂ -Rich Fluids and Precipitation and Dissolution in Rock Fractures.....	51

Determining the physical controls on biomineralization.....	52
Mineral Dissolution and Precipitation Kinetics: A Combined Atomic-Scale and Macro-Scale Investigation	53
In-Situ CO ₂ -sequestration: Measurement of Coupled Silicate Dissolution and Carbonate Precipitation	55
Testing Deep Saline Aquifers for Long-term CO ₂ Leakage Using In-Situ Noble Gases.....	56
Collaborative Research: Studies for Surface Exposure Dating in Geomorphology.....	57
Experimental Investigation into the Role of Water During the Thermal Maturation of Sedimentary Organic Matter.....	58
Isotope Fractionation by Diffusion in Liquids.....	59
LOS ALAMOS NATIONAL LABORATORY.....	62
High Resolution/High Fidelity Seismic Imaging and Parameter Estimation for Geologic Structure and Material Characterization	62
The Role of Carbon and Temperature in Determining Electrical Conductivity of Basins, Crust, and Mantle.....	63
Nonlinear Elasticity in Earth Materials	64
Nonlinear Dynamics of Fluid Flow and Contaminant Transport in the Earth's Crust from the Micro- to the Macro-scale.....	66
Improved Sensitivity Uranium Series Studies.....	67
Surface Exposure Dating in Geomorphology.....	69
Dissolution of Fe(III)(hydr)oxides by Aerobic Microorganisms.....	70
Energy Transport in Space Plasma.....	72
The Solar Wind-Magnetospheric Interaction	72
Energetic Particle Acceleration and Transport.....	73
OAK RIDGE NATIONAL LABORATORY.....	74
Volumetric Properties, Phase Relations and Reaction Kinetics of CO ₂ -CH ₄ -H ₂ -H ₂ O fluids: Effects of Injecting CO ₂ into Geological Reservoirs	74
Fundamental Research in the Geochemistry of Geothermal Systems.....	75
Ion Microprobe Studies of Fluid-Rock Interaction	77
Fundamental Research in Isotopic Fractionation of Carbonate Systems Relevant to Subsurface CO ₂ -Sequestration.....	78
Experimental studies of Hydrothermal Fluid Speciation and Fluid/Solid Interaction Employing Potentiometric Methods.....	80
Mechanisms and Rates of Isotope Exchange in Mineral-Fluid Systems.....	81
Nanoscale Complexity at the Oxide-Water Interface.....	83
PACIFIC NORTHWEST LABORATORY.....	86
The Reaction Specificity of Nanoparticles in Solution: Application to the Reaction of Nanoparticulate Iron and Iron-Bimetallic Compounds with Chlorinated Hydrocarbons and Oxyanions.....	86
Calcite Surface Chemistry: Molecular-Scale and Macroscopic Descriptions of the Influence of Impurities on Dissolution	87
Structure and Reactivity of Iron Oxide and Oxyhydroxide Surfaces.....	88
Molecular Basis for Microbial Adhesion and Geochemical Surface Reactions in Fe-reducing Bacteria: A Study Across Scales.....	91

Interactions Between Fe(III)-Reducing Bacteria and Fe Oxides: Microbial and Geochemical Dissolution Controls	93
SANDIA NATIONAL LABORATORIES	95
Evolution of Fracture Permeability	95
Micromechanical Processes in Porous Geomaterials	96
The Physics of Two-Phase Immiscible Fluid Flow in Single Fractures and Fractured Rock	97
Understanding and Predicting Solute Transport in the Presence of Multiple Time-Scales of Diffusion and Sorption.....	98
Modeling of Mesoscale Phenomena During Sequestration of Carbon Dioxide in Porous Reservoirs	100
Three Dimensional Electromagnetic Inversion	102
Effects of fluid flow on inelastic deformation and failure in dilating and compacting rock.....	103
A Systematic Study of Heterogeneity, Instrumentation, and Scale Using Physical and Numerical Experimentation.....	104
Molecular Simulations of Layered Minerals and their Interaction with Hazardous Wastes.....	106
PART II: OFF-SITE	108
AMERICAN MUSEUM OF NATURAL HISTORY.....	108
The Influence of Carbon on the Electrical Properties of Crustal Rocks.....	108
ARIZONA STATE UNIVERSITY	110
A SIMS Study of the Chemical Dynamics of Organic/Inorganic Interactions in Sedimentary Basins	110
BOSTON UNIVERSITY.....	112
Analysis and Interpretation of Multi-Scale Phenomena in Crustal Deformation Processes: Using Numerical Simulations of Complex Nonlinear Earth Systems	112
CALIFORNIA INSTITUTE OF TECHNOLOGY	114
Infrared Spectroscopy and Stable Isotope Geochemistry of Hydrous Silicate Glasses.....	114
CALIFORNIA INSTITUTE OF TECHNOLOGY	116
Isotope Tracer Studies of Diffusion in Silicates and of Geological Transport Processes Using Actinide Elements	116
UNIVERSITY OF CALIFORNIA at BERKELEY	118
Advective-Diffusive/Dispersive Transport of Chemically Reacting Species in Hydrothermal System	118
UNIVERSITY OF CALIFORNIA at BERKELEY	120
Collaborative Research: Studies for Surface Exposure Dating in Geomorphology.....	120
UNIVERSITY OF CALIFORNIA at BERKELEY	122
Dissolution of Fe(III)(hydr)Oxides by Aerobic Microorganisms	122

UNIVERSITY OF CALIFORNIA at DAVIS	124
The Kinetics of Dissociation of Aluminum-Oxygen Bonds in Aqueous Complexes	124
UNIVERSITY OF CALIFORNIA at DAVIS	126
Thermodynamics of Minerals Stable Near the Earth's Surface	126
UNIVERSITY OF CALIFORNIA at DAVIS	128
Electrochemical Measurements and Theoretical Predictions of the Thermodynamic Properties of Carbonate and Oxide Minerals	128
UNIVERSITY OF CALIFORNIA at LOS ANGELES	130
Application of $^{40}\text{Ar}/^{39}\text{Ar}$ Thermochronometry and Ion Microprobe Stable Isotope Geochemistry	130
to the Evolution of Petroleum Reservoirs and Hydrothermal Systems	130
UNIVERSITY OF CALIFORNIA at SANTA BARBARA	132
Fluid Flow in Faults: Estimating Permeability and Diagenetic Effects in a Transpressional Setting, Southern California.....	132
UNIVERSITY OF CALIFORNIA at SANTA BARBARA	134
Three-Dimensional Miscible Porous Media Flows with Viscosity Contrasts and Gravity Override..	134
UNIVERSITY OF CALIFORNIA at SANTA BARBARA	135
Magma Rheology, Mixing of Rheological Fluids, Molecular Dynamics Simulation, and Lithospheric Dynamics	135
UNIVERSITY OF CALIFORNIA at SANTA CRUZ	137
High Resolution/High Fidelity Seismic Imaging and Parameter Estimation for Geological Structure and Material Characterization.....	137
THE UNIVERSITY OF CHICAGO	142
Isotope Fractionation by Diffusion in Liquids.....	142
THE UNIVERSITY OF CHICAGO	145
GeoSoilEnviroCARS: A National Resource for Earth, Planetary, Soil and Environmental Science Research at the Advanced Photon Source	145
THE UNIVERSITY OF CHICAGO	148
Synchrotron X-ray Microprobe and Microspectroscopy Research in Low Temperature Geochemistry	148
THE CITY COLLEGE OF THE CITY UNIVERSITY OF NEW YORK	150
Particulate Dynamics in Filtration and Granular Flow	150
UNIVERSITY OF COLORADO	152
Evolution of Rock Fracture Permeability During Shearing	152

UNIVERSITY OF COLORADO	154
Nucleation and Growth Kinetics of Clays and Carbonates on Mineral Substrate.....	154
UNIVERSITY OF COLORADO	156
The Physics of Two-Phase Immiscible Fluid Flow in Single Fractures and Fractured Rock	156
UNIVERSITY OF COLORADO	159
Analysis and Interpretation of Multi-Scale Phenomena in Crustal Deformation Processes: Using Numerical Simulations of Complex Nonlinear Earth Systems	159
UNIVERSITY OF COLORADO	161
Seismic Absorption and Modulus Measurements in Single Cracks and Porous Rocks: Physical and Chemical Effects of Fluids	161
COLORADO SCHOOL OF MINES	162
Possible Vertical Migration of CO ₂ Associated with Large-Scale Injection into Subsurface Geologic Formations	162
COLORADO SCHOOL OF MINES	164
Three-dimensional analysis of seismic signatures and characterization of fluids and fractures in anisotropic formations	164
UNIVERSITY OF CONNECTICUT.....	166
Air-derived Noble Gases in Sediments: Implications for Basin Scale Hydrogeology	166
UNIVERSITY OF DELAWARE	168
Development of an Experimental Database and Theories for Prediction of Thermodynamic Properties of Aqueous Electrolytes and Nonelectrolytes of Geochemical Significance at Supercritical Temperatures and Pressures	168
UNIVERSITY OF FLORIDA	170
Evolution of surface morphology during dissolution of a rough fracture	170
GSY-USA, INC	171
The Magnetotelluric Data Simulation Project	171
UNIVERSITY OF HAWAII.....	172
Growth of faults, scaling of fault structure, and hydrologic implications	172
UNIVERSITY OF IDAHO	173
The Physics of Two-Phase Immiscible Fluid Flow in Single Fractures and Fractured Rock	173
UNIVERSITY OF ILLINOIS AT URBANA-CHAMPAIGN.....	176
Computational and Spectroscopic Investigations of Water-Carbon Dioxide Fluids and Surface Sorption Processes	176

INDIANA UNIVERSITY	179
Self-Organized Mega-Structures in Sedimentary Basins	179
INDIANA UNIVERSITY	181
Isotopically Labile Organic Hydrogen in Thermal Maturation of Organic Matter	181
THE JOHNS HOPKINS UNIVERSITY	183
Fluid Flow in Faults: Estimating Permeability and Diagenetic Effects in a Transpressional Setting, Southern California.....	183
THE JOHNS HOPKINS UNIVERSITY	185
Predictive Single-Site Protonation and Cation Adsorption Modeling.....	185
THE JOHNS HOPKINS UNIVERSITY	187
Reactions and Transport of Toxic Metals in Rock-Forming Silicates at 25°C	187
LEHIGH UNIVERSITY	188
Reactions and Transport of Toxic Metals in Rock-Forming Silicates at 25°C	188
UNIVERSITY OF MARYLAND	190
Theoretical Studies on Heavy Metal Species in Solution.....	190
MASSACHUSETTS INSTITUTE OF TECHNOLOGY	193
Evolution of pore structure and permeability of rocks under hydrothermal conditions.....	193
MASSACHUSETTS INSTITUTE OF TECHNOLOGY	195
Transport Visualization for Studying Mass Transfer and Solute Transport in Permeable Media.....	195
MASSACHUSETTS INSTITUTE OF TECHNOLOGY	196
Theoretical Studies of Landscape Erosion	196
MASSACHUSETTS INSTITUTE OF TECHNOLOGY	198
Fluid Mobility Estimation From Electroseismic Measurements: Laboratory, Field, and Theoretical Study	198
MINERALOGICAL SOCIETY OF AMERICA	200
Support of MSA and GS Short Courses and the Companion Reviews Volumes.....	200
UNIVERSITY OF MINNESOTA, TWIN CITIES	202
Magma Rheology, Mixing of Rheological Fluids, Molecular Dynamics Simulation , and Lithospheric Dynamics	202
NATIONAL ACADEMY OF SCIENCES, BOARD ON EARTH SCIENCES AND RESOURCES	204
Board on Earth Sciences and Resources and Its Activities	204

UNIVERSITY OF NEVADA, RENO	205
Growth of Faults, Scaling of Fault Structure, and Hydrogeologic Implications	205
NEW ENGLAND RESEARCH.....	207
The Role of Fracture Intersections in the Flow and Transport Properties of Rock.....	207
UNIVERSITY OF NEW MEXICO	210
Modeling of Mesoscale Phenomena During Sequestration of Carbon Dioxide in Porous Reservoirs.....	210
NEW MEXICO INSTITUTE OF MINING AND TECHNOLOGY	212
Investigation of Permeability Upscaling	212
STATE UNIVERSITY OF NEW YORK at STONY BROOK.....	214
High Precision Radiometric Dating of Sedimentary Materials	214
STATE UNIVERSITY OF NEW YORK at STONY BROOK.....	216
Medial Axis Analysis of Porous Media.....	216
STATE UNIVERSITY OF NEW YORK at STONY BROOK.....	217
Surface Chemistry of Pyrite: An Interdisciplinary Approach	217
STATE UNIVERSITY OF NEW YORK at STONY BROOK.....	219
Micromechanical Processes in Porous Geomaterials	219
NORTHWESTERN UNIVERSITY.....	221
Interactions of Pore Fluid Pressure and Inelastic Deformation of Dilating and Compacting Rock.....	221
UNIVERSITY OF NOTRE DAME	223
Dissolution of Fe(III)(hydr)oxides by Aerobic Microorganisms	223
UNIVERSITY OF OKLAHOMA	226
Development and Application of a Paleomagnetic/Geochemical Method for Constraining the Timing of Burial Diagenetic and Fluid Migration Events.....	226
OREGON STATE UNIVERSITY	228
Transport Visualization for Studying Mass Transfer and Solute Transport in Permeable Media.....	228
THE PENNSYLVANIA STATE UNIVERSITY	230
Dissolution of Feldspar in the Field and Laboratory	230
THE PENNSYLVANIA STATE UNIVERSITY	232
Critical Chemical-Mechanical Couplings that Define Permeability Modification in Pressure-Sensitive Rock Fractures.....	232
PRINCETON UNIVERSITY	234
In-situ Evaluation of Soil Organic Molecules: Functional Group Chemistry, Aggregate Structures, Metal and Mineral Surface Complexation Using Soft X-rays.....	234

PURDUE UNIVERSITY	236
Mechanical Models of Fault-Related Folding	236
PURDUE UNIVERSITY	238
Seismic Monitoring of Time-Dependent Multi-Scale Heterogeneity in Fractured Rock.....	238
RENSSELAER POLYTECHNIC INSTITUTE	240
Transport Phenomena in Fluid-Bearing Rocks.....	240
NATIONAL MUSEUM OF NATURAL HISTORY, SMITHSONIAN INSTITUTION	242
Low-T, Fluid-Ashflow-Tuff Interactions: How Rock Textures, Chemistry, and Mineralogy Reflect reaction Pathways and Influence Rock Response to Heating.....	242
UNIVERSITY OF SOUTHERN CALIFORNIA	246
Three-Dimensional Miscible Porous Media Flows with Viscosity Contrast and Gravity Override ...	246
STANFORD UNIVERSITY	247
Metal Ion Sorption at Oxide Surfaces and Oxide-Water Interfaces: Spectroscopic Studies and Modelling.....	247
STANFORD UNIVERSITY	250
Inversion of multicomponent seismic data and rock physics interpretation for evaluating lithology, fracture and fluid distribution in heterogeneous anisotropic reservoirs	250
STANFORD UNIVERSITY	252
Porous rocks with fluids: Seismic and transport properties.....	252
STANFORD UNIVERSITY	254
Diffusion of CO ₂ during Hydrate Formation and Dissolution	254
STANFORD UNIVERSITY	256
Structural Heterogeneities and Paleo-Fluid Flow in an Analogue Sandstone Reservoir	256
STANFORD UNIVERSITY	258
Coupled Fluid Deformation Effects in Earthquakes and Energy Extraction.....	258
TEMPLE UNIVERSITY	260
Surface Chemistry of Pyrite: An Interdisciplinary Approach	260
THE UNIVERSITY OF TENNESSEE	262
Completion of Kr-81 and Kr-85 Analysis Development for Hydrogeology and Testing its Validity by Assessing Aquifer Recharge Rates.....	262
TEXAS A&M UNIVERSITY	263
Time-Lapse Seismic Monitoring and Performance Assessment of CO ₂ Sequestration in Hydrocarbon Reservoirs	263

TEXAS A&M UNIVERSITY	265
Fluid-Assisted Compaction and Deformation of Reservoir Lithologies	265
TEXAS A&M UNIVERSITY	267
Experimental and analytic studies to model reaction kinetics and mass transport of carbon dioxide sequestration in depleted carbonate reservoirs	267
UNIVERSITY OF TEXAS	269
High-resolution temporal variations in groundwater chemistry: Tracing the links between climate, hydrology, and element mobility in the vadose zone	269
THE UNIVERSITY OF TEXAS	270
Thermohaline Convection in the Gulf of Mexico Sedimentary Basin, South Texas	270
THE UNIVERSITY OF TEXAS at DALLAS	272
3-D sedimentological and geophysical studies of clastic reservoir analogs: Facies architecture, reservoir properties, and flow behavior within delta front facies elements of the Cretaceous Wall Creek Member, Frontier Formation, Wyoming.....	272
TEXAS TECH UNIVERSITY	274
Modeling of Mesoscale Phenomena During Sequestration of Carbon Dioxide in Porous Reservoirs.....	274
UNIVERSITY OF UTAH	276
A Comparative Study of the Feasibility for CO ₂ Sequestration in Faulted and Fractured Sandstones in Eolian and Fluvial Deltaic Deposits	276
UTAH STATE UNIVERSITY	278
A Comparative Study of the Feasibility for CO ₂ Sequestration in Faulted and Fractured Sandstones in Eolian and Fluvial Deltaic Deposits	278
UTAH STATE UNIVERSITY	280
Growth of Faults and Scaling of Fault Structure.....	280
VIRGINIA POLYTECHNIC INSTITUTE AND STATE UNIVERSITY	282
Experimental studies in the system H ₂ O-CH ₄ -“petroleum”-salt using synthetic fluid inclusions	282
VIRGINIA POLYTECHNIC INSTITUTE AND STATE UNIVERSITY	283
Investigation of the Physical Basis of Biomineralization.....	283
VIRGINIA POLYTECHNIC INSTITUTE AND STATE UNIVERSITY	285
Microbial Community Acquisition of Nutrients from Mineral Surfaces	285
UNIVERSITY OF WASHINGTON	287
Two and Three-dimensional Magnetotelluric and Controlled Source Electromagnetic Inversion	287
UNIVERSITY OF WASHINGTON	289
Electromagnetic Imaging of Fluids in the San Andreas Fault.....	289

UNIVERSITY OF WISCONSIN	291
Three-Dimensional Transient Electromagnetic Inversion.....	291
UNIVERSITY OF WISCONSIN	292
Precipitation at the Microbe-Mineral Interface	292
UNIVERSITY OF WISCONSIN	294
Deformation and Fracture of Poorly Consolidated Media	294
UNIVERSITY OF WISCONSIN	296
Microanalysis of Stable Isotope Ratios in Low Temperature Rocks	296
UNIVERSITY OF WISCONSIN	298
Pore-Scale Simulations of Rock Deformation, Fracture, and Fluid Flow in Three Dimensions	298
WOODS HOLE OCEANOGRAPHIC INSTITUTION	299
Laboratory Constraints on the Stability of Petroleum at Elevated Temperatures: Implications for the Origin of Natural Gas	299
WOODS HOLE OCEANOGRAPHIC INSTITUTION	300
Organic Geochemistry of Outer Continental Margins and Deep Water Sediments	300
WOODS HOLE OCEANOGRAPHIC INSTITUTION	302
Evolution of Pore Structure and Permeability of Rocks under Hydrothermal Conditions.....	302
UNIVERSITY OF WYOMING	304
Mineral Dissolution and Precipitation Kinetics: A Combined Atomic-Scale and Macro-Scale Investigation Targeted Towards CO ₂ -Sequestration Data Needs.....	304
YALE UNIVERSITY	307
Plants, Weathering, and the Evolution of Atmospheric Carbon Dioxide and Oxygen	307
YALE UNIVERSITY	308
Reactive Fluid Flow and Applications to Diagenesis, Mineral Deposits, and Crustal Rocks.....	308
SUBJECT INDEX.....	310
AUTHOR INDEX	316
DOE/OBES GEOSCIENCES RESEARCH: HISTORICAL BUDGET SUMMARY	322

FORWARD

The Department of Energy supports research in the geosciences in order to provide a sound foundation of fundamental knowledge in those areas of the geosciences that are germane to the Department of Energy's many missions, and those which provide stewardship for geosciences research capabilities, primarily at the DOE National Laboratories. Excellent fundamental science that can improve and support DOE's mission needs will also provide basic knowledge applicable to many other areas of earth science beyond DOE's borders. The Geosciences Research Program resides within the Division of Chemical Sciences, Geosciences and Biosciences, part of the Office of Basic Energy Sciences of the Office of Science. The participants in this program include researchers at Department of Energy laboratories, academic institutions, and other governmental agencies. These activities are formalized by a contract or grant between the Department of Energy and the organization performing the work, providing funds for salaries, equipment, research materials, and overhead. Collaborative work among these institutions is encouraged. The summaries in this document, prepared by the investigators, describe the scope of the individual projects. The Geosciences Research Program includes research in the two broad areas of geophysics and geochemistry. Within these areas, topics of research interest include Earth dynamics, properties of Earth materials, rock mechanics, seismic, electromagnetic and radar underground imaging, geochemistry, biogeochemistry, rock-fluid interactions, hydrogeology, coupled reactive fluid flow and transport, resource exploration and evaluation, and geomagnetic solar-terrestrial interactions. All such research is related either directly or indirectly to the Department of Energy's long-range technological needs. Because of the variety of the research needs in the different applied DOE programs, fundamental approaches with multiple potential applications are favored. Further information on the Geosciences Research Program, including recent program activities and highlights, may be found on the Geosciences Programs home page at: <http://www.sc.doe.gov/production/bes/geo/geohome.html>

THE GEOSCIENCES RESEARCH PROGRAM IN THE OFFICE OF BASIC ENERGY SCIENCES

The Geosciences Research Program is directed by the Department of Energy's (DOE's) Office of Science (SC) through its Office of Basic Energy Sciences (OBES). The Geosciences Research Program emphasizes research leading to fundamental understanding of Earth's natural processes and properties that will advance the forefront of scientific knowledge, as well as help solve geosciences-related problems in multiple DOE mission areas. Activities in the Geosciences Research Program are directed toward building the long-term fundamental knowledge base necessary to provide for energy technologies of the future. Future energy technologies and their individual roles in satisfying the nation's energy needs cannot be easily predicted. It is clear, however, that these future energy technologies will involve consumption of energy and mineral resources and generation of technological wastes. The Earth is a source for energy and mineral resources, and is also the host for wastes generated by technological enterprise. Viable energy technologies for the future must contribute to a national energy enterprise that is efficient, economical, and environmentally sound.

The Geosciences Research Program is divided into two broad categories ***Geophysics*** and ***Geochemistry***.

Geophysics: Improving geophysical interrogation of the Earth's crust through better collection and analysis of seismic and electromagnetic data; improving understanding of geophysical signatures of fluids and fluid-bearing reservoirs; and characterizing geologic structures better.

Geochemistry: Investigating geochemistry of mineral-fluid interactions through studies of rates and mechanisms of reactions at the atomistic/molecular scale; studying coupled flow and reactivity in porous and fractured rocks; and tracking of mineral-mineral and mineral-fluid processes using isotopes.

The program evolves with time and progress in these and related fields. Individual research projects supported by this program at DOE national laboratories, academic institutions, research centers, and other federal agencies typically have components in more than one of the categories or subcategories listed. In addition, it is common for research activities to involve a high level of collaboration between investigators and different institutions. Cross-cutting issues include: improving understanding of basic properties of rocks, minerals, and fluids; determining physical, chemical, and mechanical properties of multi-phase, heterogeneous, anisotropic systems; improving analysis of rock deformation, flow, fracture, and failure, and characterization of fluid transport properties of large-scale geologic structures. Research progress, in addition, will be based on developing advanced analytical instrumentation and computational methods, including: higher-resolution geophysical imaging and inversion tools, angstrom-scale resolution analysis of heterogeneous minerals with x-ray and neutron methods, and advancing computational modeling and algorithm development.

PART I: ON-SITE

ARGONNE NATIONAL LABORATORY

Environmental Research Division, Bldg. 203
Argonne, Illinois 60439

CONTRACT: W-31-109-Eng-38

CATEGORY: Geochemistry

PERSON IN CHARGE: P. Fenter

Mineral-Fluid Interactions: Synchrotron Radiation Studies at the Advanced Photon Source

Paul Fenter (630) 252-7053, fax (630) 252-7415, Fenter@anl.gov; Neil C. Sturchio University of Illinois at Chicago; Michael J. Bedzyk Northwestern University

Website: http://www.anl.gov/ER/GPG_wp/index.html

Objectives: The objective of this program is to advance the basic understanding of rock-fluid and soil-fluid interactions through experimental studies of atomic-scale processes at mineral-fluid interfaces. This is crucial to establishing the relation between atomic-scale processes and macroscopic geochemical transport in natural systems.

Project Description: The principal approach is to observe single-crystal mineral surfaces in situ during chemically controlled reactions with fluids, using X-ray scattering, standing-wave, and absorption techniques with high-brilliance synchrotron radiation. These techniques provide high-resolution atomic-scale structural information that cannot be acquired by any other means. Experiments are being performed on common rock- and soil-forming minerals under conditions representative of geochemical environments near the earth's surface. Types of reactions being investigated include dissolution-precipitation, adsorption-desorption, and oxidation-reduction.

Results: Progress during the past year included further successful demonstrations of the ability to perform in situ X-ray reflectivity, diffraction, and standing-wave studies of reacting mineral surfaces under chemically controlled conditions. Experiments were conducted to characterize the mechanism and kinetics of orthoclase dissolution as a function of crystallographic orientation. Dissolution measurements of the (010) surface at acidic pH reveals a dissolution process that is similar to that previously observed for the (001) surface. The data, however, reveal a very different variation of dissolution rate as a function of temperature, revealing a substantially smaller effective activation energy for dissolution. The structure of the (010) surface was measured through high resolution

X-ray reflectivity to assess the structural origin of these differences in dissolution kinetics. Additional measurements of dissolution kinetics for the (001) surface reveal a strong variation of dissolution rate as a function of pH. The structure of fluorapatite natural growth surfaces was probed with X-ray reflectivity showing molecularly-flat surfaces with a well-defined termination. X-ray reflectivity was used to probe organic-mineral interactions through measurements of 1-hydroxyethane-1,1-diphosphonic acid adsorbed to barite (001) and (210) cleavage surfaces, and fluorapatite(100) natural growth surface.

Experimental studies of ion adsorption on muscovite substrates and of the structure of the quartz-water interface were continued, in collaboration with K. L. Nagy (University of Colorado).

BROOKHAVEN NATIONAL LABORATORY

Upton, Long Island, New York 11973-5000

Contract: DE-AC02-98CH10886

CATEGORY : Geophysics

Study of the Microgeometry of Geological Materials Using Synchrotron Computed Microtomography

K. W. Jones (631) 344-4588, fax (631) 344-5271, kwj@bnl.gov ; H. Feng (973) 655-7549, fax (973) 655-4072, fengh@mail.montclair.edu

Website: <http://www.bnl.gov/rocks>

Objectives: The objective of this project is to gain improved knowledge of the properties and behavior of geological materials on a grain-size scale. Measurements are made to determine: 1) the microgeometry of typical rock types, 2) changes in the microgeometry of the rocks as a function of applied pressure, 3) fluid-flow paths through the rocks, and 4) changes in the rock composition caused by fluid-rock interactions.

Project Description: Experimental data is obtained using the technique of synchrotron computed microtomography (CMT). Intense x-ray beams from the Brookhaven National Synchrotron Light Source pass through the sample and strike an area scintillator detector. Light from the scintillator is detected with a charge-coupled device and stored for later analysis. The tomographic volume is calculated by analyzing a series of the two dimensional views which have been obtained as the sample is rotated around an axis normal to the x-ray beam. The maximum number of voxels in the final volume is about 10^{10} voxels. The minimum voxel size is about .003 mm on an edge.

Results: Several samples were investigated. They exemplify the use of CMT for investigations pertinent to flow of fluids in porous media and to rock structures formed in processes involving flow of molten materials in magmas and smoker chimneys.

Modeling Fluid Flow in Porous Media: [With M. A. McGraw, B. Travis (LANL)]. Matter can be transported by water flow through porous media either as a dissolved solute or sorbed to mobile colloidal particulates. Most groundwater flow models have neglected the second transport mechanism. A LANL model is being made more realistic by inclusion of a colloidal phase. This colloid transport model is based on a probabilistic algorithm that uses pore size distribution, relative permeability, and capillary pressure curves. The model includes a coordination number, which is, roughly, the number of paths, or channels, that run into or out of each rock pore, on average. This type of model requires knowledge of the microstructure of the solid on a pore-size scale. We used CMT to obtain this information for samples of volcanic tuff from the Busted Butte study area.

The samples were a few mm in size, and the tomographic volumes were acquired with a voxel size of 0.0067 mm. Typical sections through the samples at different locations are shown in Figure 1. We are analyzing the data using the medial axis software created by W. B. Lindquist of SUNY Stony Brook to segment the tomographic data into pore space and rock space. The segmented data are then used to determine the distribution of pore sizes and connectivity of the sample. Calibration of the colloid transport model against column experiments requires a coordination number in the range of 5-7; we will compare this against the coordination numbers derived from the tomography experiments. A lattice Boltzman model simulation based on the tomographic data may also be used to generate relative permeability and capillary pressure curves for comparison with experimentally-derived curves.

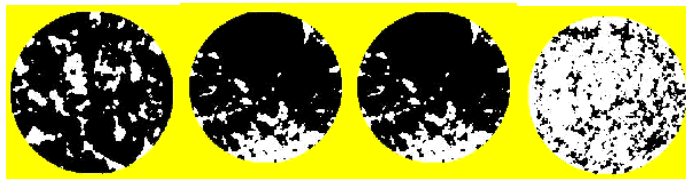


Figure 1. Four sections through a typical sample are shown. The pore space is shown in white and the rock space is shown in black. The porosity of the sample changes radically over a distance of 1-2 mm. The high spatial resolution of the synchrotron CMT apparatus is essential for obtaining a precise determination of the variation of permeability and other parameters for input into the colloidal transport model that is under development at LANL.

Structure of Jurassic Laminated Sandstone. [With J. Lincoln, Montclair State University].

The microgeometry of sandstones plays a key role in geophysical and hydrologic studies, as it is important for understanding internal flow dynamics and rock formation mechanisms. For this purpose, CMT was used to construct 3-dimensional images of Jurassic laminated sandstones from the Towaco Formation (Newark Supergroup) in New Jersey. The tomographic images effectively reveal the laminated structure of pores and solids in the sandstones. The x-ray attenuation coefficients identify different rock components within the sample. Lamination orientations are apparent in the sandstones since each lamina has a different porosity. The data can be used to calculate flow through the lamina and give insights into flow through heterogeneous non-isotropic rocks. The ability to accurately assess the sizes, shapes, and connectivity of porosity has important implications for hydrogeology and petroleum geology.

Structure of Hydrothermal Chimneys. [With W. L. Zhu, Woods Hole Oceanographic Institute].

Study of the internal microstructure of hydrothermal chimney walls has significant geochemical implications. High temperature (greater than 350°C) vent fluid flows outwards from the internal vent chimney wall as seawater seeps inward into the chimney from the outside wall. Since many geochemical reactions happen in the chimney, the chimney wall provides a good record of its geochemical history. As the chemical compositions of seawater and vent fluid are significantly different, the mineral

depositions from internal wall to outside wall may also be significantly different. We measured two chimney samples. The purpose of the study is to visualize Cu and anhydrite boundaries and pore microstructures. It is known that vent fluid is enriched in Cu and seawater is relatively enriched in sulfate. When chemical reactions happen in a hydrothermal vent, the outside wall is enriched in anhydrite and the internal wall is enriched in Cu mineral deposits. We successfully determined the porosity in specimens from different regions in the chimney and were able to identify pore space significantly smaller than shown by measurements with an industrial computed tomography scanner. We also were able to measure the structures in the interface between anhydrite and Cu regions and show how the two regions merged together.

The Aureole of the Traigh Bhàn na Sgùrra Sill, Isle of Mull: Reaction-driven Micro-cracking During Pyrometamorphism. [With M. Holness, Cambridge University]

The intrusion of a 6-m thick Tertiary gabbroic sill, in which magma flow was locally turbulent, into garnet-grade pelitic gneiss and psammite at 600 bars at Traigh Bhàn na Sgùrra on the Ross of Mull, Scotland, led to the development of a 3-m wide contact aureole. Observed reactions include muscovite breakdown, melting on quartz-feldspar grain boundaries, and isochemical breakdown of biotite and garnet. A simple, 2-stage thermal model fit to the profile of maximum temperature is consistent with a 5-month period of turbulent magma flow.

Five generations of micro-cracks occur in the psammite. The oldest predates contact metamorphism and is marked by sub-parallel fluid inclusion arrays. The next resulted from anisotropic thermal expansion due to magma intrusion. Internally-generated stresses related to an increase in volume associated with muscovite breakdown formed two further sets of cracks associated with release of H₂O and melting. Melting on quartz-feldspar grain boundaries also resulted in crack formation. The final stage of cracking was the result of anisotropic thermal contraction. Despite the high crack density at the metamorphic peak, little or no melt segregation occurred, demonstrating that micro-cracking alone is not sufficient (at least on this timescale) for melt segregation in static anatexis environments.

CMT investigations of this sample are challenging since there are only small differences in the x-ray attenuation coefficients of the several materials involved and the size of the micro-cracks is comparable to the spatial resolution of our instrument. At this time, our investigations have identified feldspar, quartz, and muscovite grains, foliation, and some indication of cracks between the feldspar grains. Further work is planned at higher spatial resolution and with improved attenuation coefficient determinations.

Contract: DE-AC02-76CH00016

CATEGORY: Geochemistry

Geochemistry of Organic Sulfur in Marine Sediments

Murthy A. Vairavamurthy (631) 344-5337, fax (631) 344-7905; vmurthy@bnl.gov

Objectives: The overall objective is to gain a fuller understanding of the geochemical role of the sulfur system in transforming sedimentary organic matter from organized structures typical of biopolymers (e.g. proteins and carbohydrates) to heterogeneous sedimentary geopolymers, such as humic substances and kerogen. A major emphasis is placed on understanding the abiotic mechanisms of sulfur incorporation into organic matter and its influence in the preservation of organic matter in marine sediments.

Program Description: Sulfur is believed to be involved in preserving organic matter in sediments, in converting this organic matter to petroleum and in controlling the timing of petroleum generation from a source rock. A fundamental geochemical issue is the mechanism of incorporation of sulfur into sedimentary organic matter. Although it is accepted that H₂S and its partial oxidation products (such as polysulfide ions) are involved, there is controversy about its molecular mechanism, and the active species involved. This project, which is aimed at understanding the formation and transformation of sedimentary organic sulfur during early diagenesis, has four major components: (1) studies of sulfur speciation in sediments, (2) mechanistic studies of organic sulfur formation, (3) mechanistic studies of the pathways of transformation of organic sulfur compounds in sediments, and (4) development of analytical methods. The suite of complementary spectroscopic and chromatographic techniques used (particularly synchrotron-radiation-based XANES spectroscopy for sulfur speciation and liquid chromatography combined with mass spectrometry, LC-MS) give detailed structural information on sulfur and its associated organic moieties

Results: The organic sulfur present in fossil fuels was originally incorporated into organic matter during the early stages of diagenesis. With time, the sulfur along with the organic matter undergoes extensive diagenetic changes to form the complex macromolecules typical of fossil fuels. We studied the macromolecular humic acid fractions isolated from a Spanish leonardite coal (Torrelapaja, Cretaceous basin belonging to the Utrillas facies) and a variety of organic-rich sediments and shales using XANES and GC/MS techniques to better understand the type of sulfur functionalities and the organic structures associated with them. Our XANES data showed both reduced and oxidized forms of sulfur. The reduced sulfur mainly consisted of thiophenic sulfur, whereas the oxidized sulfur was distributed between sulfonate and ester-bound sulfur. The predominance of heterocyclic thiophenes and the oxidized forms of sulfur reflect extensive diagenetic transformations of organic sulfur after its initial formation as thiols or organic polysulfides in reducing environments.

The XANES method was used to examine the changes in sulfur speciation in a laminated sediment sequence from Lake Titicaca, South America (16° S, 69° W) to better understand the limnological and ecological processes controlling sediment deposition and sulfur speciation on short timescales. The samples, which were taken from a piston core collected from 152 m water depth, contained a distinct sequence of laminated sediments between 167 and 153 cm depth deposited over less than about 60-100 years in the mid-Holocene period (6300 to 6150 14C cal yr BP) based on AMS radiocarbon dating. Thus, the laminations were believed to represent annual or near-annual depositional cycles. The dark-colored layer of each lamination couplet contained a significant fraction of reduced organic sulfides, with smaller fractions of iron sulfides and sulfate. In contrast, the light-colored layer of each couplet was primarily composed of sulfate and is largely devoid of iron sulfides. In all laminae, the sulfate is present as inorganic sulfate substituted in calcite. The differences in speciation likely reflect changes in productivity during sediment deposition with a higher rate of calcite deposition during the highly productive summer months. The export of calcite to the sediments was reduced during lower productivity winter months. These data illustrate the utility of S K-edge XANES for the analysis of laminated sediments and support the hypothesis that these laminations were formed annually.

LAWRENCE BERKELEY NATIONAL LABORATORY

CONTRACT: DE-AC03-76SF00098

PERSON IN CHARGE: G. Bodvarsson

CATEGORY: Geophysics

Computation of Seismic Wavefields in Complex Media

V. A. Korneev (510) 486-7214, fax (510) 486-5686, vakorneev@lbl.gov

Objectives: The main goal of this project is the developing new processing technologies, which will improve the quality and resolution of seismic images for complex media, as well as understanding their connections with physical processes in rocks.

Project Description: A significant part of the project helps to improve our understanding of seismic wave propagation in an active fault zone. Specific features of the recorded waves are attributed to the structural and physical properties of the fault, which allow extraction of more detailed information from the data. This includes extensive numerical modeling of seismic wave propagation in the fault zones and analysis and interpretation of recorded data. We use the Parkfield data as one application of the new forward modeling techniques developed in this work in a crustal scale. A unique data set was recorded in Weyburn field (Canada) for horizontal crosswell time-lapse survey. An innovative inverse scheme for guided wave tomography is applied for both datasets and allowed to obtain first of the kind high-resolution images of thin low velocity layers. Another component of the project includes studies of the frequency dependence of seismic reflections from a thin (compared to the dominant wavelength), fluid-saturated layer, where some intriguing and potentially important effects were found. This includes analysis of both ultrasonic lab data and seismic field data, as well as analytical and numerical modeling.

Results: Numerical modeling and a growing number of observations have argued for the propagation of fault-zone guided waves (FZGW) within a San Andreas fault zone that is 100 to 200 m wide at seismogenic depths and with 20 to 40% lower shear-wave velocity than the adjacent unfaulted media. Thousands of microearthquakes recorded since 1987 by the borehole seismic network at Parkfield provide a comprehensive data set we have used to characterize the nature of wave propagation in the San Andreas Fault zone there. We confirm that FZGW at Parkfield are generated within the fault zone, that they are most prominent late in the coda of S. The amplitude guided wave tomographic inversion allowed obtaining a unique image (Fig.1) of inner structure of the fault zone, with resolution by a factor of ten exceeding a resolution of travel-time P- and S- wave tomography. The results show clearly that FZGW are most effectively generated in a well-defined part of the fault zone when it lies in the source-to-receiver path of the direct P and S waves. This feature plunges to the northwest through the region of highest seismicity and it separates locked and slipping sections of the fault as determined from

both geodesy and microearthquake recurrence rates. Finite-difference modeling of the observed wave field yields a sharply bounded region of low attenuation within the fault zone. We interpret this localized zone of FZGW generation to be the NW edge of the M6 asperity at Parkfield, the low attenuation due most likely to dewatering by fracture closure and/or fault-normal compression and changes in fracture orientation due to complex stress field in the boundary of creeping and locked zones of the San Andreas Fault.

The obtained image reveal its high correlation with other geophysical spatially dependent, such as slip rate, stress change and velocities of seismic wave propagation, which suggest their common origin.

This study shows that FZGW can be used for amplitude tomographic inversion giving high resolution and robust images of the narrow low velocity layers. The zone of FZGW generation includes several significant features in the fault zone - the region of shallow velocity change in the Vibroseis monitoring, high seismicity, the largest earthquakes and associated high slip rate, the 1966 M6 hypocenter, and the transition from locked to creeping behavior.

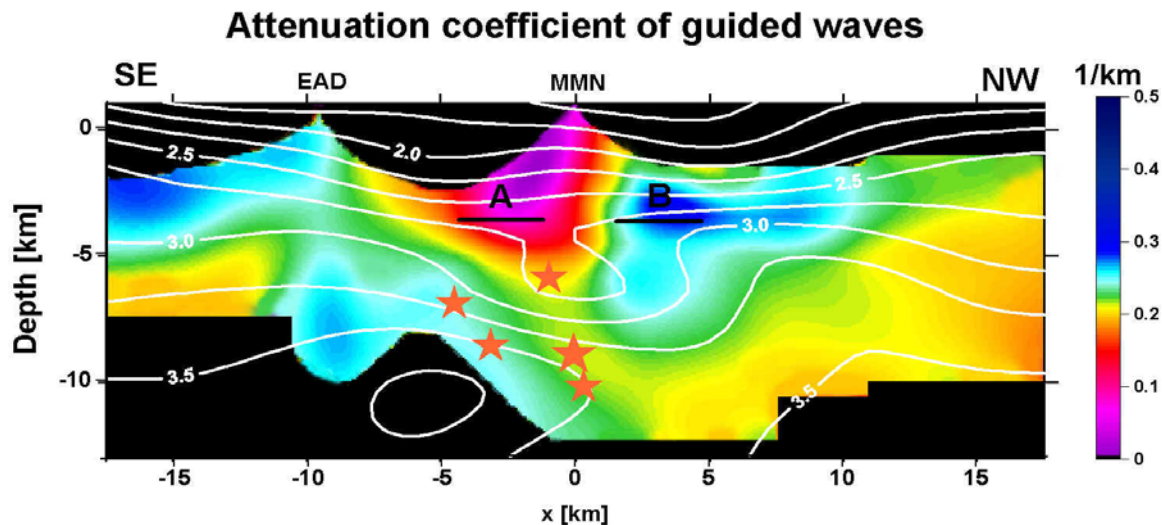


Fig. 1 In-fault image of the FZGW tomographic reconstruction showing the NW-plunging zone of inferred strong fault zone guided wave generation, Vs contours, 1987-1998 seismicity (small red stars for M>4 events), and the 1966 M6 hypocenter.

The physical mechanism of seismic attenuation variation within a FZ requires further investigation. Most likely it is associated with fractures closure and opening due to loading stress changes. Laboratory data of time-lapse seismic attenuation measurements for fractured rocks during increasing of normal load show steady increase of recorded amplitude reaching a maximum value shortly before rock destruction. The obtained spatial distribution of attenuation for SAF at Parkfield reveals very similar behavior of stressed rocks with seismic failure prone zone at SE side of the attenuation anomaly. Such mechanism gives physical interpretation of

cumulative attenuation, as being approximately proportional to elastic energy drop along the fault zone. The process of fracture opening and development also involves dewatering of rocks and water pressure changes. The understanding of relations between attenuation of FZGW and fracturing processes, stress accumulation and occurrence of earthquakes is very important for earthquake understanding and predictions.

The locations of dramatic changes in all these characteristics correspond to locked-creeping sections boundary. The evolution and profile of the Middle Mountain Ridge showing up on the NW side of the elevation curve is likely to be a result of gradual vertical stress release during creeping history of this section of SAF. These results revealed high importance of guided waves for fault zone studies. Guided waves propagate in the low velocity cores of fault zone and therefore directly affected by processes and changes which take place there. They allow produce high-resolution images of the fault zone's inner structure. The connection between guided waves and other fault zone characteristics is evident. Guided waves can be an invaluable source of information about upcoming seismic events and can be used for monitoring purposes. The relations between FZGW parameters and FZ rock properties need further investigations.

2) The frequency dependence study of seismic reflections from a thin (compared to the dominant wavelength), fluid-saturated layer was conducted using laboratory and field data. Reflections from a thin, water-saturated layer have increased amplitude and delayed travel time at low frequencies if compared with reflections from a gas-saturated layer. This effect was observed for both ultrasonic lab data and seismic field data. We compared the results of laboratory modeling with a frictional-viscous theoretical model and found that low (< 5) values of the attenuation parameter Q and its approximate proportionality to frequency can explain the observations. Our explanation is that the cause of very low Q is internal friction between fluid bearing elements of a rock formation. The frequency dependent amplitude and phase reflection properties can be used for detecting and monitoring thin liquid saturated layers.

Joint Inversion for Subsurface Imaging

K.H.Lee (510) 486-7468, fax (510) 486-5686, KHLee@lbl.gov; H.F.Morrison, M.Hoversten, D.Vasco

Objectives: To develop a joint inversion methodology using geophysical data to predict subsurface hydrologic properties. The underlying concept of using the geophysical data to predict the hydrologic properties is borrowed directly from the well-established field of well logging. Here borehole geophysical measurements of sonic velocity, electrical resistivity and density are used jointly to estimate porosity and saturation (usually oil/water saturation). It is the objective of this proposal to extend these concepts to the mapping of hydrological properties in the interwell volume using both in-hole and large-scale cross-hole and hole-to-surface geophysics.

Project description: Accurate mapping of geophysical and hydrological parameters are increasingly more important in the broader study of groundwater supply, development of long-

term injection strategy for CO₂ sequestration, characterization and monitoring of petroleum reservoirs and environmental remediation processes, and in almost all aspects of subsurface engineering in general. Geophysical methods can map the distribution of seismic velocity and electrical conductivity beneath the surface and between holes. These physical properties are dependent on density, porosity, fluid saturation, clay content, and in some circumstances, permeability. While general quantitative relationships are elusive, on a site-specific basis this geophysical data can provide spatial information that is ideal for the interpolation of well log data and for constraining or conditioning the inversion of data from pumping tests. The relationship between seismic properties, conductivity, and the hydrologic parameters are now so well known that we propose to develop a means to jointly invert the geophysical and well data to a distribution of properties that satisfies all the field data.

Results: To assess the feasibility of deriving hydrological properties directly, we have developed a joint inversion technique using EM and seismic travel-time data. Inversion parameters are the rock porosity and the fluid electrical conductivity instead of the usual bulk electrical conductivity and seismic velocity. The substitution is based on simple empirical relationships such as Arch's law and the Wyllie time average equation. To begin we chose a simplest earth model in which the formation is fully saturated and the P-wave velocities in the rock matrix and pore fluid are fixed, so the traveltimes are only a function of porosity. For this simple model the bulk electrical conductivity is a function of fluid conductivity and porosity. The inversion is based on a least-square criteria that minimize the misfit. A smoothness constraint is implemented to reduce non-uniqueness. To simulate EM responses we chose a model that is axially symmetric about the transmitter borehole. Numerical simulation is carried out with the algorithm based on the Born approximation technique. The bulk electrical conductivity used for the EM simulation is estimated using a simplified Archie's law. A straight ray path is assumed for the seismic method, and travel-time data are calculated based on the simplified Wyllie equation.

A model (Figure 1) containing three horizontal slabs with various conductivity and porosity is used to verify the proposed approach. All three heterogeneities are reasonably well resolved in terms of the two hydrological properties: porosity and fluid conductivity, respectively. The optimum result of the joint inversion has been obtained by alternating the selection of inversion parameters, in which only one parameter is allowed to change while the other parameter is held fixed at each iteration.

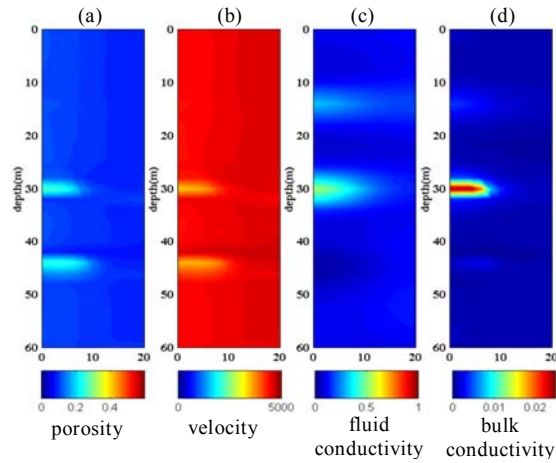
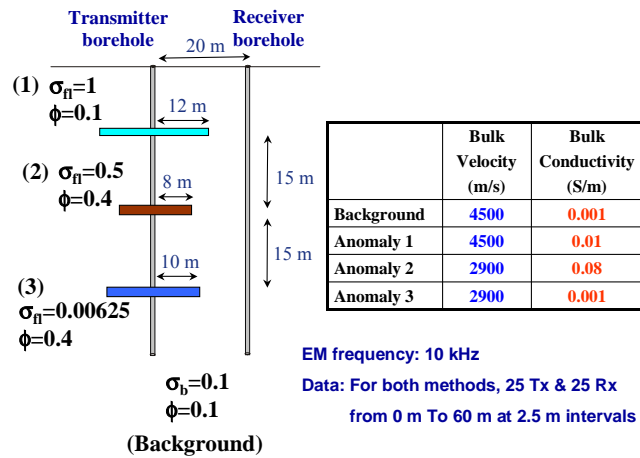


Figure 1. A synthetic model used for joint inversion study is shown on the top. Shown on the bottom is the inversion result for: (a) formation porosity; (b) calculated velocity; (c) fluid conductivity; and (d) calculated bulk conductivity.

Center for Computational Seismology (CCS)

T.V. McEvilly, (510) 486-7316, fax (510) 486-5686, tvmceville@lbl.gov; E.L. Majer; L.R. Johnson

Objectives: The Center for Computational Seismology (CCS) serves as the core data processing, computation and visualization facility for seismology-related research at LBNL. As such, it will be integral to our critical efforts in mapping the distribution and migration of fluids in the subsurface, a problem requiring new approaches in seismic waveform inversion techniques that can take into account the presence and effects of diffracted waves. A wide range of research projects relies upon CCS resources for development and application of methods for characterization, process definition, and process monitoring in the rock-fluid-thermochemical subsurface environment. Pursuing an objective of providing modern tools for seismological research, the Center is designed and operated to provide a focused environment for research in modern computational seismology by scientists whose efforts at any time may be distributed among diverse research projects. A large number of varied, separately funded research projects, from many different sponsors, rely upon this resource for intellectual exchange as well as computational needs. Ph.D. theses and journal publications reveal a spectrum of effort from the most fundamental theoretical studies to field applications at all scales.

Project Description: CCS provides a specially equipped and staffed computational facility to support and advance a wide-ranging program of seismological research. Beyond computers, work stations, seismic processing packages and visualization capabilities, it is a physical facility in which scientists pursuing individual research interact with other scientists and technical support staff in a multidisciplinary intellectual environment. CCS supports research in the general areas of wave propagation, geophysical inverse methods, earthquake and explosion source theory, seismic imaging, borehole geophysics, four-dimensional process monitoring and visualization technology.

Results: Results from the diverse seismological program at CCS are best demonstrated in the CCS research output. Major accomplishments flow largely from the breadth of research support provided by CCS, and the cross-fertilization between applications and fundamental studies. Significant recent results involve successful imaging of contaminant flow zones in fractured basalt, development of borehole orbital vibrator technology and promising results in CO₂ monitoring with borehole imaging methodology. Findings for a facility and scientific environment such as that provided by CCS must be defined in the context of the multidisciplinary research base that is supported there, rather than project-specific accomplishments (those appear in other sections of this report). It is fair to attribute a large part of the scientific reputation in seismology at LBNL to the CCS environment.

Deformation and Fracture of Poorly Consolidated Media

L.R.Myer, (510) 486-6456, fax (510) 486-5686, LRMyer@lbl.gov ; K.T.Nihei (510) 486-5349, fax (510) 486-5686, KTNihei@lbl.gov

Objectives: Rocks with small intergranular cohesion can be a potential threat to the stability of boreholes and other stress-bearing rock structures. Their mechanical behavior is intermediate between that of rock and soil. This study examines the effect of micromechanical properties of weak granular rock on macroscopic properties such as load-displacement response, ultimate strength, and failure mode.

Project Descriptions: In our previous research, a technique to fabricate weakly cemented granular rocks (artificial sandstone) was developed using dried sodium silicate as intergranular cement. Using this technique, we performed a series of parametric studies on the effect of grain-scale properties including intergranular cementation, and porosity. The focus of the final stage of the research was on the effect of confining stress on the failure of weakly cemented granular rock. To this end, we performed a series of triaxial compression tests on the weakly cemented artificial sandstone samples. In addition to these experiments, we made detailed observations of intergranular cementation as a function of cement volume occupying the pore space using scanning electron microscopy (SEM) and optical microscopy.

Results: The SEM and optical microscope revealed surprisingly small bonding areas between contacting sand grains. For cement contents below $S=0.5\%$, the sodium silicate cement could hardly be seen even though the uniaxial compression strength of rock was as high as 2 MPa. For larger cement contents, relatively even coating of the cement on the grain surface was observed, which is consistent with the result of our previous analysis based on Dvorkin-Nur cemented grain models (Dvorkin-Nur, 1996) using measured compressional and shear wave velocities of the rock samples.

During the triaxial compression tests, the failure strength of the laboratory-fabricated weakly cemented granular rock samples exhibited a strong sensitivity to the confining stress. This is due to the small intergranular cohesive strength of the weakly cemented rock compared to the increase in intergranular friction that increases with confining stress. The change in the rock strength is also accompanied by changes in the rock failure mode (see Figure 1). From near-zero confining stress up to 100 psi of confining stress, cylindrical samples of weakly cemented rock (sodium silicate cement volume/pore space volume $S=0.5\%$, porosity 35.5%) exhibited a range of mode failure modes from brittle extensile failure to ductile failure exhibiting multiple, conjugate shear bands. Such a strong sensitivity of the rock strength and failure mode to the confining stress implies that the grain-scale properties of weakly cemented rock can have a large impact on the stability and sanding of oil and gas producing wells drilled within such rocks.

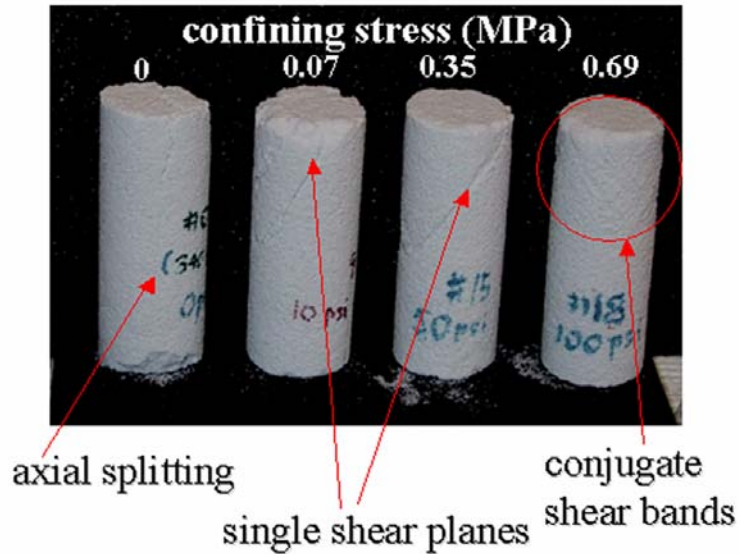


Figure 1 Strong sensitivity of rock failure mode observed for weakly cemented granular rock (synthetic sandstone). A small change in confining stress resulted in failure modes ranging from brittle extensile failure to ductile shear failure.

Decomposition of Scattering and Intrinsic Attenuation on Rock with Heterogeneous Multiphase Fluids Distributions

K.T.Nihei, (510) 486-5349, fax (510) 486-5686, KTNihei@lbl.gov; L.R.Myer (510) 486-6456, fax (510) 486-5686, LRMyer@lbl.gov

Objectives: The overall focus of this project is a fundamental investigation of scattering and intrinsic attenuation of seismic waves in rock with heterogeneous distributions of fluids and gas. This research represents a departure from past rock physics studies on seismic attenuation in that the emphasis here is not a detailed study of a specific attenuation mechanism, but rather to investigate theoretical and laboratory methods for obtaining separate estimates of scattering and intrinsic attenuation in rock with heterogeneous pore fluid distributions. It is anticipated that methods for obtaining separate estimates of intrinsic and scattering attenuation may lead to higher resolution methods for monitoring the movement of fluids in the subsurface.

This project combines laboratory, numerical, and theoretical studies to the investigation of scattering and intrinsic attenuation in rock with heterogeneous fluid distributions. The objectives of this project are threefold: (1) to adapt and further refine methods for decomposing scattering and intrinsic attenuation in rock with heterogeneous multiphase fluids, (2) to apply these methods to laboratory seismic measurements in porous rock with heterogeneous fluid distributions and compare these results with direct laboratory measurements, and (3) to examine a new method for focusing seismic waves in heterogeneous media using time reversal mirrors. These objectives are addressed in three tasks to be performed over a period of three years.

Project Description: In this project, laboratory, theoretical, and numerical studies are combined to investigate methods for estimating scattering and intrinsic attenuation in rock with heterogeneous distributions of gas and fluid. The focus is on sandstone and carbonates under conditions in which the relative saturation of miscible and immiscible liquids (e.g., water and oil) and gas (e.g., CO₂) vary. Decomposition of the attenuation will be conducted to compare the contributions from scattering and intrinsic attenuation and related to the characteristics of introduced heterogeneity obtained from X-ray CT images. Numerical and theoretical models will be performed to help interpret the results of the laboratory experiments and to investigate the effect of both attenuation mechanisms on the characteristics of the waves. Laboratory and numerical studies of wave focusing on selected heterogeneities using elastic time reversal mirrors will also be investigated. The effects of intrinsic attenuation on the time reversal focusing process and methods for correcting for intrinsic attenuation will be examined.

Results: During the second year of this project, we have focused our efforts on acoustic and elastic imaging methodologies for mapping intrinsic attenuation in the presence of scattering heterogeneities. These imaging methods are based on nonlinear full-waveform inversion using the adjoint state method. A finite difference code is used to compute the numerical gradients required by the iterative nonlinear inversion scheme. The code, developed by our collaborator at Kyoto University (T. Watanabe), solves the viscoacoustic wave equation in the frequency domain using an LUD matrix solver to allow rapid gradient calculations for multiple sources. A number of simulations were performed using this code for faulted layer models with variable intrinsic attenuation. These simulations revealed that the best estimates of intrinsic attenuation were obtained using a scheme that first inverted for the best velocity model assuming zero intrinsic attenuation, followed by an inversion for the intrinsic attenuation using the best velocity model.

To test the performance of this inversion scheme on non-synthetic data, we constructed a scanning stage that allows crosswell viscoacoustic measurements to be performed in the laboratory. The first test was performed in a water tank with three acrylic bars with diameters 0.5, 1.0, and 2.0 inches. We fabricated broadband P-wave sources and receivers from piezofilm cylinders. By driving the source below its first resonance with a pulse, we were able to acquire broadband crosswell data centered at 100 kHz for 16 sources and 31 receivers. The first attempt at full-waveform viscoacoustic inversion for velocity and intrinsic attenuation is displayed in Fig. 1. The velocity image shows a reasonable reconstruction of the three acrylic bars with characteristic artifacts (blue spots) resulting from limited illumination of the targets by the crosswell acquisition geometry. The intrinsic attenuation image recovers the locations of the three acrylic bars with the correct intrinsic attenuation ($Q_1=30$), however, with substantial smearing. We have noticed that a much sharper reconstruction of Q_1 was obtained in the inversion of synthetic data, and are investigating possible reasons for this discrepancy.

As a first step towards full-waveform viscoelastic imaging, we have developed a 2D frequency domain staggered grid finite difference code that uses an iterative matrix solver (TFQMR). We have also developed a monofrequency time domain code that provides the magnitude and phase of the wavefield after running the code a prescribed time out to steady state. These codes are

being integrated into a conjugate gradient full-waveform inversion scheme for the complex moduli of isotropic and anisotropic heterogeneous media.

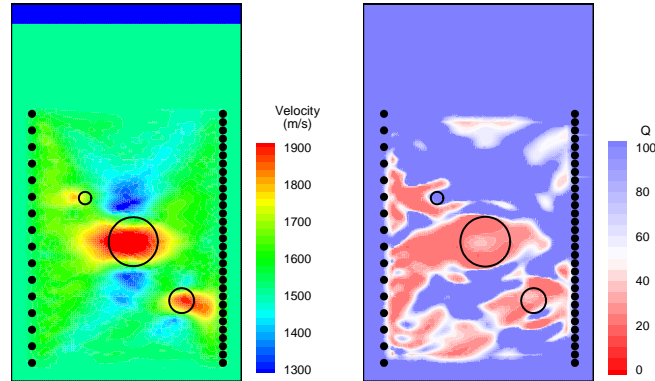


Figure 1. Velocity (left) and quality factor (right) from viscoacoustic inversion of laboratory data.

Unsaturated Fast Flow in Fractured Rock: Testing Film Flow and Aperture Influence

T.K. Tokunaga, (510) 486-7176, fax (510) 486-7797, tktokunaga@lbl.gov

Objectives: The nature of unsaturated fast-flow in fractured rocks needs to be understood in order to obtain reasonable constraints on vadose zone transport. Water films along unsaturated fractures have recently been shown to be capable of supporting fast flow and transport, and revealed limitations of existing aperture-based models. In this project, theoretical considerations and experiments are combined to improve our understanding of unsaturated flow in fractured rocks.

Project Description: Recently, the concept of film flow was introduced as a possible process by which preferential flow could occur along truly unsaturated fractured rock. Our work concerns water films on fracture surfaces under near-zero (negative) matric potentials, and examines the possibility of fast, unsaturated flow under "tension". "Films" in this context are a complex network of thick pendular regions that form within topographic depressions and thin films on topographic ridges. Thus, the thickness and connectivity of pendular film regions is expected to be important in controlling film flow on individual fracture surfaces. We showed that at matric potentials greater than that needed to saturate the rock matrix, transmissive water films can develop on fracture surfaces. The matric potential dependence of the average film thickness, the film transmissivity and film hydraulic diffusivity have been measured on fracture surfaces of

Bishop Tuff, a basalt, and roughened glass, using equilibrium, steady-state and transient methods. The water “films” investigated in the previous study as well as the present one develop on rough surfaces, range in average thickness from about 1 to 50 μm , and flow in the laminar regime. In the FY 2001 work, studies were continued on the general conditions necessary for stable film flow and saturated fracture flow under low average seepage rates. We are specifically examining the importance of flow path convergence in deep, unsaturated fractured rock formations. Fast flow paths are difficult to locate in deep unsaturated fractured rock formations, but in recent years detection of such features by geochemical analyses have been reported. The conceptual model being developed has relevance in understanding very sparsely distributed fast flow paths in the subsurface and their potential impact on subsurface waste isolation and contaminant transport.

Results: Flow through unsaturated fractured rock occurs via a number of processes, including flow through rock matrix blocks, flow along fractures via capillary films, and flow in saturated fractures. We recently showed that matric potentials close to zero (greater than -1 kPa) are necessary for development of fast film flow. This energy constraint requires that capillary film flow is strongly gravity-selective. This consideration, along with recognition that flow is largely gravity driven in deep unsaturated zones, led to a model of monotonic convergent flow along fracture pathways. This model is the 3-dimensional unsaturated zone analog to 2-dimensional stream-river convergence familiar in surface water hydrology. For the case of deep unsaturated rock formations, we are trying to determine average effective land surface catchment areas associated with active fracture flow paths. We have run preliminary tests of this model in laboratory replicas of fractured rock systems at 2 scales (30 cm and 80 cm). These tests indicate that monotonic convergence of flow paths in unsaturated fractured rock formations is oversimplistic, and that the probability of flow path divergence needs to be determined for specific systems. Our latest efforts are directed on determining such probabilities, and their dependence on fracture scale.

Prediction and Evaluation of Coupled Processes for CO₂ Disposal in Aquifers

Karsten Pruess, (510) 486-6732, fax (510) 486-5686, K_Pruess@lbl.gov; Chin-Fu Tsang (510) 486-5782, fax (510) 486-5686, CFTsang@lbl.gov

Objectives: Evaluate the physical and chemical processes that would be induced by large-scale CO₂ injection into brine aquifers. Develop and demonstrate numerical simulation capabilities for CO₂ disposal.

Project Description: The purpose of the research is to develop a systematic, rational, and mechanistic understanding of the coupled processes that would be induced by injection of CO₂ into aquifers. This is being accomplished by means of conceptual, mathematical, and numerical models that are based on rigorous continuum theories of fluid dynamics, coupled with detailed rock fracture mechanics and chemical speciation and reaction path analyses. Field experience and data from natural CO₂ reservoirs and engineered aquifer gas storage systems will be used, as

will be laboratory data and generally accepted physical and chemical principles for multiphase flow, geochemical alteration, and rock mechanical effects. By developing a mechanistic understanding of the relevant processes, this research will provide a sound basis for evaluating the feasibility of CO₂ disposal in different hydrogeologic environments, including fractured rock systems, and will provide engineering tools for the design, implementation, and monitoring of CO₂ disposal systems in brine aquifers.

Results: Three interrelated numerical simulation codes have been developed that address, respectively, issues of fluid dynamics (TOUGH2/ECO₂), reactive chemical transport (TOUGHREACT/ECO₂), and geomechanics (TOUGH-FLAC). TOUGH2/ECO₂ has been used to study immiscible displacement of brine by supercritical CO₂ for a range of scales and hydrogeologic conditions. Buoyancy effects tend to drive CO₂ towards the top of the permeable interval, causing bypassing of significant formation volumes and reducing storage capacity. A favorable side effect of this tendency towards side-by-side flow of CO₂ and water is diminished phase interference, and a corresponding reduction in fluid pressures at the injection well. Formation heterogeneities may actually enhance storage capacity, by reducing rates of buoyant upflow of CO₂ and thereby improving sweep efficiency. CO₂ leakage along a fault has a potential for self-enhancement, due to the lower viscosity and density of CO₂ compared to brine (see Figure 1). High-resolution studies of brine displacement by CO₂ have shown fingering with widths of the order of 10 cm or less, suggesting that fingering instability is unlikely to have much practical significance.

A reactive geochemical transport model TOUGHREACT/ECO₂ for evaluating long-term CO₂ disposal in deep aquifers has been developed. The model has been used to analyze mineral alteration, CO₂ sequestration by secondary carbonates, and reservoir porosity changes in a 1-D radial flow field for a homogeneous Gulf Coast sediment. Under conditions considered in our simulations, CO₂ trapping by secondary carbonate minerals such as calcite (CaCO₃), dolomite (CaMg(CO₃)₂), siderite (FeCO₃), and dawsonite (NaAlCO₃(OH)₂) could occur in the presence of high pressure CO₂. Variations in precipitation of secondary carbonate minerals strongly depend on rock mineral composition and their kinetic reaction rates. CO₂ mineral-trapping capability after 10,000 years is comparable to CO₂ dissolution in pore waters (2-5 kg CO₂ per cubic meter medium). Under favorable conditions, such as increased abundance of chlorite minerals (e.g. clinochlore Mg₅Al₂Si₃O₁₀(OH)₈), the capacity can be as large as 10 kg CO₂ per cubic meter medium due to an increase in dolomite precipitation. Carbon dioxide-induced rock mineral alteration and the addition of CO₂ mass as secondary carbonates to the solid matrix generally results in decreases in reservoir porosity and permeability.

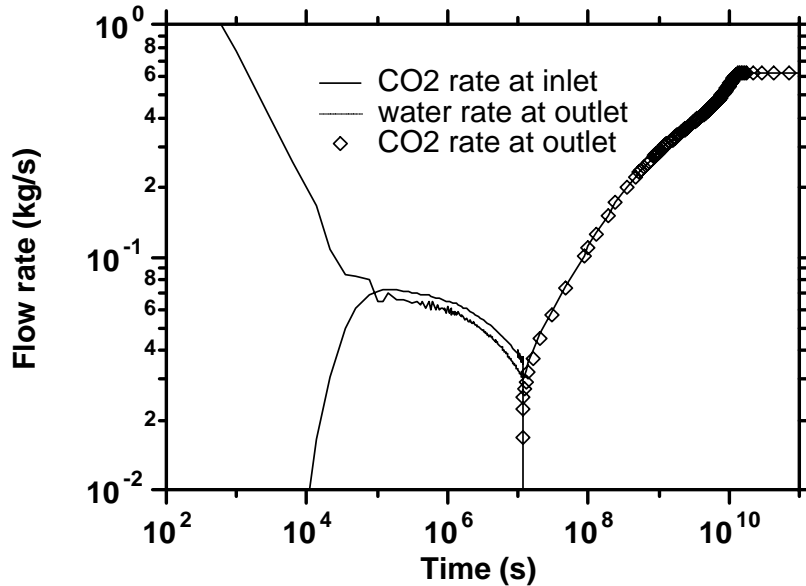


Figure 1. Flow rates per unit length of a fault zone for CO₂ leakage from a disposal aquifer. The large rates at early time ($< 10^5$ s) are due to the imposed step change in CO₂ pressure at the bottom of the fault. Flowrates slowly decline due to relative permeability effects as the CO₂ displacement front migrates up the fault (10^5 to 10^7 s). Subsequently the flowing CO₂ continues to remove moisture from the fault, reducing phase interference and causing CO₂ discharge rates to increase by a factor of approximately 20, until steady-state flow conditions are reached after about 10^{10} s.

Geomechanical aspects of CO₂ sequestration have been studied using a simulator TOUGH-FLAC that was newly developed in this project. The simulator is based on linked execution of TOUGH2 and FLAC3D, which is an established and widely used code for advanced geomechanics analysis. A linked TOUGH-FLAC simulation can utilize the latest developments in TOUGH2 for modeling brine-CO₂ mixtures under supercritical conditions, and in addition, geomechanical aspects and effects of coupling between fluid flow and rock mechanics are analyzed using the FLAC3D module.

Using TOUGH-FLAC, the hydromechanical changes associated with CO₂ injection into brine formations have been studied. The analysis demonstrates how a large-scale CO₂ injection operation results in a gradual increase of aquifer pressure, which could reach close to the lithostatic stress after years of injection. Such aquifer pressure increase will induce a number of hydromechanical interactions and geomechanical responses through changes in the effective stress field in both the injection aquifer and the overlying semi-permeable caprock. A general reduction in the vertical effective stress induces vertical expansion of the aquifer, which can be significant and can be monitored on the ground surface. A relatively slow increase of the aquifer pressure during a typical constant rate injection will induce poroelastic stresses in the caprock which prevent catastrophic mechanical rock failure in the form of hydraulic fracturing through a caprock. Instead, the principal rock mechanics effect will be shear-slip along pre-existing faults and fractures occurring in the lower part of the caprock near the injection aquifer. The analysis shows that although shear-slip would be induced in the lower part of the caprock, it is not likely

to propagate a rock failure zone through the upper part of the cap if preventive operational actions are taken. Thus, monitoring of seismic events in the lower part of the cap together with monitoring of ground surface movement are essential for controlling the hydromechanical responses during a CO₂ injection operation.

Colloid Transport in Unsaturated Porous Media and Rock Fractures

Jiamin Wan, (510) 486-6004, fax (510) 495-7797, jwan@lbl.gov

Objectives: The current understanding of colloid transport is largely based on the classic filtration theory used in saturated porous media. Some recent studies have led to identification of several important aspects of vadose zone colloid transport that still need to be understood. The overall objective of this project is to obtain a comprehensive understanding of colloid transport in partially saturated porous media and rock fractures.

Project Description: The basic physics and chemistry unique to vadose zone colloid transport is a consequence of the existence of a second immiscible fluid phase, gas. Traditional filtration theory cannot be directly applied in the vadose zone colloid transport because of the coexistence of air and water. In the 1997 to 1999 period, we focused on studies of colloids being strained by becoming trapped within thin water films in unsaturated porous media, and introduced the concept of “film straining”. Our recent research has been focused on quantifying the partitioning of surface-active colloids at the air-water interfaces. Much effort has been devoted to characterizing surface accumulations of colloids. Previously developed methods include surface microlayer sampling and jet drop collection. Because of the large uncertainties in thicknesses and interfacial areas, results are often reported as the enrichment factors for a given estimated thickness. We have recently developed a simple dynamic method to quantify colloid surface excesses at air-water interfaces without requiring assumptions concerning the thickness of interfacial regions. During the 1999 to 2000 period, we measured partition coefficients of different clay minerals at the air-water interface, primarily under environmentally relevant solution chemistry conditions.

Results: The affinity of clay colloids to the air-water interface was quantitatively measured using a bubble column method. The affinities of clay particles to the air-water interface are reported as partition coefficients (K), in a manner analogous to surface-active solutes. Five types of dilute clay suspensions were measured: Ca-montmorillonite, Na-montmorillonite, bentonite clay, illite, and kaolinite, under varying pH and ionic strength conditions. In order to obtain results that are directly relevant to typical subsurface environments, no surfactants were used, and most experiments were conducted at low values of ionic strength. Na- montmorillonite and bentonite clay were found surface excluded from the air-water interface at any given pH and ionic strength. Ca-montmorillonite and bentonite clay are slightly surface-active at the air-water interface with increased K values at lower pH. Kaolinite exhibited extremely high affinity to the air-water interface at pH below 7. The strong pH dependence of the K values suggests that electrostatic force might be the governing force for partitioning of the clay colloids at the air-water interface.

CATEGORY: Geochemistry

PERSON IN CHARGE: Bodvarsson

Integrated Isotopic Studies of Geochemical Processes

Donald J. DePaolo, (510) 486-4975, fax (510) 643-5064, fax (510) 642-9520, depaolo@socrates.berkeley.edu or djdepaolo@lbl.gov; B. Mack Kennedy (510) 486-6451, fax (510) 486-5496, bmkennedy@lbl.gov

Objective: Combine high-precision measurements of isotopic ratios in natural materials with mathematical models to understand the spatial and time scales of geochemical processes of interest for energy management.

Project Description: Isotopic measurements of Sr, Ca, Fe, O, C, H, He, Ne, Ar, Xe, Pb, Nd, and U are used to address problems of mass transport in fluid-rock systems, interpretation of past global climatic change, crustal magmatic and tectonic processes, and Quaternary geochronology. Most geological transport processes cannot be modeled accurately from first principles due to heterogeneity on many scales and complex coupling between processes. The tracers provided by natural isotopic variations measure the net effects of these complex processes, and provide the critical calibration of models that can make the models useful for prediction. Our aim is to advance the state of the art of the isotopic approaches, and to use these advances to investigate fundamental issues in geochemistry. Mathematical models are developed to help extend the application of isotopic measurements to natural systems. Modeling and systematic measurements of simple natural systems are supplemented by efforts to improve sampling methodologies and measurement techniques such as micro-sampling of geological materials, high-precision measurement of small samples by MC-ICPMS and TIMS, and rapid low-blank chemical separation of trace metals. All efforts are aimed at improved characterization of natural rock and fluid systems relevant to environmental remediation, geothermal and fossil energy resources, carbon- and water cycle science, and nuclear waste isolation.

Results: (1) Natural variations of Sr, O and U isotopes in fluids are being investigated as a means to measure in situ rates of chemical reactions in groundwater and during diagenesis of sediments. The objective is to develop a database from which to further evaluate the large discrepancies between natural reaction timescales and those measured in the laboratory and predicted by thermodynamically based kinetic models. A second objective is to use the reaction timescale as a clock for evaluating the rates of mass transport in fluid-rock systems. To this end we are studying fluid and solid isotopic characteristics in arid vadose zones, aquifers, deep sea sediments, and geothermal systems. Emphasis is now being placed on developing U isotopes as a sensitive probe of local rates of mineral dissolution. This approach is based on the competition between alpha recoil processes and dissolution. When applied to fine grained deep sea sediments, the derived bulk dissolution timescale is about 1 million years, which is about 10,000 times slower than predicted. When combined with data on soils and older sediments, the bulk

dissolution rates of both silicate (feldspar) and carbonate vary by a factor of 1 million, correlate very well with age, and do not correlate with grain size. The alpha recoil losses from solids may also be useful for measuring the timescale of comminution of grains during erosion, which may contribute to understanding the rates of weathering and sediment transport. The U isotope method is being combined with Sr isotope measurements as a means of measuring vadose zone and groundwater fluid fluxes.

(2) The natural variation of Fe isotope ratios is being investigated in components of the Earth's weathering cycle, and as a means of tracking the sources and utilization of Fe in the carbon cycle. This investigation is mainly focused on improving the understanding of natural variations of Fe isotopes, the mechanisms that control Fe isotope fractionation, and improving analytical procedures for the measurements. The reproducibility of the measurements by TIMS has been improved and the protocols for measuring Fe by multi-collector ICPMS have been established.

(3) There is a continuing need for improved geochronology in studies of Quaternary geology, the time period that is most relevant for understanding future environmental change. The U-Th-He method is being investigated for application to age determinations on volcanic rocks. This method can theoretically be used to measure ages as young as a few thousand years and as old as several million years, and hence could span the gaps often encountered with existing methods. Measurements are focused on rocks of known age. Results indicate that minerals suitable for dating can be separated from volcanic rocks, but that an awareness of competing nuclear processes and geometric effects is needed to fully interpret the age data.

(4) Simple analytical models have been developed to evaluate and understand the natural global variations of the stable isotopic composition (O, D/H) of precipitation. The models indicate that the isotopic composition of high latitude precipitation provides a strongly attenuated record of past temperature changes, but that the attenuation coefficients may be determinable. Low latitude precipitation has large systematic isotopic variations that are correlated with regional evaporation-precipitation imbalances. Both the temperature and P-E effects are critical for interpreting isotopic records of past climate changes.

(5) A mathematical model has been developed that describes the effects of matrix pore fluid diffusion on the rates of isotopic exchange between fluids and rocks in geo-hydrological systems that are contained in fractured rocks. The model describes a simple dual-porosity system with parallel equidistant fractures. The effects of matrix diffusion on the isotopes of a particular element are shown to depend on the ratio of the diffusive reaction length for that element (L_d) to the fracture spacing (b). If isotopic data are available for two or more elements with different L_d values, it may be possible to use the model to estimate the spacing of the primary fluid-carrying fractures in natural systems. Using Sr and O isotopic data from mid-ocean ridge hydrothermal vent fluids, an average fracture spacing of 1 to 4 meters is deduced.

Clay Mineral Surface Geochemistry

Garrison Sposito, (510) 643-8297, fax (510) 643-2940, gsposito@lbl.gov

Website: http://esd.lbl.gov/GEO/aqueous_geochem/index.html

Objectives: The current objective of this project is to obtain a fundamental understanding of atomistic-scale processes at clay mineral-fluid interfaces using molecular simulation.

Project Description: The principal technique used is Monte Carlo simulation based on the Metropolis algorithm. We performed Monte Carlo simulations of the structural properties of hydration water on a 2:1 layer type dioctahedral aluminosilicate with the muscovite formula $K_2(Al_2, Si_6)Al_4O_{20}(OH)_4$. The model potential functions used to represent water-water, counterion-counterion, counterion-mineral, and water-mineral interactions were MCY-type parameters which have been tested extensively and successfully for 2:1 clay mineral hydrates in our earlier projects, including K-montmorillonite, which is isostructural with muscovite. Pair correlations, density profiles of water oxygens and counterions, and visualization of the local coordination were used to compare the atomistic details of the simulated mica-water interface to recent experimental measurements using X-ray reflectivity.

Results: Our results show the existence of an adsorbed layer of water molecules bound intimately to the ditrigonal cavities in the muscovite surface and surmounted by a network of hydration water molecules into which K^+ counterions are interposed consistently with hydrogen bonding of the water to the surface O. Our calculations support the hydration water structure proposed in a recent X-ray reflectivity study while providing additional molecular details not fully accessible to this experimental methodology.

Figure 1 compares the water O density profile we obtained by MC simulation with that derived from reflectivity measurements. The match between the experimental and simulated profiles within 4 Å from the surface O is excellent, encouraging a direct interpretation of the two principal features in terms of adsorbed water species. The visualization of the water molecules that contribute solely to the first peak (denoted “a”) shows clearly that they are indeed associated with the ditrigonal cavities in the mineral surface.

The second peak in the O density profile (denoted “b” in Fig. 1) corresponds to adsorbed water molecules distributed laterally at approximately 1.3 per surface cavity (the ratio of the height of the second peak to that of the first), as also reported in the reflectivity study. Visualization revealed that most of these water molecules are oriented with one of their OH groups pointing toward the mineral surface O consistently with hydrogen bond formation. However, the water molecules are interspersed among the K^+ counterions, which reside in two distinct planes at 2.3 and 2.7 Å from the surface O. The corresponding adsorbed K^+ species are coordinated respectively to 7 surface O and 6 water O, or to 3 surface O and 9 water O, with two of the water molecules being adsorbed near a ditrigonal cavity in the latter case. These strongly adsorbed water molecules prevent closer access of the counterion to the mineral surface.

Our simulation results are consistent with liquid-like disorder for the hydrate as a whole, as also suggested in the X-ray reflectivity study on the basis of the water O density profile tending to approach the bulk liquid limit after only a few oscillations (Fig.1). Our results show stronger oscillations, but are consistent with the same trend.

Liquid-like character of the hydration water also is apparent from our calculations of the average O-O intermolecular coordination number (N_{OO}) using simulated radial distribution functions. We find $N_{OO} = 5.1$ for the coordination number of water O around a central water O, as opposed to $N_{OO} = 5.2$ for the bulk liquid based on a simulation using the MCY potential. (The experimental value is 5.4.) Overall, therefore, the structure of water adsorbed by micaceous minerals appears to be more disordered than that of ice I_h .

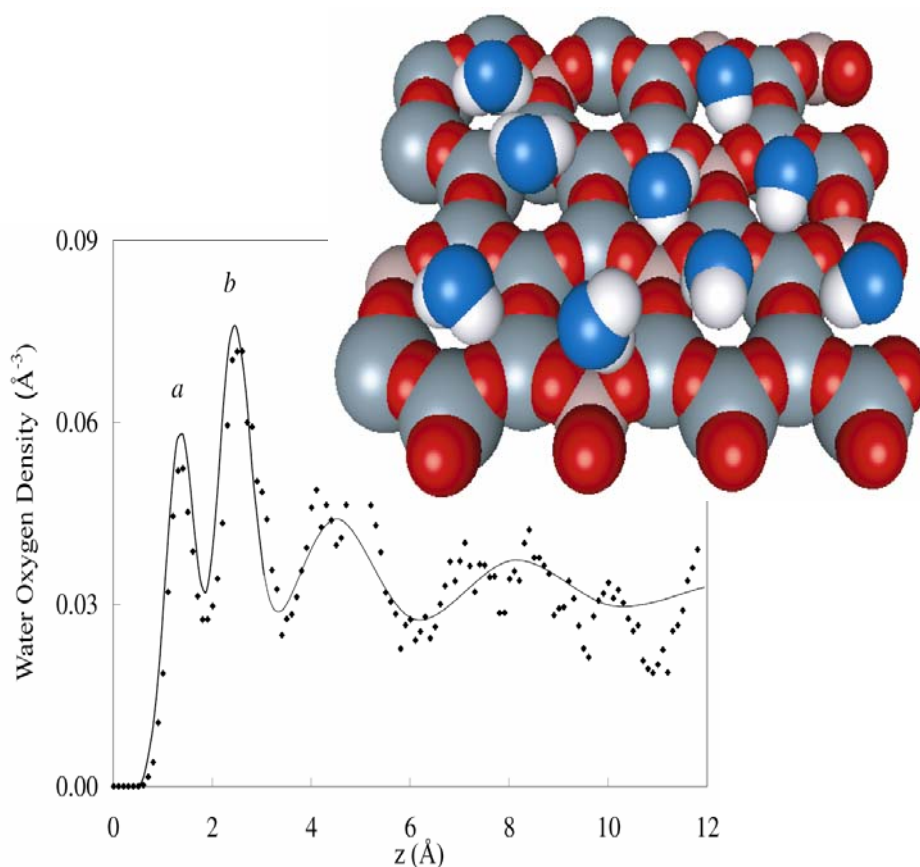


Figure 1. Water O density distribution (lower left) on muscovite as a function of the distance z from the mean surface oxygen position. The solid curve is from recent X-ray reflectivity results, while the data points are the results from MC simulation; *a*: water molecules adsorbed near ditrigonal cavities; *b*: hydration water. Visualization (upper right) of the adsorbed water molecules represented by peak *a* shows that they are adsorbed near the cavities in the mica surface.

Complexation and Precipitation Processes on Mineral Surfaces

*Glenn A. Waychunas, (510) 495-2224, fax (510) 486-7152, GAWaychunas@lbl.gov;
James A. Davis, USGS Menlo Park, CA, James R. Rustad PNNL Richland WA; Y.R. Shen
Physics Dept. UC Berkeley*

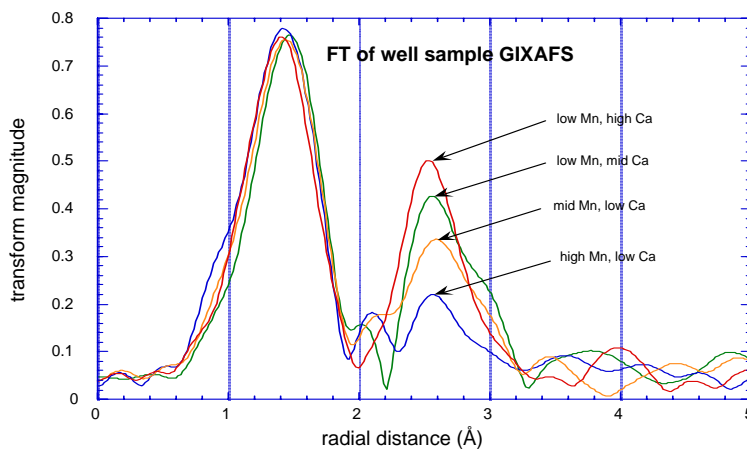
Website: http://www.esd.lbl.gov/GEO/aqueous_geochem/synbased_gaw.shtml

Objectives: Comparison of the reactivity of perfectly prepared mineral surfaces with degraded perfect surfaces simulating surface defects and with perfect surfaces exposed to natural conditions; Characterization of the effects of water undersaturation on precipitate formation; Determination of the nature of water structure near the mineral-water interface, and how it is affected by sorption and precipitation processes, pH, ionic strength and surface defects. Simulation of surface water IR spectra collected via sum frequency generation (SFG) spectroscopy.

Project Description: The project continues earlier work examining the nature of quartz surface coatings formed over time in the Cape Cod USGS site aquifer. These samples are withdrawn periodically to reveal coating formation and quartz surface degradation. Characterization methods include synchrotron-based x-ray absorption spectroscopy in grazing incidence mode (GIXAS) and total reflection x-ray fluorescence spectroscopy (TRXRF), transmission electron microscopy (TEM) and atomic force microscopy (AFM). The use of GIXAS gives us structure sensitivity to extremely small amounts of surface species, and TRXRF procedures allow us not only to measure surface composition in the femtomole range, but also allow depth profiling of surface composition in the nanometer range. A second part of the project focuses on the role of water in stabilizing sorbed complexes and early precipitates on quartz and other mineral surfaces.

For the latter work we are utilizing sum frequency (SFG) spectroscopy in collaboration with Prof. Ron Shen's group on the UC Berkeley campus. This method allows us to obtain the IR spectrum of water molecules just at the solution-mineral interface, and determine how they are affected by varying surface charge (solution pH), ionic strength of the solution, the formation of surface complexes, and defects on the surface (steps, terraces, dislocations). For many sorption complexes it has been postulated that a certain number of hydrogen bonds must be formed at the surface for their stabilization, yet experimental measurement of this bonding has not been available. SFG spectroscopy allows us to measure the relative orientations of water molecules and their degree of H-bonding to other waters and surface species. We are examining a suite of minerals having different surface properties, including quartz, hematite, corundum and pyrite. Crystals can be prepared with highly perfect surfaces, or with particular arrangements and densities of growth steps and terraces. We can also vary the total thickness of water on a surface to approximate undersaturated conditions. Another aspect of this research is determination of the nature of water structure on surfaces as a function of water coverage. We wish to determine if the closest water molecules to a mineral surface are affected by the number of overlying water layers, and if this changes reactivity and the ability to stabilize sorption complexes.

Results: Perfect quartz wafers extracted from the Cape Cod site aquifer after 1.5 years showed a continuing buildup of surface material, but still only nanometer-thick precipitates. The trend previously observed of Ca concentration affecting the amount and structural integrity of ferric precipitates was verified. TRXRF studies conducted over a range of incidence angles near the critical angle for total reflection show that the Fe precipitates are not completely mixed with Ca phases, but instead are usually on top of nanometer layers rich in Ca. The presence of Ca is interesting by itself, as the pH and chemistry of the water in the aquifer is inconsistent with Ca carbonate formation. It is therefore likely that the Ca represents microbial activity on the surface, either locally changing pH conditions to affect carbonate formation, or carrying Ca in their cellular material or membranes. AFM and TEM characterization is in progress to identify specific Ca phases and domain topology. SFG work was begun on perfect quartz crystals with several different orientations. The initial phase will be to determine the interface water molecule orientation distribution as a function of solution pH and type of (hkl) surface. We are currently preparing perfect mineral crystal surfaces for extensive studies of quartz, corundum and hematite interface water. Simulation of SFG spectra is beginning through a collaboration with James Rustad at PNNL.



Fourier Transforms of the GIXAFS taken on the Fe edge for Cape Cod aquifer samples aged 8 months. First peak is Fe-O distance with constant coordination number of 6. Second peak is Fe-Fe distance with components at ca. 2.6 and 3.0 Å (uncorrected for phase shifts). These second peaks show changing numbers of edge- and corner-sharing Fe polyhedra as a function of Mn and Ca composition. High Mn is associated with poorly crystalline Fe oxyhydroxide, while high Ca is associated with highly crystalline Fe oxyhydroxide.

Development of Isotope Techniques for Reservoir and Aquifer Characterization

B. Mack Kennedy, (510) 486-6451, fax (510) 486-5496, bmkennedy@lbl.gov

Website: <http://www-esd.lbl.gov/CIG/noblegas/noblegas.shtml>

Objectives: Based on results from prior studies, isotopic characterization of fluids associated with hydrocarbons and groundwater aquifers are useful for mapping regional fluid migration and preferred flow paths, identifying fluid sources, and estimating fluid flow rates. However, the potential utility of isotope techniques to identify reservoir flow units, compartments, and fluid loss to overlying strata has not been extensively exploited.

Project Description: Efficient and safe sequestration of large quantities of CO₂ will require reliable characterization of potential storage formations, reservoirs and aquifers. Many oil and gas reservoirs are complexly partitioned by differing structural, petrologic and stratigraphic controls that will inhibit efficient CO₂ injection and limit reservoir potential. In groundwater aquifers, long term storage requires effective traps with minimal leakage to overlying strata. To maximize CO₂ sequestration efficiency, it will be necessary to address these and similar issues related to reservoir and aquifer characterization. We believe this can be accomplished by merging geophysical techniques, which provide structural and imaging information, with isotope and tracer techniques, that can identify fluid sources and flow paths, zones of fluid mixing, and isolated fluid compartments, and 2-D fluid flow models that can set limits on fluid transit times and leakage rates.

Results: During FY2000, we joined a pilot field scale test of a CO₂ injection in the Lost Hills oil and gas field in the San Joaquin Basin, California. The test consists of three parallel projects: seismic and electrical imaging, co-injection of chemical and isotopic tracers, and chemical and isotopic analyses of production fluids before, during and after CO₂ injection. As samples become available they will be analyzed for bulk gas chemistry, noble gas abundance and isotopic compositions, and the isotopic compositions of carbon in CO₂ and CH₄.

Air-Derived Noble Gases in Sediments: Implications For Basin Scale Hydrogeology.

B. Mack Kennedy, (510) 486-6451, fax (510) 486-5496, bmkennedy@lbl.gov ; T. Torgersen University of Connecticut, (860) 405-9094, fax (860) 405-9153, Thomas.Torgersen@Uconn.edu

Website: <http://www-esd.lbl.gov/CIG/noblegas/noblegas.shtml>

Objectives: This research project (with the University of Connecticut) evaluates the processes which produce, dissolve and distribute noble gases and noble gas isotopes among liquid hydrocarbon, gaseous hydrocarbon and aqueous phases. This redirected project will: (1) identify and isolate carrier phases of the various air-derived noble gas components in

sedimentary rocks, (2) investigate processes responsible for acquisition and trapping of the components in their sedimentary carrier phases, and (3) evaluate mechanisms that release these noble gas components.

Project Description: The mechanisms, processes and time scales of fluid flow in sedimentary basins represents a fundamental question in the Earth Sciences with direct application to exploration and exploitation strategies for energy and mineral resources. An explanation is needed for the mechanism by which Ne and/or Xe can be enriched on earth materials relative to the other noble gases, how these enrichments can be retained on a geologic time scale, and what processes release these components to the hydrologic system in which they are observed. This project will investigate (i) young sediment recovered in DSDP/ODP drill holes, (ii) outcrop samples from the Monterey formation (<20Myr), and (iii) drill core from the Elk Hills field as well as specific samples of opportunity. Samples will be characterized with respect to composition and geochemistry and a suite of chemically defined fractions will be used to investigate the fractions holding sorbed noble gas components. We will also investigate DSDP/ODP samples from various environments that have different initial compositions and have undergone different diagenesis patterns.

Results: This is a new direction for this project. Measurements of noble gas abundances in hydrocarbon fluids, conducted under the previous grant, provide ample evidence that naturally occurring fluids within the Earth's crust contain at least three distinct 'air-derived' noble gas components: (1) water saturated with air (i.e. groundwater), (2) a heavy (Kr, Xe) noble gas enriched component believed to be associated with the hydrocarbon source rock (Torgersen and Kennedy, 1999) and (3) a Ne-enriched component (Kennedy et al, 2002). Identifying the source of components #2 and #3 and understanding the where, when, and how these components are added to the hydrologic system will provide important constraints to basin scale hydrogeology, such as fluid source, flow path, and re-charge temperature. Because the enrichment patterns appear to be smooth functions of noble gas mass, adsorption on solids is often invoked as a potential source of the enrichment patterns. However, thermodynamics predicts preferential adsorption of heavy noble gases relative to the light noble gases, yet Podosek et al. (1980) found that approximately half the samples of sedimentary rocks analyzed for noble gases contained a Ne-enriched component and in many cases, simultaneous Xe and Ne enrichments were found. A literature review suggests that the enriched components are associated with a host rock type or specific carrier phases. For instance, Xe-enrichments are strongly correlated with carbon-rich phases isolated from shales (e.g. Frick and Chang, 1977). It is clear that an explanation is needed for the mechanism by which Ne and/or Xe can be enriched on earth materials relative to the other noble gases, how these enrichments can be retained on a geologic time scale, and what processes eventually release these components to the hydrologic system in which they are observed. One possibility for explaining the Ne and Xe enrichments is the labyrinth-with-constrictions model proposed by Wacker et al., (1985), which will be used as a guide for this project. This model has the advantage that it can explain the very large noble gas enrichment factors observed in natural samples [$F(\text{Ng}) = 500-10,000$], simultaneous enrichment of Ne and Xe, as well as the rapid transition from physisorption to chemisorption apparently needed to explain long term retention. Establishing the lifetime for adsorption under physisorption kinetics and desorption under chemisorption kinetics through a study of noble gas 'trapping' via labyrinth-with-constrictions may provide specific insight into nano-technologies.

Reactive Chemical Transport in Structured Porous Media: X-ray Microprobe and Micro-XANES Studies

T.K. Tokunaga, (510) 486-7176, fax (510) 486-7797, tktokunaga@lbl.gov

Objectives: In subsurface reactive transport, large differences in chemical composition can be sustained in boundary regions such as sediment-water interfaces, interior regions of soil aggregates, and surfaces of fractured rocks. Studies of reactive transport in such boundary zones require information on chemical speciation with appropriate spatial and temporal resolution.

Project Description: Predicting transport of trace elements between various environmental compartments is currently often unsuccessful, partly due to lack of relevant information at compartment boundaries. Batch studies can yield insights into kinetics and equilibrium in well-mixed systems, but much of the subsurface is very poorly mixed. Without in-situ, spatially- and temporally-resolved chemical information, transport between compartments can only be described with system-specific, nonmechanistic, mass transfer models. In this project, the synchrotron x-ray microprobe and micro-XANES techniques are used to obtain such measurements in a variety of critical microenvironments. Past efforts in this project focused on selenium transport and reduction in two types of microenvironments, that found at surface water-sediment boundaries, and that found within soil aggregates. In FY 1998, the project emphasis shifted to consider reactive transport of Cr included flow-through experiments in columns of aggregated soils, including spatially-resolved, real-time tracking of initial contamination processes within soil aggregates, and later characterization of Cr redistribution upon long-term drying. The complexity of reactive transport in such systems with macropore flow and intraaggregate diffusion-redox motivated simpler FY 1999-2001 studies focused only on the latter processes.

Results: The FY 2001 studies focused on Cr(VI) diffusion and reduction to Cr(III) within synthetic and natural soil aggregates. Experiments were conducted on Altamont clay soil. The alkalinity of this soil minimized the extent of Cr(VI) sorption on mineral surfaces. A range of initial redox conditions was established within aggregates by infusing solutions containing different concentrations of organic carbon (0 to 800 ppm, as tryptic soy broth) and incubation until steady redox profiles were established. Cr(VI) was then diffused into aggregates at initial concentrations up to 10,000 ppm. Micro-XANES mapping was done at beamline X26A, National Synchrotron Light Source. Micro-XANES mapping of Cr in aggregates showed (1) deeper Cr diffusion in systems with lower organic carbon and higher Cr concentrations, (2) reduction of Cr(VI) to Cr(III) during transport, and (3) very sharp termination of Cr fronts in more reducing aggregates. The latter phenomenon results from rapidly increasing reduction rates over very short distances (< 10 mm). These results show that contaminated and uncontaminated zones within soils can coexist in very close (mm) proximity, such that bulk average chemical speciation can not meaningfully describe these systems. The small fractions of unreduced Cr(VI) remaining in these soils reside along oxic, exterior surfaces. The persistence of Cr(VI) along exterior surfaces of aggregates is significant since this more soluble and toxic form resides along faster transport paths, i.e., along macropore channels. The full range of diffusion-reduction behavior displayed in systems with different initial organic carbon and different levels

of Cr is well represented through Thiele analyses of diffusion and reaction rates. The latter rates are obtained through long-term studies of Cr reduction and through fitting measured Cr profiles to a diffusion-reduction model.

LAWRENCE LIVERMORE NATIONAL LABORATORY

University of California
Livermore, California 94550

CONTRACT: W-6405-ENG-48

CATEGORY: Geophysics

PERSON IN CHARGE: F. J. Ryerson

Water distribution in partially saturated porous materials

J. J. Roberts, (925) 422-7108, fax (925) 423-1057, roberts17@llnl.gov

Objective: To determine the electrical properties of water and CO₂ saturated and partially-saturated porous materials at a variety of experimental conditions and to utilize the experimentally determined electrical properties to investigate the relationships between electrical transport and other transport properties. These results are used to invert field EM measurements for fluid content and to develop better methods of remotely tracking subsurface injectate and detect permeable fractures.

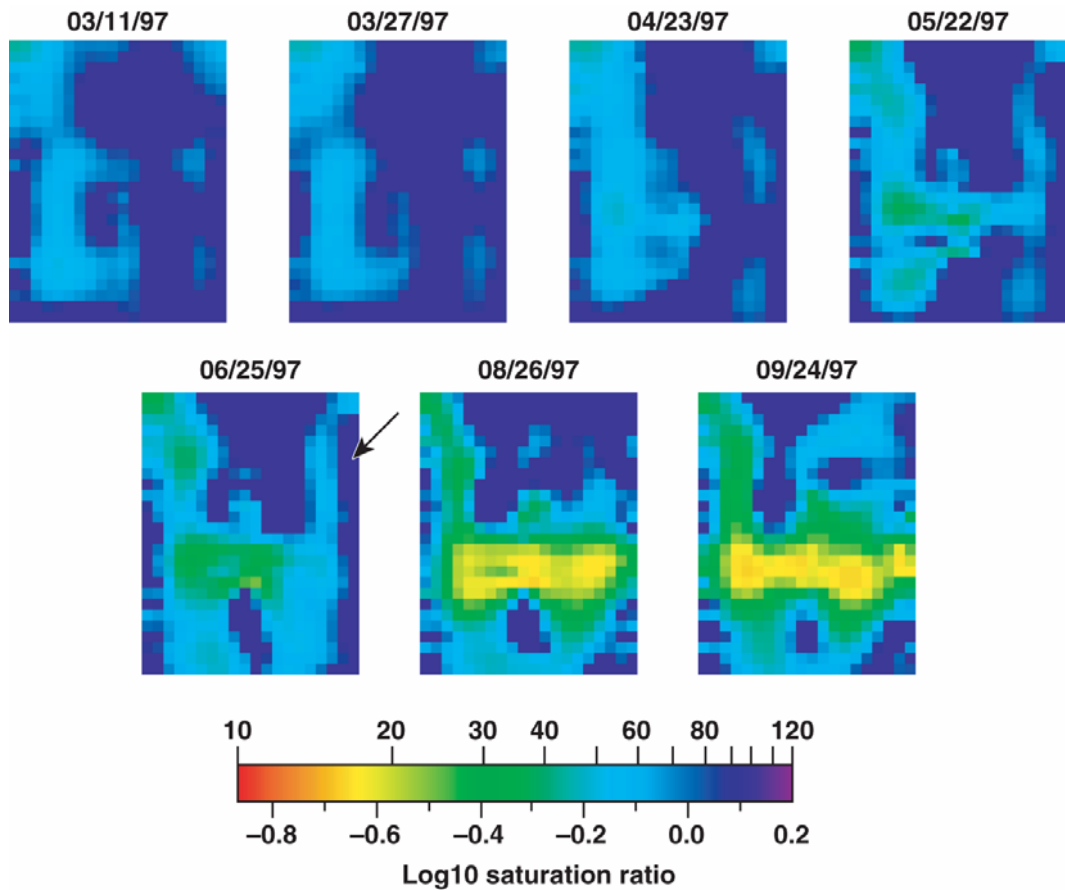
Project Description: This experimental is study designed to measure the frequency dependent electrical properties of porous materials and relate the results to other transport properties. Measurements include dielectric constant and electrical resistivity as functions of saturation, temperature and microstructural properties and include monitoring the resistivity of materials as they become fluid-, steam-, and CO₂-saturated. The complex impedance is measured because impedance spectra provide information regarding the number and arrangement of conduction mechanisms, distribution of liquid phase, and microstructural properties. These measurements are of particular importance because field electrical measurements in unsaturated regions (including electrical resistance tomography, electromagnetic depth sounding, and induced polarization) depend on reliable laboratory measurements for accurate interpretation. A number of geophysical problems including remediation, enhanced oil recovery, geothermal reservoir evaluation and site monitoring depend on reliable information regarding the interconnectedness and distribution of the fluid phase.

Results: Measurements of electrical properties during CO₂ injection were performed using the modified apparatus and are now routine. Laboratory impedance measurements were performed on sandstones and a number of samples from sites of geologic interest including siltstones from the Lost Hills, CA EOR site, tuff from Awibengkok, Indonesia geothermal field, and welded tuff from the Fran Ridge, NV Large Block Test site.

Results on samples from the Lost Hills EOR site indicate that there are discernable differences in the resistivities of samples containing brine, oil and CO₂. Although the contrast between oil and

CO₂ saturated samples is small, there is evidence that dielectric properties might best discriminate between the two pore fluids. The results have been used by the Fossil Energy Program to better understand their crosswell EM field data during a CO₂ injection project.

A second key result was the measurement of electrical properties of welded tuff as a function of saturation and temperature up to 145°C on both intact and fractured samples. A model was constructed that predicts saturation as a function of resistivity and temperature and was used to invert electrical resistance tomography data taken at the LBT. The resulting saturation maps (below) show significant improvement over previous inversion attempts as verified using neutron logging results. An additional result is the ability to locate active fractures using time-dependent electrical measurements. This is of direct benefit to the Geothermal Energy Program.



ERT images of saturation in the LBT as a function of elapsed time (indicated above each image) based on laboratory measurements of tuff resistivity. Scale shows absolute water content and saturation ratio (assuming a starting saturation of 75%). Heater horizon is about 1/3 from the bottom of the images and is the region displaying the most dryout. Arrow on 06/25/97 image indicates a drying fracture that rewet by 08/26/97. Review of geomechanical data shows movement in that region of the block prior to the redistribution of water.

Three-dimensional analysis of seismic signatures and characterizations of fluids and fractures in anisotropic formations

P.A. Berge, (925) 423-4829, fax (925) 423-1057, berge@llnl.gov; J. G. Berryman (925) 423-2905, fax (925) 422-1002, berryman1@llnl.gov

Objectives: Our major objective is to obtain constraints on lithology in fluid-filled anisotropic rocks by using rock physics theories for anisotropic and poroelastic media. We are collaborating with investigators on related OBES projects at the Colorado School of Mines and Stanford University, who are developing techniques for obtaining anisotropy parameters from seismic reflection data (CSM) and relating laboratory measurement information to modeling and field data (Stanford). By using our theoretical methods to model the anisotropy parameters recovered from seismic data, we can find ways to improve analysis of seismic reflection data collected in areas where the geology is complicated by anisotropy and heterogeneity.

Project Description: CSM collaborators are generalizing anisotropic velocity analysis techniques to account properly for vertical inhomogeneity and dipping structure, so that the technique will be applicable to a wide range of exploration problems. The LLNL/Stanford group is working on developing and analyzing rock physics models that describe transversely isotropic media, particularly to determine how these models may constrain lithology. Stanford is focusing more on laboratory measurements and anisotropic signatures of fractured rocks, and LLNL is focusing on fluid effects and poroelasticity in anisotropic rocks. Topics of research include determining what constraints on lithology can be found from the anisotropy and poroelasticity parameters and what information is sufficient and necessary for the constraints. The overlying questions are how to do lithologic interpretation of the anisotropic parameters obtained from field data, and the possibility of incorporating shear-wave data into the velocity analysis and lithology interpretation.

Results: LLNL researchers have developed a new method for using P and S velocities to obtain information about rock saturation and tested it using laboratory data that provided velocities at known saturation conditions. This work is in press in Geophysics and was presented at the 2001 annual Fall meeting of the American Geophysical Union (AGU) and the 2002 annual meeting of the Environmental and Engineering Geophysical Society. It also produced a patent. LLNL researchers also showed how rock physics methods can be used to interpret seismic data from the Geysers geothermal field, a region where fluids and fractures control the velocities and seismic anisotropy has been observed in earthquake traveltimes. Results relating seismic velocities to fracture concentration and distribution were presented at the 2001 annual meeting of the Seismological Society of America and the Geothermal Resource Council meeting, as well as the 2001 AGU meeting. LLNL researchers also showed how effective medium theories can explain discrepancies between measured shear modulus behavior and Gassmann's equations. These results were published in Physical Review E in 2001. Current research focuses on developing better rock physics methods for estimating seismic properties of anisotropic poroelastic rocks. An abstract with preliminary results was submitted to the 2002 Biot Conference on Poromechanics.

Physical Properties of Heterogeneous Rocks Containing Fluids

J. G. Berryman, (925) 423-2905, fax (925) 423-6907, berryman1@llnl.gov

Objectives: Our main objective is to understand significant factors affecting physical properties of heterogeneous rocks in order (1) to improve our ability to predict rock behavior from knowledge of rock components and pore fluids and (2) to improve our ability to interpret geophysical field data. One new tool developed to accomplish this objective is the discovery by the PI of exact results in poroelasticity and thermoelasticity for two component composite rocks and the application of these ideas to effective medium theories for poroelastic composites. This project exploits these as well as other new results, with the expectation that new insight into the elasticity and poroelasticity of rocks will result. Such insight has proven to be important for understanding partial melt in both the upper and lower mantle, for clarifying earthquake source mechanisms, for interpreting seismic reflection survey data for oil and gas exploration, for oil field engineering practices related to drilling and pumping, and for related issues in environmental cleanup of DOE sites. This type of information is important for interpretation of both seismic and electrical geophysical field data, and is useful to both oil reservoir engineers and hazard cleanup activities.

Project Description: Four major approaches are being considered in this project: (1) partial saturation data analysis showing that the Lamé' lambda parameter is most important for analyzing liquid content of rocks and that shear modulus predictions for higher frequency data needs to incorporate changes caused by liquid content, (2) continuing development and use of a generalization of Eshelby's formula from elasticity theory for poroelastic and thermoelastic composite inclusions analysis problems, (3) double-porosity/dual-permeability methods for fractured reservoirs, and (4) applications of rigorous viscoelastic bounds to rock/fluid mixtures. These types of results are all of interest in the oil and gas industry. The same basic framework can also be employed to treat reservoir characterization problems, especially regarding the effects of changing stress on matrix and fracture permeability in double-porosity models used for reservoir pumpdown studies. In addition to single-fluid reservoir analysis, related ideas have been applied to partial saturation problems, in which both gas and oil, or gas and water may be present and distributed throughout the reservoir volume in a complicated, inhomogeneous manner. Related ideas (Gassmann's fluid-substitution formulas) can play a very significant role in interpretation of seismic AVO (amplitude versus offset) data used as direct hydrocarbon indicators.

Results: One exciting area of the work in the last two years has been analysis of partial and patchy saturation of rocks. This work had built on previously funded BES work in anisotropy, wherein it was determined that the most important variable determining Thomsen's parameters in anisotropy analysis is (somewhat surprisingly) the Lamé' elasticity parameter known as lambda. For rocks containing fluids, we have shown theoretically, and by extensive studies of published laboratory data, that this is also the parameter that depends most sensitively on the pore fluid's physical properties. Thus, plots of seismic velocity (both compressional and shear are required) emphasizing changes in lambda have the power not only to determine the magnitude of the liquid saturation present, but also (and this was also a big surprise to all of us)

to distinguish homogeneous from inhomogeneous (patchy) saturation. One paper on this topic was published last year in *Journal of the Acoustical Society of America* and another will appear in the March-April, 2002, issue of *Geophysics*. Our most recent work in this area shows that seismic impedance (density times velocity) data that are typically obtained in seismic reflection surveys for oil exploration can also be used to accomplish the same results, as can well-log data when both compressional and shear velocities are measured. This fact has significant implications for improvements to seismic AVO and bright spot analysis. Gas-saturated zone are especially easy to detect this way. In collaboration with researchers at the University of Wisconsin, we had previously developed methods to determine and in some cases drastically reduce the number of elastic coefficients required to describe the behavior of a double-porosity system in the presence of changing pore pressure for applications to reservoir pumpdown. An extension of this work in collaboration with Steven Pride (from France, on sabbatical at Stanford last year) has been accepted for publication by the *Journal of Geophysical Research*. Other related work was published previously in *International Journal of Rock Mechanics* describing methods to study elastic wave propagation through such media. The resulting equations permit the parameters determining wave speed and attenuation to be decoupled, thus opening up the possibility of theoretical explanations for data that could not be explained before by Biot's simpler theory. Extensions of this work continue through studies of methods to estimate coefficients in these equations that can be computed from a knowledge of the constituents and their physical properties. Work with Pride is almost completed at this writing and will be submitted to the *Journal of the Acoustical Society of America* this Spring. New uses of the differential effective medium theory have been made this year, again in collaboration with Pride and Wang, to understand how the presence of pore fluids affects the shear modulus during higher frequency wave propagation experiments. Some related work with Wang was published in *Physical Review E* last summer. Especially with respect to the double-porosity studies, a number of surprising results have been obtained, including some new exact results for multicomponent poroelastic systems that had not been previously anticipated.

Geophysical monitoring of carbon dioxide sequestration using electrical resistance tomography (ERT)

R.L. Newmark, (925) 423-3644, fax (925) 422-3925, newmark@llnl.gov; A.L. Ramirez, 925-42-6909, fax (925) 422-3925, ramirez3@llnl.gov; W. D. Daily (925) 422-8623, fax (925) 422-2495, daily1@llnl.gov

Objectives: the objective of this project is to evaluate the applicability of high resolution electrical imaging techniques to monitor CO₂ injection and migration, and to evaluate their potential for detecting leaks or leak pathways.

Project Description: Numerical simulations and bench-scale modeling are being used to investigate the range of conditions and configurations under which electrical resistance tomography (ERT) methods may be used to monitor the geophysical changes resulting from CO₂

injection and migration. The results of these studies will be directed toward the design of a field survey. The primary activities and goals of the research will be to:

1. Investigate the sensitivity of high-resolution electrical imaging methods to key geophysical and chemical parameters pertinent to CO₂ injection scenarios.
2. Determine the operational issues pertinent to process control and performance assessment.
3. Determine the sensitivity of high-resolution electrical imaging methods to different measurement configurations, reflecting operational field survey design constraints.
4. Design and conduct a field survey to demonstrate the applicability of high-resolution electrical imaging methods to monitor CO₂ injection and migration, and to evaluate their potential for detecting leaks or leak pathways.

Results: This year's effort focused on benchmarking the numerical simulations with experiments conducted with physical models. We used laboratory physical scale models to control experimental conditions including the electrical conductivity of the background formation, the position and size of target anomalies, the electrical contrasts between target and background and the electrode configuration, including the use of vertical well casings as long electrodes. The physical model provides data with realistic data errors, which are not present in computer simulation data (even when synthetic but unrealistic errors are included in the analysis). The strategy is to compare the known physical models with the reconstructed images and from this comparison evaluate the strengths and weaknesses of ERT under different conditions. These measurements form a link between numerical simulations and field surveys.

Using either point electrode arrays or long electrodes, both conductive and resistive targets can be imaged using ERT. Targets with high electrical contrast with the background have the poorest match, especially highly conductive anomalies. Anomalies are typically of larger size and lower contrast than the actual targets. Images of targets with lower electrical contrast show better spatial reconstruction. This result is consistent with the properties of the reconstruction algorithm, which searches for the numerical model of smoothly varying electrical conductivity. By comparing experimental and numerical results of point and long electrode surveys, we have identified previously undiscovered factors effecting ERT image fidelity. These include sensitivities to the symmetry of the measurement schedule, automated weighting of individual data, and the possible effect of induced polarization for certain materials used in the physical models. These results increase our confidence in our ability to predict ERT performance under realistic field conditions. We are applying this understanding to the design of field surveys.

Application of Geophysical Tomographic Imagery to the Development of Subsurface Flow and Transport Models

C.R. Carrigan, (925) 422-3941, fax (925) 423-1997, carrigan1@llnl.gov; Jon Newell RPI, (518) 276-6433, newelj@rpi.edu

Objective: To address two fundamental subsurface flow imaging problems during the tenure of this research. One problem has to do with exploring the important capability to soft condition a numerical model of subsurface flow and transport using electric resistance and impedance tomography (ERT and EIT) observations of a groundwater infiltration event. The anticipated result is the ability to develop a 3-D realization of infiltration exhibiting a behavior that is in good agreement with parameters measured during a field experiment. The other problem has to do with improving our understanding of how EIT and particularly the electrical phase component of imaging can help elucidate subsurface flow processes.

Project Description: This proposed research has the goal of utilizing subsurface electrical imaging not just as a means to characterize the soil structure by mapping different soil types at a site but also as a way of obtaining quantitative information about how a site will respond hydrologically to an infiltration event. To do this, we will utilize new data and model integration methodologies in conjunction with benchscale experiments to validate the integration methods. We will also investigate what can be learned about porous flow and transport using two important electrical imaging methods -- electric resistance tomography (ERT) and electric impedance tomography (EIT). The proposed work combines laboratory imaging experiments, computer simulations and a highly instrumented field site, called the Vadose Zone Observatory (VZO) that are all virtually developed. To carry out the bench scale laboratory experiments, we will collaborate with research faculty and students at Rensselaer Polytechnic Institute (RPI), a member institution of the NSF Center for Subsurface Sensing and Imaging Systems (CenSSIS). The investigators at LLNL will carry out all computer intensive modeling and data integration activities required for conditioning infiltration simulations involving the synthesized, bench scale experimental and field-site environments to be considered and the VZO will provide imaging data sets for producing a testable hydrologic characterization of a well-characterized field environment in the later part of this three-year project.

Results: The project was initiated only at the end of calendar year 2001 and the RPI collaborators (Professor Jon Newell and students) only received their first year's funding in 2002. The first year's proposed work is in progress and on schedule. At LLNL this includes considering the soft conditioning of model realizations of heterogeneous porous media using ERT data from the VZO. At RPI, Professor Newell and student have designed and are constructing a laboratory bench scale infiltration experiment that will be monitored using both ERT and EIT imaging techniques that were developed for biomedical imaging.

CATEGORY: Geochemistry

PERSON IN CHARGE: **F. J. Ryerson**

Reactive Transport of CO₂-Rich Fluids and Precipitation and Dissolution in Rock Fractures

W. B. Durham, (925) 422-7046, fax (925) 423-1057, durham1@llnl.gov; W. L. Bourcier; E. A. Burton

Objective: The objective of this research is to measure local rates of dissolution and precipitation on the walls of individual fractures and the presence of CO₂-rich fluids and correlate differences in reaction rates to changes local fracture aperture. Much use will be made of high-resolution physical topography measurement and numerical simulation of reactive flow.

Project Description: The project entails refurbishing a hot-reactive-flow pressure vessel used in earlier years in this laboratory and applying it to the reactive flow problem. We will build on past successes using a similar experimental strategy, with the main difference being the high concentration of CO₂ in the reactive fluid, a condition that requires the use of elevated temperature and pressure. The experiments and simulations will be done on rock samples containing a single laboratory-made or natural fracture. Detailed imaging of the fracture aperture before and after alteration will be coordinated with measurements of fracture deformation, permeability, dispersivity, and effluent composition, all as functions of pressure, temperature, temperature gradient, time, rock composition, fluid velocity, and fluid composition. For the most part we will work with simple but relevant systems in order to maximize our understanding and impact: samples will be monomineralic rocks with low porosity and low bulk permeability (such as quartzites and marbles), under fully saturated, single-phase flow conditions. We will attempt measurements in undersaturated, dual-porosity, and more chemically complex settings as success dictates.

Results: Flow simulations were redone in a fundamentally different manner, and now show flow patterns with more precision. The new simulations have the additional advantage that transport of dissolved minerals and surface reaction can be included, and that work is in progress. Along with reactive flow experiments being carried out on Carrara marble, additional experiments are underway in analog KDP (potassium di-hydrogen phosphate) fractures. This material not only reacts at convenient rates in the laboratory, but it is sufficiently transparent that imaging of the fracture is possible during the fluid flow experiment. This allows direct measurement of fracture apertures during reactive flow experiments using light transmission techniques.

Determining the physical controls on biomineralization

Jim De Yoreo, (925) 423-4240, fax (925) 422-6892, deyoreo1@llnl.gov ; Patricia Dove (540) 231-2444, fax (540) 231-3386, dove@vt.edu

Objectives: The objective of this project is to test the hypothesis that the precise control over crystallization exerted by living organisms during biomineralization is due to modifications of kinetic and energetic parameters caused by site-specific interactions between functional groups on proteins and peptides and crystal surfaces.

Project description: In order to obtain a microscopic understanding of the reaction mechanisms and physical controls on calcite and brushite formation, we are using atomic force microscopy (AFM) to investigate the effect of growth modifiers on nucleation, step dynamics, and surface morphology. These modifiers include Mg and Sr, amino acids, and peptides. By measuring the dependence of critical step length on supersaturation, we are determining the step edge free energy, which controls the equilibrium surface morphology. From the dependence of step speed on concentration we are extracting the equilibrium solubility and the kinetic coefficient for step motion. The latter provides a measure of the activation barrier to step motion. The changes in these parameters caused by the additives provide an understanding of the mechanism by which they alter growth. Finally, we are using patterned surfaces of self-assembled monolayers to investigate the controls of surface chemistry on nucleation.

Results: The addition of Mg impedes step propagation speed at the intersection of the two step types on calcite. This effect can be explained by taking into account the strain caused by differential incorporation of Mg, which creates a strain near the intersection that is large enough to produce a measurable decrease in effective supersaturation. Unlike Mg^{2+} , Sr^{2+} , which is a larger ion, acts to pin steps, creating a dead zone at low supersaturation where no growth occurs.

Because brushite exhibits extreme anisotropy in bonding, step speed, and step roughness, analysis of the step edge and terrace width fluctuations provides us with information about molecular controls on step dynamics. For example, from the temporal correlations of the step fluctuations, we have found that molecular motion along the steps occurs by detachment from the step, followed by diffusion and reattachment rather than by diffusion along the step.

Finally, using a micro-printing method to produce patterns of self-assembled monolayers (SAMs), we investigated the nucleation of calcite crystals on the COOH terminated alkane thiols. All crystals nucleated on the COOH regions at the (001) face of calcite. Furthermore, under certain conditions about half of the sites supported the nucleation of aragonite rather than calcite.

Mineral Dissolution and Precipitation Kinetics: A Combined Atomic-Scale and Macro-Scale Investigation

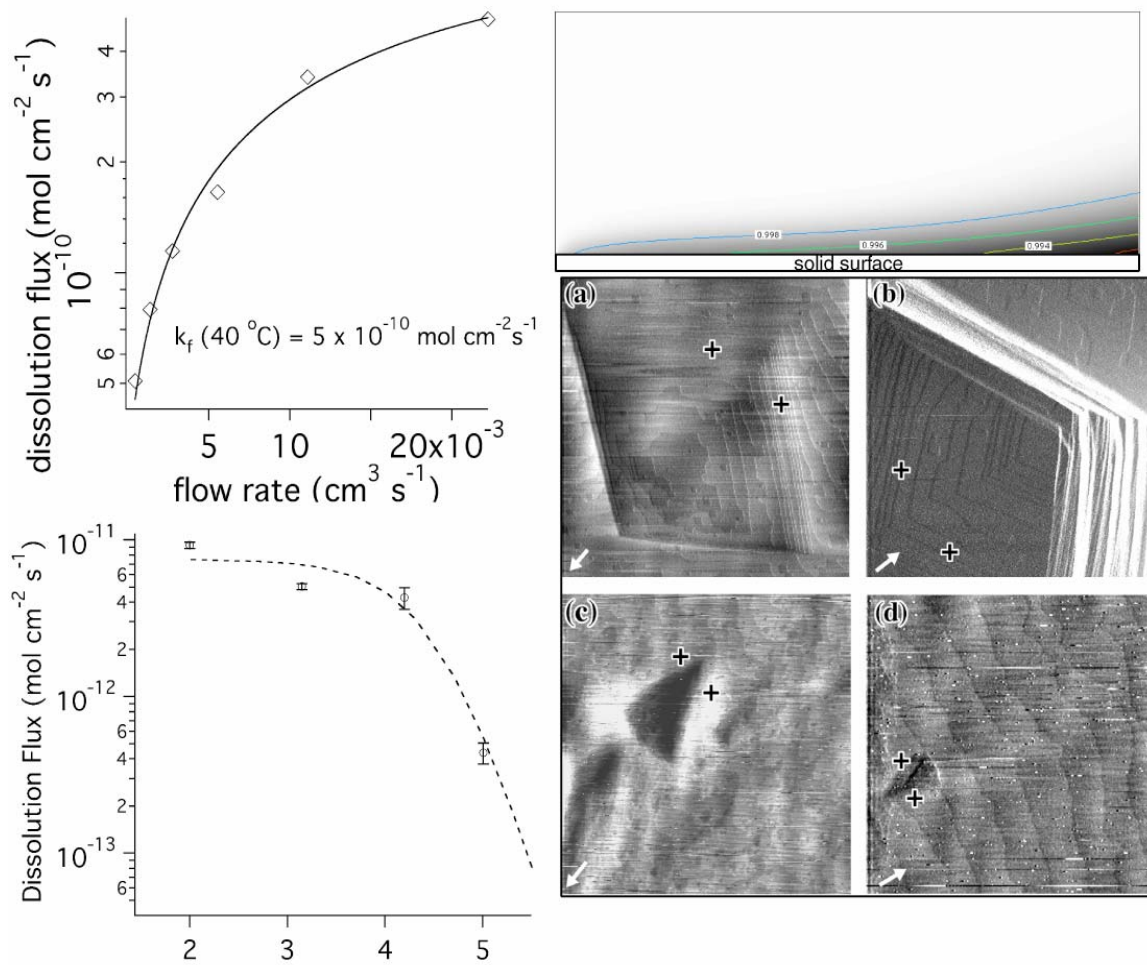
Kevin G. Knauss, (925) 422-1372, fax (925) 422-0208, knauss@llnl.gov; Carrick M. Eggleston (307) 766-6769, fax (307) 766-6679, carrick@uwyo.edu; Steven R. Higgins (307) 766-3318, fax (307) 766-6679, shiggins@uwyo.edu

Objectives: The primary objective for this research program is to develop an appropriate mechanistic understanding of carbonate mineral dissolution and growth through extensive experimentation at both microscopic and macroscopic length-scales.

Project Description: This project utilizes a combined atomic-scale and macro-scale study of mineral/fluid interaction that is designed to improve our understanding of, and ability to predict the course of, mineral dissolution and precipitation processes specifically affecting coupled silicate mineral dissolution and carbonate mineral growth expected as part of a CO₂ sequestration strategy of injection into deep aquifers. Our atomic-scale studies utilize a Hydrothermal Atomic Force Microscope (HAFM) for molecular-level experiments on the kinetics of nucleation, step motion and other phenomena on mineral surfaces under conditions relevant to CO₂-sequestration. The same conditions used in HAFM experiments will also be investigated with macroscopic hydrothermal reactors (for stoichiometric rate data) and geochemical reactive transport codes. This approach will allow us to address many still-open questions concerning the exact forms for rate laws near and far from equilibrium, the microscopic interpretation of these rate laws, the activation energies and formation energies for key microscopic surface structures (*e.g.*, steps, kinks), and the impact of specific aquifer solute catalysts and inhibitors on the dissolution and growth processes.

Results: During work on an enhanced HAFM, the importance of understanding solution composition *at the HAFM imaging location on the mineral surface* has come into stark focus. Much of the mineral dissolution and growth literature in the field of geochemistry tends to discount the importance of transport control on kinetics, but we have found that this cannot always be assumed. Here we will summarize our major findings utilizing the HAFM in experiments on carbonate dissolution under well-defined hydrodynamics.

We have studied the dissolution of magnesite and calcite (104) surfaces under a wide variety of conditions. Our main conclusions in the magnesite studies are that step density, rather than step velocity, is a strong function of pH near the surface and that the step orientation is sensitive to pH. In these studies, we definitively demonstrate that mass transport is only important at very low fluid velocities for magnesite, but that studies of calcite dissolution are generally in the mixed transport-kinetics controlled regime (even at high fluid velocities) where quantitative information can only be obtained by accounting for the transport components. We also have found that alkaline earth carbonate secondary precipitate formation on calcite surfaces significantly alters the net flux of Ca²⁺ and may passivate the CaCO₃ surface from further reaction.



Clockwise from upper left (1) Dissolution rate of calcite versus fluid flow rate in the HAFM at 40°C with an inlet $\text{pH} = 7$. The solid line is a theoretical model fit with one experimental parameter. (2) Two-dimensional concentration map ($1.0 \text{ mm} \times 0.4 \text{ mm}$) in the HAFM fluid cell calculated for magnesite dissolution with a flow rate of $1.4 \times 10^{-3} \text{ cm}^3 \text{ s}^{-1}$ at $\text{pH} = -\log[\text{H}^+] = 4.2$ at 60°C . The AFM tip scans the solid surface near the lower right corner of this map. Contours indicate the ratio of the spatially varying proton concentration to the inlet proton concentration, $[\text{H}^+]_{x,y}/[\text{H}^+]_{\text{inlet}}$. (3) HAFM images of magnesite during dissolution at 60°C with inlet $\text{pH} =$ (a) 5.0 (image size: $6.7 \mu\text{m} \times 6.7 \mu\text{m}$), (b) 4.2 (image size: $2.0 \mu\text{m} \times 2.0 \mu\text{m}$), (c) 3.2 (image size: $7.0 \mu\text{m} \times 7.0 \mu\text{m}$), (d) 2.0 (image size: $6.6 \mu\text{m} \times 6.6 \mu\text{m}$). Arrows indicate absolute sample orientation, showing rotational relationship among images. (4) Surface reaction limiting dissolution rate of magnesite as a function of pH at 60°C . The dashed line is a theoretical fit to a model based on proton adsorption as a pre-equilibrium step.

In-Situ CO₂-sequestration: Measurement of Coupled Silicate Dissolution and Carbonate Precipitation

Susan A. Carroll, (510) 423-5694, carroll6@llnl.gov; Kevin G. Knauss knauss1@llnl.gov

Objectives: The objective of this research is to measure dissolution and precipitation rates important to the mineralization of dissolved carbon at conditions relevant to CO₂ sequestration. Determination of mineral dissolution and precipitation kinetics is fundamental to the successful disposal of greenhouse CO₂-rich gases in aquifers, because reservoir storage capacity is directly related to the conversion rates of CO₂ to carbonate minerals. The reaction of CO₂ and water with unstable silicate minerals to produce more stable silicates (e.g. clays) and solid carbonates is the natural weathering process which is a dominant part of the long-term global geochemical cycling process. Our kinetic research will feed directly into promising reaction-transport codes that will evaluate aquifer storage of dissolved CO₂ and mineral carbonates, and resulting changes in porosity and permeability.

Project Description: Our approach is to conduct single and multi-mineral dissolution and precipitation experiments and reaction transport experiments in Ca-Al-Si-CO₂ and CaCO₃ systems as a function of pCO₂, pH and temperature. Supercritical CO₂ experiments simulate the reactive front of CO₂ plume and aquifer water and are designed to measure the available source of calcium for storage of CO₂ as carbonates and the source of aluminum and silica for the precipitation of secondary minerals that will effect aquifer porosity and permeability.

Results: We focussed our work in FY2001 on feldspar dissolution experiments as a function of temperature and dissolved aluminum concentrations needed to numerically describe the rate dependence on pH, dissolved Al, and temperature.

In our experiments we took advantage of retrograde solubility of aluminum hydroxides, such as gibbsite, at acid pH to study the effect of dissolved aluminum on feldspar dissolution. Our results show that dissolved aluminum inhibits labradorite dissolution until a secondary phase (gibbsite) precipitates from solution. This suggests that feldspar dissolution will be higher in waters saturated with secondary phases than in undersaturated waters. This is important because a large portion of the affected aquifer will have a temperature and/or pH, which promotes precipitation of secondary phases.

We calculate the activation energy from the temperature dependence of labradorite dissolution rates normalized to the silicon release at a constant flow rate (0.9 ml min⁻¹), because higher release rates of Na, Ca, and Al relative to silica were observed at 30 and 60°C. It is important that the temperature dependence be in terms of a constant flow rate at this point in our study, because labradorite dissolution appears is affected by aqueous aluminum, which changes as a function of flow rate. We calculate $E_a = 9.53$ (kcal mol⁻¹). This value is slightly lower than E_a ranging from 11.5 to 15.9 (kcal mol⁻¹) reported from other labradorite studies in acid solutions (pH 1-4, T 5-70°C)

In FY2002 we are once again taking advantage of the retrograde aluminum solubility to experimentally study coupled feldspar dissolution and gibbsite precipitation.

Testing Deep Saline Aquifers for Long-term CO₂ Leakage Using In-Situ Noble Gases

G.J. Nimz, (925) 423-2766, fax (925) 422-0208, nimz1@llnl.gov; G.B. Hudson, LLNL (925) 423-2947, hudson5@llnl.gov

Objectives: The intent of this project is to develop techniques based on noble gas isotopes for the purpose of testing deep saline aquifers for long-term leakage of gases. Such aquifers have been suggested as repositories for industry-derived CO₂ effectively sequestering this “greenhouse” gas rather than releasing it to the atmosphere. Some noble gas nuclides, notably ⁴He, ²¹Ne, ⁴⁰Ar, and ^{134,136}Xe, are produced in-situ in aquifers continuously over geologic time, and accumulate in measurable excess abundances. If CO₂ is capable of leaking as a gas either continuously or episodically, these noble gas nuclides would likely also be affected, and their full accumulation would not be observed.

Project Description: There are two primary methods by which the nuclides of interest to this project are produced in the subsurface, neutron nuclear reactions (²¹Ne, ⁴⁰Ar) and natural spontaneous fission of ²³⁸U (^{134,136}Xe). As a measure of the expected subsurface production of these gaseous species, two non-gaseous nuclides which are also produced by these two methods can also be measured (³⁶Cl produced by neutron reactions, ¹²⁹I produced by fission). In addition, a positive correlation might also be expected between ⁴He, produced during the radioactive decay of ²³⁸U and the fission-produced nuclides, providing another measure of expected subsurface production. The approach taken in this project is to measure the relative abundances of these nuclides in geologic materials and deep saline fluids to investigate the possible usefulness of the gaseous nuclides in testing deep aquifers for leakage.

Results: We have investigated our basic assumptions through the combined analysis of ³⁶Cl and ¹²⁹I in a variety of aquifer lithologies. Carbonate aquifers provide a very low U-Th environment, providing an endmember case. We analyzed a suite of Gulf Coast carbonate brines for ³⁶Cl/Cl which had previously been analyzed for ¹²⁹I/I (Moran et al, 1995). The suite produced ³⁶Cl/Cl = 5.2E-15 ± 2.1E-15. Assuming the aquifer Th/U ratio to be ~2, common for carbonates, the ³⁶Cl/Cl ratio implies [U] ≈ 1.35 and [Th] ≈ 2.70. This U concentration would produce a calculated ¹²⁹I/I ratio of 30E-14, assuming a spontaneous fission half-life of ~7E+15a and a fission yield of 0.04%, both within the range of published values. This calculated ¹²⁹I/I ratio compares well with the measured values of 27E-14 ± 6E-14, suggesting that the ³⁶Cl/Cl and ¹²⁹I/I ratios are accurately reflecting aquifer [U] and [Th]. Another endmember test was provided by saline waters from a young andesitic volcanic complex associated with geothermal activity. The mean age of the complex is several million years, old enough for ³⁶Cl to exhibit andesitic in-situ values, but sufficiently young that ¹²⁹I would still exhibit depleted mantle values. Average ³⁶Cl/Cl ≈ 6.5E-15, implying [U] ≈ 1, too high for depleted mantle. Average ¹²⁹I/I ≈ 5.7E-13, suitable for mantle [U]/[I] ≈ 2, at any [U]. This demonstrates a situation in which both ³⁶Cl and

^{129}I reflect isotopic equilibrium with aquifer rock, but only ^{36}Cl is able to reflect aquifer [U]. Other tests demonstrate the importance of considering interactions between deep saline waters and shallower meteoric waters. This is an important screening criterion for CO_2 sequestration, since such interaction must be avoided. A deep saline arkosic sandstone and mafic igneous aquifer complex in central Nevada produced uniform $^{36}\text{Cl}/\text{Cl}$ ratios of $50\text{E}-15 \pm 5\text{E}-15$. This implies $[\text{U}] \approx 7$, far too high based on published [U] for similar outcrop rocks in the region. Analysis of shallower regional waters suggests the measured $^{36}\text{Cl}/\text{Cl}$ represents mixing of meteoric and saline waters. Similarly, a non-carbonate saline aquifer system in central Iowa produced a range of $^{36}\text{Cl}/\text{Cl} \approx 5\text{E}-15$ to $450\text{E}-15$. In an attempt to understand these values from the perspective of recharge age, ^4He was measured and helium ages were calculated. The correlation again implies meteoric mixing. For those samples with very old ages and low $^{36}\text{Cl}/\text{Cl}$, $^{129}\text{I}/\text{I}$ values are being obtained. Low flux rates require $^{129}\text{I}/\text{I}$ sensitivity in the low 10^{-13} range. This is near the common background for ^{129}I by accelerator mass spectrometry ($\sim 10^{-14}$), and required a stabilization of our analytical abilities for ^{129}I . This was accomplished this year by an enhanced beamline and adjustments to an ESA analyzer. Repeatable backgrounds of $\sim 10^{-14}$ are now available for use in this project.

Collaborative Research: Studies for Surface Exposure Dating in Geomorphology

R. C. Finkel, (925) 422-2044, fax (925) 422-1002, finkell@llnl.gov; M. W. Caffee, K. Nishiizumi (510) 643-9361, fax (510) 643-1433, kuni@ssl.berkeley.edu, Lawrence Berkeley National Laboratory; W. E. Dietrich (510) 642-2633, bill@seismo.berkeley.edu; R. C. Reedy, Los Alamos National Laboratory

Objective: An experimental and theoretical program to fully develop the systematics of *in situ* produced cosmogenic nuclides in terrestrial surface samples and to apply their measurement to the dating of surface features and processes.

Project Description: Surface exposure dating utilizing cosmogenic nuclides is now acknowledged as a successful means with which to date many terrestrial surfaces. It is also recognized that there are many new applications for these techniques. Although the method rests on a firm physical and geochemical foundation, some of the parameters required for interpreting results are only poorly known. This project includes determination of precise production rates and production depth profiles, studies of altitude and latitude effects, intercalibration with other methods, and isolation of *in situ* produced nuclides from lithologies other than quartz. The effort will focus on chemical isolation of cosmogenic nuclides of geologic and artificially exposed samples, on implementation of surface exposure dating methods using new radionuclides such as *in situ* ^{14}C and pure spallation ^{36}Cl , measurements of proton and neutron cross sections and improvement of theoretical production rate calculations.

Results: We continue to work on development of a reliable method for determine *in situ* produced ^{14}C in geologic samples, especially quartz, by a step-wise heating technique to separate *in situ* produced ^{14}C from meteoric ^{14}C . The extraction line consists of three sub-systems: carrier and flow gas measurement and aliquotting, sample heating, and CO_2 purification. We have replaced the old 4:1 $\text{N}_2\text{-O}_2\text{-CO}_2$ carrier gas mixture with a new carrier gas mixture that consists of $\text{He-O}_2\text{-CO-CO}_2$. The total background in blank quartz that was collected from deep in the Homestake mine in South Dakota, is about $2\text{-}5 \times 10^5$ atoms/g of ^{14}C . We also measured ^{14}C in quartz samples collected at the Transantarctic Mountains in Antarctica. These are demonstrably saturated in ^{14}C activity, based on ^{10}Be and ^{26}Al concentrations. Our duplicate results indicate that we are recovering more than 95 % of the expected *in situ* produced ^{14}C in the quartz.

Although quartz is the best mineral for studies of cosmogenic nuclide surface exposure dating, quartz is rare in many geological settings. We are working on extending the range of geologic applications by developing a method for using olivine. We are developing a method for separating *in situ* produced ^{10}Be from meteoric ^{10}Be using stepwise leaching methods. In order to test our methods, we have measured ^{10}Be in recently erupted volcanic olivine from Hawaii (Kilauea) and Iceland, where we don't expect to find ^{10}Be from subduction. Surprisingly, olivine from both volcanoes contains an appreciable amount of ^{10}Be . This finding suggests that unexpected reaction between basaltic magma and hydrothermally altered oceanic crust may occur.

Experimental Investigation into the Role of Water During the Thermal Maturation of Sedimentary Organic Matter

Roald N. Leif, (925) 422-246, fax (925) 422-020, leif1@llnl.gov; Robert S. Maxwell (925) 423-499, maxwell7@llnl.gov

Objective: The primary objective for this research program is to identify the significant aqueous-organic chemical reactions important to understanding the role of water in petroleum formation.

Project Description: The generation of oil by the geological maturation of sedimentary organic matter is primarily a thermal process involving a complex mix of free-radical hydrocarbon cracking reactions. The presence of water has been shown to participate in the process of oil formation. The degree to which water is involved and the precise mechanisms by which this interaction occurs are still uncertain. This research project is focused on the following: (1) identifying the reaction pathways between water and organic matter, (2) evaluating the potential of water to act as a net source of hydrogen during the thermal maturation of sedimentary organic matter, and (3) determining the effects of solution composition, organic matter type and mineral components.

The experiments are performed in Dickson-type flexible gold bag rocking autoclaves. Both NMR and GC-MS analyses are used to obtain information about the bulk properties of the

mixtures and detailed information of individual components in the reacted solutions. This work is aided by the use of isotopic labeling to provide insight to help establish reaction mechanisms under varied experimental conditions.

Results: Recent experiments have shown how hydrogen from water is incorporated into saturated alkanes via alkene isomerization of transient olefins, one of the primary products resulting from free-radical β -scission reactions. Hydration of double bonds occurs readily, although this is a thermodynamically unfavored reaction. As expected, the steady-state concentration of these hydroxylated species (e.g. alcohols) is very low but they can react further by acting as reducing agents, donating hydrogen to result in the formation of ketones. This oxidative pathway can continue to produce organic acids and ultimately carbon dioxide. This is one of the reaction pathways that produces the elevated levels of carbon dioxide in hydrous pyrolysis experiments. We are currently learning more about the reductive branch of the hydrolytic disproportionation of alkanes, specifically the ultimate fate of hydrogen during this process. The production of hydrogen gas under these conditions is essentially a dead-end by-product, an unreactive reservoir of the hydrogen, but some of the reducing potential goes back into the hydrocarbon pool by a reaction pathway opened up through the presence of water. The presence of water appears to inhibit the formation of the high molecular weight polycondensed aromatic hydrocarbons. There is a strong driving force to form aromatic hydrocarbons, but hydrogen, donated from the alcohols, can react with "coke-precursor" molecules, thereby interfering with the oxidative, coke-forming pathway to result in the observed decrease in high molecular weight polycyclic aromatic hydrocarbons, shifting the distribution towards more alkylated polycyclic aromatic hydrocarbons. In essence, water decreases the "reaction severity" as compared to parallel experiments with no water present.

Isotope Fractionation by Diffusion in Liquids

Ian D. Hutcheon, (925) 422-4481, fax (925) 422-3160, hutcheon1@llnl.gov; Ross W. Williams (925) 423-8769, fax (925) 422-3160, williams141@llnl.gov; Frank M. Richter (773) 702-8118, fax (773) 915-9505, richter@geosci.uchicago.edu; John N. Christensen (510) 486-6735, fax (510) 486-5496, jnchristensen@lbl.gov

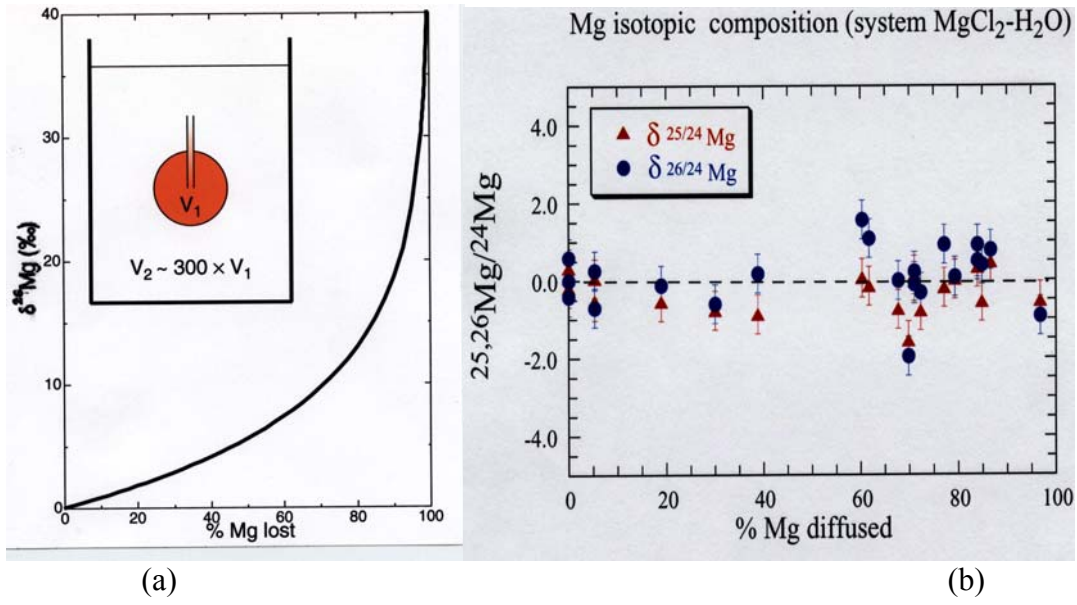
Objectives: The overall objective of this research effort is to document and quantify kinetic isotope fractionations during chemical diffusion in liquids ranging from silicate melts to water.

Project Description: The Lawrence Livermore National Laboratory part of this project involves measuring isotope fractionation of dissolved species by diffusion in water. The design of the diffusion experiment is shown in part (a) of the Figure below. A small spherical chamber filled with a salt solution (e.g., 1 N MgCl_2) is connected to a much larger water filled reservoir by a small cylindrical tube with an inner diameter of about 1 mm. The time over which the concentration evolves is long compared to how long it takes for diffusion to maintain a uniform concentration in the small chamber and because of the large volume ratio, the concentration of

salt in the larger reservoir is negligible. Under these conditions, the concentration in the small chamber will decay exponentially with a decay rate proportional to the diffusivity of the dissolved salt in water. If species of different isotopic composition have slightly different diffusivity, the system will be a Rayleigh fractionator and the residue of salt in the small chamber will become progressively enriched in the more slowly diffusing species, presumably those containing the heavier isotopes. The isotopic enrichment of a fraction F is given by $C_2/C_1 = F^{1-\alpha}$, with $\alpha = D_1/D_2$, where D_1 and D_2 are the diffusivities of species C_1 and C_2 .

Results: We have measured the fractionation of Mg isotopes during the diffusion of MgCl_2 in water in experiments ranging from one day to four months. The Mg concentration was measured by atomic absorption and confirmed the exponential decay due to diffusion of the Mg concentration in the small chamber. The Mg isotope composition was measured using a multi-collector ICP-MS (a Micromass IsoProbe). The ion beams of ^{24}Mg , ^{25}Mg and ^{26}Mg were measured simultaneously on Faraday cup detectors and corrected for instrumental mass-dependent fractionation, i.e., mass bias, using empirical factors derived from standard analyses.

Figure b shows that there was no detectable fractionation of Mg isotopes even when more than 95% of the initial Mg in the small chamber had diffused away. Even if we were to assume a precision of no better than $\pm 1\%$, the fractionation factor α for Mg^{2+} in water must be such that $\tilde{\alpha}_1 < 0.00025$ (compared to $\tilde{\alpha}_1 = 0.008$ that we have measured for Ca^{2+} in silicate melts). The most obvious explanation for this surprising lack of measurable isotopic fractionation of Mg during diffusion in water is that Mg^{2+} diffuses along with a large hydration sphere, sufficiently large to dilute the effect of the mass of the isotopes of Mg in terms of their effect on the mobility of diffusing unit. The problem with this explanation is that the hydration sphere needs to be of the order of 100 water molecules. We are in the process of repeating the diffusion/isotope fractionation experiments with ionic species with lower ionic potential, which we expect will have smaller amounts of water bound up in their hydration spheres. We plan to measure Cl isotopes to check whether they may have been fractionated as Cl diffused out of the small chamber.



(a) The inset shows the experimental design of the diffusion in water experiments. The graph shows the result of a calculation for the isotopic fractionation of the Mg remaining in the sphere as a function of the amount of Mg lost to the larger chamber by diffusion. For the purpose of this calculation it was assumed that Mg isotopes fractionate by diffusion in water by the same fractionation factor as we measured earlier for Ca isotopes diffusing in a silicate melt ($\alpha=0.1$). (b) $^{26}\text{Mg}/^{24}\text{Mg}$ and $^{25}\text{Mg}/^{24}\text{Mg}$ (in per mil deviation relative to the initial isotopic ratio) measured in water taken from the small spherical chamber plotted against the % Mg lost from the chamber by diffusion. The data show no appreciable fractionation by diffusion in water, in marked contrast to the degree of fractionation that occurs by diffusion in gases and in silicate melts.

LOS ALAMOS NATIONAL LABORATORY

University of California
Los Alamos, New Mexico 87545

Contract: W-7405-ENG-36

Person in Charge: D. R. Janecky (505) 665-0253; fax (505) 665-8118; janecky@lanl.gov

Website: <http://www-emtd.lanl.gov/bes/Program.html>

CATEGORY: Geophysics

High Resolution/High Fidelity Seismic Imaging and Parameter Estimation for Geologic Structure and Material Characterization

*M. Fehler, (505) 667-1925, fax (505) 667-8487, fehler@seismo5.lanl.gov; Ru-Shan Wu
U.C. Santa Cruz*

Objectives: Our objectives are to use wave equation migration to improve the quality of information that can be obtained from seismic images. We also seek to exploit the natural advantages of our methods for providing reflection amplitude vs. angle information that can be used to infer *in situ* parameters like rock properties and fluid type and content.

Project Description: We propose enhancements to the high-resolution/ high fidelity multi-domain seismic imaging techniques that we have developed to date. We also propose to exploit natural advantages of our methods for providing reflection amplitude vs. angle information that can be used to infer *in situ* parameters like rock properties and fluid type and content. We will also begin to develop methods for imaging using multi-component data and elastic wavefield extrapolation.

High Resolution/High Fidelity (HR/HF) seismic imaging is critically important for both energy resource management (oil/gas exploration/production) and CO₂ sequestration. As oil/gas exploration is done in more complicated and difficult geological areas, more sophisticated imaging methods for complex structures are needed to pinpoint the targets. High-Resolution/High Fidelity seismic imaging will help in characterizing the crack distribution, fluid and gas content and changes of reservoir parameters during operation of reservoirs for production or during environmental protection efforts such as those involving nuclear waste disposal, CO₂ sequestration, and groundwater contamination monitoring and remediation. High Resolution refers to the improved resolution obtained with wave equation based imaging techniques compared with ray-based methods. High Fidelity refers to the improved amplitude information that can be obtained when using wave equation based methods.

Results: During the past year, we have continued investigations into the Split-Step Pade migration operator that was originally developed during the first year of the project. We also initiated an effort to develop velocity models from synthetic data, where the velocity model is known and images have been obtained using many of our wave-equation based migration operators as well as from ray-based Kirchhoff migration. Our goal in this work is to determine how errors in the velocity model used for migration can impact the resulting image. We initially investigated the impact of velocity model errors by introducing changes in the known velocity model and migrating using the changed velocity model. However, we believe that we need to introduce realistic errors and that this is best done using a conventional velocity analysis approach, which we are now doing. We are also investigating an approach for developing images for various incident angles onto each layer within the image. This is a first step in developing an amplitude vs. angle analysis approach. In the area of wave propagation in heterogeneous media, we are developing methods to explain the envelope of waveforms using the Markov and radiative transfer theories. By fitting numerical waveforms using these semi-analytical approaches, we are gaining insight into the importance of scattering mechanisms on seismic wave propagation.

The Role of Carbon and Temperature in Determining Electrical Conductivity of Basins, Crust, and Mantle.

T. J. Shankland, (505) 667-4907, fax (505) 667-8487, shankland@lanl.gov; A. G. Duba, (510) 422-7306, fax (510) 423-1057, alduba@llnl.gov; E. A. Mathez, American Museum of Natural History, (212) 769-5379, fax (212) 769-5339, mathez@amnh.org

Objectives: The intent of this work is to comprehend the electrical conduction mechanisms in carbon-bearing rocks and in mantle minerals for the purpose of relating electrical conductivity (σ) measured in the field to the nature and origin of carbon in crustal rocks and to temperature in the mantle.

Project Description: Electrical conductivity depends strongly on temperature T and on the presence of other phases such carbon, fluids, or ore minerals at the lower temperatures of the crust and basins. One research approach is to measure σ of mantle minerals as functions of temperature, orientation, oxygen fugacity fO_2 , and iron content. These data supply the best models for "electrogeotherms" yet available. Another approach is to document textures of carbon in crustal rocks from basins and metamorphic zones and relate them to rock conductivity. The key to high conductivity in rocks is the extent to which the conductors form an interconnected network. In this case, the nature of the carbon is determined by time-of-flight mass spectroscopy, and its distribution is determined by electron microbeam techniques in the same samples used for conductivity measurement.

Results: In order to explore the many-faceted problem of carbon distribution and detection in rocks and its influence on electrical conductivity, the PIs of this project convened an

interdisciplinary workshop that included forty petrologists and geophysicists from Europe and North America. It was held at the American Museum of Natural History in New York City April 18 and 19, 2001.

Although general consensus was reached on the importance of carbon in producing upper crustal electrical conductivity anomalies, the situation for the lower crust was much less clear. One problem is simply that some lower crustal features are unseeable because uplift, by whatever mechanism, modifies microstructure and generally modifies geochemistry, even subtly, in fresh rocks. Although geophysical methods lack spatial and temporal resolution and laboratory deformation experiments shakily match in-situ crustal conditions, geophysical researchers were more confident of carbon as an explanation of conductivity anomalies than were most petrologists present. For instance, there was no consensus on what constitutes viable mechanisms for mobilizing and precipitating carbon at pressures and temperatures of the deep crust. Further, there is the problem that thermodynamic equilibrium may not prevail on microcracks because of unknown kinetic and shear effects and because the carbon may not be purely graphitic. However, veins of graphite described from New Hampshire show field evidence for the mobility and precipitation of copious graphite in veins with or without graphitized wall rocks in sillimanite-grade schists, and gneisses. The location of the graphite veins appears to be tectonically controlled, with deposition near the top and possibly much deeper in the lower crust. Unresolved issues that need further attention include: measurement of electrical properties of hydrous minerals that may be stable in the crust; how the interconnectivity of carbon can be dynamically maintained at lower crustal to upper-mantle conditions where equilibrium conditions would tend to produce isolated graphite crystals; and experimental observations of mechanisms for destruction of interconnected carbon films during laboratory simulation of near-surface crustal conditions.

Nonlinear Elasticity in Earth Materials

P. A. Johnson, (505) 667-8936, fax (505) 667-8487, paj@lanl.gov; J. A. TenCate, T. J. Shankland, E. Smith; R. A. Guyer

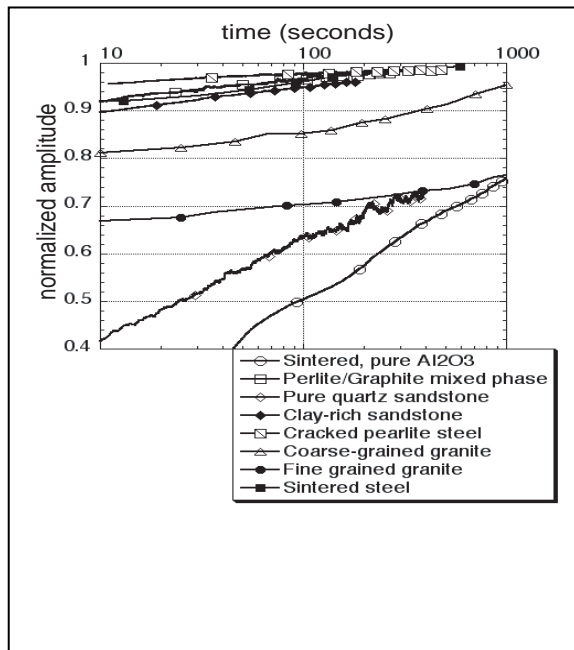
Objectives: Research objectives are to investigate the physical manifestations of nonlinear elasticity in rock, and to characterize nonlinear properties of rocks and other solids that exhibit similar behavior, such as compressed powdered metals and materials that are damaged. Of primary importance is determining the origin of nonlinear behavior, relating this quantitatively to nonlinear response, and developing and applying a holistic model describing the nonlinear response of rock over broad stress-strain-frequency ranges so that practical applications can proceed.

Project Description: Increasingly rapid progress is being made in the field of dynamic nonlinear elasticity of earth materials. Roughly fifteen years ago three groups of scientists (at Los Alamos, at the Institute of Applied Physics, and the Institute of Physics of the Earth in Russia) independently initiated this research field. Early and continued OBES support has been

instrumental in making it possible for this research field to flourish. Today the field of dynamic nonlinear elasticity of earth materials has recognized importance in the domains of geomaterials, materials science, and strong ground motion, and there are an ever-increasing number of researchers working within it.

Rocks display unique elastic behavior. They are extremely nonlinear, being hysteretic, possessing discrete memory, and having slow dynamics [a long term memory of strain]. Although some of these types of nonlinearities may exist in, for example, powdered metals, it is rocks where these characteristics were first observed. It is now clear that rocks are part of a large class of materials, possibly a universality class. This is still speculative, but determining whether or not we have discovered such a class is part of our ongoing work. The class of materials includes rock, damaged solids, compressed powdered metals, and we are finding others as we study more and more materials. Further, nonlinear behavior plays a central role in developing new methods with which to characterize material properties, for instance, interrogating the elastic microstructure of rock, determining if a material is damaged, or monitoring progressive damage. Nonlinear attributes of rock have important consequences on processes in the earth such as earthquake strong ground motion, reservoir subsidence, seismic wave propagation and attenuation, stress fatigue damage, hydraulic fracturing, etc. Our work involves developing a comprehensive theoretical and experimental framework that (1) employs static and dynamic laboratory investigation of materials to provide a macroscopic and microscopic description of the elastic state, and (2) provides for turning the microscopic description into a prescription for material properties that can be used to predict change in stress state, both static and dynamic.

Results: The features in an earth solid that determine its elasticity are the same features that control access by fluids, aging, chemical reaction, etc. (flat pores, grain contacts, cracks, etc.).



These features commonly make up 1% or less of the total volume. Understanding how these “soft” portions of the material behave is the key to understanding how the bulk material behaves. We have discovered a remarkable tool for probing the elastically soft portion of geomaterials, called slow dynamics.

Figure 1. Examples of slow dynamical behavior induced by a broad-frequency band source for various materials: a sintered alumina ceramic; a pearlite/graphite mixed phase metal; a very pure quartz sandstone bonded by silica and microcrystalline quartz; a sandstone that contains clay, secondary clay minerals, and calcium carbonate in the pore space, bonded by calcite and quartz; a perlitic steel engine bearing cap containing a very small crack; and samples of coarse- and fine-grained granite. In each material, the eigenmode amplitude (proportional to Q) is shown.

Surprisingly, we have discovered that many other materials respond like earth materials in their slow dynamical behavior, including certain ceramics and metals, at the very least.

Remarkably, this behavior takes place in materials that are wildly diverse in their physical, meso-geometrical and chemical makeup, e.g., the strain memory of an object composed of an alumina ceramic is manifest like that of sandstone, limestone, granite and concrete. In contrast, an object composed of ordinary 5180 (mostly) perlitic steel, for instance, exhibits no memory of dynamic wave excitation; however, if the pearlite contains even a very small crack, the macroscopic strain memory of the object, due to the crack, appears like that of the martensite, the rock, etc. The figure illustrates such findings.

Our group is the first ever to report such findings. Slow dynamics are destined to be a sensitive probe of the micromechanics of material systems, and may be the primary manifestation of a new universality class. The use of slow dynamics as a probe of nanoscale material properties may well become a new domain of research.

This work is leading quickly to applications in damage diagnostics and nondestructive testing of materials. At least two companies have begun manufacturing devices for this purpose.

Nonlinear Dynamics of Fluid Flow and Contaminant Transport in the Earth's Crust from the Micro- to the Macro-scale

B. J. Travis, (505) 667-1254, fax (505) 665-3687, bjt@vega.lanl.gov; D. Yuen U. of Minnesota, 612-624-1868, fax 612-624-8861, davey@krissy.msi.umn.edu]

Website: www.ees5.lanl.gov/models/index.html

Objectives: The objective is to develop numerical simulations of complex fluid dynamical phenomena in the Earth's crust by both continuum and discrete-particle methods, with particular emphasis on coupling processes occurring on different spatial and temporal scales.

Project Description: This is a collaborative effort with Prof. David Yuen of the University of Minnesota, Geophysics Dept, to develop and apply computational models to capture interaction of complex fluid flow processes in the earth's crust over a range of scales. Prof. Yuen's focus is on multi-scale dissipative particle methods. The LANL part focuses on multi-scale continuum methods, in particular, use of fractal functions in a predictive mode, i.e., as solutions of governing partial differential equations in which coefficients of the equations are fractal functions. Important transport properties of geologic media, such as permeability, are known to be approximately fractal over a wide range of length scales, from cm to km. Fractals have seen much application in a descriptive mode; but ours is the first successful use of them in a predictive mode for subsurface flow and transport problems. After development of the particle and continuum methods separately, our goal is to merge them into a single hybrid algorithm capable of capturing a greater range of scales than either can alone, and apply these new

algorithms to multi-scale transport problems of national interest, such as transport of microbial pathogens through soil and rock and contamination of water supplies.

Results: The main goal of the first three years has been achieved, ie, development of particle-based and continuum-based algorithms for multi-scale/up-scale analysis of complex fluid flows. Specific milestones in FY01 included:

Fractal interpolating functions (fif) have been applied to 1-D flow and transport equations (Travis, 2002) as a proof of principle, providing solutions that capture dynamics at all scales.

Fif representations have been integrated to provide sub-gridscale homogenizations that can be used in traditional finite difference or finite element solutions of porous flow and transport.

We have demonstrated the capability to solve inverse problems for a large-scale simulation of 3-D flow in the Earth's crust (Bunge, Hagelberg & Travis, 2002). Inverse methodology allows us to answer questions such as, given the present-time observations of a fluid flow, what was the state of that fluid system at an earlier time?

A framework for simulating complex fluid and heat flow in the Earth's crust has been implemented (Dutrow, Travis, Gable & Henry, 2001).

The fif methodology is being extended to 2-D and 3-D geometries and is being implemented in existing finite difference porous flow and transport computer codes. Coupling a DPD particle algorithm, which is very effective at representing dynamics at nanometer to mm scales (e.g., capturing dynamics between pathogen cell membrane and soil pore structure and water and mineral content) with our continuum multi-scale FIF algorithm (cm-to-km scale) will allow us to quantify scale interactions and make predictions about transport from the nano-scale to the km scale, providing a single model coupled across an enormous scale range.

CATEGORY Geochemistry

Improved Sensitivity Uranium Series Studies

M.T. Murrell, (505) 667-4299, fax (505) 665-4955, mmurrell@lanl.gov; S.J. Goldstein (505) 665-4793

Objectives: The goal of this project is to provide unique information on the behavior of U-series members in the environment using improved capabilities for Quaternary dating.

Project Description: Uranium-series disequilibria techniques are well-established and valuable tools for geochronology and geochemistry. Such measurements have typically been made by decay counting; however, there are considerable advantages in using mass spectrometric

techniques. The general goal of the current project is to apply mass spectrometric methods to answer basic questions in Quaternary dating and geochemistry. Emphasis is placed on a multi-element concordia approach and improving sensitivity for these elements. This work provides information on the recent evolution of magmatic systems and also has application to natural hazard risk assessment, paleoclimate studies, and the carbon cycle. In this way, our research contributes to an improved understanding of fundamental Earth processes that can be used as a foundation for efficient, effective, and environmentally sound use of energy resources, and to provide an improved scientific basis for advanced energy and environmental technologies.

Results: Over the last year, we have reoccupied our clean laboratory and mass spectrometry facility (RC45), damaged in the Cerro Grande Fire and subsequently refurbished, and completed an extensive (>50) set of actinide blanks on our operations and laboratories before resuming this research.

After 5 months of installation and detailed testing, our new multi-collector ICP mass spectrometer has been accepted by us. The Isoprobe consists of a total of 17 collectors including 8 channels of simultaneous ion-counting. It met all of our testing specifications - beating most of them by a factor of two. The first project on this instrument will be the measurement of low level thorium isotopes in natural waters. This new instrumentation will greatly improve our sensitivity for the long-lived U-series members.

We have measured U concentrations and $^{234}\text{U}/^{238}\text{U}$ ratios for a set of dusty ice samples from the base of the GISP-2 Greenland ice core, at a depth of approximately 3 km. The goal of this work was to further test the Fireman recoil-based model for producing uranium-series disequilibria in dusty ice on samples known to be > 150,000 years in age. We separated the samples into several fractions by filtration and analyzed the < 0.05 μm or “dissolved” fraction first. This fraction had exceedingly high U concentrations (2-5 ppb U), which correlate with dust concentrations (>0.20 μm) for these samples. These U concentrations are a factor of 1000 higher than measured for the “dissolved” ice at Allan Hills. We hypothesize that the high U concentrations, their correlation with dust concentration, and $^{234}\text{U}/^{238}\text{U}$ activity ratios below 1 are most consistent with incorporation of very fine (<0.05 μm) dust particles in the “dissolved” fraction of these samples. Consequently, this study points out that certain samples may not be applicable for this method (they may not be suitable in dust characteristics: size, origin, or amount). For extremely dusty samples such as these, more stringent separation of dust, perhaps by ultrafiltration, may also be necessary to separate the dissolved and particulate components.

In addition to the above activities, we have a number of other ongoing studies that include: 1) the residence time of Hawaiian magmas at different stages of volcano evolution and in different settings in the same volcano; 2) the spatial and temporal evolution of travertines in Nevada; 3) temporal and spatial evolution of MORB at the Northern Gorda Ridge, the Axial Valley of the Mid-Atlantic Ridge, and the EPR, and 4) ventilation ages for deep-ocean water, both presently and during the past glacial maximum using U-series dates for deep-sea corals.

Surface Exposure Dating in Geomorphology

Robert Reedy, (505) 667-5446; fax (505) 665-4414, rreedy@lanl.gov; K. Nishiizumi Univ. Calif., Berkeley, 510-643-9361, kuni@ssl.berkeley.edu; W. E. Dietrich UCB; R. C. Finkel LLNL

Objectives: The production systematics of nuclides made *in situ* in terrestrial surface samples by cosmic rays and the use of these cosmogenic nuclides to date and characterize young (<1 Ma) surfaces are studied.

Project Description: Geological samples start accumulating cosmogenic stable and radioactive nuclides such as 0.7-Ma Al-26 once they are formed very near the Earth's surface or brought to the surface from depths of many meters. These nuclides are often the only way to characterize the recent surface record of such samples, such as dating when they were exposed on the Earth's surface or inferring erosion rates. Studies include dating major glacial, fluvial, and earthquake events. To interpret the measurements of the concentrations of these nuclides in surface samples requires good rates for their production. This project uses measurements of cosmogenic nuclides in well-characterized samples plus numerical simulations using computer codes developed at LANL and cross sections for the relevant nuclear reactions to get better production systematics for many in-situ-produced cosmogenic nuclides as a function of target composition, elevation, and geomagnetic latitude.

Results: Cross sections for the production of these nuclides continue to be compiled and evaluated. Many neutron-induced cross sections are different from the proton-induced ones often assumed to apply for neutrons. Status reports on such cross sections have been presented at several international conferences. Work continues to be done on measuring more needed neutron cross sections at the Los Alamos Neutron Scattering Center and other sources of energetic neutrons.

We have gotten the latest version of the code MCNPX developed at LANL and are testing it for our specific application. Initial tests have been good. The code is being modified for our specific application.

Collaborations have been maintained with groups exposing artificial samples on the Earth's surface and with others measuring cosmogenic nuclides in natural samples. I am helping Dr. Ian Graham of the Institute of Geological and Nuclear Science of New Zealand on interpreting his recent measurements for a range of geomagnetic latitudes and elevations in the Southern Hemisphere. These measurements include rates from portable neutron monitors and concentrations of radionuclides produced in artificial samples. A detailed report on these measurements and their interpretation is being prepared and will be presented soon at an international conference.

Dissolution of Fe(III)(hydr)oxides by Aerobic Microorganisms

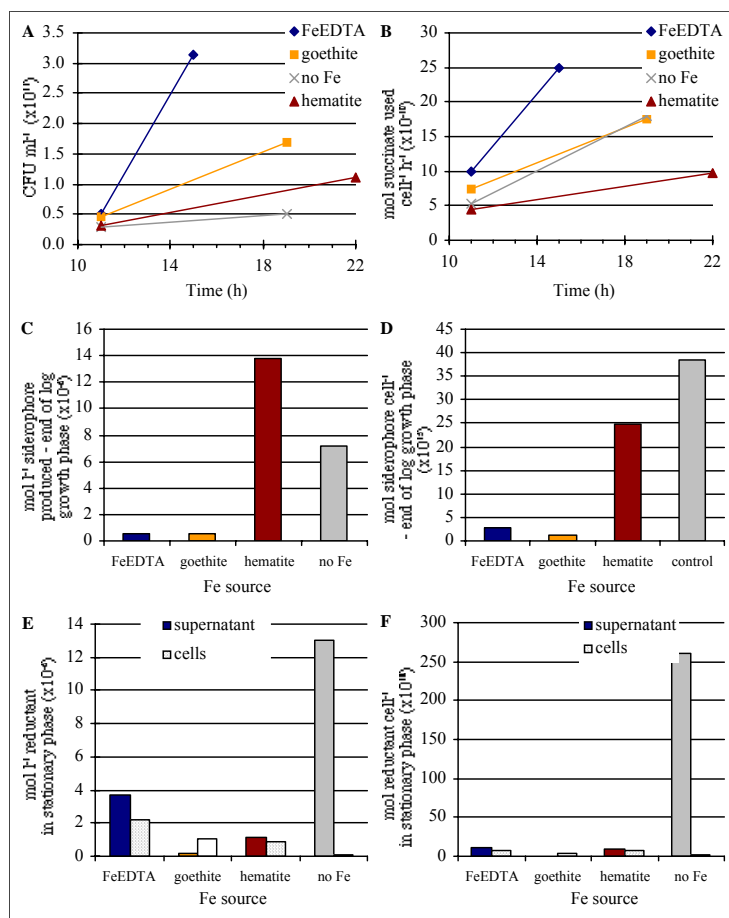
Larry Hersman, (505) 667-2779, fax (505) 665-6894, hersman@lanl.gov; P. Maurice, Notre Dame University; Garrison Sposito, U.C., Berkeley

Objective: Our overall objective is to determine the mechanisms of iron release during microbially enhanced iron oxide dissolution by an aerobic microorganism. The results of several of our experiments performed in our first funding cycle lead us to believe that aerobic microorganisms used a reductive dissolution process to acquire iron from hematite (α -Fe₂O₃). We therefore proposed to use a combination of biochemical and analytical techniques to determine the compounds and conditions responsible for the microbially enhanced dissolution. We report here the progress of our work to date, at LANL.

Project Description: The purpose of this research is to investigate the mechanisms used by aerobic microorganisms to obtain Fe for growth. Currently little is known about Fe oxide dissolution processes in oxic environments. Understanding these mechanisms is fundamental to a wide range of bio-geo-chemical processes. For example, Fe oxides sorb a variety organic and inorganic pollutants, therefore understanding the mechanisms of dissolution is important to understanding pollutant transport phenomena. Los Alamos National Laboratory is investigating the growth characteristics of a *Pseudomonas* sp. whose only source of Fe is either hematite or goethite. Additionally, we supply siderophore for siderophore mediated investigations at UC Berkeley and provide microbially reacted, Fe oxide surfaces for AFM analysis at Notre Dame University.

Results:

Siderophore characterization (P. mendocina): Using electrospray MS/MS, Emily Dertz at UC Berkeley (collaboration with Ken Raymond) has determined the molecular ion is at 929 g/mol. The 173.0 peak suggests that the ornithine (first determined by HPLC analysis) is actually Orn (N-OH, N-acyl) and located on one end of the siderophore (see Fig 3 for example of ornithine type siderophore). This is a common modification that yields a hydroxamate siderophore. The five amide proton resonances in the H NMR suggest a 5 amino acid long peptide chain, which is attached to a long aliphatic side chain. Based upon this NMR work and previous HPLC pico-Tag analysis, 2 modified ornithines (as described above), 1 B hydroxyaspartic acid, 1 serine and the unknown amino acid should make up the peptide backbone. Finally, there is evidence (NMR) of an alkene moiety in the siderophore based upon NMR spectra. This appears to be a part of the aliphatic side chain



Microbial Growth and Energy Use.

Growth was measured over time by taking the absorbance of the samples at 600 nm. **(A)** The fastest and most abundant growth occurs when the cells are grown in the presence of FeEDTA, followed by goethite, hematite, and no Fe. For the determination of energy use, we took samples at the beginning and end of log growth phase, filtered each sample, and measured the amount of succinate still present in the solution by HPLC (Supelcogel C-610H column, 0.1 M phosphoric acid mobile phase) and compared these results to a previously established standard curve. **(B)** The most energy (per cell) is used by the cells grown in the presence of FeEDTA - and at the fastest rate, followed by goethite and no Fe which have similar rates, and finally the cells grown in the presence of hematite use the least amount over the longest period of time.

Siderophore Production. **(C)** Understandably, very little siderophore (less than $1 \mu\text{M}$ total concentration) is produced when FeEDTA is present; however, very little siderophore is produced in the presence of goethite, as well. Expectedly, almost $14 \mu\text{M}$ siderophore is produced in the presence of hematite and about $7 \mu\text{M}$ in the presence of no Fe. **(D)** Although the population of cells present in the hematite flasks produce a greater total concentration of siderophore, the cells in the presence of no Fe produce more siderophore on a per cell basis.

Reductant Production. **(E)** The reductant analysis revealed that cells grown in the presence of hematite and goethite produce a very small total concentration of reductant as a population ($\sim 1 \mu\text{M}$ in the supernatant and $\sim 0.75 \mu\text{M}$ cell-bound), the cells grown in the presence of FeEDTA produce 2 to 3 times that amount, and the cells grown with no Fe added produce a large quantity of reductant in the supernatant ($\sim 13 \mu\text{M}$) and essentially no cell-bound reductant. **(F)** On a per cell basis, the cells in the no Fe flasks produce the most reductant (supernatant only); the individual cells in the FeEDTA and hematite flasks produce similar (small) amounts of reductant to one another, followed by an even smaller amount of reductant being produced in the presence of goethite.

CATEGORY Solar-Terrestrial Physics

Energy Transport in Space Plasma

S. P. Gary, (505) 667-3807, fax (505) 665-7395, pgary@lanl.gov,

Website: *http://nis-www.lanl.gov/~pgary/*

Objectives: The long-term goal of this research is to understand the flow of plasma energy in the near-Earth space environment from a small-scale point of view. The objective of this research is to use plasma theory, simulations, and data analysis to express the consequences of plasma microinstabilities as concise relationships that may be used in large-scale models of space plasmas that describe the solar-terrestrial interaction.

Project Description: Particle velocity distributions and parameters observed by Los Alamos plasma instruments on scientific spacecraft as well as computer simulations are used to carry out fundamental studies of plasma instabilities and associated transport in and near the solar wind, the Earth's bow shock, and the terrestrial magnetosphere.

Results: Our most important accomplishment in 2001 was the demonstration that relatively steep power law magnetic fluctuation spectra observed at relatively short wavelengths in the solar wind do not, as is commonly believed, correspond to collisionless dissipation of the waves. Rather, we have argued that such power spectra appear as a result of the dispersive properties of magnetosonic/whistler modes.

The Solar Wind-Magnetospheric Interaction

J. Birn, (505) 667-9232, fax (505) 665-3332, jbirn@lanl.gov

Objectives: The goal of this research is to further the understanding of the structure and dynamics of the Earth's magnetosphere, coupled to the fast-flowing solar wind plasma on the one hand and to the ionosphere on the other.

Project Description: The focus of this research is the investigation of the large-scale structure and evolution of the Earth's magnetosphere, using theory, numerical modeling, and correlative studies of data from multiple sites within and near the magnetosphere (including the Earth itself as well as scientific satellites).

Results: Our most significant accomplishment in 2001 was obtained from our further investigations of the formation of thin current sheets in the magnetotail. Using a quasi-static approach, we showed that modest boundary perturbations can lead to critical states characterized

by strong current intensification. For perturbations exceeding a critical limit, equilibria that satisfy the conservation of entropy, topology and magnetic flux, cease to exist, indicating the onset of catastrophic evolution.

Energetic Particle Acceleration and Transport

G. D. Reeves, (505) 665-3877, fax (505) 665-7395, reeves@lanl.gov

Website: *leadbelly.lanl.gov/reeves.html*

Objectives: The overall goals of this project are (1) to better understand the acceleration and transport of energetic particles during magnetic storms, substorms, relativistic electron enhancements, solar energetic particle events, and other magnetospheric processes, (2) to develop empirical models of the structure and dynamics of the Earth's radiation belts and other energetic particle regions, and (3) to develop a better understanding of the space environment as a system and to better understand the effects of the space environment on spacecraft and their operations.

Project Description: This effort concerns the analysis of energetic particle data from a variety of US programmatic and NASA scientific satellites. Those include the series of geosynchronous spacecraft that carry Los Alamos energetic particle detectors, the GPS satellites which also carry Los Alamos energetic particle detectors, NASA's POLAR satellite, and others. The energies of the particles of interest range from keV to hundreds of MeV. The lower end of this range lies somewhat above the thermal plasma energies and is therefore sensitive to local acceleration processes such as magnetospheric substorms. The higher end of the energy range is well suited to the study of energetic particles in the earth's radiation belts and those that can penetrate the Earth's magnetic field, such as galactic cosmic rays and particles produced in solar flares. We also investigate the effects of those particles on spacecraft systems and instrumentation.

Results: Our most important accomplishment in 2001 derived from our analysis of relativistic electron fluxes as measured from the POLAR spacecraft in the northern hemisphere of the terrestrial magnetosphere. We identified all times of magnetic storms, and looked for correlations between those storms and electron fluxes. Contrary to the common assumption about the relationship between storms and relativistic electron events, we found no significant dependence between electron fluxes and storm magnitudes. We also found that the pre-existing and final electron fluxes are uncorrelated, so it appears that the pre-existing population is not simply pumped up by storm effects.

OAK RIDGE NATIONAL LABORATORY

University of Tennessee – Battelle, LLC
Oak Ridge, Tennessee 37831

CONTRACT: DE-AC05-96OR22464

CATEGORY: Geochemistry

PERSON IN CHARGE: David. R. Cole

Volumetric Properties, Phase Relations and Reaction Kinetics of CO₂-CH₄-H₂-H₂O Fluids: Effects of Injecting CO₂ into Geological Reservoirs

J.G. Blencoe, (865) 574-7041, fax (865) 574-4961, blencoejg@ornl.gov, L.M. Anovitz; M.T. Naney

Objectives: Experiments, thermodynamic analyses, and equation-of-state (EOS) modeling are being performed to gain a predictive understanding of the geochemical behavior of CO₂ and CH₄ in deep porous and permeable rocks. Results of the research will have numerous practical applications in technologies for sequestering CO₂ in geological reservoirs.

Project Description: Experiments are conducted with binary and ternary mixtures of CO₂, CH₄, and H₂O at temperature-pressure conditions similar to those encountered in deep aquifers, sedimentary basins, and geothermal resource areas. Volumetric properties and liquid-vapor phase relations are determined with high precision and accuracy using a unique, vibrating-tube densimeter (VTD) designed for operation at 30-500°C and 5-200 MPa. Experimentally measured volumetric properties and phase relations for fluid mixtures are modeled using theoretically based (semi-empirical) formulations. Laboratory experiments and thermodynamic modeling are closely integrated to optimize the efficiency and effectiveness of data acquisition and EOS development.

Results: This year important progress was made in determining the upper baric stabilities of liquid-vapor assemblages in the CO₂-H₂O system at high-subcritical temperatures (275-360°C).

Experimental investigations of vapor-liquid equilibria (VLE) in the CO₂-H₂O system have produced inconsistent results (Tödheide and Franck, 1963; Takenouchi and Kennedy, 1964; Seitz and Blencoe, 1997). To resolve the discrepancies between the VLE data for high-subcritical temperatures (275-360°C), experiments are being performed to measure the pressure (*P*)-mole fraction CO₂ (*X*_{CO₂}) limits of the CO₂-H₂O L-V region at 275, 300, 325 and 350°C. To date, results have been obtained for 300 and 350°C. The data were collected using a custom designed, vibrating U-tube densimeter operable at 30-500°C, 5-200 MPa. The experimental method developed to obtain the results involves detection of the pressure of the bivariant reaction $F = L + V$ (F = single-phase CO₂-H₂O fluid) for a series of fluid compositions at a

fixed temperature. The first step in the procedure is to create an isobaric-isothermal, physically isolated and chemically homogeneous sample of “high-pressure” CO₂-H₂O fluid of known composition. Fluid pressure is then lowered slowly at constant temperature. Pressure readings and matching values for τ (the period of vibration of the U-tube) are recorded at 0.1 or 0.2 MPa intervals. When the fluid begins to separate into two phases (liquid + vapor), a distinct inflection is observed in the trend of P vs. τ . Considering all potential sources of error in the technique, we estimate that measured upper baric L-V stabilities are accurate to ± 0.2 MPa. This accuracy is far superior to the pressure-measurement accuracies claimed in *any* previous investigation of CO₂-H₂O VLE.

Our new VLE data for 300°C agree closely with the results obtained by Takenouchi and Kennedy (1964) and Seitz and Blencoe (1997). In contrast, the data obtained by Tödheide and Franck (1963) indicate upper baric stabilities for L + V that are as much as 10 MPa above those suggested by the more recent results. Thus, it is evident that the data obtained by Tödheide and Franck (1963) are seriously in error. The sharp discrepancies between the VLE data presented by Tödheide and Franck (1963) and Takenouchi and Kennedy (1964) have been the subject of intense debate for more than 35 years. Taken together, the data obtained in the present study and those acquired in the earlier work of Seitz and Blencoe (1997) strongly suggest that the results reported by Takenouchi and Kennedy (1964) are more reliable than those obtained by Tödheide and Franck (1963). Thus, an important step has been taken toward final resolution of a longstanding controversy in geochemistry.

However, our new VLE data also indicate a CO₂-H₂O L-V stability field for 350°C that is significantly smaller than the one determined by Takenouchi and Kennedy (1964). In addition, the Takenouchi and Kennedy (1964) L-V stability field for 325°C exhibits a P - X_{CO_2} morphology that is distinctly different from those manifested by the CO₂-H₂O L-V regions for 300 and 350°C that we have determined in our vibrating-tube experiments. Thus, it is evident that additional vibrating-tube measurements of CO₂-H₂O VLE are required to establish the exact P - X_{CO_2} dimensions of the CO₂-H₂O L-V region at 275-360°C.

Fundamental Research in the Geochemistry of Geothermal Systems

J. Horita, (865) 576-2750, fax 865-574-4961, horitaj@ornl.gov], D. R. Cole; A. A. Chialvo

Objectives: The objective of this project is to provide fundamental information on geochemical reactions that play pivotal roles in a wide range of geological processes, but that specifically impact reservoir dynamics, corrosion, and heat extraction in active geothermal systems. Kinetic and equilibrium partitioning of stable C-O-H isotopes, and other fluid-solid interactions are primary subject areas for this research.

Project Description: At Oak Ridge National Laboratory, a long-term basic research program in experimental hydrothermal geochemistry, stable isotope geochemistry, and igneous petrology has led to the development of unique methodologies for extracting rigorous and unambiguous information on a wide range of geochemical processes. This capability permits the efficient and definitive examination of specific problems hampering the ability to quantitatively model fluid-rock interaction processes related to the discovery and exploitation of geothermal resources. Research topics in this project are selected in close cooperation with geothermal industry representatives and are frequently augmented by parallel research on more applied aspects of the same problems funded by the U.S. Department of Energy's Geothermal and Wind Technologies Program.

Results We obtained experimental data of isotopic partitioning for the NaI liquid-vapor system at 160-385°C. The D/H isotope effects of 4 molal NaI solutions are about twice those by NaCl solutions at 20-50°C, but differences between the two salts decrease with increasing temperature. Above 200°C, the effects of NaI and NaCl become indistinguishable, supporting the hypothesis that with increasing temperature the hydration shell of halide ions in aqueous solutions expands significantly and that the hydration water molecules become more like "bulk-solvent water". Similar experimental data show that the $^{18}\text{O}/^{16}\text{O}$ isotope effects of CsCl is very similar to that of KCl at 200 and 300°C, suggesting that both K^+ and Cs^+ ions exhibit "structure-making" behavior at elevated temperatures.

In collaboration with CalEnergy, we initiated a comprehensive sampling and analytical program of hot, hypersaline brines collected from wells at Salton Sea geothermal system, California. Of a total of 51 samples of injection and production fluids obtained, the temperature and salinity of the fluids range as high as 181°C and 31.5 wt-%, respectively. We employed analytical methods, which employ the principle of isotopic equilibration between gases (H_2 and CO_2) and brines. Except for a blank sample, the isotopic compositions of all brine and steam samples fall into a narrow range (δD values from -65.9 to -55.7‰ and $\delta^{18}\text{O}$ values from -1.35 to 2.41‰). In the context of the isotope salt effects, our new isotopic data of Salton Sea brines are consistent with those in the literature. The blank sample (SLT IID16 Blank) from canal waters, which originate from the Colorado River, has very low δD and $\delta^{18}\text{O}$ values and can be readily distinguished isotopically from the production fluids. All pairs of production brine and steam samples have very similar D/H ratios, while $^{18}\text{O}/^{16}\text{O}$ ratios of brines are 2.0 to 2.5 ‰ greater than those of corresponding steam samples. This relation is expected, because with increasing temperature, the equilibrium D/H fractionation factor between water and steam decreases rapidly. At about 220°C, D/H ratios of coexisting water and steam become indistinguishable and above this temperature steam becomes more enriched in deuterium than water ("cross-over"). On the other hand, liquid water is always more enriched in ^{18}O compared to vapor.

We have conducted molecular-based simulations to understand isotopic fractionation of simple molecular fluids. The differences in thermophysical properties of isotopes have a purely quantum origin, which can be investigated in terms of classical mechanical mechanics based on the Helmholtz free energy. An important feature of this approach is that there is no need to introduce the harmonic-oscillator approximation, and most importantly, all required quantities are readily available as time averages from classical molecular-dynamics simulations. A

preliminary simulation analysis for liquid-vapor ^{36}Ar - ^{40}Ar isotope partitioning as a function of the absolute temperature from 81 to 120K agree well with the corresponding experimental results in the literature.

Ion Microprobe Studies of Fluid-Rock Interaction

L.R. Riciputi, (865) 574-2449, fax 865-576-8559; i79@ornl.gov], D. R. Cole; M. Fayek

Objectives: The objective of this research is to investigate how the microscale elemental and isotopic record, accessible using ion microprobe analysis, can be used to understand mass transfer processes occurring during fluid-rock interaction at low to moderate temperatures in the earth's crust, studying both natural and experimental samples.

Project Description: In this project, the ability of ORNL's Cameca 4f ion microprobe to obtain quantitative element and light (H, B, C, O, S) isotope ratio analyses with a 5-30 micron spatial resolution are being developed and applied to studies of fluid-rock interactions in a variety of settings, in both natural and experimental systems. The ion microprobe data is typically integrated with information obtained using a variety of other techniques, petrographic studies, conventional bulk gas source and thermal ionization isotope ratio analyses, electron microprobe, and fluid inclusion analysis. Primary areas of investigation include (1) use of the microscale isotope record to study mass transport during large-scale fluid-rock events, (2) determination of both diffusion rates and equilibrium water-mineral isotope partitioning factors in the O, H, and C systems, and (3) utilizing microscale isotopic and elemental disequilibrium in natural settings to study the duration of fluid-rock events.

Results: Our study of authigenic K-feldspar and quartz cements from the Mount Simon Sandstone in the Illinois Basin (and surrounding areas) to resolve the multiple the regional events that precipitated the widespread K-feldspar and quartz cements across the mid-continent at ~400Ma is nearly complete. SIMS trace element analyses suggest that there are regional trends in some trace elements that support the idea of regional flow paths. Much of this work was conducted by Zhensheng Chen for his Ph.D. at UTK.

Continued microscale investigation of oxygen isotope zonations in the Boehls Butte Anorthosite, Idaho to better understand fluid-rock interactions during the alteration of this anorthosite has revealed that feldspars from a sample of schist proximal to the anorthosite has homogeneous oxygen isotope profiles. The lack of oxygen isotope profiles suggests that there was a profound difference in hydraulic properties of the two rock types during uplift. Analyses of two samples of the Bitterroot Anorthosite, which is located 50 km distant from the Boehls Butte revealed variable oxygen isotopic compositions, suggesting that the processes at Boehls Butte may have a regional expression.

We have made considerable progress on our work to investigate hydrogen transport mechanisms in glasses at low (30-150°C) temperatures. Experiments of up to two and a half

years duration show that the diffusion coefficient is a function of both time and the water content of the obsidian, and that the surface concentration is also time-dependent. Modeling of these results shows that the effects of diffusion-induced stress and surface relaxation, coupled with a compositionally-dependent diffusion coefficient can successfully reproduce both the shapes of the diffusion profiles and their temporal evolution.

Our study of quartz cements from the Proterozoic Athabasca and Thelon basins, Canada, and the McArthur Basin, Australia shows that quartz cements from these basins exhibit petrographic characteristics suggesting quartz cementation began at shallow depth before mineralizing fluids were present. To estimate the depth of quartz cementation, we coupled quartz cement stratigraphy (from petrography) with high precision *in-situ* ion probe-generated $\delta^{18}\text{O}$ data ($n=81$) from 10 μm areas. The $\delta^{18}\text{O}$ data from over 20 samples show that early quartz cements in these Proterozoic basins began at or near the surface at < 1 km burial depth. Reports of such early phases are rare due to the limitations of existing techniques to resolve individual phases. Understanding the timing of pore-occluding quartz cement is important in the case of ancient sandstones because these cement phases can transform aquifers into diagenetic aquicludes and can potentially either stop or redirect mineralizing fluid flow.

We have developed a number of new *in situ* ion microprobe techniques for the isotopic analysis of uranium-bearing minerals, including (1) Development of uraninite standard for $\delta^{18}\text{O}$ ion microprobe analysis and (2) Development of uraninite standards for U-Pb ion microprobe isotopic analysis. Using these carefully chemically and isotopically calibrated standards, we developed instrumental ion-yield fractionation factor (α_{SIMS}) curves, defined by equations that describe the relationship between the “true” values for $^{206}\text{Pb}/^{238}\text{U}$ and $^{207}\text{Pb}/^{235}\text{U}$ vs. the $^{206}\text{Pb}^+/^{238}\text{U}^+$ and $^{207}\text{Pb}^+/^{235}\text{U}^+$ values that were determined by SIMS. These calibration curves have significantly improved the precision of U-Pb ages obtained by SIMS, and permit the *in situ* detailed characterization of uranium-bearing minerals at the μm -scale, which is necessary to monitor the behavior and migration of uranium and other radionuclides over large spatial and temporal scales. We have been utilizing these standards to study uranium deposits from Athabasca, Canada and the Oklo-Oelobondo natural fission reactors, Gabon. Our results suggests that, if analyzed at the microscale, these deposits are very sensitive temporal monitors of global- and regional-scale thermotectonic events, and preserve a relatively complete record of major geologic events.

Fundamental Research in Isotopic Fractionation of Carbonate Systems Relevant to Subsurface CO₂-Sequestration

J. Horita, (865) 576-2750, fax (865) 574-4961, horitaj@ornl.gov ; D. R. Cole

Objectives: The objective of this project is to understand and quantify several key reactions controlling kinetic and equilibrium isotope partitioning during the precipitation, recrystallization, and transformation of carbonate minerals (calcite, dolomite, siderite) in CO₂-

rich fluids at conditions encountered in various geologic settings (groundwater, deep aquifers, sedimentary basins, geothermal systems, etc). This information is needed to monitor and model large volumes of CO₂ injected into the subsurface.

Project Description: This project is currently focused on: a) mechanisms, rates, and isotopic fractionation during slow to rapid precipitation of calcite from CO₂-rich solutions at low temperatures (<100°C) and b) recrystallization and replacement of calcite and dolomite in CO₂-rich fluids at moderately elevated temperatures (100-300°C), both as function of several key variables (temperature, pCO₂, ionic strength, microbial activity, etc.).

Results: The kinetics of oxygen isotope exchange between CO₂ and various aqueous chloride salt solutions have been measured at temperatures ranging from 15 to 50°C. Data for KCl, NaCl, NH₄Cl, MgCl₂, CaCl₂, and AlCl₃ allow the identification of systematic behavior. The measured rate constants governing the first order isotope exchange kinetics range from a factor of 2 to a factor of 20 smaller than those for CO₂-pure water. Reaction half-times strongly depend on the ionic charge and radius, and molality. The effects of solution molality are approximately additive, suggesting the possibility of linking the kinetic data to the thermodynamic properties of the system. The activation energies determined for the temperature dependence of the rate constants for various solutions are of the order of 20 kJ/mol.

A new methodology was developed for determining linear growth rates of calcite (CaCO₃) from aqueous solutions under “chemo-stat” conditions. Our new method can directly measure the height of small (>5 nm) growth steps on a single crystal of calcite over a linear scanning range of 1 – 5 mm, using a stylus-based profilometer. Growth patterns of the same calcite samples were also observed by atomic force microscopy. AFM showed that coverage by new layers of calcite is not uniform even within the same cleaved surface of calcite and that numerous rhombic pits bounded by [441] and [481] with 78 and 102° angles occur in size ranging from a few to tens of μm. A histogram of step heights shows distinct patterns characterized by many high plateaus and deep valleys with an average height is 106±64 nm for 219 min duration (29±17 nm/hr). The methodology develop in this study can determine directly 2-dimensional growth profiles on the order of nm and μm in height and lateral resolution, respectively, over a long lateral range (several mm to cm) on the mineral surface.

Variations in the extent of oxygen isotope exchange have been measured in the system calcite-H₂O±CO₂±NaCl as a function of T(300-700°C), P (25 – 200 MPa), NaCl (0 – 5m), and X(CO₂) (up to 0.18). There is a pronounced increase in the rate of oxygen exchange with increasing T, P and salinity associated with enhanced solubility and Oswald ripening of calcite grains. The presence of CO₂ tends to dampen the growth rates, and hence the oxygen exchange rates decrease with increasing X(CO₂). Results from these high P-T-X experiments can be extrapolated to lower temperature-pressure conditions appropriate for CO₂ sequestration, circumventing the intractable problem of experimentally sluggish isotopic exchange at low temperatures.

Experimental studies of Hydrothermal Fluid Speciation and Fluid/Solid Interaction Employing Potentiometric Methods

D.J. Wesolowski, (865) 574-6903, fax (865) 574-4961, wesolowskid@ornl.gov; P. Bénézeth

Objective: The objective of this project is to utilize ORNL's unique, high temperature, hydrogen-electrode, pH-measurement cells and other potentiometric approaches to study aqueous reactions and water/mineral interactions relevant to DOE's geoscience mission areas. The results find broad application in waste isolation, geothermal and fossil fuel utilization, and electrical power generation.

Project Description: The pH is considered the master variable in aqueous systems, controlling the nature of dissolved species, the rates of homogeneous and heterogeneous reactions, the solubility and absorptivity of rock minerals, the transport and deposition of contaminants and ore components, the volatility of mineral acids and the thermal stability of organic acids. In this program we develop and use unique experimental facilities to directly measure the pH of aqueous solutions and the activities of important dissolved ions over broad ranges of temperature, salinity and pH, and use these measurements to quantify the dissociation constants of inorganic and organic acids and bases, the hydrolysis and complexation of metal ions in solution and the solubilities and surface adsorption properties of minerals.

Results: Studies of the solubility and reaction rates of oxides and hydroxides to high temperatures with *in situ* pH measurement have been a major focus of this effort. The solubilities of zinc and nickel oxides were studied by flow-through cell techniques with on line acid injection from 150 to 350°C as a function of pH. In neutral pH regions, solubility of zinc oxide is higher (104 to 200ppb total dissolved zinc, depending on temperature) than previously measured in our laboratory (50ppb, Bénézeth et al., 1999), but substantially lower than previous estimates available in the scientific literature. It is believed that deposition of ZnO or a zinc hydroxide phase must have occurred in the hydrogen-electrode concentration cell (HECC) sample lines in the earlier study; a problem that is overcome in the flow cell by injecting acid into the sample line before the solution is cooled to room temperature. The nickel results differ significantly from those of previous studies, particularly in mildly basic solutions where the solubility remained independent of pH and was lower than previously reported. Only two nickel species in solution (Ni^{2+} and $\text{Ni}(\text{OH})_2^0$) are needed to model the entire data set.

The dissolution/precipitation rates of boehmite (AlOOH), gibbsite and bayerite ($\text{Al}(\text{OH})_3$) were studied at low temperatures (30 to 90°C) in $\text{NaOH-NaAl}(\text{OH})_4$ solutions or mixed $\text{NaNO}_3\text{-NaOH-NaAl}(\text{OH})_4$ solutions, which are predominant in Hanford High Level Waste Storage Tank supernatant and Savannah River waste cleanup procedures. The results obtained show that bayerite dissolved more rapidly than gibbsite, which in turn dissolves at least ten times more rapidly than boehmite, for a given initial solution composition and temperature. We found also that in all cases increasing ionic strength decreases the dissolution rate, independently of the total NaOH concentration, for all phases and temperatures studied.

In collaboration with Dr. Vincent Salters of Florida State University, we performed titrations of the standard Suwanee River Fulvic Acid (SRFA) to determine the acid/base behavior of the organic ligand functional groups and the total acidity. Experiments have been performed with the hydrogen electrode (from 25 to 100°C) and glass electrode concentration cells (at 25, 35 and 50°C) on SRFA at 0.03 and 0.1 and 0.5 molal ionic strength and some experiments were performed with a Rare Earth Element, neodymium, to measure the complexation constants between Nd^{3+} and the fulvic acid. To our knowledge, this is the first study that probes into the temperature dependency of fulvic acid protonation and REE binding. The results are currently being fitted both with FITEQL 4.0, FIT (NICCA-DONNAN) and ORGLS programs. Finally, we investigated the effect of sorption of a representative divalent transition metal ion (Zn^{2+}), and the effects of various amine buffers used in power plants as pH buffers, on the surface charge of magnetite (Fe_3O_4) to 250°C in dilute solutions of sodium trifluoromethanesulfonate (NaTr). We have found that none of the currently used pH buffers (ammonia, morpholine, ethanolamine, dimethylamine) have detectable effects on the point of zero charge or the zeta potential of magnetite, relative to that of the NaTr medium itself. However, Zn^{2+} adsorbs strongly on magnetite surfaces, and enhances negative surface charge density on the mineral surface at pH's above the point of zero charge.

Mechanisms and Rates of Isotope Exchange in Mineral-Fluid Systems

D. R. Cole, (865) 574-5473, fax (865) 574-4961, coledr@ornl.gov] ; L. R. Riciputi; J. Horita

Objective: The major objective of this research is to measure the rates of isotopic exchange between mineral and fluids controlled by one of two general mechanisms: surface reactions leading to recrystallization and volume diffusion.

Project Description: Equilibrium isotope fractionation factors and rates of isotopic exchange (via diffusion or mineral transformation mechanisms) form the cornerstones for interpretation of stable isotope data from natural systems. Microscale studies (high precision of small sample sizes or *in situ* spot analysis) of mineral-fluid interaction in natural systems indicate that: (a) isotopic heterogeneity and disequilibrium may be more widespread than previously realized, (b) isotopic disequilibrium can occur at high as well as low temperatures, (c) different minerals exhibit varying susceptibilities to retrograde fractionation and re-equilibration, and (d) the mechanisms of isotopic exchange are varied depending on the prevailing geochemical conditions (e.g., temperature, pressure, fluid chemistry, fluid/solid ratio, etc.). Because of the recent advances in analytical techniques, the need for accurate, reliable fractionation factors and rate constants has never been greater. Realizing this need, we have focused our BES research on the experimental determination of rates and equilibrium fractionations for a variety of geologically relevant mineral-fluid (gas) systems for which data are either lacking, limited or, in some cases, controversial.

Results: A substantial effort was made to review all of the existing information on rates and mechanisms of isotope exchange, and the equilibrium fractionation factors for O, C, and H. This work culminated in the form of two chapters for the Reviews in Mineralogy Vol. 43 on “Stable Isotope Geochemistry” edited by J. W. Valley and D. R. Cole. In the case of the rates review, topics included (a) isotope behavior in homogeneous systems, both aqueous and gaseous, (b) rates in systems where mineral reactions control exchange, and (c) diffusion of light elements in either crystalline, amorphous or melt systems. A major deficiency was noted in our understanding of the mechanisms and rates of hydrogen isotope exchange in heterogeneous mineral-gas-solution systems. The review on equilibrium isotope exchange focused on the quantum mechanical explanation of isotope partitioning, experimental methods to measure the fractionation factors, and a summary of the experimental and empirical fractionation factors for O, C and H in gaseous, aqueous, mineral and melt system. An obvious deficiency in our understanding of hydrogen isotope fractionation was also revealed in this review activity.

A study was initiated on the hydrogen diffusivity in biotite and muscovite reacted with D₂O at elevated temperatures (600-800°C) and pressures (up to 200 MPa). The objective was to examine diffusion parallel to the plate direction (fast direction). Even for very short duration experiments (1 – 3 days), ion microprobe profiles were essentially flat for profile depths of several microns indicating much faster transport in this crystallographic orientation than previously estimated from bulk exchange studies. Rough estimates of the diffusivities based on these data suggest values of between 10⁻¹⁰ and 10⁻¹² cm²/s for the temperature range investigated. We observed slightly faster rates in the biotite compared to the muscovite. This work was conducted in collaboration with Dr. Tom Chacko of the University of Alberta.

A study was initiated on the kinetics and isotope exchange accompanying dolomite breakdown to periclase + calcite +CO₂, a reaction common to contact metamorphic systems, but still poorly understood. Experiments have been conducted at 800°C and 50 MPa for varying durations using natural dolomite (powdered from a large gem-quality single crystal) reacted with CO₂. Although this P-T-X condition is well above the stability boundary for the dolomite breakdown, the decomposition kinetics are quite sluggish – i.e. only 30% breakdown after 14 days. This work was conducted in collaboration with T. Labotka and L. Anovitz of UTK.

Reactions between fluids (gases) and solids can be described by a kinetic analysis based on the “shrinking core” conceptual model, according to which a layer of solid product (if any) forms around an unreacted core. The progress of the reaction is described by differential equations relating the consumption of the solid reactant (or equivalently, the radius of unreacted core) to the transport of the fluid (or gaseous) reactant and its reaction at the particle surface. These differential equations for the radius of the unreacted core are usually solved subject to the assumption that the rate of reaction is completely controlled by (a) mass-transfer from the bulk of the fluid (or gas) phase to the surface of the particle; (b) diffusion through the solid product layer; or (c) reaction at the interface between the product layer and the unreacted core. A general numerical method has been developed and applied to the problem of formation of albite alteration rims on coarse-grain plagioclase feldspar phenocrysts from the Rico, CO hydrothermal system. Specifically, the model was used to describe the oxygen isotope patterns measured in grains exhibiting varying degrees of albite replacement. Using known rates of

reaction and diffusion, simulation of conditions at Rico ($T = 150\text{-}300^\circ\text{C}$; $P = 1$ kbar; salinity = 1 m NaCl) indicates that narrow rims (10-100's micron) formed at low T 's (150-200°C) took 100,000 to 1 million yrs to develop, whereas thicker rims (up to 1 mm) formed at higher T 's (250-300°C) took only 50,000 to 100,000 yrs to develop. These times represent integrated values, but are consistent with the timing of convective fluid turnover in magma-hydrothermal systems. P. Larson of Wash. State Univ. and C. Mora of UTK contributed to this effort.

To get a better understanding of the coupled reaction-diffusion behavior observed in systems like Rico, we initiated cation exchange experiments at 600°C and 200 MPa where albite was reacted with either 1 or 2 m KCl doped with ^{18}O and D, and sanadine was reacted with 1 or 2 m NaCl doped with ^{18}O and D, for periods of 4, 5 and 6 days. Images were produced of the cation and ^{18}O isotope patterns in run products using backscatter electrons and the ion microprobe, respectively. Qualitatively, there is a reasonably good match between the distribution and extent of newly formed reaction rims and the ^{18}O -enriched zones. Further image analysis is required to test the actual degree of correlation. T. Labotka of UTK participated in this work.

Nanoscale Complexity at the Oxide-Water Interface

D.J. Wesolowski, (865) 574-6903, fax (865) 574-4961, wesolowskid@ornl.gov; A.A. Chialvo, D.A. Palmer, P.T. Cummings, P. Bénézeth, B. Gu and W. Hamilton at Oak Ridge National Laboratory; P. Fenter, N.C. Sturchio and Z. Zhang at Argonne National Laboratory; S. Lvov and J.D. Kubicki at Penn State University; M.L. Machesky at Illinois State Water Survey

Objective: The objective of this project is to focus a wide range of unique capabilities and expertise on the molecular-level structure and reactivity of the electrical double layer (EDL) formed at the interface between aqueous solutions and mineral surfaces over a wide range of environmental conditions. Studies include surface titrations and electrophoresis measurements, synchrotron x-ray and neutron scattering and reflection, ab initio calculations and molecular dynamics simulations.

Project Description: The pH- and temperature-dependent charging of oxide surfaces by reaction with water, and the association of solution counterions with the charged surface, form an interfacial region, the EDL, which results from a complex interplay of electrostatic and van der Waals forces, quantum effects, lattice strain, ion hydration and hydrogen bonding in solution, and specific binding of solute ions with the surface and one another. The nature of the EDL controls many processes at many scales, such as nanoparticle assembly and alteration, crystal growth rates and morphologies, bacterial attachment and nutrient uptake, colloid transport and flocculation, corrosion and fouling in the power, chemical and materials industries, and contaminant transport and adsorption in aquifers. It is only within the last few years that X-ray and neutron sources are becoming available that have sufficient energies and intensities to unambiguously measure the geometries and bonding environments of surface species, solution ions and solvent structures within the EDL *in situ*. There is very little information available on

mineral/solution interfacial phenomena at elevated temperatures, and, with the exception of our unique pH titration and electrophoresis results, almost nothing quantitative is known about EDL phenomena at temperatures above 100°C. Furthermore, there have been very few truly integrated efforts to achieve a greater understanding of this critical interfacial phenomenon, combining expertise in aqueous, electrochemical, materials, X-ray, neutron and computational sciences.

Results: Rutile (TiO₂) was chosen as the primary phase for the bulk of our current studies, because it is highly insoluble and exhibits a relatively simple surface structure. We have completed a large matrix of pH-titrations of submicron rutile powders in RbCl solutions (0.03m and 0.30m) with and without low concentrations (0.001m) of Sr²⁺ and Zn²⁺ at temperatures of 25 to 250°C. Zinc was found to bind much more strongly with the rutile surface, and to release nearly twice as many surface protons than strontium, with high degrees of adsorption observed at pH's well below the point of zero charge of the surface in the absence of these strongly-sorbed ions. These salts were selected because they are ideal for the associated synchrotron X-ray standing wave and reflectivity studies being conducted on rutile single crystal (110 and 010) surfaces. The latter studies have demonstrated that Sr²⁺ binds to rutile surfaces as an inner sphere species associated with four adjacent surface oxygen atoms, while Zn²⁺ forms bidentate surface complexes. However, both of these divalent ions and Rb⁺, as well as adsorbed water molecules all appear to occupy a position approximately three angstroms above the mineral surface. Attempts to simulate the EDL, using a featureless surface with a charge density similar to that observed in our pH titrations, as well as the rutile 110 surface generated from ab initio calculations, both indicate ion distributions in the EDL qualitatively similar to our experimental observations. Electrophoretic mobility studies have also been successfully performed with rutile powders, in pure water and dilute NaCl solutions at temperatures to 200°C, that indicate pH's of zero net surface charge as a function of temperature that are in good agreement with our surface titration results. Combining these experimental and computational results will provide powerful constraints on the detailed geometries and reaction mechanisms controlling interfacial phenomena.

Neutron scattering studies designed to elucidate the structural details of large organic species (such as cetyltrimethylammonium ion, CTA⁺) require spherical nanoparticles with extremely uniform particle diameters. Thus far we have been unable to obtain or synthesize titania nanoparticles with the required monodispersivity, but we have made excellent progress with the synthesis of silica nanoparticles (ca. 20nm diameter) with high monodispersivity. Results of a recent small-angle-neutron scattering experiment conducted at the Manuel Lujan Jr. Neutron Scattering Center at Los Alamos National Laboratory are now being analyzed. Preliminary analysis suggests that the geometrical orientation of the linear CTA⁺ ions sorbed to the negatively charged silica nanoparticle surfaces can be determined.

A three-day workshop was held at ORNL in July of 2001 during which all co-PI's were able to present and discuss their results and plan subsequent experimental studies. This workshop was also attended by members of an NSF-funded Nanoscale Interdisciplinary Research Team, lead by J. Banfield (UC Berkeley), A. Navrotsky (UC Davis), P. Cummings (UT Knoxville) and M.K. Ridley (Texas Tech), whose goal is to determine the effect of particle size on the thermodynamic properties and surface reactivities of naturally-occurring metal oxide

nanoparticles. A collaborative relationship has been established between these two research groups, and many of our new results were presented in a three-day symposium entitled “Complexity at the Oxide-Water Interface: Mineral Surfaces and Nanoparticles” held at the American Chemical Society National Meeting in Orlando, Florida, April 7-11, 2002.

PACIFIC NORTHWEST LABORATORY

Battelle, PNNL
Richland, WA

CONTRACT: DE-AC06-76RLO 1830

CATEGORY: Geochemistry

PERSON IN CHARGE: A. Felmy

The Reaction Specificity of Nanoparticles in Solution: Application to the Reaction of Nanoparticulate Iron and Iron-Bimetallic Compounds with Chlorinated Hydrocarbons and Oxyanions

D.R. Baer, (509) 376-1609, fax (509) 376-5106, l don.baer@pnl.gov; P. G. Tratnyek (503) 748-1023, fax 503-748-1273, tratnyek@ese.ogi.edu

Objectives: The principal objective of this study is to understand the fundamental mechanisms responsible for the enhanced reactivity and selectivity of reactive metal, bimetallic and oxide nanoparticles toward chlorinated hydrocarbons and environmentally important mobile oxyanions.

Project Description: Iron and iron bimetallic nanoparticles have been shown to have a greatly increased reactivity towards a variety of environmentally important solute species including chlorinated hydrocarbons, reducible oxyanions, and metal ions and produce different, and often more environmentally safe, reaction products in comparison to the byproducts using microscale iron surfaces. These changes occur for particles of the size range where significant variations in electronic and magnetic properties are induced for pure metal particles. However, the iron particles will have the additional complication of a reaction layer that forms on the surface in solution. The differences in selectivity are believed to relate to unique structural and chemical features of Fe(0) near the solution and/or Fe(II) in the oxide film layers. They may be induced by the changes in the electronic structure of the nano-sized particles or changes in the structure of the films formed on the particles in solution. In order to establish and quantify these effects, this project involves a coupled experimental and modeling research program for studying reactive metal, bimetallic and oxide nanoparticles toward chlorinated hydrocarbons and environmentally important mobile oxyanions.

Results: This project is only recently been initiated.

Calcite Surface Chemistry: Molecular-Scale and Macroscopic Descriptions of the Influence of Impurities on Dissolution

D.R. Baer, (509) 376-1609, fax (509) 376-5106, don.baer@pnl.gov; J.E. Amonette (509) 376-5565, fax (509) 376-3650, jim.amonette@pnl.gov

Objectives: The purpose of this program is to develop a fundamental, microscopic understanding of the site-specific reaction mechanisms of the impact of solution impurities on calcite dissolution.

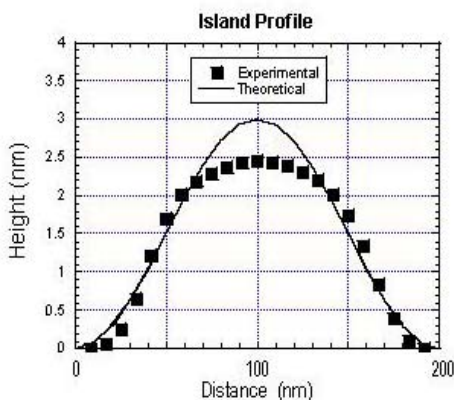
Project Description: This project involves an interdisciplinary theoretical and experimental effort designed to gain a fundamental, molecular level understanding of carbonate mineral surface structure and chemistry including the impact of surface sorbates and precipitates on the surface reactivity. Carbonate minerals coprecipitate and sequester contaminants in soils and sediments and serve as a major reservoir in the global carbon cycle. The project seeks to obtain a new level of understanding of the roles of impurities in calcite dissolution. Specific work proposed includes: (1) scanning probe microscopy (SPM) measurements of step motion during dissolution as impacted by a systematically selected series of divalent cation impurities, (2) theoretical calculations of the binding energies (and diffusion rates) for these cations as related to terrace, step, and kink sites on the calcite surface, (3) vertical scanning optical interferometry (VSI) measurements of overall dissolution and local dissolution rates as influenced by pit formation and precipitates, (4) synchrotron x-ray, surface analysis and other measurements of impurity concentration, locations and binding energies. Impurity interactions will range from single-site adsorption to surface and step incorporation and nano-phase precipitation. The combined efforts will provide new insight regarding interactions of impurities with specific sites on the calcite surface and their impact on dissolution.

Results: The differing impacts of a variety of metal cations on dissolution and growth reactions on the calcite surface have been examined using in-solution atomic force microscopy (AFM) and other methods. The addition of manganese (Mn^{+2}) to the solution at concentrations above $0.5 \mu\text{M}$ inhibits the dissolution of calcite, but when concentrations reach $1 \mu\text{M}$, a new phase forms on the surface. This new phase is rod-like with lengths up to microns long, a well defined constant thickness of 8 atomic layers and widths of approximately 200 nm. The cross section of this mixed $\text{Mn}_x\text{Ca}_{1-x}\text{CO}_3$ nano phase has been modeled using a Glued Wetting Layer Model. A comparison of the calculated and experimental cross sections of these nano rods is shown in Fig. 1. Although the width of the rod appears to fit this energy minimization model, the elongated shape is partially determined by a very rapid rate of adsorption at specific kink sites.

An effort to link molecular-scale to more macroscopic observations is made through the use of vertical scanning interferometry (VSI), which can rapidly and non-invasively map the topography of surfaces with a vertical resolution of $<1 \text{ nm}$ and a focal depth on the order of mm. Currently, the areal field of view of the technique is on the order of 1 mm^2 with horizontal resolution of about $1 \mu\text{m}$. Thus, VSI combines a vertical resolution close to that of AFM with the rapid data collection (on the order of a few seconds), large focal depth, and large field of view typical of optical microscopy. The large depth of focus, in particular, allows for precise

measurements (ca. 1% relative) of surface-height over an area larger than possible for scanning probe microscopy. As such, vertical scanning interferometry, provides complementary information to the AFM that facilitates scaling of microscopic processes to bulk rates. The Mn^{+2} system has been studied by both AFM and VSI. For this system the impact of solution chemistry on overall dissolution rate as determined by VSI and step velocity as determined from AFM are in excellent agreement.

The impacts of the addition of other cations to the solution, such as Sr^{2+} , Co^{+2} , Ca^{+2} and Mg^{+2} are under investigation. Although Sr^{2+} , Co^{+2} , Ca^{+2} and Mn^{+2} in solution slow dissolution of calcite, adding Mg^{+2} to the solution enhances the rate of dissolution. Whereas many of the impurity effects we observe can be explained by site blocking in a terrace ledge kink model, the impact of the Mg^{+2} may also involve changes to the surface or step energy.



Glued wetting layer model prediction of MnCaCO_3 precipitate cross section.

Structure and Reactivity of Iron Oxide and Oxyhydroxide Surfaces

J.R. Rustad, (509) 376-3979, fax (509) 376-3650, james.rustad@pnl.gov; A.R. Felmy 509-376-4079; fax 509-376-3650; ar.felmy@pnl.gov, D.A. Dixon (509) 372-4999, fax (509) 376-3650; david.dixon@pnl.gov; M. Dupuis (509) 376-4921, fax (509) 376-0420, michel.dupuis@pnl.gov

Objectives: This project is focused on developing large-scale molecular dynamics simulation methods to better understand chemical speciation at oxide-water interfaces.

Project Description: Through assimilation of the results of diverse experiments in surface science, aqueous chemistry, crystal chemistry and accurate *ab initio* electronic structure calculations, we are constructing a comprehensive simulation capability for oxide-water interfaces. Components of these simulations include reactive surface functional groups, sorbing anions and metals, and explicit calculation of the influences of solvent and the electric double layer. Massively parallel computer codes using this simulation model are being applied to problems having length scales of 5-10 nanometers. Within the last year, we have been using this capability to investigate redox reactions involving ferrous iron and Cr(VI,V,IV) both in aqueous solution and at the iron oxide-water interface.

Results: Umbrella sampling molecular dynamics methods are being used to study redox processes involving ferrous iron and Cr(VI,V,IV) species in solution and at ferric oxide surfaces. The molecular dynamics potential model was compared with *ab initio* calculations on water and proton binding energies for $\text{Fe}(\text{H}_2\text{O})_6^{3+}$, $\text{Fe}(\text{H}_2\text{O})_6^{2+}$, $\text{Fe}(\text{OH})(\text{H}_2\text{O})_5^{2+}$, $\text{H}_n\text{CrO}_4^{n-2}$, $\text{H}_n\text{CrO}_4^{(n-3)}$, and $\text{H}_n\text{CrO}_4^{(n-4)}$. It has also been benchmarked against known redox potentials of Fe in aqueous solution as a function of pH. We have found, for example, that the calculated energy difference between Fe(II)-Fe(III) hydroxo-aquo complexes correlates perfectly with the measured redox potential of the same couples in aqueous solution. Likewise, the hydroxide binding energies of $\text{Cr}(\text{OH})_4^{(+2,+1,0)}$ for Cr(VI,V,IV) correlate perfectly with the *ab initio* calculations. This indicates that the tight binding approximation is actually quite reasonable, and the zero level of energy can be defined with respect to the ionization potential of Fe(II) and the electron affinity of Cr(VI,V,IV) without loss of generality. The umbrella sampling technique is the same as that used by the pioneering study of Kucharski et al (1988) (J. Chem. Phys. 89, 3248). The possibility of extending this work, coupling the electron transfer with proton transfer, which is possible in our approach, opens up a whole new realm of fundamental redox processes for computational investigation.

In our initial studies we have placed $\text{Fe}(\text{OH})_2$ and H_2CrO_4 in a solution of 210 water molecules at fixed distances from 5-10 Å. For this composition the system contains $\text{Fe}(\text{H}_2\text{O})_6^{2+}$, HCrO_4^- , and OH^- . As the electron is gradually transferred, by slowly changing the Fe charge to 3+ and the Cr charge to 5+, the species evolve towards $\text{Fe}(\text{OH})_2(\text{H}_2\text{O})_6^+$ and H_2CrO_4^- , that is the electron transfer is coupled with hydroxide complexation by the Fe(III) and proton transfer to Cr(V). Further investigations will focus on barriers to redox reactions and the changes that occur in the speciation and barriers in interfacial geometries. Our recent prediction of an interfacial hydroxide ion layer could play a large role in facilitating the transfer of an electron from Fe(II) in the vicinity of the interface due to stabilization of Fe(III) by the hydroxide ions. Such an interfacial mechanism involving near-surface aqueous hydroxide ions may be more appealing than direct catalysis involving surface complexation (i.e. involving Fe-O-Fe bonds) because of the less restrictive steric factors involved in the aqueous mechanism.

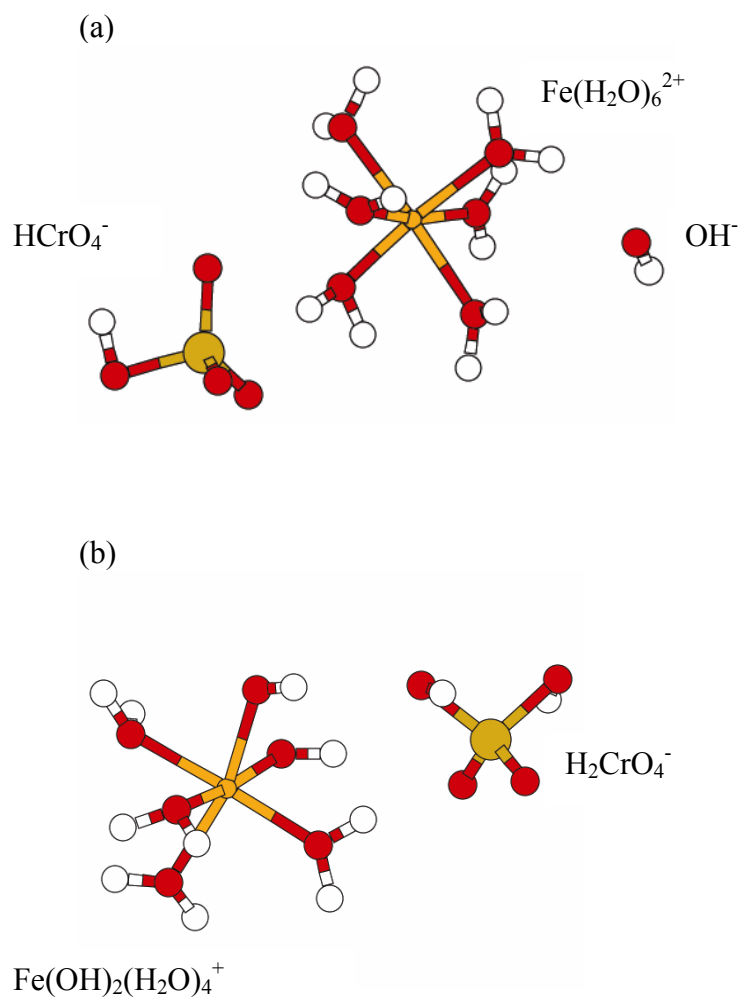


Figure 1. Simulated electron transfer between Fe(II) and Cr(VI) where the fraction of the electron transferred, δ_e , is (a) 0.0 and (b) 0.75, that is, for the electronic configuration Fe(2.75)-Cr(5.25). By $\delta_e=0.75$, the chromate species has changed from HCrO_4^- to H_2CrO_4^- . The images are from simulations embedded in 210 water molecules (not shown). Fe-Cr distance is fixed at 5 Å in these images.

Molecular Basis for Microbial Adhesion and Geochemical Surface Reactions in Fe-reducing Bacteria: A Study Across Scales

T.P. Straatsma, (509) 375-2802, fax (509) 375-6631, tps@pnl.gov; D.A. Dixon (509) 372-4999, fax (509) 376-6631, david.dixon@pnl.gov; A.R. Felmy (509) 376-4079, fax (509) 376-3650, ar.felmy@pnl.gov

Objectives: This project is focused on developing the theoretical understanding of the processes in subsurface environments that determine the uptake of ions by bacterial membranes and the adsorption of bacteria to geochemical surfaces.

Project Description: Using molecular level *ab initio* electronic structure calculations of small molecular clusters, molecular dynamics investigations of large molecular systems, and predictions of macroscopic geochemical reactions using thermodynamic and kinetic models, a theoretical modeling capability is developed for the study of the interactions of lipopolysaccharides located on the outer membrane of gram-negative bacteria with mineral surfaces and how such interactions affect metal uptake and mineral dissolution. This modeling capability will be applied to better understand and predict the molecular processes involved in microbial metal binding, microbial attachment to mineral surfaces, and, eventually, oxidation/reduction reactions (electron transfer) that can occur at these surfaces and are mediated by the bacterial exterior surface. This project focuses on the LPS membrane of *Pseudomonas aeruginosa*, a ubiquitous bacterium found in the subsurface.

Results: An accurate molecular model for the lipopolysaccharide (LPS) molecule of *Pseudomonas aeruginosa* has been developed, and used to construct a model for the LPS outer membrane. Molecular dynamics simulations of this membrane have been carried out. Calculated properties from this model agree very well with available experimental data for this type of membrane. The calculated surface area per lipid unit is 0.40 nm^2 , and in excellent agreement with the experimental value of 0.41 nm^2 . The calculated potential difference across the membrane of 85 mV compares well with reported experimental values of 100 mV for similar LPS membranes. Analysis of the simulations have identified specific structural and energetic properties of the membrane that are of importance for the way the membrane provides ion binding sites, and interacts with external mineral surfaces. To study the interaction of LPS membranes with mineral surfaces, a molecular model for the 110 face of goethite has been developed that is consistent with the biomolecular force field used in the model of the LPS membrane. A computational mineral fragment model has been designed to reproduce the electrostatic potential of a periodic slab.

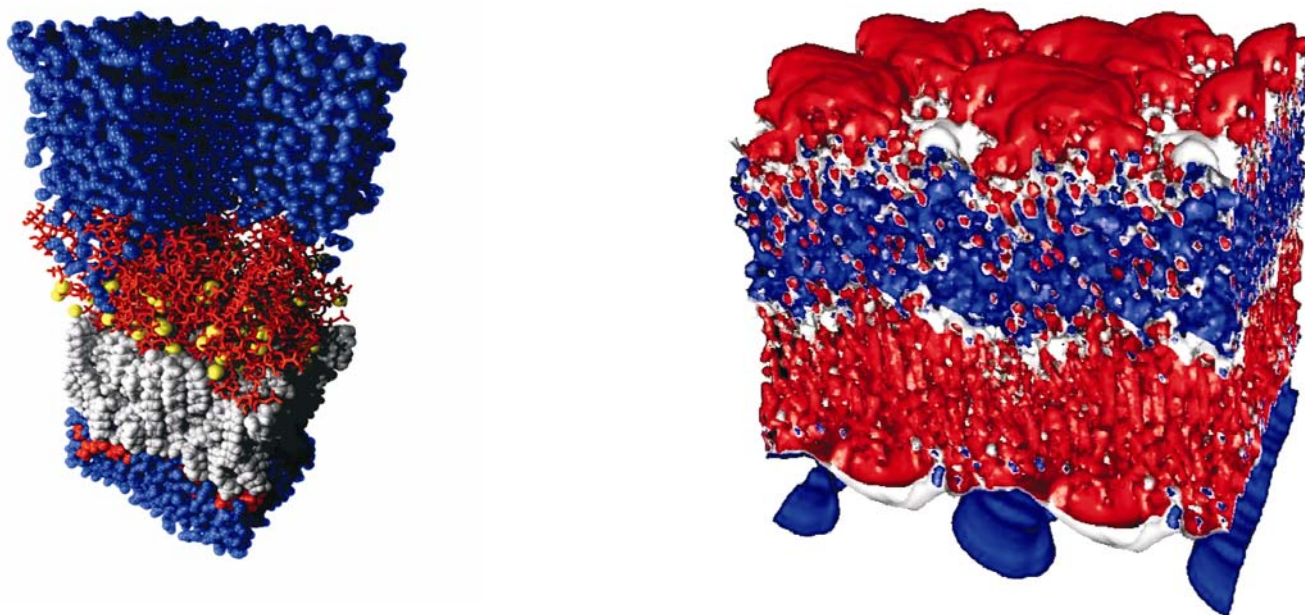


Figure 1. Molecular structure (left) and electrostatic potential shown as the isocontours at -150 mV in red and $+150$ mV in blue (right) of the assembled LPS membrane of *Pseudomonas aeruginosa*.

Interactions Between Fe(III)-Reducing Bacteria and Fe Oxides: Microbial and Geochemical Dissolution Controls

J. M. Zachara, (509) 376-3254, fax (509) 376-3650, john.zachara@pnl.gov; J. K. Fredrickson (509) 376-7063, fax (509) 376-1321, jim.fredrickson@pnl.gov; K. M. Rosso (509) 376-7762, fax (509) 376-3650, kevin.rosso@pnl.gov; C. Liu (509) 376-0129; fax (509) 376-3650, chongxuan.liu@pnl.gov

Objectives: The bacterial utilization of Fe(III) oxides as an electron acceptor is an important, but poorly understood component of the iron biogeochemical cycle. Such utilization alters the surface and internal properties of the Fe(III) oxide, and markedly changes their overall physicochemical behavior and reactivity. Research is underway in this project to better define the interfacial electron transduction process between bacteria and Fe(III) oxides, and to explore the implications of such electron transfer to Fe(III) oxide surface chemistry and solid phase transformations.

Results: Recent research has focused on three activities: 1.) a scanning probe microscopy study of the evolution of surface structure on tabular hematite that accompanied bacterial reduction by *Shewanella putrefaciens*, 2.) a kinetic, spectroscopic investigation of the reduction rates of different morphologic types of hematite by bioreduced, anthraquinone disulfonate (an electron shuttle compound known to stimulate electron transfer from bacteria to Fe(III) oxides), and 3.) a Mossbauer spectroscopic evaluation of the biogeochemical mechanisms involved in the bacterial transformation of ferrihydrite (a poorly crystalline Fe(III) oxide) to green rust (a highly reactive layered Fe(III)/Fe(II) hydroxide). We have made many important findings. *S. putrefaciens* (our test organism) has been shown to utilize a non-local electron disposal mechanism involving a soluble electron transducing agent. Electron flux is not directed through the organism/oxide contact region as originally believed. Also found is that the fundamental rate of electron transfer through direct organism-oxide contact is quite slow. The biomineralization process has been found to be complex, with dependencies noted on thermodynamics, rate of electron supply, and presence/absence of minor sorbed and aqueous ions that may inhibit or catalyze solid-phase rearrangement. Shown in Figure 1 are Mossbauer spectra of a Si-containing ferrihydrite after 0, 1, and 8 days exposure to an iron-reducing bacterium. Ours is the first report of the biosynthesis of this mineral phase, which occurs only in the presence of trace phosphate and only at specific, bacterially regulated Fe(II) flux rates. Next years research will continue to explore kinetic issues involved in bacterial electron transduction to Fe(III) oxides, and biogeochemical and mineral physical factors controlling the nature of biomineralization products.

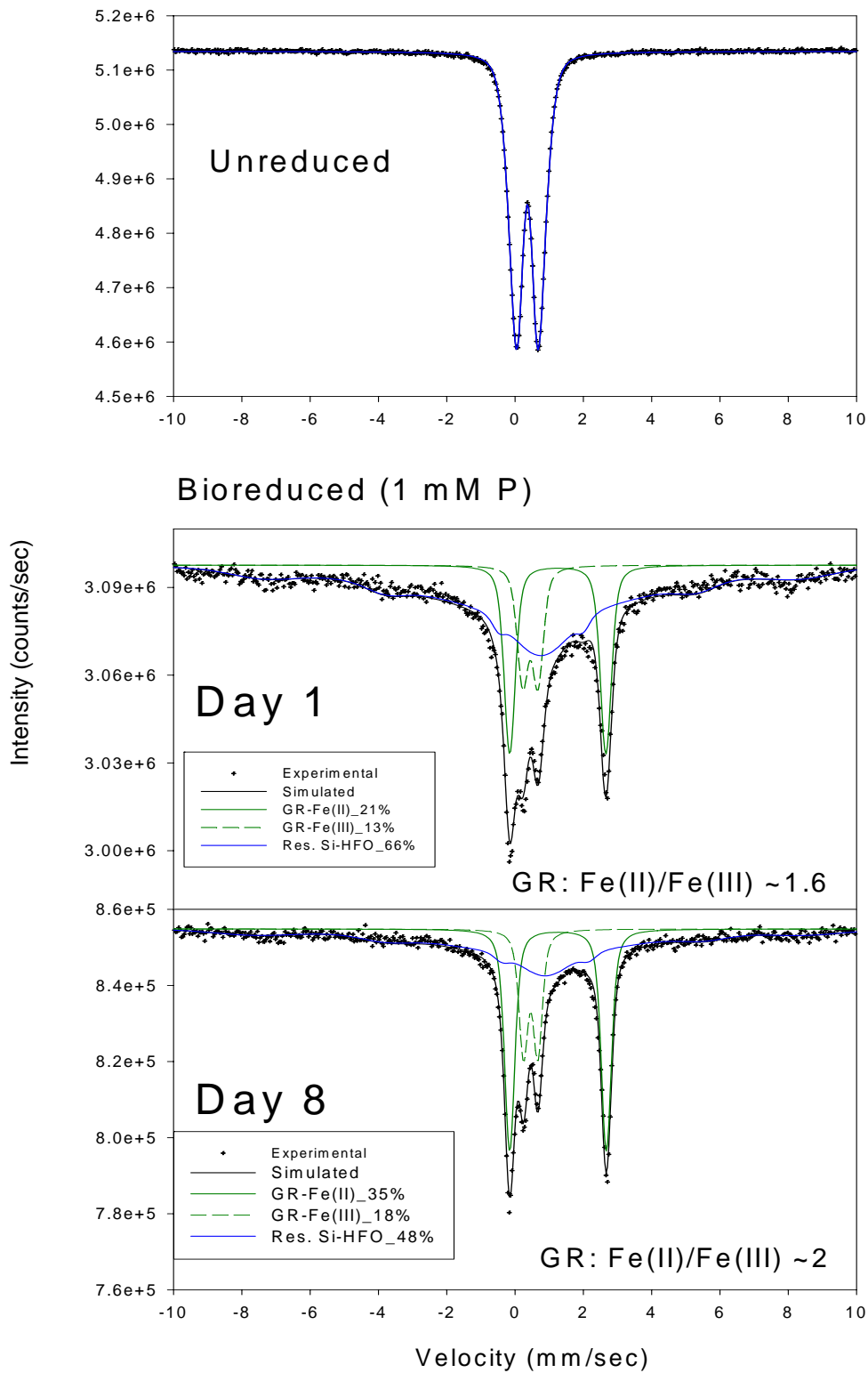


Figure 1. Mossbauer spectra of Si-containing ferrihydrite after 0, 1, and 8 days exposure *S. putrefaciens*. The ferrihydrite is transformed to carbonate-green rust by the bacteria. The Fe(II)/Fe(III) ratio changes with incubation time and structural carbonate originates from the bacterial metabolism of lactate that was added as a carbon source. Residual, but more crystalline ferrihydrite remains.

SANDIA NATIONAL LABORATORIES

Lockheed Martin
Albuquerque, New Mexico 87185

Contract: DE-AC04-94AL85000

CATEGORY: Geophysics

PERSON IN CHARGE: Henry R. Westrich

Evolution of Fracture Permeability

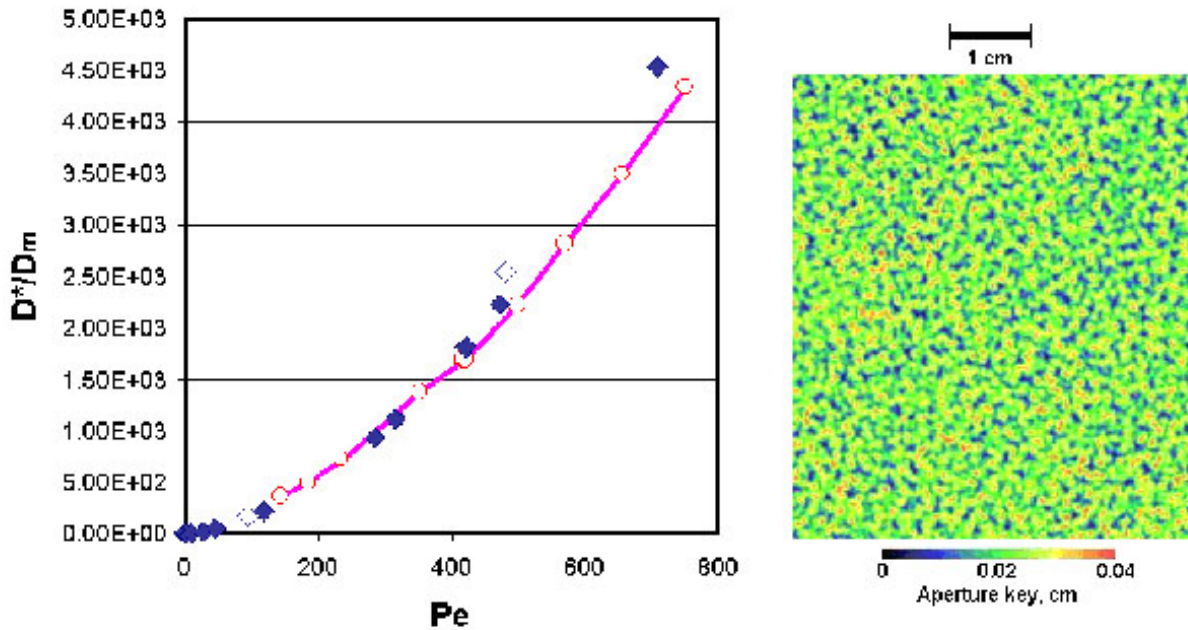
*Harlan W. Stockman, (702) 363-8522, hwstock@sandia.gov; C. Jove-Colon; S. Brown
New England Research*

Objectives: To develop and test models for dissolution/precipitation in fractures, particularly fracture intersections.

Project Description: The Geochemistry Department at Sandia is modeling a set of dissolution/precipitation experiments. The experiments are performed by S. Brown of New England Research, and are described elsewhere in this summary document. The tests involve water and brine flow through intersecting fractures in polycrystalline gypsum.

The purpose of the modeling is to extend the range of the experiments, by varying conditions that are difficult or impossible to vary in the laboratory. In addition, by providing detailed maps of concentration and velocity variations, the modeling elucidates the causes of dissolution, precipitation, and enhanced mixing along fracture planes and at fracture intersections. The models help determine which, of competing hypotheses, best explain the observed dissolution patterns.

Results: In FY02, modeling efforts were concentrated on validation for flow in very large (30 million node) simulations. We obtained good agreement with the dispersion experiments of Detwiler et al. (Water Resources Research, v36, p 1611), as shown in the figure below. The lattice Boltzmann (LB) codes were optimized (up to factor 20 improvement in speed), and new boundary conditions added. A key aspect is the validation of models for surface reaction; we are cooperating with the Ford Bone and Joint Center to model reaction and precipitation in human bone, and this collaboration will provide valuable experimental constraints. In addition, rotating-disk measurements are underway at Sandia to determine dissolution rate laws for polycrystalline gypsum, as a necessary constraint on models for the full-scale fracture experiments.



Comparison of LB and Experimental Results for Dispersion (D^*) as function of Peclet Number. Left: The pink line and circles are experimental results; the filled and open diamonds are LB calculations for symmetric (more probable) and asymmetric apertures. Right: a portion of the experimental aperture field.

Micromechanical Processes in Porous Geomaterials

Joanne T. Fredrich, (505) 844-2096, fredrich@sandia.gov; Teng-fong Wong, State University of New York at Stony Brook

Objectives: This project focuses on the systematic investigation of the microscale characteristics of natural earth materials, and how these micro-scale characteristics control the macroscopic deformation and transport behavior. The research uses an integrated approach consisting of experimental rock mechanics testing, quantitative 2D and 3D microscopy and statistical microgeometric characterization, and theoretical and numerical analyses. The objective is to enhance fundamental understanding of failure and transport processes in geologic materials, and thereby strengthen the theoretical basis for the application of laboratory results to various technological operations of importance.

Project Description: Knowledge of the microscale characteristics and behavior of rocks is important for several energy-related applications, including global climate change and carbon management; oil field geoscience; geotechnical engineering efforts such as design and assessment of geologic nuclear waste repositories; and environmental remediation efforts at contaminated DOE and/or DoD installations. We use an integrated approach consisting of experimental rock mechanics testing, quantitative microscopy, and theoretical and numerical analyses. The experimental investigation provides a detailed understanding of the microstructure

of geologic materials and how the microscale characteristics affect macroscale behavior including brittle failure and fluid transport. Detailed and quantitative microstructural studies complement laboratory rock mechanics experiments. The results are used to formulate and evaluate theoretical and numerical models of rock deformation and fluid flow.

Results: (1) Some additional quantitative microscopy was performed to complete our study of the micromechanics of compaction in an analogue reservoir sandstone. Revisions to a manuscript based on this work that was submitted and accepted for publication in Spec. Publ. Geol. Soc. Lond. were completed. (2) Quantitative three-dimensional image analysis of several synchrotron computed microtomographic experiments performed at the APS on pristine and deformed samples of Castlegate sandstone and synthetic sandstones has been performed to derive two-phase descriptions of the porous medium. We continue to collaborate with W. Brent Lindquist in this area, and we apply his 3dma code developed under his separate BES funding in our work at Sandia. (3) The processed three-dimensional image data for the four samples of synthetic sandstone at resolution of 3.34 micron were mapped to our three-dimensional lattice Boltzmann (LB) single-phase fluid flow simulator and used to derive numerical predictions of intrinsic permeability. The numerical data were compared with direct laboratory measurements of intrinsic permeability performed on the same samples. Results were presented at the 2000 Fall AGU meeting and a manuscript is in preparation. (4) Analysis of the synchrotron microtomographic data sets collected on Castlegate sandstone (that are significantly larger in size than the synthetic sandstone data sets), is in progress. LB flow simulations have been performed on several subsets of the experimental image data, and those results as well as quantitative three-dimensional microstructural analysis, are being analyzed further.

The Physics of Two-Phase Immiscible Fluid Flow in Single Fractures and Fractured Rock

Robert J. Glass, (505) 844-5606, rjglass@sandia.gov; H. Rajaram University of Colorado, Boulder; M. J. Nicholl University of Idaho

Objectives: Employ detailed physical experiments and high-resolution numerical simulations to develop a quantitative understanding of the critical processes controlling two-phase flow and transport in fractures. Fundamental understanding may subsequently be abstracted for application to large-scale problems in petroleum extraction, isolation of hazardous or radioactive waste, remediation of subsurface contaminants, and CO₂ sequestration.

Project Description: Under two-phase immiscible flow conditions, fluid flow and solute transport characteristics of the fracture are controlled by the geometry of the respective phases. In turn, phase geometry is determined by a combination of aperture variability, phase accessibility, capillary and viscous effects associated with the two-phase flow processes themselves, and external forces such as gravity. Also, if one of the fluids is slightly soluble in the other, mass transfer between the phases will influence phase geometry.

In this collaborative project between Sandia National Laboratories, the University of Colorado at Boulder, and the University of Idaho, systematic physical experimentation is coupled with concurrent numerical simulation to explore the factors controlling phase geometry, flow, transport, and inter-phase mass transfer in rough-walled fractures. A high-resolution light-transmission technique has been developed to allow accurate experimental measurements (aperture, phase geometry, solute concentration) in transparent analog fractures. Use of this technique will lead to data of unprecedented accuracy for evaluating current understanding of fundamental processes, and motivate refinement of theoretical concepts.

Results: A depth-averaged model was developed for dissolution of a non-aqueous phase liquid (NAPL) entrapped in a variable aperture fracture. The model couples fluid flow, transport of the dissolved NAPL, inter-phase mass transfer and NAPL-water interface movement. The relevant fundamental processes are incorporated at appropriate levels of resolution and thus our model does not require any empirical parameters to describe inter-phase mass transfer. Model simulations were compared to a NAPL dissolution experiment carried out in a transparent analog glass fracture (15.4 x 30.3-cm) under constant flow conditions. The evolution of the entrapped NAPL geometry during dissolution was measured using our high-resolution light-transmission techniques, at a 0.0155 x 0.0155-cm resolution. The model accurately predicted both the change in overall NAPL saturation with time, and the evolution of the entrapped NAPL geometry. This is perhaps the first instance of close agreement between simulations and experiments on NAPL dissolution without any empirical treatment of inter-phase mass transfer.

In comparison to a saturated fracture, transient solute transport through a variable aperture fracture containing an entrapped fluid phase will be characterized by enhanced dispersion and pronounced non-Fickian behavior. Transport experiments in a partially saturated fracture were used to evaluate a three-dimensional particle-tracking simulator, which employs a quasi-three dimensional velocity field based on the Reynolds equation. The particle-tracking model was in qualitatively good agreement with experiments. It was able to predict 85% of the relative increase in dispersion resulting from the entrapped phase. It also reproduces the experimentally observed nonlinear relationship between solute dispersion and Peclet number, which suggests that Taylor dispersion effects are potentially significant even in partially saturated fractures.

Understanding and Predicting Solute Transport in the Presence of Multiple Time-Scales of Diffusion and Sorption

Lucy C. Meigs, (505) 844-2375, lcmeigs@sandia.gov; Roy Haggerty, Oregon State University; Charles Harvey, Massachusetts Institute of Technology

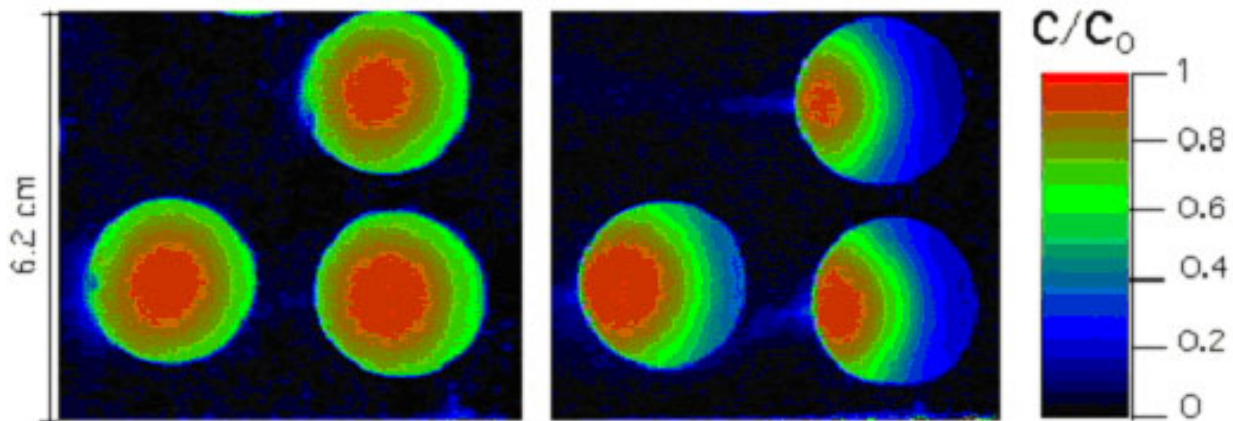
Objectives: This research seeks: (1) to determine when small scale permeability structures cause solute spreading to be dominated by classical dispersion and when it causes solute spreading to be dominated by mass transfer; and (2) to develop models for predicting the effects of mass transfer over diverse time and length scales.

Project Description: Our approach is to conduct numerical simulations and laboratory experiments in heterogeneous media using conventional column techniques and novel transport visualization techniques. We are conducting numerical and laboratory experiments (1) to map transport regimes (conditions under which different equations adequately describe transport), (2) to apply mass transfer models developed at one time and space scale to larger scales, and (3) to investigate reactive transport with mass transfer.

Results: Numerical simulations and experimental work demonstrate that the upscaled solute transport behavior of a conservative solute is determined, not only by the standard spatial statistics of hydraulic conductivity, but also by the connectedness of the hydraulic conductivity field. Results demonstrate that hydraulic conductivity fields with the same standard spatial statistics may, or may not, produce mass-transfer behavior in a conservative solute depending on the connectedness characteristics of the media. Furthermore, mass transfer may be driven by both diffusion and advection.

We have developed a method, using tracer experiments conducted at different velocities, to construct a residence time distribution for the immobile domain that describes mass transfer by diffusion in heterogeneous media over a wide range of time scales. The scaling behavior of breakthrough curves can be predicted with this residence time distribution. For media with multiple rates of mass transfer, the use of the traditional single-rate model (i.e., exponential residence time distribution) gives poor predictions of transport when the scale of experiments and predictions differ. Our work has also shown that mass transfer driven by advection is important in some cases (see Figure). Building upon the diffusion work, we have begun to extend our residence-time methodology to fully capture both advective and diffusive mass transfer.

We have also developed a method using colorimetric chemical reactions to visualize reactive transport in porous media. Using this method we have demonstrated that commonly used models that assume perfect mixing between two reactants at the pores scale as they are transported through a porous media can over predict the product formed. We have begun to make the first steps toward quantifying reactive transport in a highly heterogeneous medium, something that will have wide applicability to subsurface transport problems.



Comparison of solute concentration within low permeability regions for experiments conducted in two different transport regimes. The flow rate (1.32ml/min) and elapsed time (approx. 525 min.) are the same for both the diffusive mass transfer (left) and advective mass transfer (right) regime images. The right-hand figure, where solute is transported in and out of the bleb via advection, clearly shows the importance of advective mass transfer.

Modeling of Mesoscale Phenomena During Sequestration of Carbon Dioxide in Porous Reservoirs

*Lisa Mondy, (505) 844-1755, lamondy@sandia.gov, A.Graham, Texas Tech University;
M. Ingber, University of New Mexico*

Objectives: The purpose of this program is to combine experiments, computations, and theory to make fundamental advances in our ability to predict transport phenomena in concentrated, multiphase, disperse systems, particularly when flowing through geologic media.

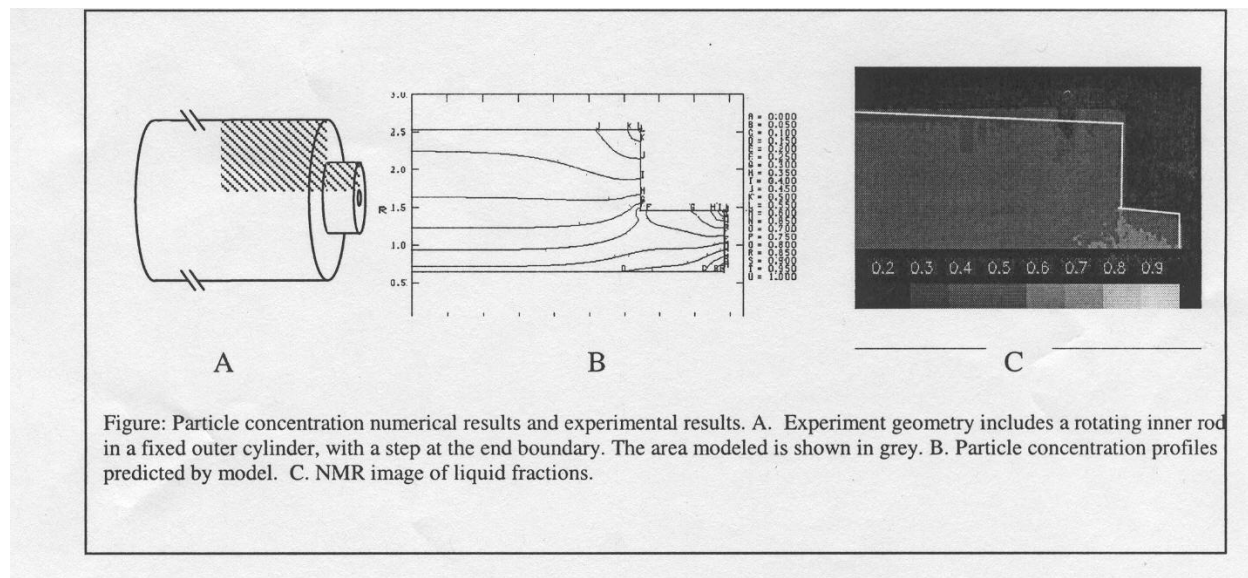
Project Description: Processes for the sequestration of carbon dioxide in porous reservoirs involve several components of multiphase flows. If hydraulic fracturing is used to develop local "sweet spots" (zones of high permeability), the flow and resulting distribution of the proppant can have a large impact on the subsequent sequestration process. Even without hydraulic fracturing, the creation of precipitates can drastically alter the characteristics of the porous formation itself. Furthermore, emulsions can form and fingering can take place at the supercritical CO₂/brine interface. In order to be of use in designing effective CO₂ sequestration processes, significant enhancements to currently available continuum-level suspension flow models are required. Both experimentation and high performance computing at the mesoscopic level are used to obtain microstructural information that is necessary for the development and refinement of the continuum models.

Results: The continuum models originally developed by Phillips et al. (1992) and Nott and Brady (1994) have been improved and implemented into a general-purpose finite element computer code. Results show good agreement with experimental measurements based on nuclear magnetic resonance (NMR) imaging in idealized three-dimensional flows (see Fig.)

Normal stress contributions are modeled, which results in accurate predictions of suspended particle migration in curvilinear flows. The improved model also allows for non-neutrally buoyant particles and non-Newtonian suspending liquids.

Massively parallel computing has allowed particle level simulations, based on the boundary element method (BEM), with up to three thousand particles. Volume averaging of the stress tensor has been added to the codes to allow prediction of average macroscopically observed transport properties from particle scale simulations. These simulations lead to detailed information on individual particle and fluid motion that is unobtainable through experiments. For example, highly accurate transient calculations of collections of particles in nonlinear shear fields have demonstrated that particles in inhomogeneous shear fields migrate in the direction of the lower shear rate. This is, to our knowledge, the first explanation of this phenomenon from first principle physics. These very fundamental studies are elucidating the fundamental physics that govern the particle transport phenomena in multiphase systems.

This work is complemented by experimental work to provide insights and benchmarks. A study of apparent particle slip in confined geometries has been performed. Due to the finite size of the particles, suspensions of particles form a boundary layer near containing walls. The walls impose an ordering of the particles that extends several particle diameters into the bulk suspension. In constrained geometries such as the small channels in porous media, this boundary layer can extend over the entire channel. NMR imaging is used to determine the mesoscale structure and falling and rolling balls are used to investigate the mechanical properties at locations ranging from the centerline to the walls of the containing cylinder. It was found that there exists markedly non-Newtonian wall effects in concentrated suspensions in which the volume fraction of particles is greater than 0.2. At these higher concentrations, wall effects are much larger and extend further into the suspension than in Newtonian fluids.



Three Dimensional Electromagnetic Inversion

Gregory A. Newman, (505) 844-8158, ganewma@sandia.gov; D. L. Alumbaugh, University of Wisconsin-Madison

Objectives: This project seeks to develop a three-dimensional imaging capability for transient electromagnetic fields in a manner similarly developed for seismic wavefields for high resolution imaging of the subsurface. Specific applications considered include the characterization of DOE hazardous waste sites and nuclear waste repositories, oil and gas exploration and monitoring of sequestered CO₂ in gas-depleted reservoirs.

Project Description: The objective of this project is to develop a full 3D inversion capability for transient electromagnetic fields. Although the development of practical multidimensional TEM inversion methods are just beginning, seismic imaging techniques have advanced the idea of back propagating or migrating the wavefield into the earth in order to image the subsurface. By applying a similar concept for electromagnetic fields, imaging algorithms will be developed, which employ either a conjugate gradient search or a full Newton iteration for an optimal solution. These algorithms will be governed by the diffusive Maxwell's equation and is efficiently implemented by back propagating the data residuals into the model. To achieve realistic model complexity, the algorithms will use finite difference methods for computing the predicted data and cost functional gradients and matrix-vector products required for the Newton iteration. Parallel computing platforms will also be utilized for reasonable computation times.

State of the practice TEM data analysis employs layered (1D) inversion of individual 'soundings', and then 'stitching' the results together to provide a 2D or 3D interpretations. This can result in artifacts and misinterpretation in areas of complex subsurface structure. Code development occurring at Sandia National Laboratories under this project is providing forward and inversion algorithms that can properly account for complex 3D geometries. Simulations at the University of Wisconsin are employing the new codes to analyze problems important to the DOE. Specific topics being addressed include crosswell and singlewell monitoring of CO₂ sequestration processes, and identifying where standard TEM processing breaks down when inverting data collected over dipping structures. The various analyses involve; 1) visualizing the current systems that are induced by a rapidly terminating current source in or over a 3D model; 2) analyzing and comparing the data that would be measured by different source-receiver configurations and offsets; 3) using linear inversion theory to define how the spatial sensitivity of the different source-receiver configurations to the 3D model changes over time; 4) 1D inversion of simulated profile data over various 3D structures to determine artifacts that develop in the resulting images.

Results: Implementation of the 3D finite difference modeling code on single and parallel processors is now completed. This code solves the diffusive Maxwell equations in the presence of the air-earth interface, using an explicit time stepping scheme and has been check for a range of simple earth models. Both loop and grounded source fields can be simulated. A borehole version of the code, which neglects the air-earth interface condition, is also available. This later code is now being employed in an experiment design study to access the applicability of the

TEM method for monitoring sequestered CO₂. Both non-linear conjugate gradient and Newton solutions, using the finite difference code, are also under development and will employ back propagation to efficiently compute the functional gradients and matrix-vector products required for the Newton iteration. Parallel versions of these inversion algorithms are to be completed within the next few months.

The forward modeling codes developed at Sandia has been employed to simulate measurements made before and after a CO₂ flood in the Maljamar Oil Field of New Mexico; the reservoir model was provided by scientists at Lawrence Livermore National Laboratories. Preliminary modeling using simulation of measured fields at receiver positions and current visualization has shown that a CO₂ injection may be detectable as long as it is injected into a region that is relatively conductive compared to the injection zone itself. A second important finding is that quick (1e-6 seconds) current termination in the transmitter can provide enhanced sensitivity to resistive units at very early times. If the termination time is 1e-5 seconds this sensitivity is lost.

The 'geologic dip' study has shown that if the geology consists of a resistor over a conductor, stitched 1D inversions of central loop sounding data can provide realistic estimates of the true structure up to dips of approximately 27 degrees. In addition, even though artifacts appear for dips that are greater than this value, the artifacts become more focused near the center of the dipping interface; for a 90-degree dip only those stations immediately adjacent to the dipping interface are affected. However, when a conductor overlies a resistor, then the method is very insensitive to the dip-angle. In fact the profile data resulting over a structure that dips at 27 degrees is almost identical to that collected over a vertical-contact.

Effects of fluid flow on inelastic deformation and failure in dilating and compacting rock

W. A. Olsson, (505) 844-7344, waolss@sandia.gov; D.J. Holcomb

Objectives: One of the proposed strategies for mitigation of carbon dioxide emissions is the sequestration of CO₂ in depleted oil or gas reservoirs. For the implementation of this strategy, it is critically important to understand how production of the original contents of the reservoir has changed the stress and deformation states and the properties of the rocks making up the reservoir trap. For example, certain low-permeability deformation structures, such as compaction bands and shear bands, may compartmentalize a hydrocarbon reservoir before or during production. Thus, inelastic deformation resulting from tectonic stress or stresses created during production of oil or gas, or reinflation with CO₂, may produce structures that interfere with fluid migration and make the reservoir unattractive as a potential producer of oil and gas or repository of CO₂.

Project Description: We are applying coordinated experimental and theoretical techniques to the problem of nonhomogeneous compaction through an existing university-national laboratory collaboration. J. W. Rudnicki at Northwestern University, is addressing the theoretical and numerical aspects; and W. A. Olsson and D. J. Holcomb at Sandia National Laboratories are designing and carrying out the experimental part of the program. Deformation experiments are

being performed on porous sandstone characteristic of oil and gas reservoirs. There are three main objectives of this work: (1) Illuminate the phenomenology of dilatant/compactive rock containing pore fluid in the drained and the undrained response, and test predictions of developing theory. Triaxial compression experiments on Castlegate sandstone (porosity = 28%) under certain conditions lead to nonuniform compaction. We wish to better understand the dynamics of the compaction process in these experiments and to determine the parameter space over which nonuniform compaction occurs. (2) Collect the appropriate constitutive data constrained and suggested by developing theoretical models. Because porous rock is known to have a cap on the yield surface, this is being addressed especially with regard to its relation to nonuniform compaction. (3) Design well-posed experiments that can be used as validation tests against a numerical implementation of the theory to be developed as part of this research.

Results: We measured permeability across compaction bands during their formation and subsequent propagation. Acoustic emissions (AE) were monitored continuously throughout the experiments, allowing spatial and temporal location of the events. In addition, simultaneous fluid flow measurements were made axially across the specimens during the experiments. Permeability changed by one order of magnitude as shear stress was increased to peak stress, which is associated with the development of the compaction bands. The apparent permeability was found to drop dramatically upon formation of one or more compaction bands, and then continued to decrease steadily with propagation of the bands across the specimens. The change in apparent permeability as the AE zones traverse the specimens was an additional 2 orders of magnitude.

A Systematic Study of Heterogeneity, Instrumentation, and Scale Using Physical and Numerical Experimentation

Vincent C. Tidwell, (505) 844-6025, vctidwe@sandia.gov; John L. Wilson, New Mexico Institute of Mining and Technology

Objectives: The goal of this research is to enhance fundamental understanding of upscaling processes through systematic physical and numerical experimentation. The acquired understanding will be used to modify and, where necessary, offer alternative models of upscaling. The resulting models will provide the academic and practitioner alike an improved means of characterizing and simulating multiscale, heterogeneous formations.

Project Description: Parameterization of porous media flow and transport models is often complicated by the inability to make measurements at the desired scale of analysis. This disparity in scales necessitates the use of some averaging or upscaling model to compute the required effective media properties. To challenge these models and our associated understanding, laboratory experiments involving the collection of over 200,000 permeability values from six different heterogeneous blocks of rock using six different scales of measurement were conducted. Now efforts are made to generalize these results to a broader spectrum of instruments, scales, and material properties. Specifically, we build upon the concept of the

spatial weighting function to develop theoretical upscaling models for a variety of hydraulic instruments (e.g., pump and slug tests). These investigations are accomplished numerically employing adjoint state analysis. To extend the scales of analysis, these weighting functions are used to interpret existing field-scale data where multiple instruments operating over different scales were used to measure the same material property. Finally, we extend our studies to other parameters by investigating the effects of permeability upscaling on solute transport processes, in particular macrodispersion.

Results: The effects of spatial variability on solute transport are well recognized; however, few data sets provide both visual and quantitative evidence of this relationship. Using X-ray absorption imaging we were able to quantitatively visualize solute transport in an exhaustively characterized slab of rock. Specifically, experiments were conducted on a 30 by 30 by 2.5-cm thick slab of cross-stratified sandstone exhibiting nested scales of heterogeneity. Characterization of the rock slab involved the collection of 8649 permeability measurements from each face of the rock slab using a computer automated gas minipermeameter (0.15 cm ID tip seal). Additionally, the spatial distribution of porosity was measured by way of X-ray absorption imaging (0.25 by 0.25 mm² resolution). Transport experiments were then conducted under steady-state flow conditions using a conservative tracer. Tests were conducted parallel, normal, and diagonal to stratification with both point and line sources subject to slug and continuous tracer injection. Two-dimensional digital images of the solute concentration fields at select times during the tracer experiments were acquired in addition to conventional breakthrough curves. Results show solute pathways to be strongly influenced by the spatial permeability/porosity patterns of the sandstone slab. Specifically, solute dispersion was found to scale linearly with distance when flow was oriented parallel to stratification while complex, non-linear scaling relations were encountered when flows were forced to cross the stratification. Additionally, the calculated dispersion coefficients vary spatially and by the orientation and mode of injection.

The relationship between pore-scale heterogeneity and permeability for a slab of Massillon Sandstone was investigated. Petrographic and scanning electron microscopy analysis were conducted on thin sections (twenty thin sections divided into sextants) taken from one-inch diameter core samples, while permeability data were collected with a gas minipermeameter from both the core samples and the rock slab (collected prior to coring). Results suggest surprisingly poor correlation between the measured pore characteristics and the calculated permeability. We ascribe this poor correlation to the diagenetic history of the rock sample. Specifically, compaction, as well as the precipitation of authigenic iron oxide, quartz overgrowth cement and clay minerals acted to reduce permeability, whereas secondary porosity created by the dissolution of these cements and detrital grains locally increased permeability. This interplay between cement precipitation and secondary porosity dissolution appears responsible for the complex relationship between permeability and pore scale characteristics.

CATEGORY: Geochemistry

PERSON IN CHARGE: Henry R. Westrich

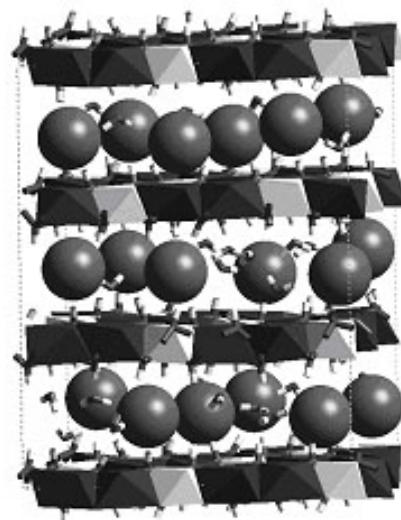
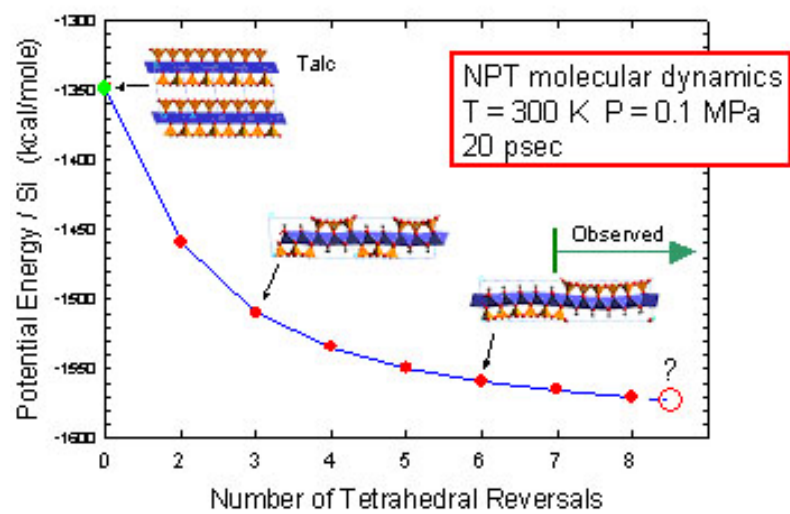
Molecular Simulations of Layered Minerals and their Interaction with Hazardous Wastes

Randall T. Cygan, (505) 844-721, rtcygan@sandia.gov; Louise J. Criscenti; David M. Teter

Objectives: Examine the interaction of selected metal ions, anions, and organic contaminants on the external and interlayer surfaces of layered minerals using various computational chemistry tools. The molecular simulations will improve our understanding of the fundamental mechanisms of adsorption processes and may help to predict and optimize environmental approaches for the mitigation of hazardous waste.

Project Description: Modeling of layered minerals (clays and layered double hydroxides) and their interactions with aqueous solutions combines energy minimization and molecular dynamics methods. One approach uses a fully flexible, empirically derived forcefield to describe the energy of all atomic interactions. Bulk structures, relaxed surface structures, and intercalation processes are evaluated and compared to experimental and spectroscopic findings for validation. More sophisticated calculations incorporate state-of-the-art quantum methods that complement the forcefield models. Ab initio approaches based on density functional theory (DFT) are used to examine the electronic structure of various layered minerals. Massively parallel computers provide the capability to obtain fully optimized periodic structures for large unit cell structures typical for these complex layered minerals. Electron density distributions, deformation maps, HOMO/LUMO extents, and electrostatic potentials are used to evaluate the crystallographic control and mechanisms for contaminant sorption. This project is being performed in collaboration with Andrey G. Kalinichev (University of Illinois), R. James Kirkpatrick (University of Illinois), and Kate Wright (University College of London).

Results: A molecular mechanics forcefield that was developed for modeling hydrous phases was used to simulate the bulk structure of various layered phases, and to examine the swelling behavior of smectite clays such as montmorillonite and beidellite. Molecular dynamics results are in excellent agreement with available crystal structure refinements, and with several quantum optimizations (DFT using GGA) that provide further validation. The clayff forcefield offers a computationally efficient approach for simulating large molecular configurations relating to environmentally important systems such as clays, hydroxides, oxyhydroxides, double layered hydroxides, their interlayers and external surfaces, and aqueous solutions. The accompanying figure provides examples of the theoretical approach for simulating complex phases. The clayff forcefield reproduces the unique wave-like structure and stability of antigorite (left) and the layered structure and chloride interlayer dynamics of hydrotalcite (right).



PART II: OFF-SITE

AMERICAN MUSEUM OF NATURAL HISTORY

Department of Earth and Planetary Sciences,
New York, NY 10024

Grant : DE-FG02-92ER14265

The Influence of Carbon on the Electrical Properties of Crustal Rocks

E.A. Mathez, (212) 769-5379, fax (212) 769-5339, mathez@amnh.org

Objectives: The intent of this work is to comprehend the electrical conduction mechanisms in carbon-bearing rocks and in mantle minerals for the purpose of relating electrical conductivity measured in the field to the nature and origin of carbon in crustal rocks and to temperature in the mantle.

Project Description: Electrical conductivity depends strongly on temperature and on the presence of other phases such carbon, fluids, or ore minerals at the lower temperatures of the crust and basins. One research approach is to measure conductivity of mantle minerals as functions of temperature, orientation, oxygen fugacity $\bar{Y}O_2$, and iron content. These data supply the best models for "electrogeotherms" yet available. Another approach is to document textures of carbon in crustal rocks from basins and metamorphic zones and relate them to rock conductivity. In this case the nature of the carbon is determined by time-of-flight mass spectroscopy (ToF-SIMS) and its distribution determined by electron microbeam techniques in the same samples used for conductivity measurement.

Results: An interdisciplinary workshop attended by forty petrologists and geophysicists from Europe and North America was convened at the American Museum of Natural History on 18-19 April, 2001 to discuss carbon in rocks and its influence of electrical conductivity. The program featured prepared lectures and informal presentations and discussion. Processes of carbon precipitation in fractures, mobility during heating, and redistribution during uplift-exhumation retrograde metamorphism were discussed. While there was general consensus that carbon may cause upper-crustal conductivity anomalies, understanding lower crustal conductivity is more difficult because uplift modifies microstructure and geochemistry, geophysical methods lack resolution, and laboratory experiments do not adequately match conditions. Several issues needing further attention were identified, and a report on the workshop was published in EOS.

A pilot project was conducted using ToF-SIMS to characterize carbons in 3.8 Ga old amphibolite (volcanoclastic sediment) from the Isua greenstone belt, Greenland. Graphitic carbon with $\delta^{13}C$ of about -19 per mil had been found in the rock and interpreted to indicate a biogenic source. The ToF-SIMS work demonstrates the presence of a hydrocarbon fraction, suggesting that some

of the carbon could have been introduced after metamorphism. The questions are how this material formed and how it influences carbon isotopic composition.

ARIZONA STATE UNIVERSITY

Center for Solid State Science
Box 871704
Tempe AZ 85287-1704

Grant: DE-FG03-94ER14414

A SIMS Study of the Chemical Dynamics of Organic/Inorganic Interactions in Sedimentary Basins

Richard L. Hervig, (480) 965-3107, fax (480) 965-9004, richard.hervig@asu.edu; Lynda Williams (480) 965-0829, fax (480) 965-9004, lynda.williams@asu.edu

Objectives: Microanalyses of boron isotopes, along with more common isotopes (N, S, O) in kerogen are being obtained to determine their variation in hydrocarbon-producing sedimentary basins. The goal is to determine the timing of release of these elements from the organic compounds during thermal maturation, and their isotopic fractionation.

Project Description: Analyses of kerogen by secondary ion mass spectrometry (SIMS) may be an ideal method for discovering trace element chemical variations that can be useful in understanding organic/inorganic interactions. SIMS has the unique capability of analyzing trace elements without chemical extraction or mineral separations that often induce isotopic fractionation. Measured changes in minor components of kerogens and clay minerals may be a more useful tracer of the geochemical dynamics of the sedimentary system than the major elements because few (if any) other minerals incorporate B and N at the reaction temperatures of oil and gas maturation, while major elements are involved in a variety of diagenetic reactions. Measured trace element variations will be linked to changes in the major elements (C, O and S isotopes). This integrated trace element and isotopic study of kerogen will test the hypothesis that variations in B and N in diagenetic clay minerals are a result of their release from a hydrocarbon source rock. The results should lead to a better understanding of mass transfer between organic and inorganic components of sedimentary basins and hydrocarbon migration.

Results: The initial efforts of this research through 2001 were to survey the B-content and $\delta^{11}\text{B}$ of a variety of organic kerogen types and thermal maturity. We examined kerogen in polished thin section from type I, II, and III source rocks (Green River shale, Wilcox lignite, New Albany shale and Ghareb limestone). The results showed a large range in B-content (up to 600 ppm), with very light $\delta^{11}\text{B}$ values ranging from -10 to -33‰. It was not possible, however, to focus the primary ion beam on a region that did not overlap silicate material, so some of the analyzed boron may not have been organically bound. Further examinations were made on coals. Samples were selected from the Penn. State Coal Repository, from the Argonne National Lab Premium Coal collection, and from NIST standards. The samples were powders pressed into pellets for SIMS analyses. An aliquot of each coal was washed in mannitol to remove adsorbed-B contaminants, and compared to the unwashed coals. We found that the mannitol washed coals were significantly depleted in B compared to the unwashed coals, but there was little effect on

the measured $\delta^{11}\text{B}$ values. Coals washed in mannitol had B contents ranging from 5 to 150 ppm. The unwashed coals had B contents up to 1370 ppm. We found no correlation between B-contents and ash% (ash content <15%) in the coals. There is a decline in B content with increasing thermal maturity. There is also a correlation between the ratios of B/C and O/C, indicating the decline in B and O with increasing thermal maturity. There is no correlation with H. The $\delta^{11}\text{B}$ values of the coals ranged from -5 to -55‰. These results indicate that organic matter is a source of isotopically light B in thermally mature sedimentary basins.

BOSTON UNIVERSITY

Center for Computational Science and Department of Physics
590 Commonwealth Ave.
Boston, MA 02215

Grant: DE-FG03-95ER14499

Analysis and Interpretation of Multi-Scale Phenomena in Crustal Deformation Processes: Using Numerical Simulations of Complex Nonlinear Earth Systems

*W. Klein, (617) 353-2188, fax (617) 353-9393, klein@buphy.bu.edu; John B. Rundle
(303) 492-5642, fax (303) 492-5070, rundle@cires.colorado.edu*

Objectives: To develop a physical understanding of the origins of geodetic crustal strains in nonlinear geomechanical systems, to examine the space-time patterns and correlations that occur in these systems, and to use these patterns to forecast the future activity that may produce disasters affecting a wide variety of critical energy facilities.

Project Description: The complex earth system generates a variety of phenomena that are highly non-linear and operate over a broad range of spatial and temporal scales. Signatures of these processes include scaling (fractal distributions), global and local self-organization, intermittancy, chaos and the emergence of coherent space-time structures and patterns. We are using massively parallel simulations to model geodynamical effects observed in earthquake systems in order to determine the origin of these phenomena. These investigations and the theoretical efforts done in parallel are particularly aimed at quantifying the limits of predictability for disasters such as earthquakes that occur within the earth system. We are currently continuing our development of the theoretical and computational tools that allow us to both obtain sufficient data on realistic models and to analyze the data we obtain. From these simulations we will then predict geodetic and other deformation associated with impending earthquakes to be tested against Global Positioning System, Synthetic Aperture Radar, seismicity and other field data.

Results: We have made significant advances in several areas. These include:

1) Advances in identification, analysis, and interpretation of multi-scale emergent space-time patterns in numerical simulations of earthquake fault systems. Most computational and theoretical work to date has focused on understanding the behavior of single faults. We studied the types of emergent space-time patterns of earthquake activity that occur on a given interacting fault network, how the patterns scale in space and time, how they are related to the inherently unobservable underlying dynamics of stress accumulation, and their sensitivity to changes in the underlying model parameters. Our results imply that many of the significant dynamical properties of earthquakes, including the form of the Gutenberg-Richter relation for the fault network, can only be understood in the context of the topologically complex network as a whole, rather than of the individual faults.

2) Scale dependence of Self-Organizing Threshold Systems, with Applications to Earthquakes and Other Systems. Threshold systems are known to be some of the most important nonlinear, self-organizing systems in nature, including networks of earthquake faults, neural networks, superconductors and semiconductors, and the World Wide Web, as well as political, social, and ecological systems. All of these systems have dynamics that are strongly correlated in space and time, and all typically display a multiplicity of spatial and temporal scales. In all of these systems, long-range interactions induce the existence of locally ergodic dynamics. The existence of dissipative effects leads to the appearance of a “leaky threshold” dynamics, equivalent to a new scaling field that controls the size of nucleation events relative to the size of the background fluctuations. As part of this year’s research effort, Rundle was a co-organizer (with D.L. Turcotte and H. Frauenfelder, both members of NAS) of the second NAS Arthur M. Sackler Colloquium at the NAS Beckman Center, Irvine, California, held March 23-24, 2001. Topic of the colloquium was “Self-Organizing Complex Systems”.

3) PDPC patterns of earthquakes: Implications for scaling in space & time. Earthquake dynamics are considered to be a paradigm for strongly correlated, high dimensional driven threshold systems such as neural networks and magnetized domains in ferromagnets. In general, these studies have focused on scaling, critical phenomena and nucleation arising from analysis of simulation data, as well as on space-time patterns of activity seen in such simulations. The more difficult problem of understanding the physical meaning of the space-time patterns of activity, leading to new methods to forecast the future evolution of large events in the system, has been only infrequently addressed. During this year, we continued to develop and improve new methods for understanding the observable space-time patterns of activity in driven mean field threshold systems, based on the idea that many of these systems are characterized by pure phase dynamics, whose mathematics is isomorphic to the mathematics of quantum mechanics. Application of these method to earthquake data from a typical, seismically active region, southern California, has shown that the method holds considerable promise for forecasting the temporal occurrence of the largest future events.

4) Green’s functions & analysis of actively deforming regions including volcanoes. we have examined surface deformation in two volcanic regions, Long Valley caldera in California , and Mayon volcano in the Philippines. Our work, as always, has been in collaboration with the Spanish group at the University Complutense de Madrid, under the direction of Professor Jose Fernandez-Torres. In the former case of Long Valley, we modeled both deformation and gravity changes in an attempt to identify possible precursors of an eruption. Our results obtained by inverting these data indicate that errors can be introduced if all types of data are not considered simultaneously in the modeling process. In the case of Mayon volcano in the Philippines, we found that this type of joint modeling of the gravity and deformation data produces results that are far more plausible than previous results produced by modeling such data independently.

CALIFORNIA INSTITUTE OF TECHNOLOGY

Division of Geological and Planetary Sciences
Pasadena, California 91125

Grant: DE-FG03-85ER13445

Infrared Spectroscopy and Stable Isotope Geochemistry of Hydrous Silicate Glasses

E. Stolper, (626) 395-6504, fax (626) 568-0935, ems@expet.gps.caltech.edu

Objectives: The focus of this project is the application of experimental petrology, infrared spectroscopy, and stable isotope geochemistry to problems in petrology and geochemistry, with particular emphasis on the behavior of magmatic systems and variations of CO₂ content and isotopic composition in the atmosphere.

Project Description: Part 1 of this project has as its focus the determination of oxygen isotope fractionations between CO₂ gas, olivine mineral, and silicate melts. It involves experimental determinations of oxygen isotope fractionation in CO₂ vapor-silicate melt systems and in olivine-silicate melt systems. Part 2 is the study of the isotopic compositions and concentrations of CO₂ and H₂O in the air in the Los Angeles area. One-liter samples have been collected in evacuated glass bulbs every one to two days, purified by vacuum extraction techniques, analyzed for concentration by manometry, and analyzed for isotopic composition by conventional gas-source mass spectrometry. The data are compared with a set collected here in 1972-73, as well as with the NOAA-CMDL network data, and with air pollutant data from the South Coast Air Quality Management District.

Results: *Part 1:* We conducted experiments constraining oxygen isotope fractionations between CO₂ vapor and Na-rich melilitic melt at 1 bar and 1250 and 1400°C. This simple composition is often used as an analogue for basaltic melts. The fractionation factor constrained by bracketed experiments is 2.65 ± 0.25 ‰ ($\pm 2\sigma$; n=92) at 1250°C and 2.16 ± 0.16 ‰ (2σ ; n=16) at 1400°C. These values are independent of Na content over the range investigated (7.5 to 13.0 wt. % Na₂O). We combine these data with the known reduced partition function ratio of CO₂ to obtain an equation describing the reduced partition function ratio of Na-rich melilite melt as a function of temperature. We also fit previously measured CO₂-melt or -glass fractionations to obtain temperature-dependent reduced partition function ratios for all experimentally studied melts and glasses (including silica, rhyolite, albite, anorthite, Na-rich melilite, and basalt). The systematics of these data suggest that reduced partition function ratios of silicate melts can be approximated either by using the Garlick index (a measure of the polymerization of the melt) or by describing melts as mixtures of normative minerals or equivalent melt compositions. These systematics suggest oxygen isotope fractionation between basalt and olivine at 1300°C of approximately 0.3-0.5‰, consistent with most (but not all) basalt glass-olivine fractionations measured in terrestrial and lunar basalts.

Part 2: We continued our sampling of air, primarily in Pasadena but also in a few other locations, and determining the concentration of CO₂ and its $\delta^{13}\text{C}$ and $\delta^{18}\text{O}$. Our focus has

continued to be on developing sampling protocols, and during the current grant period we have brought on-line an automatic sampler that will allow detailed analysis of variability of the composition of urban air over many time scales. This project has the potential to elucidating sources and amounts of pollution and to complement other measurements of urban atmospheres being routinely made to monitor air quality. This project was a major activity of Sam Epstein, and in the five months since his death, we have been pulling together the data for several publications. A draft of one manuscript is nearly complete.

We have collected 1-liter samples every one to two days for over three years on the Caltech campus and compared our results for CO₂ concentrations and isotopic compositions with a set of data collected during 1972-73 in a similar location. Excellent correlations between concentration and $\delta^{13}\text{C}$ confirm that the area has had an increase in CO₂ concentration accompanied by a lightening of the heavy endmember (clean air). Candidates for the light, "pollutant" end member include automobile exhaust, exhaust from burning natural gas, and human breath exhalation. The trend for the air samples in Pasadena very closely corresponds to automobile exhaust, although some lighter natural gas component must be important, since the Pasadena air data point to a lighter end member than exhaust from burning oil. The composition of the pollutant end member in the Los Angeles area is much lighter than most other locations that have been sampled by the NOAA-CMDL network. Interestingly, the composition of this end member has not changed over the past 30 years. The temporal pattern of the CO₂ data for the Caltech campus show very good correlation with NO₂ data from Los Angeles County's Air Quality Management District for sites ranging from Hawthorne, near the ocean, to Pomona, well inland of Pasadena, demonstrating that we are not observing local conditions.

We have obtained an infrared CO₂-H₂O analyzer, which is continuously collecting concentration data, allowing us to address more questions, such as diurnal variations and variations with location, since the analyzer is portable. We have started to study effects of different weather patterns, such as Santa Ana winds and the common marine layer. The marine layer creates a unique pattern in the diurnal variations observed, virtually eliminating the overnight increase in CO₂ concentration observed on clear nights. This change is due either to the dissolution of the CO₂ in the fog, removing it from the air, or the dilution of the CO₂ produced on the land, by the respiration of the plants, by clean, marine air.

CALIFORNIA INSTITUTE OF TECHNOLOGY

Division of Geological and Planetary Sciences
Pasadena, CA 91125

Grant: DE-FG03-88ER13851

Isotope Tracer Studies of Diffusion in Silicates and of Geological Transport Processes Using Actinide Elements

G. J. Wasserburg, (626) 395-6139, fax (626) 796-9823, isotopes@gps.caltech.edu

Objectives: The initial aims of this project have not been modified.

Project Results: Several new projects have been initiated.

1) A study of the concentrations of all the Platinum Group Elements and Re was conducted in a deep sea drill core which included the KT boundary. The purpose was to find out the extent to which these elements migrated within the section and whether there was significant differential migration. It was found that all of the PGEs and Re were subject to some migration that appears to be diffusive. The effective diffusion coefficient for all elements was the same, so that elemental fractionation by post-depositional migration would not occur. In the PGE peak, the Os/Ir ratio was 1/10 of the chondritic value. This relationship persists through most of the overlying section. In the epicontinental sections containing the KT layer, the ratio was found to be chondritic. It follows that the removal of Os from seawater must be dominantly controlled by sedimentation in different selected areas within the deep sea and that the apparent lifetime of both Os and Re are, in fact, due to a mixture of two mechanisms—one of which dominantly removes the Os into reduced oceanic sedimentary basins, and the other into deep sea sediments. A model is presented for the PGE and Re, and it is shown that differential removal of these elements occurs in fundamentally different depositional regimes. We propose that this controls the ratio Os/Ir in major areas of deep sea clay deposition. The Os/Ir ratio in deep sea clay sections is proposed as a monitor of the areal extent of reduced oceanic sedimentary basins. A paper has been submitted covering this research

2) The study of U-Th series nuclides in groundwaters at the Brookhaven National Laboratory has stimulated us to investigate transport in old, slow-moving aquifers in arid climates. We selected the Ojo Alamo Aquifer in New Mexico, where the average rainfall is 22 cm/yr. It has been found that the ages of the groundwaters range up to 25 ka. The purpose was to investigate the transport of U-Th series nuclides and their daughter products in an old, slow-moving groundwater mass as a means of understanding water-rock interactions and to compare the results with a temperate zone aquifer. It was found that ^{232}Th is approximately at saturation and supports the view of Tricca et al. (2001) that Th is precipitated irreversibly upon weathering, leaving surface coatings of ^{232}Th and ^{230}Th on aquifer grains. Uranium in the aquifer waters has very high $\delta^{234}\text{U} \sim 8000$ ‰ and low ^{238}U concentrations. These levels can be explained by low weathering rates in the aquifer ($w_{238\text{U}} \sim 2 \times 10^{-18}$ to $2 \times 10^{-17} \text{ s}^{-1}$) using a continuous flow, water-rock interaction model.

The Ra isotopes are roughly in secular equilibrium in spite of their very different mean life times. The ^{222}Rn and ^{228}Ra isotopes in the aquifer correspond to $\sim 10\%$ of the net production rate of the bulk rock. This is interpreted to reflect an earlier formed irreversible surface coating of Th which provides Ra and Rn to the aquifer waters. The surface waters which appear to be feeding the aquifer have low $\delta^{234}\text{U}$ and high ^{238}U concentrations. The flow model shows that it is not possible to obtain the high $\delta^{234}\text{U}$ and low ^{238}U values in the aquifer, if these are representative of the vadose zone input. It follows that the old aquifer waters studied can not be fed by the present vadose zone input unless they are greatly diluted with waters with very low U concentrations. If the present sampling of vadose zone sources is representative of the present input, then this requires that there was a major change in water input, with much larger rainfall some several thousand years ago. This may represent a climatic change in the Southwest. A paper has been finished and submitted for publication.

3) A study of Sm and Nd concentrations and isotopic compositions in waters and soil profiles in a tropical watershed (Cameroon) was carried out. The purpose was to understand the evolution of REE in weathering of granitic type rocks where there is a large residual layer of laterite (~ 8 meters thick) overlying the parent rock. The study was reasonably complete and a manuscript is in preparation. The senior author, Dr. Jerome Viers, had to return to France for a new position as Assistant Professor in Toulouse.

4) A new project has just been initiated with Dr. Damien Lemarchand. The purpose of this study is to determine whether there is a relationship between Ca and B isotopic fractionation. The techniques are now being refined and a study is underway to find a possible relations between temperature, pH, and isotopic fractionation of Ca and B in a selected set of carbonates

UNIVERSITY OF CALIFORNIA at BERKELEY

Department of Earth and Planetary Science
Berkeley, California 94720

Grant: DE-FG03-85ER13419

Advective-Diffusive/Dispersive Transport of Chemically Reacting Species in Hydrothermal System

*Harold C. Helgeson, (510) 642-1251, fax (510) 643-9980,
brogie@socrates.berkeley.edu*

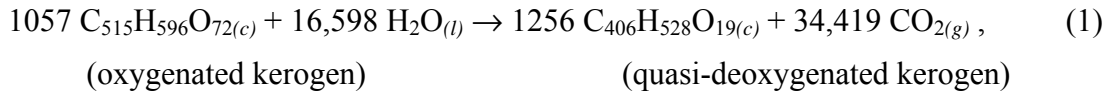
Objectives: The overall research objective of this project is to quantify the reaction process responsible for the generation of petroleum in sedimentary basins using thermodynamic calculations and compositional information to characterize metastable equilibrium states (Shock, 1988; Helgeson et al, 1993; Seewald, 1994) and the causes and consequences of irreversible reactions in hydrocarbon source rocks and reservoirs.

Project Description: The formation and evolution of petroleum in sedimentary basins is generally attributed to the thermal catagenesis of kerogen; *i.e.* kinetically controlled irreversible generation from kerogen of high molecular weight liquid hydrocarbons in bitumen and their progressive conversion to the lighter species that predominate in petroleum because of increasing time and temperature with increasing depth of burial. This widely accepted time/temperature paradigm is based largely on extrapolation of the results of laboratory pyrolysis experiments to the natural process of petroleum generation by correlating the products of the experiments with observed changes in kerogen composition with depth in sedimentary basins. However, high-temperature pyrolysis experiments are by design irreversible, and the extent to which the results of these experiments represent, or can even be reliably extrapolated to account for petroleum generation in nature has never been adequately documented.

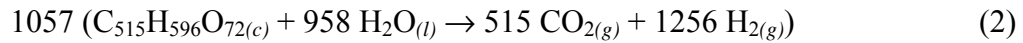
Although the phenomenological association of petroleum generation and maturation with increasing temperature and time during burial is self-evident, the causal implications of this association are highly questionable. In fact, it has been shown that in closed systems, source rocks with hydrogen-rich organic matter may retain their petroleum generating potential at temperatures far greater than those normally associated with the formation of crude oils. It can be demonstrated that degradation of organic matter with increasing depth is an oxidation/reduction process that requires the presence of H₂O.

Theoretical considerations and thermodynamic calculations have led to the hypothesis that hydrolytic disproportionation of hydrocarbons plays a crucial role in the diagenetic deoxygenation of immature kerogen, as well as the generation and maturation of crude oil in hydrocarbon source rocks. Recent field and laboratory evidence supporting this hypothesis indicates that hydrolytic disproportionation of organic matter is not only a dominant process in petroleum source rocks and reservoir systems, but that it plays a widespread and important role in ore deposition and high-temperature metasomatism of sedimentary, granitic, and mantle-derived rocks.

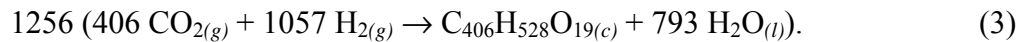
Results: Research carried out in the current budget period has been primarily concerned with characterizing the mass transfer accompanying diagenetic deoxygenation of immature kerogen in sedimentary basins. Ample evidence indicates that large amounts of CO₂ are produced during diagenetic deoxygenation and hydrogenation of kerogen as it reacts with H₂O during burial of source rocks in the upper part of sedimentary basins (Price and Wenger, 2000), which is consistent with the overall irreversible hydrolytic disproportionation reaction represented by



where the subscripts (*c*), (*l*), and (*g*) refer to the crystalline, liquid, and gas states, respectively. This reaction corresponds to the sum of two half-reactions after cross multiplying by the reaction coefficients for H_{2(g)}; *i.e.*



and



Reaction (1) is favored in relatively shallow or otherwise uncompacted source rocks with high porosities and permeabilities which are open to interstitial flow of water into the rock in response to the escape of CO_{2(g)} produced by the reaction. Under these conditions, for every mole of H₂O that enters the source rock and is consumed by reaction (1), ~ 2 moles of CO₂ are produced by combining the mole of oxygen derived from H₂O with ~ 2 moles of carbon and ~ 3 moles of oxygen extracted from the immature oxygen-rich reactant (C₅₁₅H₅₉₆O_{72(c)}). In the process, 2 moles of hydrogen derived from H₂O are consumed by conversion of 0.064 moles of the reactant kerogen to ~ 0.076 moles of C₄₀₆H₅₂₈O_{19(c)}. As the reaction proceeds and all of the C₅₁₅H₅₉₆O_{72(c)} kerogen is converted to C₄₀₆H₅₂₈O_{19(c)}, the weight percent hydrogen in the kerogen increases by ~ 23 percent from ~ 7.5 to ~ 9.3 percent of the kerogen, which corresponds to a substantial increase in the oil generation potential of the source rock. Comprehensive mass transfer calculations are planned to further characterize this process.

UNIVERSITY OF CALIFORNIA at BERKELEY

Space Sciences Laboratory
Berkeley, California 94720-7450

Grant: DE-FG03-96ER14676

Collaborative Research: Studies for Surface Exposure Dating in Geomorphology

K. Nishiizumi, (510) 643-9361, fax (510) 643-1433, kuni@ssl.berkeley.edu; W. E. Dietrich (510) 642-2633, bill@seismo.berkeley.edu; M. W. Caffee, R. C. Finkel, Lawrence Livermore National Laboratory; R. C. Reedy, Los Alamos National Laborator

Objective: An experimental and theoretical program to fully develop the systematics of *in situ* produced cosmogenic nuclides in terrestrial surface samples and to apply their measurement to the dating of surface features and processes.

Project Description: Surface exposure dating utilizing cosmogenic nuclides is now acknowledged as a successful means with which to date many terrestrial surfaces. It is also recognized that there are many new applications for these techniques. Although the method rests on a firm physical and geochemical foundation, some of the parameters required for interpreting results are only poorly known. This project includes determination of precise production rates and production depth profiles, studies of altitude and latitude effects, intercalibration with other methods, and isolation of *in situ* produced nuclides from lithologies other than quartz. The effort will focus on chemical isolation of cosmogenic nuclides of geologic and artificially exposed samples, on implementation of surface exposure dating methods using new radionuclides such as *in situ* ^{14}C and pure spallation ^{36}Cl , measurements of proton and neutron cross sections and improvement of theoretical production rate calculations.

Results: We continue to work on development of a reliable method for determine *in situ* produced ^{14}C in geologic samples, especially quartz, by a step-wise heating technique to separate *in situ* produced ^{14}C from meteoric ^{14}C . The extraction line consists of three sub-systems: carrier and flow gas measurement and aliquotting, sample heating, and CO_2 purification. We have replaced the old 4:1 $\text{N}_2\text{-O}_2\text{-CO}_2$ carrier gas mixture with a new carrier gas mixture that consists of $\text{He-O}_2\text{-CO-CO}_2$. The total background in blank quartz that was collected from deep in the Homestake mine in South Dakota, is about $2\text{-}5 \times 10^5$ atoms/g of ^{14}C . We also measured ^{14}C in quartz samples collected at the Transantarctic Mountains in Antarctica. These are demonstrably saturated in ^{14}C activity, based on ^{10}Be and ^{26}Al concentrations. Our duplicate results indicate that we are recovering more than 95 % of the expected *in situ* produced ^{14}C in the quartz. Although quartz is the best mineral for studies of cosmogenic nuclide surface exposure dating, quartz is rare in many geological settings. We are working on extending the range of geologic applications by developing a method for using olivine. We are developing a method for separating *in situ* produced ^{10}Be from meteoric ^{10}Be using stepwise leaching methods. In order to test our methods, we have measured ^{10}Be in recently erupted volcanic olivine from Hawaii (Kilauea) and Iceland, where we don't expect to find ^{10}Be from subduction. Surprisingly, olivine from both volcanoes contains an appreciable amount of ^{10}Be . This finding suggests that

unexpected reaction between basaltic magma and hydrothermally altered oceanic crust may occur.

UNIVERSITY OF CALIFORNIA at BERKELEY

Institute of Environmental Science and Engineering
O'Brien Hall #1766
Berkeley, California 94720-1766

Grant: DE-FG03-96ER14667

Dissolution of Fe(III)(hydr)Oxides by Aerobic Microorganisms

Garrison Sposito, (510) 643-8297, fax (510) 643-2940, sposito@ce.berkeley.edu; L.E. Hersman, Los Alamos National Laboratory; P.A. Maurice, University of Notre Dame

Objectives: The overall objective of our research is to determine the rates and mechanisms whereby microbes dissolve Fe(III)(hydr)oxides in aerobic soil environments. Information about the rates and mechanisms of Fe(III)(hydr)oxide dissolution is fundamental for a wide range of hydrobiogeochemical processes, yet little is known about the mechanism of dissolution promoted by siderophore-producing microorganisms. Fe(III)(hydr)oxides sorb radionuclides and organic contaminants; thus their dissolution may cause remobilization of these sorbed pollutants. Our current studies focus on the effect of Al-for-Fe substitution in goethite on the adsorption of the hydroxamate siderophore, desferrioxamine-B (DFO), and the effect of a competing bioligand, oxalate.

Project Description: The aluminum content of four samples of Al-goethite (S1-S4) was determined from surface area determinations, acid digestion experiments, and unit-cell parameters. The Al content (100 x in $\text{Fe}_{1-x}\text{Al}_x\text{OOH}$) of the four samples was: 2.6 ± 0.7 (S1), 3.6 ± 1.2 (S2), 4.5 ± 1.1 (S3), and 10 ± 2 (S4). Adsorption of DFO (0-400 μM), oxalate (0-700 μM), or both, on Al-goethite samples was investigated in batch mode in 10 mM NaClO_4 , 5mM MES buffer at pH 5, with a solids concentration of 10 g L^{-1} . Aliquots of stock solutions containing DFO (2mM) and ^{14}C labeled oxalic acid (133 μM) were added to achieve the desired solution concentration. The samples were placed on a rotator for 1 h to equilibrate. The concentration of DFO in suspension after equilibration was determined colorimetrically as the Fe-DFO complex in the presence of excess Fe using a Shimadzu UV-160 spectrophotometer. The concentration of oxalate in suspension was determined colorimetrically in the presence of ferric salicylate. Quantitation of oxalate as ^{14}C -labeled oxalic acid also was performed using a Beckman LS9000 Scintillation counter. Electrophoretic mobility measurements on the four samples in the presence or absence of oxalate and DFO were made using a Zeta-Meter System 3.0.

Results: Oxalate (36 μM) decreased DFO adsorption on Al-goethite, regardless of DFO concentration or Al content of the samples (see table below). The presence of DFO did not affect oxalate adsorption, however. The maximum surface excess of oxalate was about 40 $\mu\text{mol g}^{-1}$, regardless of the Al content of the samples.

Adsorption of oxalate (40 μM) caused significant a decrease in the electrophoretic mobility of Al-goethite. In the presence of MES buffer and background electrolyte, the electrophoretic mobility was comparable to that observed after oxalate adsorption only.

Effect of Oxalate on the Adsorption of DFO.

Al-Goethite Sample (mole fraction Al)	[DFO] (μM)	[Oxalate] (μM)	DFO surface excess ($\mu\text{mol g}^{-1}$)
S1 (x = 0.02)	20	0	1.8
		36	1.2
	40	0	2.1
		36	1.7
	100	0	3.7
		36	2.2
S2 (x = 0.04)	20	0	1.9
		36	1.4
	40	0	2.6
		36	1.6
	100	0	2.6
		36	2.0
S3 (x = 0.05)	20	0	1.9
		36	1.1
	40	0	2.1
		36	1.7
	100	0	3.2
		36	1.5
S4 (x = 0.10)	20	0	1.3
		36	1.2
	40	0	2.5
		36	1.7
	100	0	3.5
		36	2.1

UNIVERSITY OF CALIFORNIA at DAVIS

Department of Land, Air and Water Resources,
Davis, CA 95616

Grant: DE-FG03-96ER14629

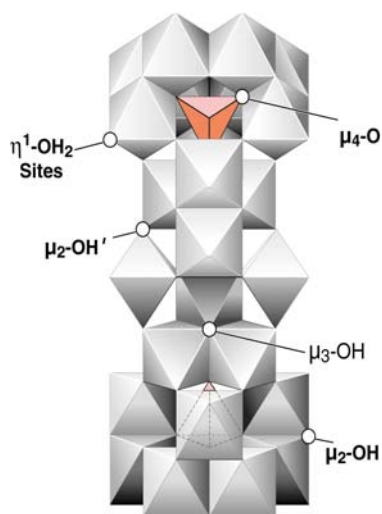
The Kinetics of Dissociation of Aluminum-Oxygen Bonds in Aqueous Complexes

William H. Casey, (916) 752-3211, fax (916) 752-1552, whcasey@ucdavis.edu

Objectives: We determine rates and mechanisms of Al(III)-O bond rupture at mineral surfaces and in dissolved aluminum complexes.

Project Description: Most of the low-temperature reactions that are geochemically important involve a bonded atom or molecule that is replaced with another. We probe these reactions at the most fundamental level in order to establish a model to predict rates for the wide range of reactions that cannot be experimentally studied.

Results: Considerable energy was expended synthesizing and purifying a large aluminum cluster (Al_{30} ; Figure) that exposes several types of oxygens to the bulk solution, including seven structurally distinct sets of bridging hydroxyls. This molecule is a rich model for the aqueous interface of aluminum (hydr)oxide minerals, since it approaches colloidal dimensions in size, yet is a dissolved complex with +18 charge. We have conducted both ^{17}O - and ^{19}F -NMR experiments to identify the reactive sites and to determine the rates of isotopic exchange between these sites and the bulk solution.



We also spent considerable time refining ^{19}F -NMR methods of tagging these large molecules. These ^{19}F -NMR spectra are particularly useful because the nucleus has $\text{spin}=1/2$, so peaks in the spectra are relatively narrow, and because fluoride can substitute for some oxygens at defined rates. All fluorines are detectable by NMR, the chemical shift is very sensitive to small changes in structure and bonding, and an enormous range of molecules are available with ^{19}F in a nonbonding site. We can therefore tag different sites in the polyoxocations.

Figure 1: The Al_{30} molecule has the stoichiometry $\text{Al}_{30}\text{O}_8(\text{OH})_{56}(\text{H}_2\text{O})_{26}^{18+}(\text{aq})$. It was crystallized by Taulelle et al., (2000) and Rowsell and Nazar (2001) and we are employing ^{17}O -NMR to determine the rates of oxygen-isotope exchange with the bulk solution. This molecule exhibits many of the properties of aluminum (hydr)oxide colloids.

Finally, we have high-pressure experiments underway in a home-built titanium NMR probe. These experiments allow us to determine the activation volumes for important geochemical reactions, such as oxygen-isotope exchange into bridging hydroxyl sites in molecules such as that shown in the figure.

UNIVERSITY OF CALIFORNIA at DAVIS

Thermochemistry Facility
Department of Chemical Engineering and Materials Sciences
One Shields Ave.
Davis, California 95616-8779

Grant : DE-FG01-97ER14749

Thermodynamics of Minerals Stable Near the Earth's Surface

Alexandra Navrotsky, (530) 752-3292, fax (530) 752-9307, anavrotsky@ucdavis.edu

Website : <http://navrotsky.engr.ucdavis.edu/>

Objectives: The goals of the project are to increase both the data base and the fundamental understanding of the thermodynamics of volatile-bearing mineral phases (amphiboles, micas, clays, zeolites, carbonates, sulfates) important to surficial, sedimentary, and shallow crustal processes.

Project Description: Using high temperature solution calorimetry, this research determines the enthalpies of formation of hydrous silicate, carbonates, and sulfates. Systematics in energetics of ionic substitutions are sought in order to predict the thermodynamics of complex multicomponent minerals. Mixing properties of mica, amphibole, clay, zeolite, sulfate, and carbonate solid solutions are also studied.

Results:

Sulfates

The thermochemistry of anhydrous sulfates (anglesite, anhydrite, arcanite, barite, celestine) was investigated by high-temperature oxide melt calorimetry and differential scanning calorimetry. Complete retention and uniform speciation of sulfur in the solvent was documented by (a) chemical analyses of the solvent ($3\text{Na}_2\text{O}\cdot 4\text{MoO}_3$) with dissolved sulfates, (b) FTIR spectroscopy confirming the absence of sulfur species in the gases above the solvent, and (c) consistency of experimental determination of the enthalpy of drop solution of SO_3 in the solvent. Thus the principal conclusion of this study is that high-temperature oxide melt calorimetry with $3\text{Na}_2\text{O}\cdot 4\text{MoO}_3$ solvent is a valid technique for measurement of enthalpies of formation of anhydrous sulfates. Enthalpies of formation of CaSO_4 , BaSO_4 , SrSO_4 , and PbSO_4 were redetermined using this method.

Jarosites and Related Phases:

The principal goal of this project is to study the thermochemistry of jarosites and related phases, which can be described by the general formula $\text{AB}_3(\text{XO}_4)_2(\text{OH})_6$, where $\text{A} = \text{K}, \text{Na}, \text{H}_3\text{O}$, $\text{B} = \text{Fe}$ (Jarosite series), Al (Alunite series) and $\text{X} = \text{S}, \text{Cr}^{\text{VI}}$. Such sulfates and related materials are important minerals in soils and sediments and important hosts for toxicants such as Cr^{6+} . The enthalpy of formation of such phases, including solid solutions, is being determined, mainly through high temperature drop solution calorimetry (in molten sodium molybdate solvent at 700

°C). Taking into account the complexity of the structure of jarosites, our study is focused on well-characterized synthetic phases, prepared either by coprecipitation methods or by hydrothermal synthesis. Full characterization includes X-ray diffraction, thermal analyses, electron probe microanalyses and Fourier transformed infrared spectroscopy. Up to now, this project has mostly dealt with the most common jarosite solid solutions occurring in nature, i.e. potassium-sodium-hydronium jarosites. Future work will deal with other solid solutions like jarosite-alunite, alunite-natroalunite, jarosite-chromium analog to jarosite. Part of this work will be done in collaboration with D. Baron from California State University in Bakersfield. These phases will be fully characterized and their enthalpy of formation will be investigated.

Hydrotalcites:

Recent interest in hydrotalcite-like materials has grown due to their role in controlling the migration of divalent metals in natural waters as well as their use as specialty chemicals and catalyst materials. Since hydrotalcites exhibit wide compositional variations, measuring thermodynamic data for each type of phase is both difficult and impractical. Our current research focuses on measuring and systematizing thermodynamic data and developing a model for enthalpies and free energies for many compounds based on a few careful measurements. Calorimetric measurements of heat of formation data for some cobalt-aluminum hydroxycarbonates show that the heat of formation from the end members (binary hydroxides and carbonates) is small, allowing these materials to be considered as thermodynamically equivalent to mechanical mixtures of the end members. We predict an increase in solubility of up to 15 orders of magnitude upon complete substitution of nitrate for carbonate in the cobalt aluminum hydrotalcite-like compound, showing the importance of the interlayer chemistry on aqueous solubility. Future research will focus on two goals: (1) relating the thermodynamic data to compositional variations, (2) testing the mechanical mixture model on other hydrotalcite-like systems.

Hydration Energetics:

We are systematizing data on the enthalpy and entropy of hydration of zeolites and clays via appropriate reactions of the type - anhydrous phase + $n\text{H}_2\text{O}$ = hydrous phase.

UNIVERSITY OF CALIFORNIA at DAVIS

Department of Chemistry
One Shields Avenue, Davis, CA 95616

Grant: DE-FG03-01ER15145

Electrochemical Measurements and Theoretical Predictions of the Thermodynamic Properties of Carbonate and Oxide Minerals

Peter A. Rock, (530) 754-8919, fax (530) 754-9057, rock@lsdo.ucdavis.edu

Objectives: To determine thermodynamic properties of carbonates hydroxycarbonates and oxides of relevance to DOE objectives and goals for CO₂ sequestration and the removal of toxic metal ions from waste water streams and aquifers.

Project Description: We are: (1) using electrochemical double-cell methods to measure the thermodynamic properties of carbonates, hydroxy carbonates and oxide solid-solution minerals that are important in soils and aquifers and in the abatement and remediation of radioactive waster waters; and, we are (2) devising and applying new theoretical approaches to the calculation of the energetics of metal carbonates, hydroxy carbonates and oxides in pure and binary phases.

Results: Using the novel electrochemical technique developed in our DOE supported research we have completed our experimental measurements on the protodolomites supplied to us by Dr. Paul Brady. We also have used our new theoretical lattice energy calculation model developed with DOE support to calculate the energy difference between randomized CaMg(CO₃)₂(ss) solid solutions and dolomite with alternating layers of Ca²⁺ and Mg²⁺ ions. The agreement between theory and experiment is good.

We have completed the analysis of our direct electrochemical double-cell determination for the hematite-to-goethite conversion $\text{FeO}_3(\text{s}) + \text{H}_2\text{O}(\ell) = \text{FeOOH}(\text{s})$ which is an important geochemical reaction in soils.

We have completed our experimental measurements on a series of high-magnesium calcites provided to us by Dr. H. Westrich. Analysis of our electrochemical results is ongoing, but is proving difficult, owing to composition changes in the solid phases in some of our cells during the measurement period. We are working to unravel these complexities. The theoretical analysis also needs to be completed, but we do not anticipate difficulties in this area based on our experience with the analysis of (Ca,Mg)CO₃ solid solutions.

We have developed a new computerized data acquisition system that enables us to increase the number of cells simultaneously under study from 18 to 42. This increase is very significant because our cell measurements usually extend over 4-to-8 months, and in some cases to over 24 months. We will be using these cells to study the thermodynamic properties of lanthanide hydroxycarbonates, such as NdOHCO₃(s) (an analogue for AmOHCO₃(s)) which are suitable

analogues for actinite hydroxycarbonates. We also are setting up the electrochemical cells necessary to determine the thermodynamic properties of hydrotalcite and Stichtite.

UNIVERSITY OF CALIFORNIA at LOS ANGELES

Department of Earth and Space Sciences
Los Angeles, CA 90095-1567

Grant: DE-FG-03-89ER14049

Application of $^{40}\text{Ar}/^{39}\text{Ar}$ Thermochronometry and Ion Microprobe Stable Isotope Geochemistry to the Evolution of Petroleum Reservoirs and Hydrothermal Systems

T.M. Harrison, (310) 825-7970, fax (310) 825-4396, tmh@argon.ess.ucla.edu

Website: <http://oro.ess.ucla.edu/doe.html>

Objectives: Understanding the rates and mechanisms involved in the formation of exploitable geological energy sources, including fossil fuel, geothermal, and fissionable materials, requires knowledge of the age of origin and subsequent thermal history of the system over geological time. The objective of this research is to assess the utility of micro-scale isotopic techniques in deriving both fluid evolution and thermal history results for crustal environments that bear upon energy exploration and reservoir assessment.

Project Description: We are using coupled application of the ion microprobe and $^{40}\text{Ar}/^{39}\text{Ar}$ thermochronometry to: (1) assess the thermal and diagenetic histories of sedimentary basins (southern San Joaquin basin, central California); (2) study the intrusion history and thermal evolution of a young geothermal system (Geysers steam field, northern California) to resolve fundamental questions regarding its origin; and (3) develop tools to investigate the stability of uraninite in the presence of fluid and radiation effects to better understand the nature of unconformity-type uranium deposits (Athabasca Basin). Some of these efforts require significant developmental work to make meaningful progress. In particular we have found it necessary to develop a robust ion microprobe calibration for isotope ratio analysis of oxygen and carbon isotopes of complex carbonate compositions in order to investigate rock-fluid interactions. Similar developments have been required to study the U-Pb and oxygen isotopic systematics of uraninites and associated phases.

Results: 1) Thermal and diagenetic histories of sedimentary basins. The ability to perform in situ, micron-scale, carbon and oxygen isotopic analyses of carbonate minerals and cements opens up the possibility of assessing long term (10^6 - 10^7 year) permeability histories of hydrocarbon reservoirs and obtaining paleoclimate histories with ultra high (annual to decadal) temporal resolution. Ion microprobe techniques for determining carbon and oxygen isotopic ratios with sub-‰ precision are now routine, but have thus far been restricted to end member carbonates because of significant compositional matrix effects on measured isotopic ratios. This represents a significant limitation for cements in sedimentary basin environments where carbonates exhibit an extensive solid solution. We synthesized a suite of complex carbonate compositions across the CaCO_3 - MgCO_3 - FeCO_3 ternary using both hydrothermal and piston-cylinder approaches. Natural specimens were used for endmember compositions and those along the dolomite-ankerite join. The oxygen and carbon isotopic compositions of mg-sized aliquots of these materials were characterized using conventional gas source mass spectrometry. Matrix effects were then obtained by comparing these data with results from ion microprobe analyses. Our

results yield the following instrumental mass fractionation (imf) relationships (in ‰): calcite-siderite $\text{imf} = -25.90 x_{\text{Fe}}^2 + 16.20 x_{\text{Fe}} - 29.19$; calcite-magnesite $\text{imf} = -37.75 x_{\text{Mg}}^2 + 4.291 x_{\text{Mg}} - 30.13$ (valid for $x_{\text{Mg}} < 0.5$); dolomite-ankerite $\text{imf} = -21.98 x_{\text{Fe}}^2 + 29.17 x_{\text{Fe}} - 34.43$; siderite-magnesite $\text{imf} = -172.8 x_{\text{Fe}}^3 + 325.0 x_{\text{Fe}}^2 - 168.7 x_{\text{Fe}} - 22.26$. Replicate measurements show that the form of these functions is preserved, although relative shifts between analytical sessions are observed.

2) Thermal energy potential of active magmatic-hydrothermal systems. The known extent and emplacement history of granitoids (1.13-1.25 Ma) within the Geysers Magmatic Complex, Sonoma County, California, cannot explain its protracted geothermal activity. Significant thermal inputs from younger sources appear to be required; the size of the system scaling with age (i.e., younger smaller bodies or older larger bodies). We have begun a systematic search for this source by: obtaining new samples from both archived sources (cuttings from over 22 bore holes penetrating the felsite) and field sampling of volcanic equivalents of intrusive granitoids; U-Pb zircon dating of these rocks; examination of melt inclusions in zircon to better constrain the initial isotopic disequilibrium in the U-Pb system in order to refine dating estimates.

3) High temporal resolution paleoclimatology from in situ oxygen and carbon isotopes of speleothem. Oxygen and carbon isotopic variations in speleothems (i.e., cave deposits) provide one of the best records of climate variations during the Pleistocene. Current methods involving gas-source measurement of $\delta^{18}\text{O}$ and $\delta^{13}\text{C}$ and U-series dating are restricted to providing data averaged over ca. 100 years and thus limit temporal resolution of the onset of regional and global climate change at the century level. Tests of hypotheses involving more rapid timescales require higher temporal, and thus spatial, resolution. Ion microprobe measurements of oxygen and carbon isotopes across a sectioned stalactite from the Soreq Cave, Israel, that had been previously dated by U-series methods yields an ultra high temporal paleoclimate record that encompasses the last glacial maximum (18 to 8.5 ka B.P.). While the ion microprobe $\delta^{18}\text{O}$ results are characterized by somewhat lower precision than conventional methods (typically 0.5‰ versus 0.1‰), they reproduce the previously defined trend with a temporal resolution that is 50 times higher. Under favorable conditions, annual resolution is feasible using the ion microprobe approach. The new data reveal well-resolved climate oscillations with a period of $\sim 10^2$ years that are not evident in the bulk analyses and suggest greater instability of glacial climate than previously appreciated.

UNIVERSITY OF CALIFORNIA at SANTA BARBARA

Department of Geological Sciences
Santa Barbara, California 93106

Grant: DE-FG02-96ER14619

Fluid Flow in Faults: Estimating Permeability and Diagenetic Effects in a Transpressional Setting, Southern California

*James R. Boles, (805) 893-3719, fax (805) 893-2314; boles@magic.geol.ucsb.edu;
Grant Garven (410) 516-8689, fax (410) 516-7933; emagarven@jhu.edu*

Objectives: This is a collaborative effort to determine the coupling of fluid mass transfer and diagenetic effects along faults that have developed in a transpressional setting. The study will contribute a practical understanding of the effects of thrusting on sediment diagenesis, fault-valve mechanics, petroleum migration and basin-scale groundwater flow in an active seismic environment.

Project Description: We have targeted three major faulted petroleum systems in southern California for study: Wheeler Ridge and Elks Hills areas in the San Joaquin Basin, the coastal faults and offshore South Ellwood Field in the Santa Barbara basin, and the bounding faults to the Long Beach Field in the Los Angeles basin. Subsurface core samples, outcrop samples, well logs, reservoir properties and published structural-seismic sections are being collected to characterize the tectonic history and diagenetic evolution for the known fault networks. These data provide constraints for finite element flow and transport models that are being developed to predict fluid pressures, flow patterns, rates of deformation, temperatures, and diagenetic patterns in the fault systems during thrusting and normal faulting. We are also monitoring modern hydrocarbon seeps along the faulted crest of the South Ellwood anticline.

Results: Professor Boles and his Ph.D. student Renee Perez have analyzed the petrology of cements and geochemistry of pore water and hydrocarbons at the Wheeler Ridge field to characterize the geochemical imprints of Quaternary-age thrusting. Permeability near the fault zone appears to decrease at depths greater than 2.4 km due to calcite cements, which impeded oil migration, while at shallower depths the porosity at the fault increases due to plagioclase dissolution and microfracturing. Geochemical fingerprinting of oil types verifies that shallow occurring oils have migrated across the fault whereas deep occurring oils have not migrated across the fault. Professor Garven and his Ph.D. student Eyal Stanislavsky have written a fully coupled, 2-D, poroelastic plane-strain numerical code to model fault-valve behavior and earthquake recurrence at Wheeler Ridge (Fig. 1). The first generation of numerical experiments reveal an initial fault failure after 45,000 years of thrust loading with pulses of geofluid migration that dissipate relatively quickly. Patterns of transient fluid flow and deformation have been evaluated for different scenarios of model boundary, rheological, and permeability conditions. Failure is strongly controlled by the ratio of host rock to fault bulk compressibility.

Studies of the Refugio-Carneros fault outcrops in the Santa Barbara area combined with the record of modern offshore seepage present a temporal picture of an evolving hydrocarbon system. Several hundred thousand years ago, hot basin fluids and hydrocarbons flowed from the deep basin and were focused at the tips of the active basin-margin faults. Massive calcite precipitated as a result of oxidation of methane to carbon dioxide when meteoric water and basin fluids mixed in the fault zone. Timing of faulting and calcite precipitation is estimated to range from 120,000 to greater than 500,000 years BP (U-Th series dates on calcite, J. Chen, Cal Tech). Preliminary models of Prof. Garven demonstrate that breaking of a seal in a deep over pressured section is required to cause rapid movement of high temperature ($>100^{\circ}\text{C}$) fluids to the surface.

Today, apparently due to several hundred thousand years of deformation, pressure has been bled off from the basin to a nearly hydrostatic gradient. Methane seepage still occurs from the crest of the faulted South Ellwood anticline. Seepage results from natural buoyancy of the gas phase rather than overpressure in the deep section. Release of gas from the fault is affected by tide height. Monitoring of methane seeps at the sea floor in 70 meters of water indicates a one meter increase in tide height decreases the flow rate about 2%. Long term (multi monthly) variation in seep rate (up to 5%) is related to formation and release of slugs of gas from the fault zone or from the underlying South Ellwood reservoir.

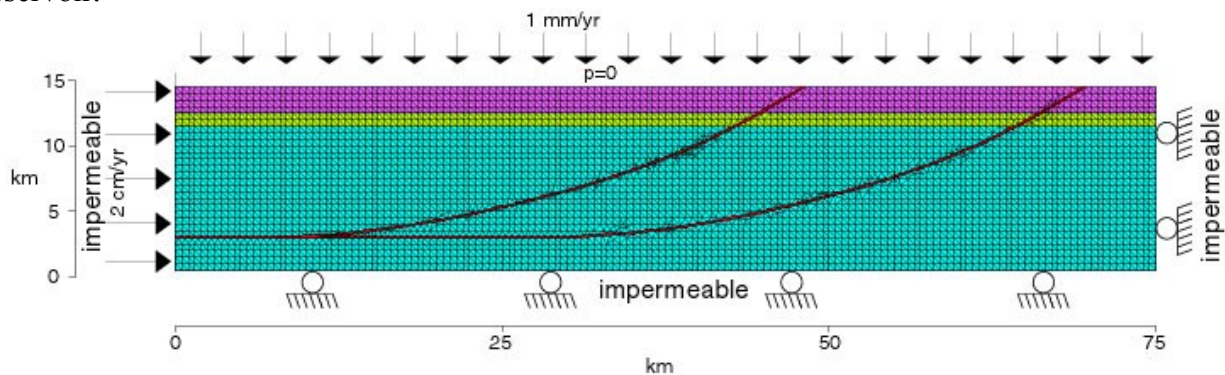


Figure 1. Finite element mesh and boundary conditions. The cross-section is subjected to compressional tectonic forces, and to shallow marine subsidence. The tectonic plate is moving at a velocity of 2 cm/yr, and the surface is subsiding at a velocity of 1 mm/yr. These boundary conditions represent the initial stage of the Wheeler Ridge (Medwedeff, 1992).

UNIVERSITY OF CALIFORNIA at SANTA BARBARA

Department of Mechanical and Environmental Engineering
Santa Barbara, California 93106

Grant: DE-FG03-00ER15114

Three-Dimensional Miscible Porous Media Flows with Viscosity Contrasts and Gravity Override

Eckart Meiburg, tel and fax: (805) 893-5278, meiburg@engineering.ucsb.edu, in collaboration with Anthony Maxworthy, Univ. of Southern California

Website: http://www.me.ucsb.edu/meiburg_web/research.html#h3

Objectives: To gain an understanding of the dynamics of miscible, variable density and viscosity flows in porous media, by means of detailed high fidelity numerical simulations. A main objective is to investigate the interaction among the effects of heterogeneity, density and viscosity fluctuations in the practically relevant quarter five-spot configuration.

Project Description: The project involves a three-dimensional computational investigation into the spatio-temporal dynamics of miscible porous media flows under the coupled effects of permeability heterogeneities, mobility contrast, and gravitational segregation. To this end, we employ high-accuracy numerical simulations based on a combination of compact finite difference and spectral methods. Our own recent two-dimensional simulations of plane, neutrally buoyant displacements and of flows with gravity override show that heterogeneities play a fundamentally different role in those flows. As a result, their role in three dimensional displacements with buoyancy effects cannot be extrapolated by combining results of different two-dimensional analyses, and a fully three-dimensional investigation is needed to obtain the necessary, qualitatively new understanding of the role of heterogeneities. Overall, the investigation aims to outline the borders between the various parameter regimes in which the displacement will be dominated by different physical mechanisms.

Results: Three-dimensional high-resolution, parallel, direct numerical simulations have been performed of miscible porous media flows for a wide range of mobility and density contrasts, both in the rectilinear and in the quarter five-spot configurations. So far the focus has been on homogeneous environments, although initial simulations of displacements in heterogeneous media have been conducted as well. The displacement processes are investigated by analyzing the mechanisms by which the vorticity components related to viscosity, density and permeability variations interact. For large values of the Peclet number and moderate density ratios, several nearly horizontal layers of the injected fluid are observed, while at larger density ratios the front becomes somewhat stabilized in the vertical direction, as most of the injected fluid is directed towards an evolving gravity tongue. We are currently focussing on the influence that the aspect ratio of the domain has on the displacement, as well as on the effects of the correlation length and variance of the heterogeneity field.

UNIVERSITY OF CALIFORNIA at SANTA BARBARA

Institute for Crustal Studies
Santa Barbara, California 93106-1100

Grant: DE-FG03-91ER14211

Magma Rheology, Mixing of Rheological Fluids, Molecular Dynamics Simulation, and Lithospheric Dynamics

F. J. Spera, (805) 893-4880, fax (805) 893-8649, spera@magma.geol.ucsb.edu, in collaboration with David Yuen, University of Minnesota

Website: <http://magma.geol.ucsb.edu/>

Objectives:

- ... Laboratory measurements of magma rheological properties on magma
- ... Determination of the structure and properties of multicomponent silicate melts and glasses at elevated temperature and pressure.
- ... Numerical modeling of porous media thermohaline convection
- ... Geochemical material balance modeling of assimilation and fractional crystallization subject to energy constraints.

Project Description: This collaborative project with D. A. Yuen at the University of Minnesota seeks to improve our understanding of the thermal, chemical, dynamical and mechanical state of the continental crust and subcrustal lithosphere with particular focus on the interactions between the various subsystems. The work-plan includes: (1) rheological laboratory measurements on melts and magmatic suspensions (2) Determination of the thermodynamical and transport properties of molten silicates by MD simulations (3) Mixing processes of rheological fluids in convection and visualization of complex processes (4) Coupling between mantle convection with temperature-dependent and non-Newtonian rheology and mantle diapirs on the thermal regime and subsidence curves of rift-related basins (5) The dynamical influences of lithospheric phase transitions on the thermal-mechanical evolution of sedimentary basins (6) The development of stress fields and criteria for faulting in the crust and finally (7) Modeling of heat and mass transport driven by thermal and compositional heterogeneities in porous media (8) Open system Geochemical modeling of magmatic systems.

Results: Results cited below are for the UCSB part of this project. Additional results are given in the summary of activities by the University of Minnesota team. Molecular Dynamics simulations for composition $\text{CaAl}_2\text{Si}_2\text{O}_8$ in a microcanonical ensemble of 1300 particles (O+Si+Al+Ca) were conducted at temperatures spanning the glass transition temperature at 1 GPa. The computer glass transition was detected at $T_g \approx 2800$ K by study of thermodynamic properties, speciation equilibria and tracer diffusivity as a function of temperature. T_g is

observed as a change in slope of enthalpy (H) versus temperature at $T = T_g \approx 2800$ K. The configurational isobaric heat capacity of supercooled melt relative to the glass is 53.3 J/K mol, within a factor of two of the experimental value. The computed isobaric heat capacity for equilibrium liquid at 3000 K, is 457 ± 35 J/K mol versus the calorimetric value of 461 J/K mol. In equilibrium liquid, speciation defined by equilibria such as $[1]O + [3]O = 2 [2]O$ and $TO4 + TO6 = 2 TO5$ are temperature-dependant with DH and DS approximately equal to -39 kJ/mol and 19 J/mol K and -10 kJ/mol and 12 J/mol, respectively in excellent agreement with laboratory values. The static structure factor for oxygen-oxygen shows that the glass transition is not associated with significant changes in the static structure. Self-diffusivity orders at fixed temperature according to $DCa > DO > DAl > DSi$ with $DCa \sim 20\%$ larger than DO and $DO \approx 2 DSi$. Activation energies for diffusion for all atoms lie in the range 170-190 kJ/mol. The small range in tracer diffusivity and activation energy (E_a) found for different atoms suggest cooperative motion is important. A given particle and its neighbors remain trapped for a finite residence time before undergoing cooperative thermally- activated rearrangement. The waiting time distribution is strongly temperature-dependent and related to the dramatic increase in structural relaxation time as temperature approaches T_g . The MD simulations are consistent with a picture of 'dynamic heterogeneity' as the ultimate cause of the sluggish dynamics as an equilibrium (ergodic) liquid becomes deeply supercooled. At some temperature above the Kauzmann temperature (TK) where the extrapolated entropy of deeply supercooled liquid equals that of crystalline solid, long lived, highly cooperative, collective particle motions take place in restricted regions of three-dimensional space.

Laboratory experiments pertaining to the viscosity of bubble-bearing rhyolite emulsions have been completed. We show that for Capillary number (Ca) in the range 10-100 the relative viscosity is a monotonically decreasing function of porosity (volume bubble-fraction) and that at 50 vol. % bubbles, the shear viscosity is smaller, by about a factor of five, relative to the single-phase (zero porosity) melt at the same pressure and temperature. In contrast, for Ca in the range 0.1 to 10 there is shear rate- dependence of the relative viscosity whereas for $Ca < 0.1$, the relative viscosity increases as the bubble content increases but no shear rate- dependence is noted.

A geochemical model (EC-RAFC) for describing the geochemical evolution of open magmatic systems subject to simultaneous assimilation, recharge and fractional crystallization has been developed and applied to a number of hydrothermal-magmatic systems. The EC-RAFC algorithm incorporates an energy conservation principle into the expressions for material balance and appears to faithfully capture many aspects of magmatic evolution in open system 'reactors'.

UNIVERSITY OF CALIFORNIA at SANTA CRUZ

Institute of Physics and Planetary Physics, UCSC
Santa Cruz, CA 95064

Grant: DE-FG03-01ER15144

High Resolution/High Fidelity Seismic Imaging and Parameter Estimation for Geological Structure and Material Characterization

R.S. Wu, (831) 459-5135, fax (831) 459-2423, wrs@es.ucsc.edu; X.B. Xie; T. Lay; E. Silver; X.Y. Wu, in collaboration with Michael Fehler, LANL

Website: <http://www.es.ucsc.edu/~acti>

Objectives: Develop high resolution/high fidelity multi-domain seismic imaging techniques and apply to local parameter estimation of reservoir structure and properties, such as reflection amplitude vs. angle information (AVA or AVO) and local reflection analysis. The imaging methods based on generalized screen propagator (GSP) need to be further developed, especially the amplitude preserving property and aperture corrections, anisotropic screen propagators, elastic screen propagators. The modeling techniques based on GSP need also be developed for the applications.

Project Description: The project is a collaborative effort between LANL and UCSC. The research at UCSC is implemented at the Modeling and Imaging Laboratory, Institute of Geophysics and Planetary Physics. The purpose of this project is to further develop and apply the new theories/methods of multi-domain one-way wave propagation to parameter estimation of reservoir structure and properties in 3D complex environments. This efficient wave equation based method can generate excellent modeling/imaging results, and high-fidelity local parameter estimation compared with the current ray based methods.

Results: Major results for this project year (FY 2001 – 10/2000-9/2001) can be summarized into three parts:

Improvement on Acoustic Imaging Method and Development of Elastic Imaging Method
Generalized screen propagators (GSP) in offset-domain for acoustic imaging have been improved (Jin, Mosher and Wu, 2001). Angle-image gathers has been obtained for both the offset-domain prestack-imaging and the shot-domain prestack-imaging (Xie and Wu, 2002). These angle-gathers (angle-dependent images) can be used for velocity model updating and local reflection analysis.

Elastic wave imaging methods have been developed and tested using synthetic data for the SEG/EAGE 2D salt model (Xie and Wu, 2002). A common-conversion point imaging method using multi-component data is developed based the elastic complex-screen propagator theory developed by us in the previous DOE project. A vector imaging condition was proposed for the

converted wave imaging. Separated P-wave and converted S-wave images can be obtained simultaneously for the purpose of getting more information on reservoir properties.

Elastic Wave Modeling by Elastic Thin-Slab and Elastic Screen Methods:

(1) Elastic complex-screen method has been extended and applied to modeling reflected multi-component elastic waves (Xie and Wu, 2001). Furthermore, an elastic thin-slab method for modeling elastic wave propagation and reflection in complex media has been developed (Wu and Wu, 2002). The thin-slab method does not invoke the narrow-angle approximation and therefore is more accurate than the complex-screen method, especially for large-angle waves. However, the method is as about twice slower than the complex-screen method, but still very efficient compared with finite difference method. In the meanwhile, the accuracy of the complex-screen method has been also improved by introducing higher order approximation in dealing with scattering patterns of different parameter perturbations without much increase of computation time.

(2) The elastic thin-slab method has been applied to AVO (amplitude versus offset) modeling. The traditional AVO modeling methods, such as the finite difference and ray-tracing methods, have great difficulties in modeling the effects of thin-beds (thinner than $\frac{1}{4}$ wavelength) and small-scale random heterogeneities. We have demonstrated the accuracy and efficiency of the elastic thin-slab method in such cases (Wu and Wu, 2002). Figure 1 shows a modeling example of the method for the thin salt-layer effects and influence of random heterogeneities to gas-sand AVO response. Model is sketched in (a), and the thin-layer effect is shown in (b). We see the strong influence of a thin salt-layer to the AVO curve. The curves in (c) show the combined effects of thin-salt-layer (20 m thick) and random heterogeneities (filled the whole model space).

Converted Wave Imaging for Steep Subsalt Structures:

The difficulties in imaging subsalt structures using conventional P-waves are well-known, especially for steep subsalt structures, due to the blockage of subsalt illumination by the high-velocity caps (salt domes). On the other hand, converted S-waves can avoid the deadly critical/post-critical reflections of P waves and therefore penetrate the salt body, providing the necessary illumination for steep subsalt structures. Conventional converted-wave imaging focuses on the ccp (common-conversion-point) images, which does not have the advantage on illuminating the steep subsalt structures. Instead, we developed a C-path imaging which still uses the P-P reflection on steep interfaces but takes the advantage of C-path penetration through the salt-body. Figure 2 shows the results of our method. Data are generated using a 2D elastic finite difference code. The image in (a) is the conventional P-wave image; the C-path image using the S-data is shown in (b). We see that only steep subsalt structures are imaged due to the nature of C-path imaging. Combining these two images after normalization we can see clearly both the flat and steep subsalt structures (c).

Plan for next year

1. Study on Amplitude Fidelity of Acoustic and Elastic Screen Propagators and Aperture Correction: Although wave-equation based propagators keep amplitude information during propagation much more faithfully than the ray method, various factors which affect the accuracy of downward propagated wave amplitudes still need a thorough study for the purpose of high fidelity imaging and local reflection analysis.

2. Development of Anisotropic Generalized Screen Propagators

3. Improvement on Modeling Methods Using Elastic Thin-Slab and Screen Propagators: We will try to extend the methods into 3D geometry.

4. Extension of AVO Analysis to AVA and Local Reflection Analysis: We will conduct preliminary study on AVA (amplitude versus angle) and more general local reflection analysis after migration/imaging, which will remove the influence of overburdens and can obtain more useful information of reservoir properties.

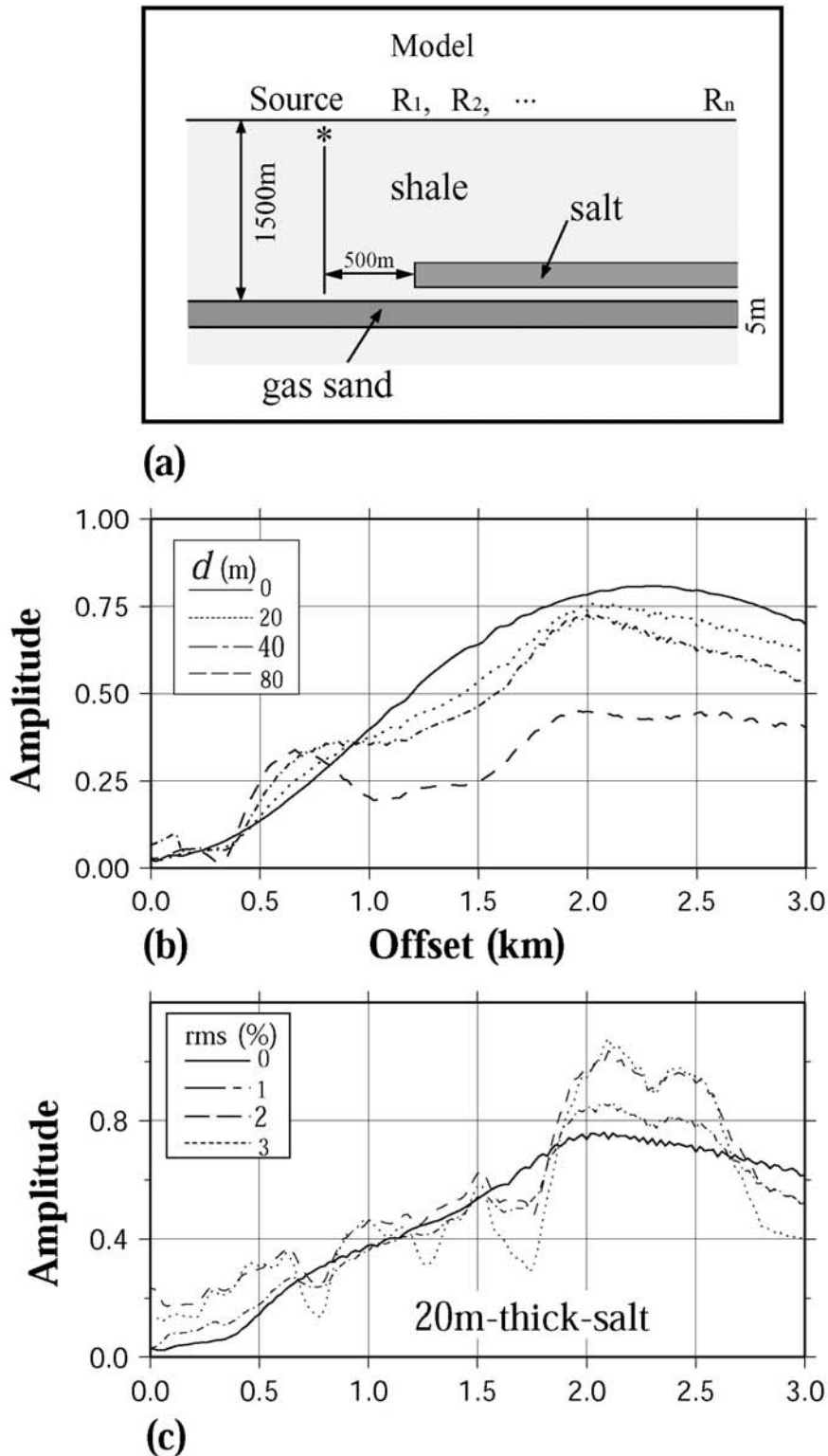
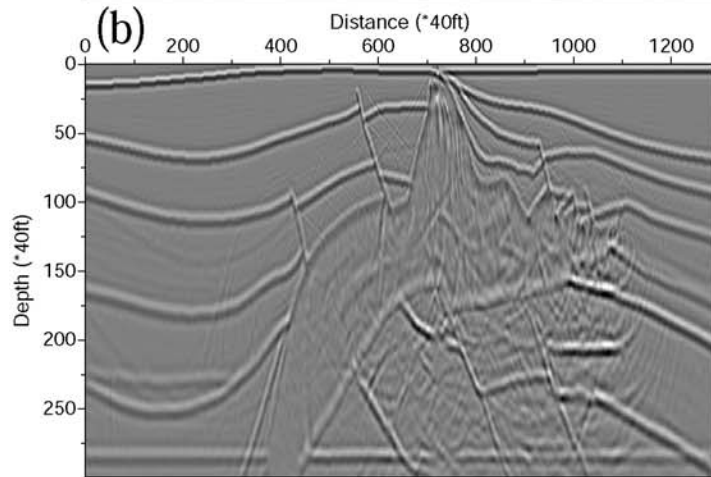
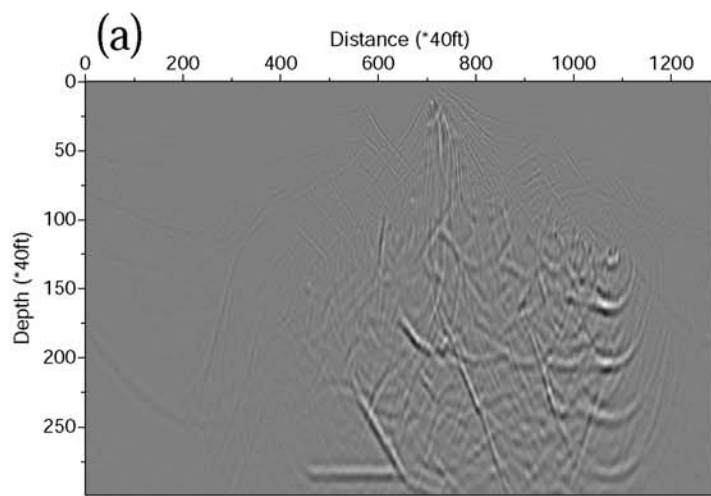
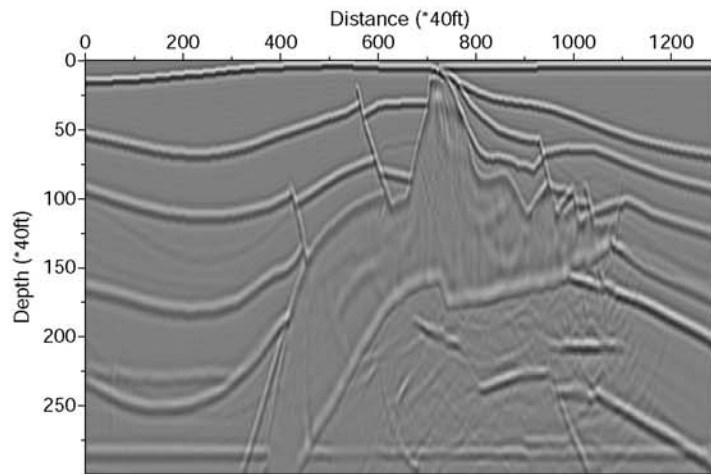


Fig. 1 Thin-bed effect and influence of random heterogeneities on AVO response of a gas sand layer: a) Model; b) AVO responses affected by a truncated thin-salt-bed with different thicknesses (0-80m); c) AVO responses with the influence of random heterogeneities (correlation length 100m in x and 40m in z) with different RMS velocity perturbations (1%, 2%, and 3%) combined with the thin-bed (20m thick) effect.



(c)

Fig. 2 Migrated images by generalized screen method using different wave paths: a) Image with P-path using P-data; b) Image with converted path (C-path) using S-data; c) summation of the two images after normalization. Both flat and steep subalt structures can be seen clearly.

THE UNIVERSITY OF CHICAGO

Department of the Geophysical Sciences
Chicago, IL 60637

Grant: DE-FG02-97ER14773

Isotope Fractionation by Diffusion in Liquids

Frank M. Richter, (773) 702-8118, fax (773) 915-9505, richter@geosci.uchicago.edu;
Ian D. Hutcheon, (925) 422-4481, fax (925) 422-3160, hutcheon1@llnl.gov, Ross W.
Williams, (925) 423-8769, fax (925) 422-3160, williams141@llnl.gov, John N.
Christensen, (510) 486-6735, fax (510) 486-5496, jnchristensen@lbl.gov

Objectives: The overall objective of our research effort is to document and quantify kinetic isotope fractionations during chemical diffusion in a variety of liquids ranging from silicate melts to water.

Project Description: The experiments designed to measure the isotopic fractionation of Ca and Li by diffusion in natural silicate melts involve diffusion couples with starting materials made from Mid-Ocean Ridge Basalt juxtaposed with a natural rhyolite glass. The diffusion couples are annealed in a piston cylinder apparatus at 1.2 GPa, and held at temperatures in the range 1350°C-1450°C for times ranging from 15.7 hours to 6 minutes. Profiles of major element concentration were measured along the length of the diffusion couples using a JEOL JSM-5800LV scanning electron microscope equipped with an Oxford Link ISIS-300 energy dispersive microanalytical system. Trace element profiles and Li isotopic compositions were measured using the modified AEI IM-20 ion microprobe. $^{44}\text{Ca}/^{40}\text{Ca}$ was measured by double spike thermal ionization mass spectrometry at the Berkeley Center for Isotope Geochemistry.

We have also been measuring the degree of isotope fractionation of dissolved species by diffusion in water. The design of the water diffusion experiments involves a small spherical chamber filled with a salt solution (e.g. 1 N MgCl_2) connected to a much larger water-filled reservoir by a small cylindrical tube with an inner diameter of about 1 mm. The time over which the concentration evolves is long compared to how long it takes for diffusion to maintain a uniform concentration in the small chamber and because of the large volume ratio, the concentration of salt in the larger reservoir remains negligibly small. Under these circumstances, the concentration in the small chamber will decay exponentially with a decay rate proportional to the diffusivity of the dissolved salt in water. If species of different isotopic composition have slightly different diffusivity, the system will be a Rayleigh fractionator and the residue of salt in the small chamber will become progressively enriched in the more slowly diffusing species, presumably those containing the heavier isotopes. The isotopic enrichment of a remaining fraction F is given by $C_2/C_1 = F^{1-\alpha}$, with $\alpha = D_1/D_2$ where D_1 and D_2 are the diffusivity of species C_1 and C_2 . The isotopic composition of Mg remaining in the inner chamber, as well as that of Mg that diffused into the outer large water reservoir was measured using a Cameca Micromass multi-collector ICPMS.

Results: Ca isotopic measurements have been made on two rhyolite-basalt diffusion couples (RB-2 and RB-3), and as shown in Figure 1, a local minimum in $\delta^{44}\text{Ca}$ of about 6‰ is produced as Ca diffuses from the basalt into the rhyolite. The Ca isotopic fractionation is in very good agreement with predictions we had made based on our earlier experiments on the relative mobility of Ca isotopes in isochemical $\text{CaO-Al}_2\text{O}_3\text{-SiO}_2$ liquids. Li isotope fractionation was also measured, and as shown in Figure 2, the fractionation of $\delta^7\text{Li}$ is about 40‰. The diffusion couples involving Li were remarkable in that they show that Li diffuses in the basalt-rhyolite system orders of magnitude faster than all the major elements (including Na and K) and more than 15 trace elements that we also measured.

We measured the fractionation of Mg isotopes during the diffusion of MgCl_2 in water by experiments ranging from one day to four months. The Mg concentration was measured by atomic absorption and confirmed the exponential decay of the Mg concentration in the small chamber. Figure 3 shows that we have not found any detectable fractionation of Mg isotopes even when more than 95% of the initial Mg has diffused out of the small inner chamber. Even if we were to assume a precision of no better than $\pm 1\%$, the fractionation factor α for Mg^{2+} in water must such that $1-\alpha < 0.00025$ (compared to $\bar{\alpha}_1 = 0.004$ that we measured for Ca and 0.03 for Li in silicate melts). The most likely explanation for this surprising lack of measurable isotopic fractionation of Mg during diffusion in water is that Mg^{2+} diffuses along with a large hydration sphere, sufficiently large to dilute the effect of the mass of the isotopes of Mg in terms of their effect on the mobility of diffusing unit.

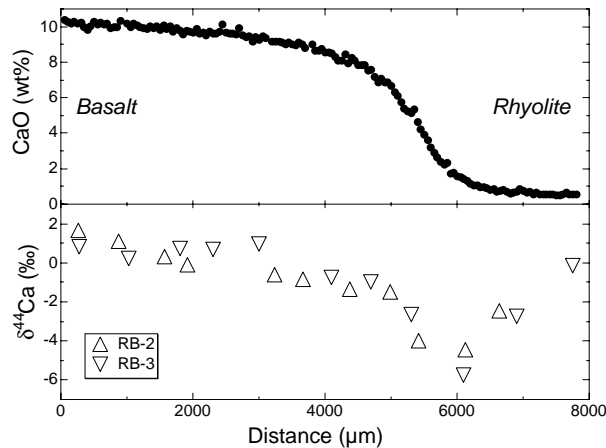


Fig. 1. Wt % CaO and Ca isotopic fractionation in diffusion couples RB-2 and RB-3. Run duration 15.7 hours, T=1450°C, P=1.2 GPa.

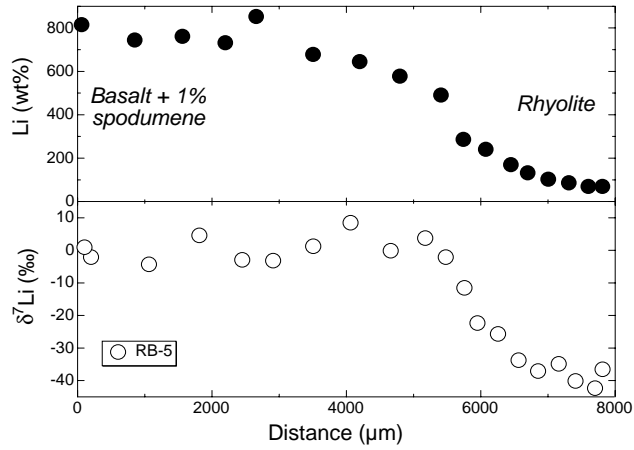


Fig. 2. Wt% Li and Li isotopic fractionation in diffusion couple RB-5. Run conditions 0,1 hours, T=1350°C, P=1.2 GPa. Note that Li has diffused further in 0.1 hours that did Ca in 15.7 hours.

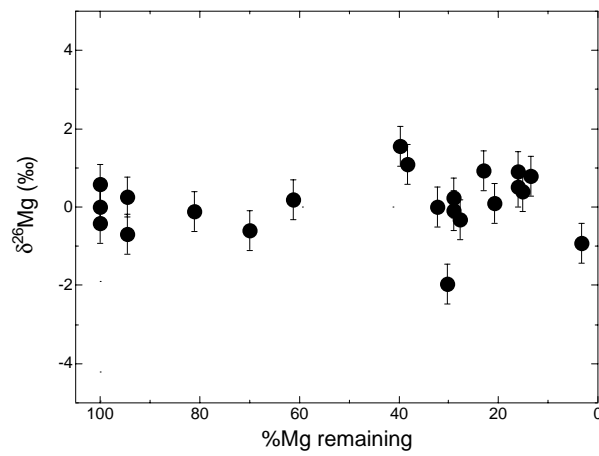


Fig. 3. Mg isotopic composition of MgCl₂ as a function of how much MgCl₂ has diffused out of a chamber designed to act as a Rayleigh fractionator

THE UNIVERSITY OF CHICAGO

Center for Advanced Radiation Sources
5640 S. Ellis Avenue
Chicago, IL 60637

Grant: DE-FG02-94ER14466

GeoSoilEnviroCARS: A National Resource for Earth, Planetary, Soil and Environmental Science Research at the Advanced Photon Source

Stephen R. Sutton, (630) 252-0426, fax (630) 252-0436, sutton@cars.uchicago.edu; Mark L. Rivers, (630) 252-0422, fax 630-252-0436, rivers@cars.uchicago.edu

Website: <http://gsecars.org>

Objectives: GeoSoilEnviroCARS is a national consortium of earth scientists whose goal is to design, construct and operate, as a national user facility, synchrotron radiation beam lines at the Advanced Photon Source, Argonne National Laboratory.

Project Description: Instrumentation for the following techniques is provided: (1) x-ray absorption fine structure spectroscopy; (2) fluorescence microprobe analysis and microtomography; (3) powder, microcrystal and surface diffraction; (4) high-pressure crystallography with diamond anvil cells and multi-anvil presses, and (5) radiography at high pressure in the multi-anvil press. Research areas include phase transitions in mantle minerals, the properties of the Earth's core, migration and remediation of toxic metals and radioisotopes in contaminated sediments, redox chemistry of transition metals at the root-soil interface and its role in agriculturally-relevant plant diseases, the chemical nature of hydrothermal fluids, chemical reactions on mineral surfaces, and petrogenesis of strategic elements.

Results: GeoSoilEnviroCARS is currently making 90% of the total beam time available to the community through a web-based proposal system at <http://gsecars.org>. In FY2001, 121 beam time proposals were received and 160 scientists and students conducted experiments. Fifty-two undulator experiments and 41 bending magnet experiments were performed for a total of 93 experiments for the year. Results included the following examples (collaborators in brackets):

Hydrothermal Fluids: (A) The coordination of copper in vapor phase inclusions coexisting with brine from the Mole Granite, NSW, Australia was studied [J. Mavrogenes (ANU) and colleagues]. Copper was found to be concentrated in the vapor inclusions and, at room temperature, uniformly distributed in the condensed fluid. X-ray absorption spectra identified the stable complexes as $[\text{Cu}(\text{OH}_2)_6]^{2+}$ at 25°C, $[\text{CuCl}_2]^-$ at 200°C, and $[\text{CuCl}(\text{OH}_2)]$ at the homogenization temperature of around 400°C. The observed, fully reversible change in copper coordination is the first direct spectroscopic evidence for vapor-phase Cu speciation and suggests that copper is transported in the vapor phase as a neutral chloride complex. (B) A special diamond cell [W. Bassett (Cornell University) and colleagues] is being utilized for dissolution and elemental partitioning studies of trace elements, e.g., Y, Th, Hf, and U, as a result of melting. Preliminary experiments were performed on zircon glasses in aqueous solutions as the system

was heated to 800°C. The goal of this work is to obtain the first in situ quantitative measurement of element partitioning between melts and aqueous fluids as well as between solids and aqueous fluids at elevated temperatures and pressures, and to directly determine the speciation of selected metals in the aqueous fluid coexisting with a silicate melt and in supercritical fluids.

Mineral-Water Interfaces: Crystal truncation rod (CTR) scattering measurements [G. Brown, Jr. (Stanford University); G. Waychunas (LBNL); and colleagues] of the hydrated α -Fe₂O₃ (0001) surface suggested oxygen (or hydroxyl) termination, similar to our previous observations on the isostructural hydrated α -Al₂O₃ (0001) surface. Detailed structural analysis is in progress with the goal of understanding the observed reactivity differences between the α -Fe₂O₃ (0001) and α -Al₂O₃ (0001) surfaces. A CTR study of Pb(II) sorption on the (0001) and (1-102) surfaces of α -Al₂O₃ was designed to determine the mode of attachment of the Pb(II) complexes on these surfaces and the magnitude of sorbate-induced surface relaxation. CTR signals associated with the sorption reaction supported previous suggestions of Pb(II) sorption at ordered surface sites and showed the technique is sensitive to <5% monolayer coverage.

Metal Contaminants: (A) Research on the cycling of arsenic within the Wells G&H wetland, Woburn, MA., [N. Keon (MIT) and colleagues] demonstrated that arsenic distribution is affected by the activity of cattails in the upper wetland sediments. Fluorescence tomographic imaging of intact cattail roots revealed a very strong correlation between arsenic and iron ($R > 0.95$) within $\sim 30 \mu\text{m}$ thick plaques. Furthermore, oxidation state tomograms showed higher As³⁺/As⁵⁺ ratios in more mature roots and a tendency for As³⁺ to occur on the interior of the iron plaque. The long-term implications are profound suggesting that both oxidation states of As are being effectively sequestered by the plants. (B) The complex interactions of aggregate microenvironments and microbial communities that control the fate of Cr(VI) contamination was studied [T. Tokunaga (LBNL) and colleagues]. Aggregates with higher available organic carbon took up greater amounts of Cr(VI) and reductively precipitated Cr(III) within shorter distances. The results suggest that the spatial distribution of microbial activity in the aggregates is related to the creation of redox gradients and to Cr(VI) reduction. Similar stratification of redox potentials, metal contaminants, and microbial communities might occur within larger sediment blocks. (C) MicroXAFS analyses [D. Roberts (University of Delaware) and colleagues] on surface soils from near the Palmerton Zn smelting plant confirmed that Zn is predominately incorporated as aeri ally deposited ZnFe₂O₄ (franklinite) particles, a byproduct of smelting ZnS containing trace amounts of Fe. The Zn speciation in the subsurface sample varied considerably but commonly as inner sphere adsorption complexes on Al and Mn oxides.

Sectoral Zonation: (A) The partitioning behavior between subsectors of apatite was previously found to be correlated with the size of the REE ion relative to Ca²⁺, for which it substitutes in the structure. Europium is the only REE that was not found to show a differential distribution between subsectors and this anomalous behavior was postulated to be the result of the presence of both Eu²⁺ and Eu³⁺, expected to show opposite partitioning behavior. The europium oxidation state was found to be mixed but surprisingly similar in adjacent sectors [J. Rakovan (Univ. of Miami – Ohio) and colleagues].

Fluid Flow: (A) A dependence of measured hydraulic properties on drainage flow rate has been observed in unsaturated porous media suggesting interference from dynamic phenomena such as air entrapment, pore-water blockage, influence of flow velocity on the solid/liquid-gas contact angle, etc.

Microtomographic imaging of a fine sand (mean particle size of 0.17 mm; KI contrast agent added to solution) showed drainage rate had a major impact on the overall amount of water retained and its microdistribution [D. Wildenschild (Tech. Univ. – Denmark) and colleagues]. For fast drainage, most of the water has preferentially drained off in a few larger pores, and the bulk of the matrix remained saturated, whereas slow drainage resulted in more uniform drainage.

THE UNIVERSITY OF CHICAGO

Center for Advanced Radiation Sources
5640 S. Ellis Avenue
Chicago, IL 60637

Grant: DE-FG02-92ER14244

Synchrotron X-ray Microprobe and Microspectroscopy Research in Low Temperature Geochemistry

Stephen R. Sutton, (630) 252-0426, fax (630) 252-0436, sutton@cars.uchicago.edu

Website: <http://www.bnl.gov/x26a/>

Objectives: The objectives are to apply a synchrotron-based x-ray microprobe for determinations of the compositions, structures, oxidation states, and bonding characteristics of earth materials with trace element sensitivity and micrometer spatial resolution.

Project Description: The project focuses on applications of the x-ray fluorescence microprobe on Beam Line X26A at the National Synchrotron Light Source (NSLS), Brookhaven National Laboratory. Research focuses on actinide incorporation in minerals and sediments, biogeochemistry of metal contaminants, mineral surface site controls on metal uptake by minerals, iron oxidation states in igneous petrogenesis, and instrumentation development.

Results: Examples of research results included the following (collaborators in parentheses).

Surface Site Preferences for Cu(II), Co(II) and U(VI) Uptake by Calcite (R. Reeder – SUNY Stony Brook): The effectiveness of metal uptake by minerals is strongly dependent on the surface characteristics of the sorbent. In one experiment, calcite single crystals were synthesized from room-temperature solutions containing Co(II) or Cu(II). Both Co(II) and Cu(II) are differentially incorporated between the nonequivalent vicinals as shown by the close correspondence between the different vicinal faces and the Co or Cu concentrations. However, the metals show opposite preferences, with Co(II) preferring different symmetrically nonequivalent sites. Related EXAFS work shows that a Jahn-Teller distortion of octahedral Cu(II) sorption complexes is most likely responsible for the different surface site preferences. In a related experiment, calcite single crystals grown in uranyl-containing solutions exhibited polygonized spiral growth hillocks composed of four vicinal surfaces, consistent with face symmetry. Micro-x-ray fluorescence analysis revealed that uranium is differentially incorporated between nonequivalent vicinal surfaces, reflecting step-selective incorporation of uranyl species during growth. Micro-x-ray absorption near-edge structure spectra from the nonequivalent vicinal faces failed to reveal any differences in speciation between the vicinals that might account for the presence of the multiple coordination environments identified by luminescence and x-ray absorption spectroscopies.

Phytoextraction and Phytoremediation of Contaminants from Soils (M. Fuhrmann – Brookhaven National Laboratory): As part of efforts to develop methods for the use of plants to remove contaminants from soils (phytoextraction), discrete localization of certain metals were found in zones

within roots and stems of several plant species. MicroXRF maps showed the distribution of Pb in the stems of EDTA treated samples (*Nicotiana tabacum*) is extensive and at a much greater concentrations than the stems of untreated samples. Also the distribution of Pb in the untreated stem showed very small, discrete localization of Pb. This may indicate that reactions at individual roots have mobilized small quantities of Pb.

Influence of Elevated Carbon Dioxide on the Biogeochemistry of Soil and Aquatic Systems (S. C. B. Myneni, Princeton University): This project examines (1) variations in soil mineralogy, mineral surface chemistry, and soil pore water chemistry as a function of elevated CO₂ in soil pore spaces, and (2) influence of these variations on vegetation and metal uptake by plants. Samples derive from Mammoth Mountain in California, the site of recent magmatic degassing of CO₂ as a result of an earthquake in 1989. X-ray microprobe studies of the variations in metal distributions (e.g., Ca, Mn and Zn) in roots and shoots of plants exposed to the CO₂ show enhanced metal uptake since the degassing event.

Iron Oxidation State as an Oxygen Fugacity Indicator (M. D. Dyar – Mount Holyoke College; J. S. Delaney – Rutgers University): (A) Iron oxidation state measurements at the microscale in plagioclase from a middle Tertiary volcanic succession in the Atascosa Mountains of south-central Arizona showed variations in oxygen fugacity undetectable in other ways. These data provide direct evidence that magmatic oxygen fugacity decreased as the lava evolved (Cartwright et al. 2000). (B) Clinopyroxene (cpx) crystals in lavas from the East African volcano Satiman (adjacent to hominid locality, Olduvai Gorge, Tanzania) have dramatic oscillatory zoning correlated with oxygen fugacity variations revealed by Fe oxidation state heterogeneity (Fe³⁺/total Fe = 25 – 45%). Fe oxidation state changes within crystals cannot be reconciled with progressive oxidation as the magma evolved. Other than the rim, the highest ferric is in the outer core of the cpx and indicate that the magma become oxidized during early growth. The subdued oxidation state changes in the mantle despite the prominent compositional changes perhaps reflect constant oxygen content during magma evolution in a closed chamber, despite the clear decrease of fO₂ between the core and mantle cpx growth stages. Fine fO₂ variations in a Satiman magma chamber can be extracted from the ferric/ferrous measurements.

Instrumentation Developments (J. Parise, SUNY Stony Brook): Recent instrumentation upgrades included the following: (1) Improved X-ray Microfocusing System: A more compact Kirkpatrick-Baez microfocusing system, including benders and controllers, was implemented providing improved spatial resolution. (2) Fast X-ray Detector: a new Canberra Si(Li) detector was installed with fast pre-amplifiers for improved count rate capability. (3) Advanced Motor Control System: A PC-based microprobe control system was installed integrating our existing CAMAC devices through a VME crate running EPICS. The new EPICS based software provides a new level of flexibility on controlling motors and detectors that was not possible in the past. (4) Microdiffraction Capability: Efforts began to integrate microdiffraction analysis with our existing fluorescence analytical capabilities. Applications are now possible combining the microbeam techniques of XRD, XRF, and XAFS.

THE CITY COLLEGE OF THE CITY UNIVERSITY OF NEW YORK

Benjamin Levich Institute & Department of Physics
New York, New York 10031

Grant: DE-FG02-93ER14327

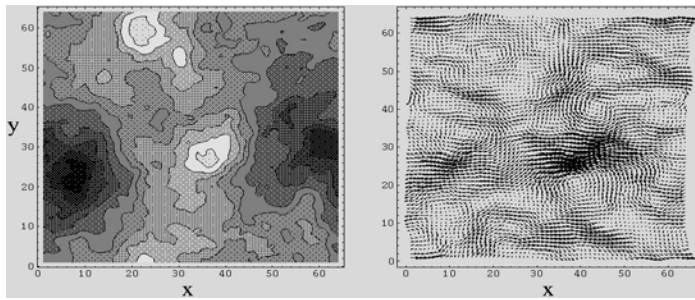
Particulate Dynamics in Filtration and Granular Flow

Joel Koplik, (212) 650-8162, fax (212) 650-6835, koplik@sci.ccny.cuny.edu

Objectives: We propose to seek a better understanding of the dynamics of collective particulate motion in deep-bed filtration processes, in flows in geological fracture systems, and in gravity-driven granular flows.

Project Description: Two general topics are under active study, a third having been completed earlier in the grant period. We are examining transport processes (fluid flow, passive tracer dynamics, and suspended particle dynamics) in geological fractures, where the rock surface is modeled as a self-affine fractal. Here we combine scaling arguments with lattice Boltzmann numerical simulations, and collaborate with an experimental group at Orsay. An independent sub-project considers the structure of the wake of an obstacle placed in a gravity-driven flow.

Results: This year's progress on the two active topics above is as follows. We have extended our previous results on permeability and passive tracer dispersion in two dimensional fractures (with no variation in the third direction) to the fully three-dimensional case. We find that the scaling behavior of the permeability and velocity fluctuations can be related to the mean aperture and roughness exponent using effective medium methods. The computed velocity fields exhibit channeling effects, and anisotropies resulting from lateral shifts in the bounding fracture surfaces. In the same fractures, simulations of passive tracer dispersion show a mixture of Taylor and geometric dispersion mechanisms acting, with the latter predominating for narrow fractures and where velocity fluctuations are large. The transit time distributions display substantial tails, corresponding to non-flowing zones in the fracture depressions. All numerical results are in qualitative agreement with experiment, with quantitative testing in progress. In the granular flow sub-project, we have developed an event-driven numerical code with particle insertion/deletion routines which maintain a slow, steady background flow in the presence of inelastic collisions and an obstacle. In the nearly elastic limit, these simulation results include transient vortex formation in the wake, and general agreement with earlier work based on other algorithms. Currently, we are studying the obstacle wake for the full range of elasticity coefficients.



Example of flow in a self-affine rough fracture.
Left: computer-generated fracture surface, shown as a contour plot, with light/dark regions corresponding to high/low elevation.
Right: fluctuations about the mean in the velocity field, when an incompressible fluid flows through the fracture in the x-direction.

UNIVERSITY OF COLORADO

Department of Geological Sciences
Boulder, CO 80309-0399

Grant: DE-FG03-95ER14518

Evolution of Rock Fracture Permeability During Shearing

Shemin Ge, (303) 492-8323, fax (303) 492-2606, ges@spot.colorado.edu, Hartmut Spetzler

Objectives: To investigate the transport characteristics in a variable aperture fracture by examining the relationship between the ratio of dispersion coefficient to molecular diffusion coefficient (DL/D_m) and Peclet number (Pe) for a multi-solute system in non-Darcian flow regimes.

Project Description: Existing understanding on solute dispersion is derived from single solute transport in Darcian flow regimes. Using the Lattice Boltzmann method, we examined the applicability of the DL/D_m - Pe relationship from a single-solute system to multi-solute situations in non-Darcian regimes. A natural fracture was used and fitted with 1000 lattice units (lu) along the fracture and an average 30 lu across. Two solutes were injected into the fracture from one end and fluid concentrations were monitored at the other end. Solute 1 has a molecular diffusion coefficient of $D_m = 0.005 \text{ lu}^2/\text{ts}$ and Solute 2 of $D_m = 0.01 \text{ lu}^2/\text{ts}$, ts is time step. For the same Pe , the fluid velocity of Solute 2 is twice that of Solute 1, consequently, the two solutes could be in different flow regimes. To obtain the dispersion coefficients, we computed the first and second moments of the solute mass using the Lattice Boltzmann variables.

Results: We conducted fluid and solute transport simulations at various flow velocities. From Reynolds number (Re) of 15, eddies were observed where the fracture aperture changes rapidly. Figure 1(a) shows the relationship between flow velocity and particle acceleration. From approximately $Re = 10$, the relation is no longer linear, but flow is still laminar because no turbulence was observed. Non-linear laminar flow is a transition from laminar to turbulent. Non-Darcian flow includes non-linear laminar and turbulent flows. With further increasing fluid velocity, the nonlinear relationship between fluid velocity and acceleration is due to turbulent flow effects.

We then examined solute transport in the fracture. Figure 1(b) shows that the DL/D_m - Pe relationships are fitted by quadratic equations in which the first term represents Taylor dispersion and the second term represents macrodispersion. Solute 1 and Solute 2 behave similarly for $Pe < 100$ in the Darcian regime. As non-Darcian flow starts from approximately $Pe = 100$ corresponding to $Re = 10$, their behaviors start to differ. The difference in DL/D_m increases as flow progresses into turbulent regimes. Taylor dispersion of Solute 2 is higher than that of Solute 1, but macro-dispersion coefficient of Solute 2 becomes negative because the turbulent flow interferes with transport along the fracture wall.

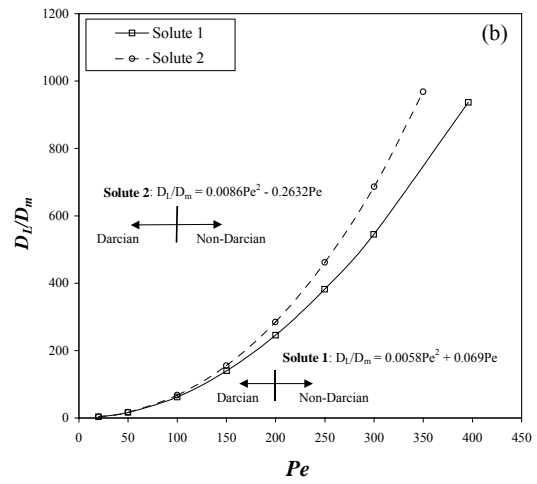
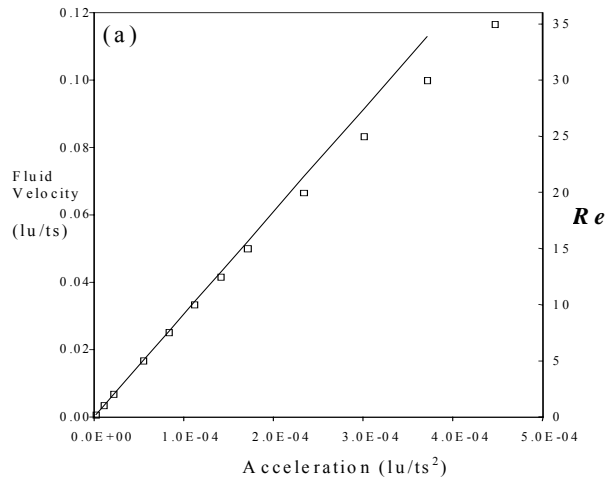


Figure 1. (a) Fluid velocity versus acceleration. Non-linear laminar flow starts at approximately $Re = 10$. (b) D_L/D_m versus Pe , the relationship of Solute 2 deviates from that of Solute 1 at $Pe=100$ where non-Darcian flow starts in Solute 2.

UNIVERSITY OF COLORADO

Department of Geological Sciences
Boulder, Colorado 80309-0399

Grant: DE-FG03-99ER14979

Nucleation and Growth Kinetics of Clays and Carbonates on Mineral Substrate

Kathryn L. Nagy, (303) 492-6187, fax (303) 492-2606, kathryn.nagy@colorado.edu

Website: <http://spot.colorado.edu/~nagyk/>

Objectives: To investigate the kinetics of nucleation and growth of clays and carbonates on mineral substrates. Data are needed to model reactive fluid flow in porous media as applied to the natural processes of soil formation and sediment diagenesis, and to engineered processes such as subsurface CO₂ sequestration.

Project Description: Secondary mineral nucleation and growth controls global cycling of elements during weathering, sequestration of contaminant metals in the environment, and fluid flow pathways in sedimentary basins. Although simulations of fluid flow now include complex reactions with minerals they still cannot reproduce natural systems because kinetic data are lacking, especially data describing heterogeneous nucleation and growth. Experiments are conducted to nucleate and grow clays and carbonate on mica and quartz as a function of solution composition and temperature. Substrate characteristics that control nucleation such as surface charge and molecular-scale structure are being evaluated. Rates are determined from solution changes in stirred-flow reactor experiments with powdered minerals and from atomic force microscopy (AFM) images of precipitate volume in single crystal experiments. In-situ synchrotron X-ray reflectivity (with P. Fenter at Argonne National Laboratory and N. Sturchio of the University of Illinois at Chicago) is also used to assess nucleation mechanisms.

Results: We characterized the cleaved basal surface of muscovite mica and crystal growth faces of quartz in aqueous solutions using X-ray reflectivity and atomic force microscopy. Reflectivity measurements were conducted in near-neutral pH solutions using bending magnet and insertion device beamlines (BESSRC-CAT) of the Advanced Photon Source (APS). Results show that the muscovite surface relaxes only slightly to a depth of one to three unit cells. In pure water, near-surface water molecules form three layers that together extend about 10 Angstroms into the solution. Water near the quartz surface does not show the same extent of layering, and near-surface relaxation of bulk crystal silicon and oxygen atoms is minimal. The muscovite(001)-solution interface structure was determined reproducibly to ~ 1 Angstrom-scale resolution in the presence of 0.01 and 0.5 molar potassium, cesium, barium, and calcium chloride solutions. Model fits to the data show that potassium and cesium sorb in a manner similar to that of classical inner sphere complexes, but calcium and barium sorb closer to the mica surface than expected for classical outer sphere complexes. Model fits also suggest that chloride could be present near the surface. Sorption of zinc to quartz (from 0.01 molar zinc chloride solutions) resulted in minimal structural differences from the interfaces in pure water. Continued experiments on muscovite include investigation of the interface structure in the presence of various monovalent (and

divalent) anions, including bicarbonate and carbonate. Experiments on quartz include nucleation of zinc-silicate clays under varying pH conditions. Experiments to form calcite on muscovite and clays on quartz are in progress using steady-state flow experiments in the fluid cell of an atomic force microscope.

UNIVERSITY OF COLORADO

Department of Civil, Env. and Arch. Engg.
Campus Box 428
Boulder CO 80309-0428

Grant: DE-FG03-96ER14590

The Physics of Two-Phase Immiscible Fluid Flow in Single Fractures and Fractured Rock

H. Rajaram, (303) 492-6604, hari@colorado.edu; R. J. Glass Sandia National Laboratories; M. J. Nicholl, University of Idaho

Objectives: Employ detailed physical experiments and high-resolution numerical simulations to develop a quantitative understanding of the critical processes controlling two-phase flow and transport in fractures. Fundamental understanding may subsequently be abstracted for application to large-scale problems in petroleum extraction, isolation of hazardous or radioactive waste, remediation of subsurface contaminants, and CO₂ sequestration.

Project Description: Under two-phase immiscible flow conditions, fluid flow and solute transport characteristics of the fracture are controlled by the geometry of the respective phases. In turn, phase geometry is determined by a combination of aperture variability, phase accessibility, capillary and viscous effects associated with the two-phase flow processes themselves, and external forces such as gravity. Also, if one of the fluids is slightly soluble in the other, mass transfer between the phases will influence phase geometry.

In this collaborative project between Sandia National Laboratories, the University of Colorado at Boulder, and the University of Idaho, systematic physical experimentation is coupled with concurrent numerical simulation to explore the factors controlling phase geometry, flow, transport, and inter-phase mass transfer in rough-walled fractures. A high-resolution light-transmission technique has been developed to allow accurate experimental measurements (aperture, phase geometry, solute concentration) in transparent analog fractures. Use of this technique will lead to data of unprecedented accuracy for evaluating current understanding of fundamental processes, and motivate refinement of theoretical concepts.

Results: A depth-averaged model was developed for dissolution of a non-aqueous phase liquid (NAPL) entrapped in a variable aperture fracture (see Figure). The model couples fluid flow, transport of the dissolved NAPL, inter-phase mass transfer and NAPL-water interface movement. The relevant fundamental processes are incorporated at appropriate levels of resolution and thus our model does not require any empirical parameters to describe inter-phase mass transfer. Model simulations were compared to a NAPL dissolution experiment carried out in a transparent analog glass fracture (15.4 x 30.3-cm) under constant flow conditions. The evolution of the entrapped NAPL geometry during dissolution was measured using our high-resolution light-transmission techniques, at a 0.0155 x 0.0155-cm resolution. The model accurately predicted both the change in overall NAPL saturation with time, and the evolution of the entrapped NAPL geometry. This is perhaps the first instance of close

agreement between simulations and experiments on NAPL dissolution without any empirical treatment of inter-phase mass transfer.

In comparison to a saturated fracture, transient solute transport through a variable aperture fracture containing an entrapped fluid phase will be characterized by enhanced dispersion and pronounced non-Fickian behavior. Transport experiments in a partially saturated fracture were used to evaluate a three-dimensional particle-tracking simulator, which employs a quasi-three dimensional velocity field based on the Reynolds equation. The particle-tracking model was in qualitatively good agreement with experiments. It was able to predict 85% of the relative increase in dispersion resulting from the entrapped phase. It also reproduces the experimentally observed nonlinear relationship between solute dispersion and Peclet number, which suggests that Taylor dispersion effects are potentially significant even in partially saturated fractures.

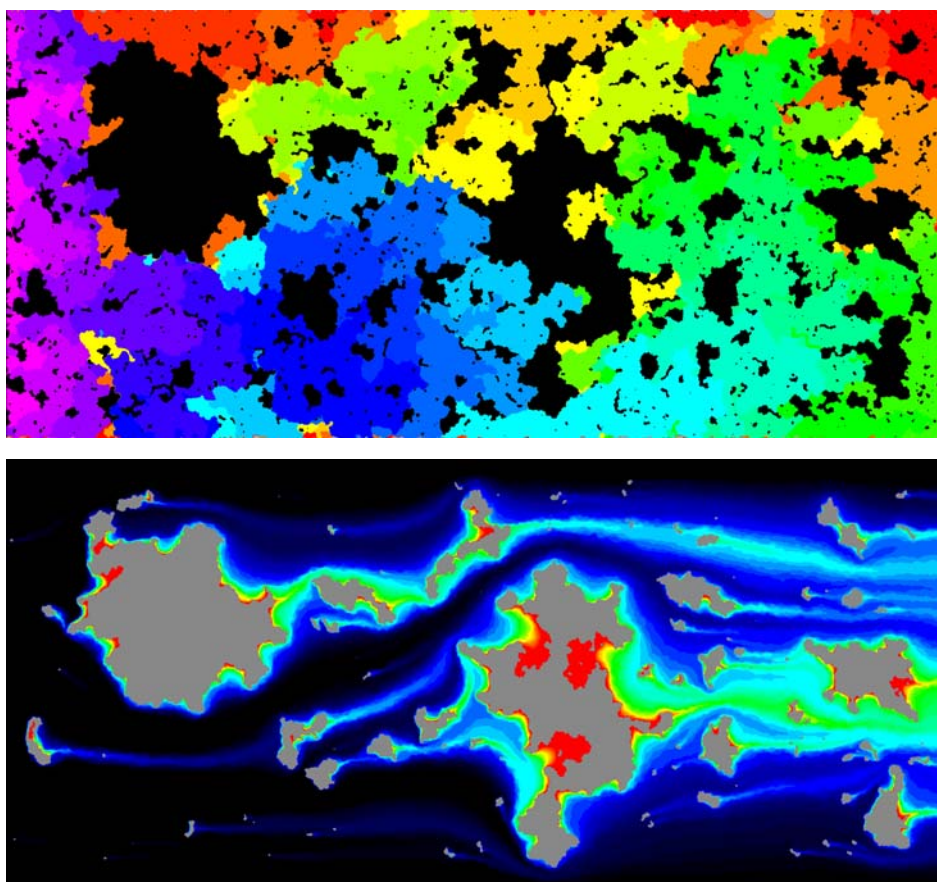


Figure 1: In context of experiments, the physics of flow, transport, phase displacement, and phase/rock dissolution are formulated and solved numerically. Top: Phase displacement in rough-walled fracture leading to entrapment of TCE (black); displacement order is shown in color from purple-blue-green-yellow-red. Bottom: Subsequent dissolution of TCE (now gray) from flowing fracture; dissolved concentrations of TCE are shown in color from blue (0) to red (TCE saturated).

Single-phase flow in a discrete fracture is commonly simulated using the Reynolds equation. Our earlier work suggested that this depth-averaged approach would underestimate head loss in regions of changing aperture. To explore this hypothesis, we implemented an ad hoc correction in the numerical formulation

of the Reynolds equation. The correction allowed us to modify local head loss according to the magnitude of local changes in aperture. Increasing the influence of changes in aperture led to increased channelization of flow and in-plane tortuosity. Calibration to experimental measurements of transmissivity on measured aperture fields led to improved estimates of longitudinal dispersivity, demonstrating the importance of adequately describing local head loss.

Finally, we developed a modified diffusion-limited aggregation (DLA) process to model immiscible viscous displacements in rough-walled fractures. Our model includes the effects of local aperture field variability to channelize flow within a fluid phase and capillarity to smooth the displacement front. Model behavior was considered in both a Hele-Shaw cell, and a variable aperture field that is correlated well below the simulation scale. Simulation results demonstrated that both local transmissivity and interfacial tension exhibit first-order influences on the development of phase structure. Local transmissivity bias channels growth into connected large apertures, while our simple density based sticking rule models capillarity and systematically smoothes the interface.

UNIVERSITY OF COLORADO

Cooperative Institute for Research in Environmental Sciences
Colorado Center for Chaos & Complexity
Department of Physics
Campus Box 216, Boulder, CO 80309

Grant: DE-FG03-95ER14499

Analysis and Interpretation of Multi-Scale Phenomena in Crustal Deformation Processes: Using Numerical Simulations of Complex Nonlinear Earth Systems

*John B. Rundle, (303) 492-5642, fax (303) 492-5070; rundle@cires.colorado.edu; W. Klein
Department of Physics, Boston University*

Objectives: To develop a physical understanding of the origins of geodetic crustal strains in nonlinear geomechanical systems, to examine the space-time patterns and correlations that occur in these systems, and to use these patterns to forecast the future activity that may produce disasters affecting a wide variety of critical energy facilities.

Project Description: The complex earth system generates a variety of phenomena that are highly non-linear and operate over a broad range of spatial and temporal scales. Signatures of these processes include scaling(fractal distributions), global and local self-organization, intermittancy, chaos and the emergence of coherent space-time structures and patterns. We are using massively parallel simulations to model geodynamical effects observed in earthquake systems in order to determine the origin of these phenomena. These investigations and the theoretical efforts done in parallel are particularly aimed at quantifying the limits of predictability for disasters such as earthquakes that occur within the earth system. We are currently continuing our development of the theoretical and computational tools that allow us to both obtain sufficient data on realistic models and to analyze the data we obtain. From these simulations we will then predict geodetic and other deformation associated with impending earthquakes to be tested against Global Positioning System, Synthetic Aperture Radar, seismicity and other field data.

Results: We have made significant advances in several areas. These include:

- 1) Advances in identification, analysis, and interpretation of multi-scale emergent space-time patterns in numerical simulations of earthquake fault systems, as well as in real fault systems. Most computational and theoretical work to date has focused on understanding the behavior of single faults. We studied the types of emergent space-time patterns of earthquake activity that occur on a given interacting fault network, how the patterns scale in space and time, how they are related to the inherently unobservable underlying dynamics of stress accumulation, and their sensitivity to changes in the underlying model parameters. Our results imply that many of the significant dynamical properties of earthquakes, including the form of the Gutenberg-Richter relation for the fault network, can only be understood in the context of the topologically complex network as a whole, rather than of the individual faults.
- 2) Scale dependence of Self-Organizing Threshold Systems, with Applications to Earthquakes and Other Systems. Threshold systems are known to be some of the most important nonlinear, self-organizing systems in nature, including networks of earthquake faults, neural networks, superconductors and semiconductors,

and the World Wide Web, as well as political, social, and ecological systems. All of these systems have dynamics that are strongly correlated in space and time, and all typically display a multiplicity of spatial and temporal scales. In all of these systems, long-range interactions induce the existence of locally ergodic dynamics. The existence of dissipative effects leads to the appearance of a “leaky threshold” dynamics, equivalent to a new scaling field that controls the size of nucleation events relative to the size of the background fluctuations. As part of this year’s research effort, Rundle was a co-organizer (with D.L. Turcotte and H. Frauenfelder, both members of NAS) of the second NAS Arthur M. Sackler Colloquium at the NAS Beckman Center, Irvine, California, held March 23-24, 2001. Topic of the colloquium was “Self-Organizing Complex Systems”. Proceedings volume will appear shortly.

3) PDPC Patterns of Earthquakes in Nature: Implications for Scaling in Space and Time. Earthquake dynamics are considered to be a paradigm for strongly correlated, high dimensional driven threshold systems such as neural networks and magnetized domains in ferromagnets. In general, these studies have focused on scaling, critical phenomena and nucleation arising from analysis of simulation data, as well as on space-time patterns of activity seen in such simulations. The more difficult problem of understanding the physical meaning of the space-time patterns of activity, leading to new methods to forecast the future evolution of large events in the system, has been only infrequently addressed. During this year, we continued to develop and improve new methods for understanding the observable space-time patterns of activity in driven mean field threshold systems, based on the idea that many of these systems are characterized by pure phase dynamics, whose mathematics is isomorphic to the mathematics of quantum mechanics. Application of these method to earthquake data from a typical, seismically active region, southern California, has shown that the method holds considerable promise for forecasting the temporal occurrence of the largest future events.

4) Green’s Functions and Analysis of Actively Deforming Regions Including Volcanoes. We have examined surface deformation in two volcanic regions, Long Valley caldera in California , and Mayon volcano in the Philippines. Our work, as always, has been in collaboration with the Spanish group at the University Complutense de Madrid, under the direction of Professor Jose Fernandez-Torres. In the former case of Long Valley, we modeled both deformation and gravity changes in an attempt to identify possible precursors of an eruption. Our results obtained by inverting these data indicate that errors can be introduced if all types of data are not considered simultaneously in the modeling process. In the case of Mayon volcano in the Philippines, we found that this type of joint modeling of the gravity and deformation data produces results that are far more plausible than previous results produced by modeling such data independently.

UNIVERSITY OF COLORADO

Cooperative Institute for Research in Environmental Sciences
Dept. of Geological Sciences
Boulder, Colorado 80309

Grant: DE-FG03-94ER14419

Seismic Absorption and Modulus Measurements in Single Cracks and Porous Rocks: Physical and Chemical Effects of Fluids

Hartmut Spetzler, (303) 492-6715, fax (303) 492-1149, spetzler@spot.colorado.edu

Objective: Our primary objective is to understand and characterize the physicochemical effects of small amounts of organic compounds on the mechanical properties of partially saturated sediments and rocks. Our ultimate goal is to develop a system for monitoring the onset of contamination at buried waste sites.

Project Description: Small amounts of organic compounds adsorbed to granular surfaces change the rock's surface properties (e.g. surface tension), which significantly change the rock's transport properties (e.g. permeability and capillary pressures) and bulk mechanical properties (e.g. compressibility and ability to dissipate energy). Fluid redistribution in a stressed, partially-saturated rock occurs via meniscus deformation and/or contact line motion, both of which require energy loss from a passing seismic wave (seismic absorption). An apparatus has been developed that harmonically stresses a rock core plug and measures subsequent deformations in the rock. The lag between the applied stress and the rock's deformation response to the stress is related to the energy dissipation due to fluid redistribution.

Results: As a result of this research, we have observed and mechanically described a new relaxation mechanism that can produce significant attenuation in rocks. This mechanism, fluid-surface contact angle hysteresis, is sensitive to the presence of organic compounds, which alter the rock's surface tension and chemistry. Contact angle hysteresis, a friction-like energy loss mechanism, is responsible for attenuation we observe in partially-saturated Berea sandstone when harmonically stressed at low frequencies (0.001 - 1 Hz) in the laboratory. Theory and lab measurements suggest that the presence of a chlorinated solvent such as TCE in sandstone produces measurable attenuation. We are currently studying the effects of different fluid saturations (water, contaminant, and gas) on attenuation at low frequencies in the laboratory and are preparing to develop a system to measure attenuation in the field during different saturation and contamination conditions. We will also extend our work to include potential effects in unconsolidated sediments. By the end of this year, we expect to have developed a better understanding of the combined effects of saturation and contamination on seismic attenuation.

COLORADO SCHOOL OF MINES

Department of Chemistry and Geochemistry
Golden, Colorado 80401

Grant DE-FG03-00ER15090

Possible Vertical Migration of CO₂ Associated with Large-Scale Injection into Subsurface Geologic Formations

Ronald W. Klusman, (303) 273-3617, fax (303) 273-3629, rklusman@mines.edu

Objective: Determine if detectable gas leakage to the surface occurs, and its magnitude, at the CO₂ overpressured Rangely, Colorado oil field. Carbon dioxide-enhanced oil recovery has been in operation at Rangely since 1986.

Project Description: One of the proposals for large-scale sequestration of fossil fuel CO₂ is deep geologic disposal in depleted oil/gas reservoirs or deep aquifers. The literature generally ignores the possibility of vertical migration of gases caused by overpressure. Overpressuring a reservoir or aquifer will be necessary in order to have acceptable rates of dispersal of injected CO₂.

This research will investigate the possibility of loss of gases from a CO₂ overpressured reservoir. Carbon dioxide has been used for enhanced oil recovery (EOR) at the large Rangely oil field, northwest Colorado since 1986. The research will evaluate the soil gas compositions and fluxes to the atmosphere for evidence of microseepage of CH₄ and/or CO₂ that originated in the reservoir at a depth of 2000 m. These data will also be supported by measurement of stable carbon isotopes and carbon-14 to ascertain possible source(s) of the gases. The winter slowing of soil microbiological processes in the cold, semiarid climate at Rangely will aid in separating the possible microseepage signal from shallow methanotrophic consumption of CH₄, and from soil respiration-produced CO₂ in soil gases. Measurements are made in both the summer and winter seasons, in order to understand the noise in the system, and possibly detect and quantify a deep-sourced soil gas signal.

Results: The work associated with the summer 2001 field campaign was completed from June 25-August 4, 2001. Measurement of soil gas concentrations and fluxes was carried out between individual trips to the field. Stable isotope measurements were completed by early fall, 2001. At the beginning of the summer of 2001, five "deep" holes were augered for installation of a nested soil gas sampling system. Three of these were on the Rangely field, one on the Mellen Hill fault, and one in a background or control area.

Summer soil gas, CH₄, concentrations are very close to atmospheric concentrations with small deviations higher or lower, reflecting microseepage and methanotrophic oxidation, respectively. Carbon dioxide soil gas concentrations typically ranged from 3-10 times atmospheric concentration, reflecting root respiration and microbial oxidation processes. Summer fluxes of CH₄ averaged 3.59 mg/m²/day and CO₂ fluxes averaged 3.80 g/m²/day. Stable isotopic measurements demonstrated a predominance

of biologically-derived carbon in the CO₂. A small positive CH₄ flux was observed, but methanotrophic oxidation was most important.

Winter 2001/2002 measurements were carried out from December 12-2001 through February 12, 2002. Concentraions of CH₄ in soil gas were similar to the summer, but CO₂ concentrations were from atmospheric concentrations to approximately three times atmospheric concentrations. Methane fluxes averaged 18.4 mg/m²/day and CO₂ fluxes averaged 0.34 g/m²/day. This demonstrates a slowing of the methanotrophic oxidation, and slowing in the production of soil gas CO₂, relative to the summer. However, stable carbon isotopic measurements of winter soil gas CO₂ still support the predominance of a biological source, not a deep source.

The "deep" holes were constructed to allow permanent sampling at depths of 1, 2, 3, 5 m, and total depth, which ranged from 7 to 9 meters. A more extensive suite of measurements, including stable carbon isotopic measurements on CH₄, as well as CO₂ were completed. These data support a small level of CH₄ microseepage from depth, but evidence of CO₂ microseepage from depth remains negative. Large volume soil gas samples were collected during the winter of 2001/2002 for purposes of carbon-14 determination of purified CO₂, which is underway.

A non-parametric two group median test was run in order to determine whether the data from the Rangely field was different from data collected over the Mellen Hill fault, and the control area, respectively. The shallow soil gas CH₄ was significantly higher over the field, compared to the control area, but soil gas CO₂ was not. The δ C-13 of soil gas CO₂ was significantly lower over the Mellen Hill fault compared to the Rangely field, reflecting more microbiological activity on the fault.

A preliminary estimate of microseepage from the Rangely field was made. Based on the difference between summer and winter, and the difference between the field and the control area, an estimate of 400 metric tonnes of CH₄/year for the entire 78 km² area of the field was obtained. This microseepage seems to be concentrated over the western part of the field. Using the winter flux of CO₂ over the field, and knowing the majority is from biological processes, a preliminary estimate of <4300 metric tonnes of CO₂ year⁻¹ over the entire Rangely field is made. This will likely be further constrained when the stable isotope and carbon-14 data for the winter of 2001/2002 is obtained.

COLORADO SCHOOL OF MINES

Center for Wave Phenomena,
Green Center,
Golden, CO 80401-1887

Grant : DE-FG03-98ER14908.

Three-dimensional analysis of seismic signatures and characterization of fluids and fractures in anisotropic formations

Prof. Ilya Tsvankin, (303) 273-3060, fax (303) 273-3478, ilya@dix.mines.edu; Prof. Vladimir Grechka and Prof. Kenneth L. Larner

Website: <http://www.cwp.mines.edu>

Objectives: The main goal of the project is to develop efficient velocity analysis and parameter estimation methods for azimuthally anisotropic reservoirs using 3-D (azimuthal) variation in seismic signatures. The anisotropic parameters can then be related to the reservoir properties which control the flow of hydrocarbons.

Project Description: The CSM group is working on the inversion of azimuthally dependent reflection traveltimes and prestack amplitudes for the effective parameters of azimuthally anisotropic media. The combination of *P*-waves and converted *PS*-waves helps to estimate a representative set of the anisotropic parameters for models containing subvertical fracture systems or tilted transversely isotropic layers. The project includes theoretical studies, development of inversion and processing algorithms and their application to 3-D seismic field data. The inverted anisotropic model is used to evaluate the physical parameters of fracture networks and the lithologic properties of source and reservoir rocks; the rock-physics part of the project is largely addressed by the groups from LLNL and Stanford University. The project results should provide a foundation for high-resolution characterization of heterogeneous anisotropic reservoirs using wide-azimuth multicomponent seismic surveys.

Results

Moveout inversion of P-wave data in laterally heterogeneous VTI media

An efficient method for inverting azimuthally-dependent *P*-wave stacking velocities in VTI (transversely isotropic with a vertical symmetry axis) media was developed and applied to synthetic data. For models with plane dipping or curved interfaces above the reflector, it is possible to reconstruct the anisotropic velocity field in depth using minimal *a priori* information.

Joint 2-D travelttime inversion of PP and PS data

Conventional-spread *PP* and *PS* traveltimes were combined with check-shot data in a velocity-analysis algorithm for layered TI media designed to estimate the vertical velocities and anisotropic parameters. Application of this methodology to a field data set produced vastly improved *PS* sections that gave a crisp image of the reservoir.

Analysis of converted PS-wave reflection coefficients for anisotropic media

Concise linearized approximations were derived for the reflection coefficients of *PS*-waves in arbitrary anisotropic media. Their analysis was used to identify the parameter combinations constrained by *PS*-wave amplitudes for a range of anisotropic fractured models.

Joint inversion of PP and PS reflection coefficients for azimuthally anisotropic media

The analytic results described above were used to devise parameter-estimation algorithms operating with azimuthally varying reflection coefficients of *PP*- and *PS*-waves. The addition of mode-converted waves helps to overcome the nonuniqueness in the amplitude-versus-offset (AVO) inversion for fractured models of HTI (TI with a horizontal symmetry axis) and orthorhombic symmetry.

Estimation of fracture parameters for models with anisotropic background

Complications caused by background anisotropy in fracture characterization were studied for the effective model formed by two orthogonal fracture sets embedded in a VTI host rock. Whereas the fracture orientation can be found directly from surface seismic data, unambiguous estimation of the fracture compliances requires information about at least one of the background parameters.

UNIVERSITY OF CONNECTICUT

Department of Marine Science
1080 Shennecossett Road
Groton, CT 06340-6097

Grant: DE-FG02-95ER14528

Air-derived Noble Gases in Sediments: Implications for Basin Scale Hydrogeology

T. Torgersen, (860) 405 9094, fax (860) 405 9153, Thomas.Torgersen@Uconn.edu

B. Mack Kennedy, LBNL, (510) 486 6451, fax (510) 486 5496, bmkennedy@lbl.gov

Objectives: This research project (with Lawrence Berkeley National Laboratory) evaluates the processes which produce, dissolve and distribute noble gases and noble gas isotopes among liquid hydrocarbon, gaseous hydrocarbon and aqueous phases. This redirected project will: (1) identify and isolate carrier phases of the various air-derived noble gas components in sedimentary rocks, (2) investigate processes responsible for acquisition and trapping of the components in their sedimentary carrier phases, and (3) evaluate mechanisms that release these noble gas components.

Project Description: The mechanisms, processes and time scales of fluid flow in sedimentary basins represents a fundamental question in the Earth Sciences with direct application to exploration and exploitation strategies for energy and mineral resources. An explanation is needed for the mechanism by which Ne and/or Xe can be enriched on earth materials relative to the other noble gases, how these enrichments can be retained on a geologic time scale, and what processes release these components to the hydrologic system in which they are observed. This project will investigate (i) young sediment recovered in DSDP/ODP drill holes, (ii) outcrop samples from the Monterey formation (<20Myr), and (iii) drill core from the Elk Hills field as well as specific samples of opportunity. Samples will be characterized with respect to composition and geochemistry and a suite of chemically defined fractions will be used to investigate the fractions holding sorbed noble gas components. We will also investigate DSDP/ODP samples from various environments that have different initial compositions and have undergone different diagenesis patterns.

Results: This is a new direction for this project. Measurements of noble gas abundances in hydrocarbon fluids, conducted under the previous grant, provide ample evidence that naturally occurring fluids within the Earth's crust contain at least three distinct 'air-derived' noble gas components: (1) water saturated with air (i.e. groundwater), (2) a heavy (Kr, Xe) noble gas enriched component believed to be associated with the hydrocarbon source rock (Torgersen and Kennedy, 1999) and (3) a Ne-enriched component (Kennedy et al, 2002). Identifying the source of components #2 and #3 and understanding the where, when, and how these components are added to the hydrologic system will provide important constraints to basin scale hydrogeology, such as fluid source, flow path, and re-charge temperature. Because the enrichment patterns appear to be smooth functions of noble gas mass, adsorption on solids is often invoked as a potential source of the enrichment patterns. However, thermodynamics predicts preferential adsorption of heavy noble gases relative to the light noble gases, yet Podosek et al. (1980) found that approximately half the samples of sedimentary rocks analyzed for

noble gases contained a Ne-enriched component and in many cases, simultaneous Xe and Ne enrichments were found. A literature review suggests that the enriched components are associated with a host rock type or specific carrier phases. For instance, Xe-enrichments are strongly correlated with carbon-rich phases isolated from shales (e.g. Frick and Chang, 1977). It is clear that an explanation is needed for the mechanism by which Ne and/or Xe can be enriched on earth materials relative to the other noble gases, how these enrichments can be retained on a geologic time scale, and what processes eventually release these components to the hydrologic system in which they are observed. One possibility for explaining the Ne and Xe enrichments is the labyrinth-with-constrictions model proposed by Wacker et al., (1985), which will be used as a guide for this project. This model has the advantage that it can explain the very large noble gas enrichment factors observed in natural samples [$F(\text{Ng}) = 500\text{-}10,000$], simultaneous enrichment of Ne and Xe, as well as the rapid transition from physisorption to chemisorption apparently needed to explain long term retention. Establishing the lifetime for adsorption under physisorption kinetics and desorption under chemisorption kinetics through a study of noble gas 'trapping' via labyrinth-with-constrictions may provide specific insight into nanotechnologies.

UNIVERSITY OF DELAWARE

Department of Chemistry and Biochemistry
Newark, Delaware 19716

Grant: DE-FG02-89ER14080

Development of an Experimental Database and Theories for Prediction of Thermodynamic Properties of Aqueous Electrolytes and Nonelectrolytes of Geochemical Significance at Supercritical Temperatures and Pressures

R. H. Wood, (302) 831-2941, fax (302) 831-6335; rwood@udel.edu), D. L. Doren (302) 831-1070, fax (302) 831-6335, doren@udel.edu; Everett L. Shock (314) 726-4258, fax (314) 935-7361, shock@zonvark.wustl.edu

Website: <http://dogstar.duch.udel.edu/wood/research.html>

Objectives: The objectives of this research are to combine new experimental measurements on heat capacities, volumes, and association constants of key compounds with theoretical equations of state and with first principals quantum mechanical predictions to generate predictions of thermodynamic data. The resulting thermodynamic data allow quantitative models of geochemical processes at high temperatures and pressures.

Project Description: This project is part of ongoing collaboration between Prof. Everett Shock of Washington University and Prof. Robert Wood of the University of Delaware, which involves 1) experimental measurements on key compounds 2) making substantial improvements in theoretical equations of state for aqueous nonelectrolytes and electrolytes based largely on these experimental measurements 3) pursuing novel applications of these equations of state to the study of high temperature/pressure geochemical processes involving aqueous fluids, and 4) Developing and using ab initio quantum calculations with Molecular Dynamics simulations to predict chemical potentials of aqueous solutes where experimental measurements are impossible or not available. The experimental work is conducted at the University of Delaware. Geochemical applications of the data are done at Washington University. Efforts to improve the equations of state and develop predictive methods are shared between the two labs, because this task in particular requires close collaboration between the two Principal Investigators.

Results: Our use of conductance measurements to get equilibrium, association constants for a variety of aqueous electrolytes at high temperature has been going very well. We have new measurements on HCl, H₂SO₄, and NaHSO₄ that are not yet interpreted. We have finished the interpretation of our high concentration NaCl results as well as high concentration literature data on KCl. This work showed that for most geochemical environments there is no need to invoke multi-ion clusters at high concentrations. We are now processing our aqueous Na₂SO₄, Li₂SO₄ and K₂SO₄ results to get the first and second association constants for these salts. The design and testing of the new heat capacity calorimeter (joint project with University Blaise Pascal) has been completed. We have improved our theoretical equations of state (working with Everett Shock at Washington State University) by using our recent experimental

data to re-parameterize the revised HKF model. We have also adopted a new equation of state to describe experimental results for a number of aqueous non-electrolytes (including ones of high polarity (alcohols, amines, acids and amides) and/or large size (hexane and benzene)).

We have further developed our new method of predicting free energies of hydration where experimental measurements are impossible. This method uses molecular dynamic simulations and ab initio quantum mechanics to make the predictions. We have shown that our new method can predict hydration free energies of ions at high temperatures with great accuracy. For instance we predicted the free energy of hydration of sodium ion plus chloride ion at 573 K as -657 kJ/mol whereas the experimental value is -661 kJ/mol. At higher temperatures the free energies of hydration are unknown and we are in the process of predicting them at a variety of state points.

UNIVERSITY OF FLORIDA

Chemical Engineering Department
Gainesville, Florida 32611-6005

Grant: DE-FG02-98ER14853

Evolution of surface morphology during dissolution of a rough fracture

Anthony JC Ladd, (352) 392-6509, fax (352) 392-9513, ladd@che.ufl.edu

Objectives: The overall research objective of this project is to develop micro-mechanical models for the dissolution of porous rocks by a chemically reacting fluid. The aim of the work is an improved understanding of how the coupling between chemical reactions, hydrostatic pressure, and fluid flow produces morphological changes in the sample.

Project Description: Numerical simulation techniques are being developed to model the flow of a chemically reacting fluid through a porous matrix. These simulations will combine a very fast fluid flow code with a stochastic simulation of the transport of chemical reactants and products. The code iterates between fluid-flow simulations and cycles of chemical transport and reaction, to predict the changes in morphology arising from the coupling between chemical reactions at the solid-fluid surfaces and the flow of fluid through the pore spaces. The motivation for this work is to explain the observations of Dr. William Durham (Lawrence Livermore National Laboratory), who found that chemical erosion tends to reduce the small-scale spatial heterogeneity in narrow fractures, while enhancing it on larger scales.

Results: A new boundary condition for the lattice-Boltzmann model was developed, which allows a no-slip condition to be specified at scales less than the resolution of the grid (R. Verberg and A.J.C. Ladd, *Lattice-Boltzmann model with sub-grid scale boundary conditions*, Phys. Rev. Lett. 84:2148-2151, 2000). Recently we examined the accuracy and stability of this boundary condition in considerable detail (R. Verberg and A.J.C. Ladd, *Accuracy and stability of a Lattice-Boltzmann model with sub-grid scale boundary conditions*, Phys. Rev. E. 65:016701, 2001). This new boundary condition allowed us to simulate acid erosion in a fractured specimen of Carrara marble, using an initial fracture topography that was obtained from Dr. W.B. Durham (Lawrence Livermore National Laboratory). These simulations accurately accounted for fluid flow and molecular transport by convection and diffusion, but did not include a detailed model of the chemical kinetics at the eroding surfaces. In a new project we are now beginning to include more sophisticated dissolution kinetics, which takes account of the equilibrium between reactants and products.

GSY-USA, INC

2261 Market St., PMB 643
San Francisco, CA 94114-1600

Grant: DE-FG03-01ER15171

The Magnetotelluric Data Simulation Project

Randall Mackie, (415) 469-8649, randy@gsy-usa.com; William Cumming, (707) 546-1245, wcumming@sonic.net

Objectives: Compute a suite of synthetic magnetotelluric responses for realistic resistivity models of important crustal features to test imaging and interpretations algorithms.

Project Description: By computing synthetic MT responses for realistic resistivity models of important crustal features, this project will provide a basis for validating research claiming improved MT imaging of similar features. Researchers will also be able to more thoroughly investigate fundamental resolution issues such as the degree to which knowledge of MT impedance transfer functions at particular noise levels can constrain the 1, 2, or 3D character of the resistivity distribution that produced them. Impedance transfer functions will be computed and distributed in an easily accessed standard format for most types of geologic targets currently receiving significant MT research funding, facilitating the transfer of new MT technology among research and industry groups. Massively parallel computers at Sandia National Laboratories, otherwise unavailable to the academic and industry MT communities, will be used to compute 3D MT responses from resistivity models that will be far more realistically detailed than any previously used in such studies. Recognized MT research leaders and industry experts have been recruited to provide representative detailed 3D models for a wide variety of models, many of which are designed to apply details available from industry to enhance the shallow sections of models of importance to academic researchers investigating more fundamental properties and processes of the Earth's crust. The resistivity models currently planned include: over-thrust for petroleum, geothermal, mining, diamond exploration, ocean-bottom MT for petroleum exploration, environmentally hazardous waste sites, and western USA tectonics.

Results: This project has only recently been initiated..

UNIVERSITY OF HAWAII

Department of Geology and Geophysics
Honolulu, Hawaii 96822

Grant: DE-FG03-95ER14525

Growth of faults, scaling of fault structure, and hydrologic implications

Stephen Martel, (808) 956-7797, fax (808) 956-5512, martel@soest.hawaii.edu; Kevin Hestir Utah State University, (801) 797-2826, fax (801) 797-1822; hestir@sunfs.math.usu.edu; James P. Evans, Utah State University, (801) 797-2826, fax (801) 797-1588, jpevans@cc.usu.edu; Jane C.S. Long University of Nevada at Reno, (702) 784-6987, fax (702) 784-1766, JCSLONG@mines.unr.edu

Website: <http://www.soest.hawaii.edu/martel/Stevem.html>

Objectives: The main research objectives are: (a) to determine how faults grow in three dimensions in brittle crystalline rocks (granites and basalts), and (b) to further develop physically based stochastic models for predicting geometric and hydrologic properties of such faults.

Project Description: We are investigating how faults of different scale grow in granite and basalt in three-dimensions. We are systematically examining the geometries, structure, and mechanics of faults with trace lengths of a few meters to several kilometers, and using this knowledge to develop physically-based stochastic models for predicting the geometry of faults over a wide range of scale and for analyzing their hydraulic behavior.

Results: Field investigation of strike-slip faults in the granitic rock of the Sierra Nevada, California, have confirmed a new mechanism for fault formation and fault growth: tearing of igneous dikes. In Sequoia National Park, concentrations of oblique fractures formed in dikes and weakened them such that the dikes failed by shearing. This process caused fault zones several kilometers long to form in Sequoia National Park, could cause even longer faults to form elsewhere, and demonstrates how opening-mode fracture processes (like dike intrusion) are an important precursor to faulting. Mechanical analyses to date indicate that a material contrast between the dikes and the granite contributes to the preferential location of the oblique fractures within the dikes. An additional source of tensile stress (perhaps generated by cooling of the dikes and granite) seems necessary to have allowed the oblique fractures to open. Interestingly, at a second site north of Sequoia National Park, concentrations of joints along some dikes appear to have acted to terminate faults growing perpendicular to the dikes. Mechanical analyses of the faults in Sequoia National Park also indicate that their seemingly irregular slip distributions reflect a strong mechanical interaction among the faults over a broad area.

UNIVERSITY OF IDAHO

Department of Materials, Metallurgical, Mining, and Geological Engineering
Moscow, ID 83844-3024

Grant: DE-FG03-01ER15122

The Physics of Two-Phase Immiscible Fluid Flow in Single Fractures and Fractured Rock

M. J. Nicholl, (208) 885-9242, fax (208) 885-2855, mnicholl@uidaho.edu; R. J. Glass Sandia National Laboratories, H. Rajaram University of Colorado, Boulder

Objectives: Employ detailed physical experiments and high-resolution numerical simulations to develop a quantitative understanding of the critical processes controlling two-phase flow and transport in fractures. Fundamental understanding may subsequently be abstracted for application to large-scale problems in petroleum extraction, isolation of hazardous or radioactive waste, remediation of subsurface contaminants, and CO₂ sequestration.

Project Description: Under two-phase immiscible flow conditions, fluid flow and solute transport characteristics of the fracture are controlled by the geometry of the respective phases. In turn, phase geometry is determined by a combination of aperture variability, phase accessibility, capillary and viscous effects associated with the two-phase flow processes themselves, and external forces such as gravity. Also, if one of the fluids is slightly soluble in the other, mass transfer between the phases will influence phase geometry.

In this collaborative project between Sandia National Laboratories, the University of Colorado at Boulder, and the University of Idaho, systematic physical experimentation is coupled with concurrent numerical simulation to explore the factors controlling phase geometry, flow, transport, and inter-phase mass transfer in rough-walled fractures. A high-resolution light-transmission technique has been developed to allow accurate experimental measurements (aperture, phase geometry, solute concentration) in transparent analog fractures. Use of this technique will lead to data of unprecedented accuracy for evaluating current understanding of fundamental processes, and motivate refinement of theoretical concepts.

Results: A depth-averaged model was developed for dissolution of a non-aqueous phase liquid (NAPL) entrapped in a variable aperture fracture (see Figure). The model couples fluid flow, transport of the dissolved NAPL, inter-phase mass transfer and NAPL-water interface movement. The relevant fundamental processes are incorporated at appropriate levels of resolution and thus our model does not require any empirical parameters to describe inter-phase mass transfer. Model simulations were compared to a NAPL dissolution experiment carried out in a transparent analog glass fracture (15.4 x 30.3-cm) under constant flow conditions. The evolution of the entrapped NAPL geometry during dissolution was measured using our high-resolution light-transmission techniques, at a 0.0155 x 0.0155-cm resolution. The model accurately predicted both the change in overall NAPL saturation with time, and the evolution of the entrapped NAPL geometry. This is perhaps the first instance of close agreement between simulations and experiments on NAPL dissolution without any empirical treatment of inter-phase mass transfer.

In comparison to a saturated fracture, transient solute transport through a variable aperture fracture containing an entrapped fluid phase will be characterized by enhanced dispersion and pronounced non-Fickian behavior. Transport experiments in a partially saturated fracture were used to evaluate a three-dimensional particle-tracking simulator, which employs a quasi-three dimensional velocity field based on the Reynolds equation. The particle-tracking model was in qualitatively good agreement with experiments. It was able to predict 85% of the relative increase in dispersion resulting from the entrapped phase. It also reproduces the experimentally observed nonlinear relationship between solute dispersion and Peclet number, which suggests that Taylor dispersion effects are potentially significant even in partially saturated fractures.

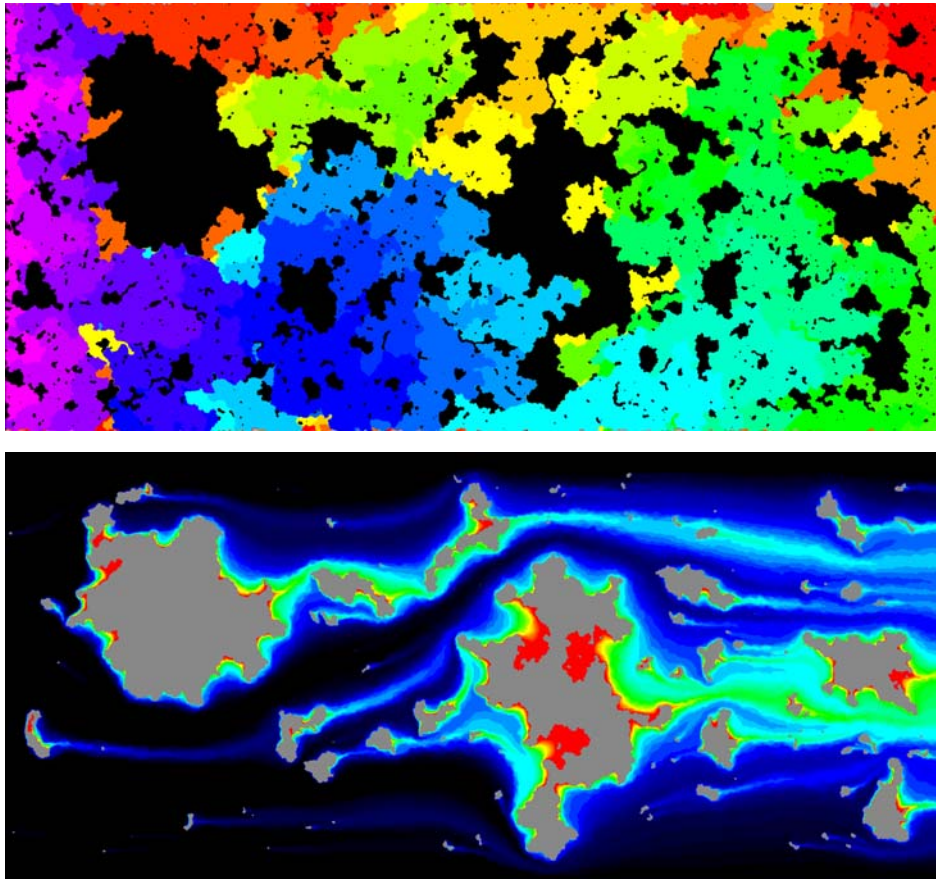


Figure 1: In context of experiments, the physics of flow, transport, phase displacement, and phase/rock dissolution are formulated and solved numerically. Top: Phase displacement in rough-walled fracture leading to entrapment of TCE (black); displacement order is shown in color from purple-blue-green-yellow-red. Bottom: Subsequent dissolution of TCE (now gray) from flowing fracture; dissolved concentrations of TCE are shown in color from blue (0) to red (TCE saturated).

Single-phase flow in a discrete fracture is commonly simulated using the Reynolds equation. Our earlier work suggested that this depth-averaged approach would underestimate head loss in regions of changing aperture. To explore this hypothesis, we implemented an ad hoc correction in the numerical formulation of the Reynolds equation. The correction allowed us to modify local head loss according to the magnitude of local changes in aperture. Increasing the influence of changes in aperture led to increased

channelization of flow and in-plane tortuosity. Calibration to experimental measurements of transmissivity on measured aperture fields led to improved estimates of longitudinal dispersivity, demonstrating the importance of adequately describing local head loss.

Finally, we developed a modified diffusion-limited aggregation (DLA) process to model immiscible viscous displacements in rough-walled fractures. Our model includes the effects of local aperture field variability to channelize flow within a fluid phase and capillarity to smooth the displacement front. Model behavior was considered in both a Hele-Shaw cell, and a variable aperture field that is correlated well below the simulation scale. Simulation results demonstrated that both local transmissivity and interfacial tension exhibit first-order influences on the development of phase structure. Local transmissivity bias channels growth into connected large apertures, while our simple density based sticking rule models capillarity and systematically smoothes the interface.

UNIVERSITY OF ILLINOIS AT URBANA-CHAMPAIGN

Department of Geology
1301 W. Green St., Urbana, IL, 61801

Grant: DE-FG02-00ER15028

Computational and Spectroscopic Investigations of Water-Carbon Dioxide Fluids and Surface Sorption Processes

R. James Kirkpatrick, (217) 333-7414, fax (217) 333-9142, kirkpat@uiuc.edu

Website: <http://www.geology.uiuc.edu/~kirkpat/index.html>

Objectives: Our efforts focus on understanding the molecular scale behavior of mineral surfaces and interlayers, the interaction of dissolved species in aqueous solutions with mineral surfaces, and the properties of geochemically relevant fluids at elevated pressures and temperatures. Such knowledge is essential to assessment and prediction of the complex chemical systems of the earth and is relevant to a wide range of natural and anthropogenic environments. To address these objectives we are taking four principal research directions:

- 1) Spectroscopic studies (NMR, FIR) of the structure and dynamics of surface and interlayer species, principally anions;
- 2) Development of molecular modeling approaches and the necessary force field parameters for examining the structure, dynamics and chemical reactions at the interfaces between minerals and aqueous fluids;
- 3) Molecular modeling studies of the structure and dynamics of ions and H₂O molecules at the interfaces between hydrous minerals and aqueous fluids and in the nanospaces of mineral interlayers;
- 4) Application of molecular modeling methods to understanding the structure and dynamics of carbonate-bearing aqueous fluids at elevated temperatures and pressures.

Project Description: Investigation of the structural environments and dynamical behavior of surface and interlayer exchanged aqueous anions in mineral-fluid systems is being undertaken using a combination of insitu NMR and FIR spectroscopy, sorption isotherm experiments and molecular dynamics (MD) computational modeling. This combination of techniques provides otherwise unobtainable, site- and species-specific information and allows integration of molecular and macroscopic perspectives. Aqueous species include CO₃⁻², HCO₃⁻, CO₂, Cl⁻, SeO₃⁻², SeO₄⁻², SO₄⁻², NO₃⁻, HPO₄⁻², and PO₄⁻³, with the counter ions Na⁺, K⁺, Cs⁺, Ca²⁺ as necessary. Solid substrate phases include single-metal hydroxides (brucite, portlandite, gibbsite) and double-metal hydroxides. MD modeling of both neat solutions and solution-mineral interfaces is central to this project.

Results:

Experimental work:

This year saw the culmination of an extensive experimental study of the structural and dynamical behavior of a wide range of geochemically important anions with layered double hydroxides (LDHs). The interaction of anions with mineral surfaces and in mineral interlayer gallery spaces is much less well understood than that of cations, and recognition of the geochemical importance of LDH phases in this regard is growing rapidly. The results provide a comprehensive framework for molecular scale understanding of the effects of anion size, conformation and charge and substrate composition and structure on the interlayer and surface structural environments of the anions, their reorientational dynamics and sorption/desorption behavior, and the macroscopic interlayer expansion. Experimental multi-nuclear, variability temperature and variable relative humidity $^{13}\text{CO}_3^{-2}$, $\text{H}^{13}\text{CO}_3^-$, $^{77}\text{SeO}_4^{-2}$, $^{77}\text{SeO}_3^{-2}$, $^{15}\text{NO}_3^-$, $^{35}\text{ClO}_4^-$, $\text{H}^{31}\text{PO}_4^{-2}$, and $^{31}\text{PO}_4^{-3}$ NMR, combined with IR spectroscopy, powder X-ray diffraction under controlled relative humidity, and water sorption isotherms demonstrate a high degree of correlation among interlayer expansion, water incorporation, and rotational dynamics of the anion at frequencies of the order of 10^4 Hz. Overall, phases that form expanded interlayer structures with two water layers contain tetrahedral oxyanions, whereas those that do not expand contain smaller or flatter anions, although anion charge also plays an important role. The structural environments and dynamical behavior of surface and interlayer anions are generally similar if the anion is either weakly or strongly held, because their local bonding environments are similar in the interlayer and on the surface. In intermediate cases, such as $^{77}\text{SeO}_3^{-2}$ and $^{15}\text{NO}_3^-$, surface anions can be dynamically, whereas those in the interlayer are rigidly held. The results have application in geochemistry, nuclear and hazardous waste management, and materials chemistry.

Computational work:

In support of the experimental work, computational molecular modeling has provided important insight into the actual structural environments and dynamical behavior of surface and interlayer species. A series of Cl^- -bearing Ca/Al, Mg/Al, Li/Al layered double hydroxides (LDH) has been simulated to investigate structural and dynamic details of the hydrogen bonding environments of anions and H_2O molecules in the interlayers of these materials, at the mineral/water interfaces, and their swelling behavior. A technique of surface atomic density maps and atomic density profiles has been developed to visualize and quantify the species- and site- specific structural data. The results are in good agreement with experimental findings and allow for quantitative understanding and interpretation of observed phenomena.

The results have shown a substantial effect of substrate charge and structure on the nanoscale structure of water at mineral surfaces. On simple metal hydroxides the H_2O molecules in direct contact with the surface are able to form structural environments comparable to those in bulk water by both donating and accepting H-bonds to and from surface OH-groups. This results in a very well developed H-bonding network formed across the interface in the solution. In contrast, on LDHs the polarizing effect of structural charge and the possibility of direct coordination of surface metal cationic sites by solution species (H_2O or anions) prevents formation of such a tetrahedrally ordered network of H-bonds in the interfacial region. The results suggest a substantial difference in the effects of the substrate on solution structure (e.g., ion clustering) in the interfacial region. Ongoing work is focused on comprehensive evaluation of the effects of surface structure and charge on interfacial water structure, its effects on sorption, and the effects of the size of the nanopores in which geochemical fluids are often held.

For carbonate-containing aqueous solutions, analysis of MD simulations of 0.5*m* Na₂CO₃ and 0.5*m* and 1.5*m* NaHCO₃ aqueous solutions under near-ambient conditions show that their structures and dynamical behavior are quite different. In Na₂CO₃ solutions, ionic clusters of Na⁺ and CO₃²⁻ are quite long-lived, and long simulation runs of up to 2 ns were needed to effectively probe the structure and dynamics of these clusters. Due to this ion cluster formation, the diffusion rates of both Na⁺ and CO₃²⁻ are ~3-6 times lower than in similar chloride solutions. In contrast, in NaHCO₃ solutions ion cluster is much less, and the diffusion rate of HCO₃⁻ is thus about the same as that of Cl⁻. Analysis of the solute hydration structure in terms of O-O and O-H radial distribution functions indicates that the negatively charged O atoms (Oc) of carbonate ions are hydrated by water molecules (Ow and Hw) in a manner similar to H₂O molecules themselves. Strong $g_{OH}(R)$ peaks at ~1.8 Å and $g_{OO}(R)$ maxima at ~4.5 Å indicate a high degree of hydrogen bonding around Oc. The hydration shells of carbonate and bicarbonate ions both contain approximately 10 water molecules, but the carbonate one is more structured due to the higher anion charge.

INDIANA UNIVERSITY

Laboratory for Computational Geodynamics
Department of Chemistry
Bloomington, Indiana 47405

Grant: DE-FG02-1ER14175

Self-Organized Mega-Structures in Sedimentary Basins

Peter J. Ortoleva, (812) 855-2717, fax (812) 855-8300, ortoleva@indiana.edu

Website: <http://www.Indiana.edu/~lcg>

Objectives: A deeper understanding of the sedimentary basin is sought to improve our ability to predict the location and characteristics of natural resources, and in the process, identify new phenomena. The approach is based on the identification of fundamental reaction, transport, and mechanical (RTM) processes, and the development of rate laws based on them, to solve the equations of mass, momentum, and energy conservation.

Project Description: The goal of this project is to gain a quantitative understanding of the origins of large-scale features in a sedimentary basin (e.g. salt tectonics, faults and fluid compartments). This understanding can be directly translated into the advancement of our fossil energy and other resource E & P activities, as well as the subsurface sequestration of CO₂ and other waste or toxic fluids. The direct goal of this project is to develop models and algorithms to understand the fundamental geosciences of these phenomena.

Results: In this year, we focused on four key fundamental issues delineating the geological history and the multiple scale challenges in quantitative modeling.

1. Multiple Scale Theory

While we are focusing on kilometer scale features, the dynamics of the large-scale phenomena of interest are dependent on the physics of the shorter scales (e.g. fault dynamics depends critically on grain scale processes such as pressure solution, breakage and overgrowth). Furthermore, the larger scale phenomena set the conditions under which the shorter scale ones must operate. In summary, the short and long scale processes are an inseparably nested cluster of effects.

To address these issues, we have developed a multiple scale asymptotic analysis of the Liouville equation. The result is a rigorous equation for the probability of the distribution of grains that accounts for six distinct timescales and three lengthscales. The theory can be applied to the full range of composite media from unlithified sediment to brittle rocks. This work will appear in Chapter VIII of the PI's upcoming monograph Mesosopic Chemical Physics.

2. Probability Functional Methods in Geological History Recreation

The phenomena of interest depend critically on the tectonic history applied to the basin at its top, side and bottom boundaries. The tectonic history is expressible in terms of the temporal evolution of the spatial distribution of heat flux, upheaval/subsidence and other factors acting at the boundaries of the basin. As the data available (seismic, well log, etc.) is sparse and only at the present day (i.e. not one hundred million years ago), we have developed a probability theory of these factors. As there is an uncountable infinity of factors (i.e. their value at all points on the boundary at all times) the probability is a functional of these space-time dependent boundary factors. Therefore, the probability is a functional of these factors. We have derived a functional differential equation for the most probable boundary tectonics scenario. We have also developed numerical techniques for solving these equations based on finite element multi-gridding and physically motivated regularized techniques. The equations are constructed using our Basin RTM crustal process simulator that accounts in three spatial dimensions for incremental stress rheology, fracture network dynamics, multi-phase flow, kerogen reactions and grain-scale processes. Having developed this information theory methodology we can more reliably model the dynamics of the basin because the boundary conditions needed to solve the partial differential equations are automatically determined using an unbiased analysis of a host of geological data. We are focusing on the application of this theory using seismic data due to its potential for remote resource detection and characterization.

3. Fluid Compartments and Salt Tectonics

Fluid compartments and salt diapirism are being analyzed as consequences of basin reaction, transport and mechanical processes. As fractures play a key role in maintaining the internal fluid communication within many compartments, and in the medium surrounding a deforming salt body, as kerogen reactions and multi-phase flow play important roles in the overpressuring of compartments, these factors are being included in the analysis. In this way, we find that the location and characteristics of fluid compartments and salt bodies depend sensitively on the tectonic and sedimentary history of the basin.

4. Fault Nonlinear Dynamic Phenomena

In the past year we have started the development of a new three dimensional fault dynamics model by integrating modules we developed earlier for the basin model, pre-existing models of the state and rate dependent friction law-type, and our new gouge evaluation model. We have several options for the model to test various concepts of seismicity. Processes in the bulk medium away from the fault surface include poro-elasticity, nonlinear irreversible deformation with yield, porous medium fluid flow, compaction, heat flow, frictional heating and fracture dynamics. For cases when the medium away from the fault surface is linear we are using our earlier experience (Ortoleva and Ross 1972, *Journal of Chemical Physics* 56(9): 4397-4400) in nonlinear integral equations to understand the onset of oscillatory slip, seismicity, failure waves, intra-fault compartments and associated fluid flow phenomena. These studies are advancing our understanding of the dynamical fault system. We are classifying fault behaviors (limit cycles, chaos and waves) and are using our rock competency model to investigate fault initiation and branching.

INDIANA UNIVERSITY

Department of Geological Sciences
Bloomington, Indiana 47405-1405

Grant: DE-FG02-00ER15032

Isotopically Labile Organic Hydrogen in Thermal Maturation of Organic Matter

A. Schimmelmann, (812) 855-7645, fax (812) 855-7961, aschimme@indiana.edu; M. Mastalerz, (812) 855-9416, fax (812) 855-2862, mmastale@indiana.edu

Website: <http://php.indiana.edu/~aschimme/hydranit.html>

Objectives: Explore the geochemical conditions and mechanisms that contribute to changes in the abundance of isotopically labile organic hydrogen in sedimentary organic matter during thermal maturation. Evaluate the diagenetic and/or paleoenvironmental significance of D/H ratios in different types of bulk kerogen, specific macerals, oil, and fractions of oil.

Project Description: Isotopically labile organic hydrogen in organic matter occupies chemical positions that participate in isotopic exchange and in chemical reactions during thermal maturation. We quantify the extent of isotopic transfer of hydrogen and nitrogen between organic matter and (i) ambient water and (ii) dissolved ammonia in long-term laboratory experiments. Natural kerogens and macerals of different type and maturity, and a large matrix of oils, fractions of these oils, and associated formation waters are isotopically characterized to assess the extent of natural hydrogen isotopic transfer during maturation and storage over geologic time. FTIR and NMR spectroscopic and petrographic methods assist in the interpretation of isotopic data. We also investigate the paleoenvironmental significance of an apparent correlation between hydrogen exchangeability and the $^{15}\text{N}/^{14}\text{N}$ ratio in stratigraphic sequences of kerogens.

Results: Organic hydrogen isotopic exchangeability in kerogen (H_{ex} , in % of total organic H) and δD_n values of non-exchangeable organic hydrogen in kerogen have been investigated spanning thermal maturation levels from lignite to graphite. H_{ex} in coal depends on thermal maturity and maceral composition. H_{ex} is highest in lignite with about 18% and decreases to around 2.5% in coals with R_o of 1.7 to ca. 5.7%. Reversing this trend, at higher rank (R_o values larger than 6%) H_{ex} increases slightly due to increasing aromaticity. A directly measured D/H ratio in bulk coal or TOC-rich rock, even after careful demineralization, reflects (1) hydrogen from various source materials, and thus the maceral composition, (2) the history of isotopic interaction along thermal maturation of organic matter with water, and (3) the presence of isotopically exchangeable organic hydrogen. The latter complication can be mitigated by isotopic double-equilibration of exchangeable hydrogen, yielding δD_n values. Our ongoing collaboration with the Australian Geological Survey on the isotopic comparison between oils (aromatic, polar, and saturated fractions of the oils, and bulk oil) and formation waters was expanded to include kerogens from a variety of identified oil source rocks. Preliminary results suggest the utility of δD_n values for oil-source rock correlation.

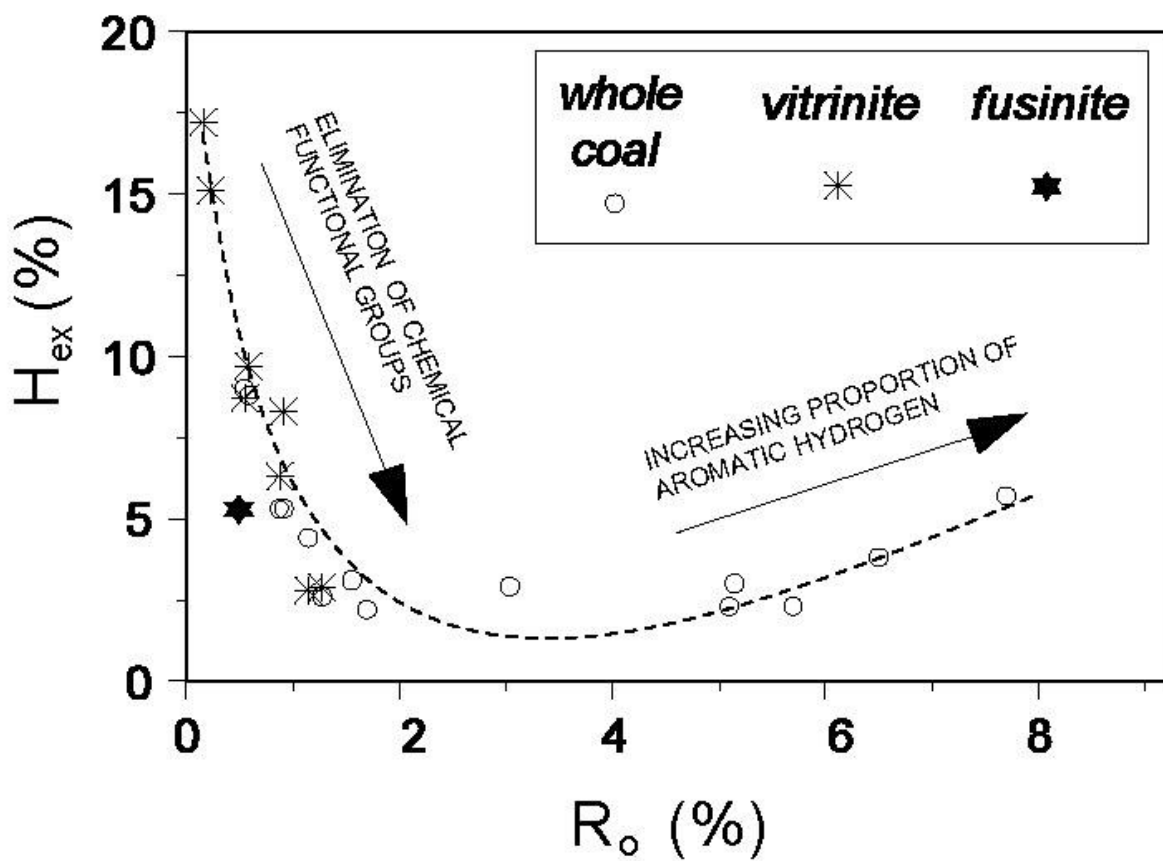


Figure 1: The isotopic exchangeability of organic hydrogen (H_{ex} , in % of total organic hydrogen) in kerogens with water hydrogen shows a distinct relationship with vitrinite reflectance (R_o), or with thermal maturity.

THE JOHNS HOPKINS UNIVERSITY

Department of Earth and Planetary Sciences
Baltimore, Maryland 21218-2687

Grant: DE-FG02-96ER14619

Fluid Flow in Faults: Estimating Permeability and Diagenetic Effects in a Transpressional Setting, Southern California

Grant Garven, (410) 516-8689, fax (410) 516-7933, garven@jhu.edu ; James R. Boles UC-Santa Barbara, (805) 893-3719, fax (805) 893-2314; boles@magic.geol.ucsb.edu

Objectives: This is a collaborative effort to determine the coupling of fluid mass transfer and diagenetic effects along faults which have developed in a transpressional setting. The study will contribute a practical understanding of the effects of thrusting on sediment diagenesis, fault-valve mechanics, petroleum migration and basin-scale groundwater flow in an active seismic environment.

Project Description: We have targeted three major faults and petroleum fields in southern California for study: Wheeler Ridge and Elks Hills in the San Joaquin Basin and the Refugio Fault in the Transverse Ranges near Santa Barbara. Subsurface core samples, outcrop samples, well logs, reservoir properties and published structural-seismic sections are being collected to characterize the tectonic history and diagenetic evolution for the known fault networks. These data provide constraints for finite element flow and transport models that are being developed to predict fluid pressures, flow patterns, rates of deformation, temperatures, and diagenetic patterns in the fault systems during thrusting and normal faulting.

Results: Jim Boles and his Ph.D. student Renee Perez have analyzed the petrology of cements and geochemistry of porewater and hydrocarbons at the Wheeler Ridge field to characterize the geochemical imprints of Quaternary-age thrusting. Permeability near the fault zone appears to decrease at depths greater than 2.4 km due to calcite cementation, which impeded oil migration, while at shallower depths the porosity increases due to plagioclase dissolution and microfracturing. Grant Garven and his Ph.D. student Eyal Stanislavsky have written a fully coupled, 2-D, poroelastic plane-strain numerical code to model fault-valve behavior and earthquake recurrence at Wheeler Ridge (Fig. 1). The first generation of numerical experiments reveal an initial fault failure after 45,000 years of thrust loading with pulses of geofluid migration that dissipate relatively quickly. Patterns of transient fluid flow and deformation have been evaluated for different scenarios of model boundary, rheological, and permeability conditions. Failure is strongly controlled by the ratio of host rock to fault bulk compressibility.

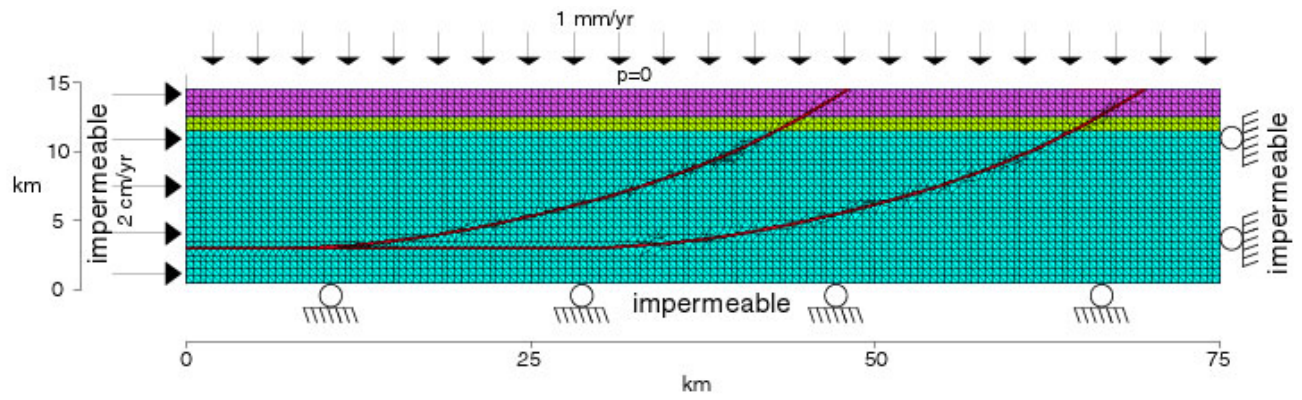


Figure 1. Finite element mesh and boundary conditions. The cross-section is subjected to compressional tectonic forces, and to shallow marine subsidence. The tectonic plate is moving at a velocity of 2 cm/yr, and the surface is subsiding at a velocity of 1 mm/yr. These boundary conditions represent the initial stage of the Wheeler Ridge (Medwedeff, 1992).

THE JOHNS HOPKINS UNIVERSITY

Dept. of Earth and Planetary Sciences
Baltimore, MD 21218.

Grant: DE-FG02-96ER-14616

Predictive Single-Site Protonation and Cation Adsorption Modeling

Dimitri A. Sverjensky, (410) 516-8568, fax (410) 516-7933, sver@jhu.edu

Objectives: The overall goal of this research is to develop a predictive model of adsorption processes at the mineral-water interface that can be applied to a fundamental understanding of the role of adsorption in geochemical processes such as weathering, diagenesis, the chemical evolution of shallow and deep groundwaters and ore-forming fluids, and the fate of contaminants in groundwaters.

Project Description: The research is aimed at generating a comprehensive, internally consistent, quantitative description of proton and cation adsorption on oxides and silicates using an extended triple layer model. The model will be developed to integrate the available experimental information on proton and cation adsorption based on internally consistent assumptions. By so doing, it will considerably facilitate the comparison of experimental data from different investigators. In addition, the model will permit predictions of surface speciation to supplement the lack of experimental adsorption data for many systems of geochemical interest. In addition, it will provide a basis for extending applications of the concept of surface complexation to oxide and silicate dissolution kinetics. The proposed extended triple layer model will include: (1) Internally consistent assumptions and methods of estimating site densities and capacitances; (2) Explicit recognition of ion solvation; (3) Explicit recognition of proton attraction-repulsion; (4) Inclusion of the extended Debye-Huckel model for aqueous ionic activity coefficients; and (5) Inclusion of a geochemical thermodynamic data file for aqueous species and minerals.

Results: For the prediction of surface charge and metal adsorption, the capacitance at the solid-water interface is a critical parameter because it gives us a relationship between surface charge, which is measurable, and surface potential, which is not measurable. By analysing surface charge measurements for a wide variety of electrolytes and oxides using a consistent model, I have shown that the capacitances have systematic trends that reveal important information about the nature of the oxide-electrolyte-water interface. For example, on rutile surfaces, ions such as sodium and potassium adsorb as inner-sphere complexes, close to the surface. In contrast, on quartz surfaces, sodium and potassium adsorb as outer-sphere complexes, much further from the surface. The specific distances are consistent with independently measured X-ray studies. This greatly improves the predictive capabilities of the extended triple-layer model.

In addition, an analysis of the adsorption of alkaline earth metals on oxides revealed that the same surface complexes apply for very different minerals. The combination of this study with the results of the capacitance study described above also suggests that the bonding on different mineral surfaces can differ greatly. For example, on rutile, it is suggested that calcium forms inner-sphere complexes, whereas on quartz, the same stoichiometry forms an outer-sphere complex. Qualitatively, these results appear to be consistent with available X-ray studies of rutile and silica surfaces. In addition, the equilibrium constants of these complexes can be related by crystal chemical and Born solvation theory.

This means that the adsorption of calcium can be predicted on many other oxides and under conditions that have yet to be investigated experimentally.

THE JOHNS HOPKINS UNIVERSITY

Dept. Earth & Planetary Sciences
3400 N. Charles St., Baltimore MD 21218

Grant: DE-FG02-00ER 14074

Reactions and Transport of Toxic Metals in Rock-Forming Silicates at 25°C

David R. Veblen (410) 516-8487, fax (410) 516-7933, dveblen@jhu.edu

Objectives: This project is a multi-pronged investigation of reactions between minerals and both toxic metal-bearing aqueous fluids and gas phase reductants. We are specifically exploring the mechanisms of oxidation-reduction reactions at the mineral-fluid and mineral-vacuum interfaces, and transport of reactive components along the grain-boundary interface in rocks.

Project Description: The project has three main components: experimental investigation of U reduction and sorption by micas; high-resolution transmission electron microscopy (HRTEM) characterization of grain boundaries; and experimental investigation of transport and sorption of heavy metals along grain boundaries. The first component includes development of X-ray photoelectron spectroscopy (XPS) methodologies to probe sorption behavior and redox reactions at mineral surfaces. The second component includes molecular-dynamical modeling of grain-boundary structures to provide insight into their transport properties. This second component also includes development of near-atomic-resolution analysis and imaging methodologies of electron-energy-loss spectroscopy (EELS), high-angle-annular-dark-field imaging (HAADF) and energy-filtered-transmission-electron-microscopy (EFTEM) in mineralogical systems. The third component combines the geochemical and mineralogical studies to elucidate transport properties and mechanisms important in Earth materials.

Results: During this first year of the three-year cycle, the geochemical work has focused on the experimental and theoretical determination of the multiplet structures of Cr2p and Mn2p as a function of bonding environment. We have now documented strong bonding environment effects on the multiplet structures of Cr2p and Mn2p that complicate interpretations of the oxidation states of Mn(IV) and Cr(III) in environmentally important minerals. Theoretical calculations are focused on whether these observations can be explained by the degree of octahedral distortion (crystallinity) or covalency of minerals. The work on Mn oxides has had an important byproduct: we have provided the first strong evidence that Mn(IV) bearing oxides can oxidize methane at 25°C and low pressures without the assistance of bacteria (Ilton, Haiduc, and Weaver, 2001).

The TEM portion of the project continues to emphasize development and application of energy-filtered techniques. Our work has produced the first, true valence imaging technique for geologic materials at the nanometer scale. Results of valence imaging for ferric and ferrous iron was presented at the Goldschmidt Conference last spring (Elbert, Ilton and Veblen, 2001). Valence imaging for titanium in highly reduced glasses has also begun and initial calibration and results will be presented in the coming spring. Our work on energy-filtered imaging of iron-bearing silicates and their boundaries has also been progressing (a portion appears in Moore, Elbert and Veblen, 2001).

LEHIGH UNIVERSITY

Dept. Earth & Environ. Sciences
31 Williams Drive
Bethlehem, PA 18015

Grant: DE-FG02-00ER14507

Reactions and Transport of Toxic Metals in Rock-Forming Silicates at 25°C

Eugene S. Ilton, (610) 758-5834, fax (610) 758-3677, esi2@Lehigh.edu

Objectives: This project is a multi-pronged investigation of reactions between minerals and both toxic metal-bearing aqueous fluids and gas phase reductants. We are specifically exploring the mechanisms of oxidation-reduction reactions at the mineral-fluid and mineral-vacuum interfaces, and transport of reactive components along the grain-boundary interface in rocks.

Project Description: The project has three main components: experimental investigation of U reduction and sorption by micas; high-resolution transmission electron microscopy (HRTEM) characterization of grain boundaries; and experimental investigation of transport and sorption of heavy metals along grain boundaries. The first component includes development of X-ray photoelectron spectroscopy (XPS) methodologies to probe sorption behavior and redox reactions at mineral surfaces. The second component includes molecular-dynamical modeling of grain-boundary structures to provide insight into their transport properties. This second component also includes development of near-atomic-resolution analysis and imaging methodologies of electron-energy-loss spectroscopy (EELS), high-angle-annular-dark-field imaging (HAADF) and energy-filtered-transmission-electron-microscopy (EFTEM) in mineralogical systems. The third component combines the geochemical and mineralogical studies to elucidate transport properties and mechanisms important in Earth materials.

Results: During this first year of the three-year cycle, the geochemical work has focused on the experimental and theoretical determination of the multiplet structures of Cr2p and Mn2p as a function of bonding environment. We have now documented strong bonding environment effects on the multiplet structures of Cr2p and Mn2p that complicate interpretations of the oxidation states of Mn(IV) and Cr(III) in environmentally important minerals. Theoretical calculations are focused on whether these observations can be explained by the degree of octahedral distortion (crystallinity) or covalency of minerals. The work on Mn oxides has had an important byproduct: we have provided the first strong evidence that Mn(IV) bearing oxides can oxidize methane at 25°C and low pressures without the assistance of bacteria (Ilton, Haiduc, and Weaver, 2001).

The TEM portion of the project continues to emphasize development and application of energy-filtered techniques. Our work has produced the first, true valence imaging technique for geologic materials at the nanometer scale. Results of valence imaging for ferric and ferrous iron was presented at the Goldschmidt Conference last spring (Elbert, Ilton and Veblen, 2001). Valence imaging for titanium in highly reduced glasses has also begun and initial calibration and results will be presented in the coming spring. Our

work on energy-filtered imaging of iron-bearing silicates and their boundaries has also been progressing (a portion appears in Moore, Elbert and Veblen, 2001).

UNIVERSITY OF MARYLAND

Department of Chemistry and Biochemistry
College Park, Maryland 20742

Grant: DE-FG02-94ER14467

Theoretical Studies on Heavy Metal Species in Solution

J. A. Tossell, (301) 405-1868, fax (301) 314-9121, tossell@chem.umd.edu

Objectives: This study utilizes the techniques of computational quantum chemistry to study the structures, energetics and properties of various metal species in solution, as components of mineral glasses, or absorbed on mineral surfaces. The focus in the past year has been on complexes of Cu(I) with thioarsenite ligands, on the energetics of the oxidation of Sb (III) species in sulfidic solutions, on computational studies of perturbations of the Al₁₃... tridecameric polyoxocation, on the electron capture decay constant of Be in its compounds and on the speciation of Si in solutions containing polyalcohols and other organic ligands.

Project Description: To understand the mechanisms of dissolution of minerals and the formation of ore deposits one must understand the structures and properties of metallic species in aqueous solution. In collaboration with Professor George Helz we recently identified a Cu thioarsenite complex which contributes greatly to the solubility of both Cu and As in sulfidic solutions in equilibrium with Cu and As sulfide minerals. A detailed discussion of the properties of this compound has now been published (*Inorg. Chem.*, 40, 6487, 2001). Our studies of speciation in arsenite and thioarsenite solutions have been extended to a study of their UV spectra, to assess the capability of UV spectroscopy for species identification and quantification (*Aquatic Geochem.*, in press, 2002). Extending upon our studies on the effect of Al³⁺(aq) hydrolysis and oligomerization on Al NMR parameters, we have calculated the structure and properties of the Al₁₃... tridecameric polyoxocation (*Geochim. Cosmochim. Acta*, 65, 2549, 2001). This species has also been used as a model site for adsorption of small molecules, modeling the adsorption process for Al oxyhydroxides, and as a test of our methods for calculating surface acidity. Finally, we have returned to the calculation of Na NMR, focusing on Na⁺ in crown-ether complexes and sodalite minerals (*J. Phys. Chem. B*, 105, 121060-11066, 2001), to determine procedures for calculating geometries and shieldings in such weakly bonded systems in preparation for further studies on hydrous aluminosilicate glasses.

Results: Recently Helz, et al. (*Environ. Sci. Technol.*, in press, 2002) reported the existence of two new Sb sulfide species, Sb₂S₅⁻² and Sb₂S₆⁻², in alkaline sulfidic solutions in equilibrium with stibnite, Sb₂S₃, and orthorhombic S. I have calculated from first principles of quantum mechanics the energetics for the oxidation of the Sb(III) sulfide dimer Sb₂S₄⁻² to the mixed Sb(III,V) dimer Sb₂S₅⁻² and then to the all Sb(V) dimer, Sb₂S₆⁻². Gas-phase reaction energies have been evaluated using polarized valence double zeta effective core potential basis sets and Moller-Plesset 2nd order treatments of electron correlation. All translational, rotational and vibrational contributions to the gas-phase reaction free energy have been calculated. Hydration energies have been obtained using the COSMO version of the self-consistent reaction field polarizable continuum method. Negative free energy changes are calculated for the

oxidation of the dianion of the III,III dimer to the III,V dimer by both small polysulfides, like S_4H^{-1} , and elemental S, modeled as S_8 . For the further oxidation of the III,V dimer to the V,V dimer the reaction free energies are calculated to be close to zero. The partially protonated Sb III,III dimer monoanion $HSb_2S_4^{-1}$ can also be oxidized, but the reaction is not so favorable as for the dianion. Comparison of the calculated aqueous deprotonation energies of $H_2Sb_2S_4$, $H_2Sb_2S_5$ and $H_2Sb_2S_6$ and their dianions with values calculated for various oxyacids indicates that the III,V and V,V dimers will have pK_{a2} values below 5, so that their dianions will be the dominant species in alkaline solutions. These results are thus consistent with the recent identification of $Sb_2S_5^{-2}$ and $Sb_2S_6^{-2}$ species by Helz, et al (2002). I have also calculated the Raman spectra of $Sb_2S_5^{-2}$ and $Sb_2S_6^{-2}$ to assist in their identification. The calculated vibrational frequencies of the III,V and V,V dimers are characteristically higher than those of the III,III dimer I previously studied. The III,V dimer may contribute shoulders to the Raman spectra previously obtained by Wood (1989).

The aluminum tridecameric polyoxocation, $AlO_4Al_{12}(OH)_{24}(H_2O)_{12}^{7+}$ is a major component in partially hydrolyzed $Al^{+3}(aq)$ solutions and has been extensively studied experimentally, mainly using vibrational and NMR spectroscopy. I recently calculated the equilibrium geometry and NMR properties of this $Al_{13}...$ polyoxocation using Hartree-Fock and density functional techniques. In the present work I carry out several different perturbations upon this polyoxocation and compute the resulting changes in its properties. Some of these perturbations have actually been carried out experimentally, while others are hypothetical. For example, one can experimentally replace the central Al[4] with other atoms, such as Ga or Ge. Protons can be removed from the exterior $-OH_2$ or $-OH$ groups to reduce the cation charge and the geometry of the molecule reoptimized. This allows a computational determination of the acidity of the $Al_{13}...$ species. Waters can be removed from the original polyoxocation to produce 5-coordinate Al and the energy for this dehydration can be compared with that for other Al oxyhydroxide species. Such coordinatively unsaturated 5-coordinate sites resemble those on the surfaces of gibbsite and bayerite and small molecules and anions like $AsO(OH)_3$ and $AsO_2(OH)_2^{-1}$ can be adsorbed on them and their reaction energetics determined. Vibrational frequencies for these adsorbed species can then be compared with experimental studies on the adsorption of these anions on Al hydroxide surfaces. Al oxyhydroxide oligomers can also be studied to assess the mechanism of formation of the $Al_{13}...$ polyoxocation. Analogous computations for Ga^{+3} oxyhydroxide oligomers give bond distances which compare well with recent experimental studies using EXAFS. Ga NMR shieldings have also been calculated for a number of oligomers, to assist in their identification and to establish trends in shielding with deprotonation and oligomerization. Calculations on such large polyoxocations at the Hartree-Fock level are quite expensive, but the expense can be enormously reduced by using approximate semiempirical MO methods, like PM3, without too great a loss of accuracy in some cases. Using such approximate methods both structures and vibrational spectra can be readily calculated.

It has recently been reported that the electron capture decay constant for 7Be varies by as much as 1.5% in different oxidic compounds of Be and that application of 400 kbar pressure to a $Be(OH)_2$ gel increases its 7Be decay constant by about 1%. Differences of such magnitude in decay rate might be useful in determining the speciation of Be in glasses, gels and aqueous solutions. We have recently calculated structures, 9Be NMR shieldings and IR/Raman spectra for both monomeric and oligomeric species of Be to assist in determining Be speciation. We here use similar methods to calculate the electron densities at the Be nucleus, which determine the rates of electron capture decay. We find that variations in the electron density at the Be nucleus in a number of oxidic compounds are only at the 0.1 -

0.4% level, as had been concluded in the 1970's. This raises doubts about the recent experimental results which show larger variations from one oxidic compound to another. The calculated ^9Be NMR shifts of these species differ by only a few ppm, but such changes are readily measurable by NMR spectroscopy, and they depend systematically on the degree of hydrolysis and the degree of oligomerization. Rough estimates of the effects of Be-O bond compression in $\text{Be}(\text{OH})_4^{2-}$ on the energy and the electron density at the nucleus indicate that several hundred kbar of pressure could increase the electron density by 1% or more, qualitatively consistent with the experimental results.

In collaboration with Prof. Nita Sahai, Dept. of Geology, Univ. of Wisconsin, I am continuing to explore the speciation of Si in solutions containing polyalcohols as ligands. Our results (Inorg. Chem., 41, 748-756, 2002) cast doubt on the original assignments of five- and six- coordinate species. This study shows the importance of having proper theoretical support for NMR assignments.

MASSACHUSETTS INSTITUTE OF TECHNOLOGY

Earth, Atmospheric and Planetary Sciences
Cambridge, MA 02139-4307

Grant: DE-FG02-00ER14

Evolution of pore structure and permeability of rocks under hydrothermal conditions

Brian Evans, (617) 253-2856, fax (617) 258-0620, brievans@mit.edu; Yves Bernabé; Ulrich Mok, Wenlu Zhu (WHOI)

Objectives: The pore structure and transport properties of rocks, including fluid permeability and electrical conductivity, can be altered by a wide variety of diagenetic, metamorphic, and tectonic processes. We are studying the interrelationships among permeability, mechanical properties, and the pore shape, under hydrothermal conditions, in mineral aggregates, with and without reactions.

Project Description: We have completed two suites of experiments and are beginning a third: 1.) Measurements of permeability and electrokinetic properties of synthetic sandstones with varying surface roughness. 2.) Measurements of evolution of permeability during the compaction of cracked and granular aggregates of quartz with varying grain size and pore-fluid chemistry at 450-800°C, in stagnant fluids, at pore pressures up to 200MPa, and at confining pressures between 200-400 MPa. 3.) Measurements of permeability in granular aggregates under similar conditions with slowly flowing pore-fluids. Current results indicate that as the mineral aggregates react and lithify, a large fraction of porosity becomes ineffective for fluid or electrical transport. Observations to quantify changes in surface roughness, porosity, and pore dimensions, will be made using standard optical, scanning electron, and laser confocal scanning optical microscopes. The image data will then be used in network models to predict the permeability. A better understanding of the processes that change porosity in the Earth is important for improving resource recovery, predicting rates of metamorphism, understanding fault mechanics and fault stability, and estimating rates of deformation by pressure solution.

Results: 1.) In a previous study, we examined the effect of chemical alteration on permeability and porosity of synthetic sandstone. For this study, we ran a similar alteration experiment after modifying the apparatus to allow continuous measurement of the electrical potential across the sample. The reaction and flow apparatus consists of an external furnace, a hydrostatic pressure vessel with water as confining fluid, two stainless-steel sample-holders connected to a pressure system that allowed independent control of pore fluid pressure. We performed a series of transient flow experiments while recording the electrical potential across the sample. The sample permeability was on the order of $8 \cdot 10^{-15}$ m², and pressure pulses decayed in a few seconds. We increased the temperature by steps, pausing to achieve thermal equilibrium at each step, and then performed transient flow experiments. During the first 8 days, we performed three such sequences with a maximum temperature of 120°C. The experiment lasted a total of 23 days, during which 58 series of transient flow tests were performed. The streaming potential demonstrated a complex hysteretic response that could not be interpreted by the standard electro-kinetic theory. We believe that the streaming potential was substantially influenced by the reaction kinetics of the alteration processes that were probably occurring on the same time scale as the

electro-kinetic experiments. The experiments could be improved by including quantitative measurements of fluid chemistry or by designing the experiments to measure properties under conditions of chemical equilibrium. The experiments illustrate some possible effects of chemical reactions during field tests, especially when cold water is injected into hot rocks.

2a.) We investigated the kinetics of crack healing in untreated and thermally cracked Sioux quartzite samples at temperatures between 300 and 600°C and at confining pressures P_c of 300 MPa. The pore fluid was either argon or distilled water; pore fluid pressure P_f varied between 50 and 250 MPa; thus, effective pressures P_{eff} were between 250 and 50 MPa. Sample permeability, k , and storage capacity, β , were continuously monitored using the oscillatory pore pressure method, with amplitudes of 1 MPa. Oscillation period ranged between 60 and 9000s. Both permeability and storage capacity decrease with time. The initial permeability of the quartzite with about 1% porosity ranges between 10^{-20} and 10^{-19} m². Transport properties change faster at higher temperature and effective pressure. For example, at about 400°C and P_{eff} = 200 MPa permeability drops by almost an order of magnitude over one day. At the same temperature, but a lower effective pressure of 100 MPa, the permeability decreases only by about a factor of two over the same time span. The decrease in permeability accelerates after 3 days at T=400°C and P_{eff} = 200 MPa. Permeabilities are then on the order of 10^{-23} m². We are analyzing geometrical distribution and fluid density of the fluid inclusions that formed during the healing.

2b.) We deformed Solnhofen limestone at 473, 523, 573 and 673 K, at confining pressures (argon) of 70 to 200 MPa, and at constant pore pressure (distilled water) of 50 MPa. Most of the limestone samples failed by dilatancy and localized deformation. The failure process is sensitive to both pressure and temperature. The stress required for the inception of dilatancy and localization increases with increasing pressure and decreasing temperature. At low pressures and temperatures, strain softening and abrupt stress drops were observed during localization. However, at higher pressure and temperature, the localization process became progressive, with strain softening and dilatancy accumulating over axial strains up to 6%. The data provide the pressure and temperature dependence of the internal friction parameter and the dilatancy factor. SEM and TEM observations are being made to measure pore geometry and dislocation microstructure.

3. *Measurements of permeability in granular aggregates under similar conditions with slowly flowing pore fluids:* We are upgrading our permeameter to conduct constant flow-rate experiments.

MASSACHUSETTS INSTITUTE OF TECHNOLOGY

Department of Civil and Environmental Engineering
Cambridge, Massachusetts 02139

Grant : DE-FG02-00ER15029

Transport Visualization for Studying Mass Transfer and Solute Transport in Permeable Media

Charles Harvey, (617) 258-0392, fax (617) 258-8850; charvey@mit.edu; Lucy Meigs, lcmeigs@sandia.gov; Roy Haggerty, haggertr@geo.orst.edu

Objectives: This research seeks: (1) to determine when the small-scale permeability structure causes solute spreading to be dominated by classical dispersion and when it causes solute spreading to be dominated by mass transfer; and (2) to understand how time-scales of mass transfer depend on physical, quantifiable characteristics of the geologic medium.

Project Description: Theoretical work is being conducted to define regimes of transport based on quantifiable measures such as dimensionless numbers. A portion of this theoretical work (and associated experiments) is focused on determining the conditions under which physical mass transfer (*i.e.*, diffusion into immobile zones) is significant, and to developing models for predicting the effects of mass transfer over long time scales. The numerical simulations are coupled with laboratory experiments using transmitted light, x-ray absorption, and conventional breakthrough curves to test and further understand the regimes of transport. Within the mass transfer regime, the geometries of flow and transport parameters that lead to multiple rates of mass transfer and scaling of transport processes are being evaluated.

Results: In order to map the regimes of transport, a method was developed for generating random hydraulic conductivity (K) fields that have highly connected flow paths or barriers, which have been found to be critical to understanding the regimes of transport. These fields share the same low-order statistics as multigaussian fields (mean, variance and covariance function), but have very different flow and transport characteristics because they are highly connected. Specifically, the results show that 2D hydraulic conductivity fields with the same basic spatial statistics, but different degrees of connectedness, may produce: (1) effective conductivities that are significantly above or below the geometric mean, (2) solute transport behavior that is best modeled through Fickian dispersion or behavior that is better modeled as rate-limited mass transfer, and (3) mass transfer that is driven that by either diffusion or advection. This work demonstrates that standard characterizations of heterogeneity may not capture the flow and transport characteristics of all aquifers.

A series of laboratory experiments are being designed to allow us to evaluate our understanding and predictions about the regimes of transport. These transport experiments are being conducted on thin chambers filled with glass beads using transmitted light to spatially map solute concentrations. Breakthrough concentrations are also being measured. Prototype experiments conducted within the mass transfer regime have enabled us to refine our experimental design.

MASSACHUSETTS INSTITUTE OF TECHNOLOGY

Department of Earth, Atmospheric, and Planetary Sciences
Cambridge, MA 02139

Grant: DE-FG02-99ER 15004

Theoretical Studies of Landscape Erosion

Daniel H. Rothman, (617) 253-7861, fax (617) 253-1699, dan@segovia.mit.edu

Website: <http://segovia.mit.edu/>

Objectives: To formulate quantitative theories for physical processes that erode landscapes and create channels and river networks, to determine unique topographic signatures of such processes, and to test predictions using digital elevation data.

Project Description: Whereas the results of large-scale landscape erosion are nearly obvious to the eye, they are notoriously difficult to predict by quantitative physical theories. Moreover, when predictions can be made, they often show that real landscapes differ only slightly from random landscapes. Therefore a better understanding of the processes that shape landscapes requires not only well-defined quantitative measures but also theories that specify the physical and geological significance of these quantities.

We study the geometry of river networks, the statistical features of the surfaces in which they are embedded, and the mechanisms of channel initiation. Network geometry is characterized by scaling laws that reflect the structure of the networks, whereas landscapes are described in terms of spatial correlations between drainage basins and the slopes they form. Aspects of each of these quantities must derive at least in part from the physical processes that incise channels and, in certain circumstances, make them regularly spaced.

Results: Using the theory of statistical geometry, we have shown that relationships between slope and drainage area can result from the basic geometric tendency for flat slopes to be associated with a convergence of flow lines that, on average, is stronger than that associated with steep slopes. Consequently, observations of relationships between slope and area, often considered an essential signature of erosive processes, do not necessarily reflect physical processes. We have specified particular combinations of landscape parameters for which the slope-area relation need not reflect any causal relation.

We have also initiated studies of channelization by subsurface or seepage flows. Using a combination of theory, experiment, and observation we are seeking to explain why seepage erosion results in regularly spaced channels. Experiments performed at a one-meter scale show that periodic channel spacing is an intrinsic aspect of the physical process in a homogeneous system composed of equal-sized glass beads. Numerical models constructed to study this process are able to reproduce the observed channel spacing.

They also show that channel spacing decreases with increasing slope, as we have observed in natural systems.

MASSACHUSETTS INSTITUTE OF TECHNOLOGY

Earth Resources Laboratory
Department of Earth, Atmospheric, and Planetary Sciences
Cambridge, Massachusetts 02139

Grant: DE-FG02-00ER15041

Fluid Mobility Estimation From Electroseismic Measurements: Laboratory, Field, and Theoretical Study

M. Nafi Toksöz, (617) 253-7852, fax (617) 253-6385; toksoz@erl.mit.edu ; Daniel R. Burns

Objectives: The objective of this project is to develop improved theoretical models, obtain higher quality laboratory data, and investigate field applications of the seismoelectric or electroseismic phenomena for the purpose of estimating in-situ permeability values.

Project Description: Permeability is a parameter of critical importance for the simulation of and prediction of hydrocarbon production, groundwater contaminant transport, and the viability of underground sequestration of CO₂. In the seismoelectric application, a propagating seismic wave initiates fluid motion in a permeable formation. Because of fluid ion adsorption on grain surfaces of the rock, an excess charge exists in the moving fluid, which induces an electrical field that can be measured. The measured electrical field is a function of the pore fluid properties, the rock matrix, and the pore geometry (which controls the permeability). The key parameter relating the electrical field to the rock permeability is the streaming current coupling coefficient, which is the ratio of the induced electrical current to the applied pressure gradient. Although, to first order, the DC streaming potential coupling coefficient does not change with permeability (except for very tight rocks), the frequency dependent behavior of the coupling coefficient can be related to permeability.

We study these phenomena primarily through the use of laboratory experiments, augmented by theoretical modeling and small-scale field measurements, to understand how the frequency-dependent electrical field can be related to the permeability.

Results

Scale-Model Experiments

In this second year of the project we have focussed our efforts in two areas of laboratory experimentation: scale model seismoelectric measurements and NMR imaging of pore-scale fluid flow. In the last few years our focus in scale-model lab experiments was on near-borehole measurements, that is, measuring the electrical field generated by an acoustic logging signal in a borehole surrounded by a permeable formation. During the past year, however, we have constructed two lab experiments specifically designed to look away from the borehole into the inter-well region. We have also made the decision to look in more detail at characterizing fractures since they represent significant conduits for fluid flow within a reservoir. In the first experiment, we investigated the possibility of measuring an

electrical signal generated by the fracturing of a rock sample, such as during a hydrofracture. To test this concept, we measured the electrical signals generated during the fracturing of a cylindrical rock sample under pressure. The results indicate that when the sample is wet, an electroseismic signal is generated due to motion of the charged fluid in the fracture. Signals related to piezoelectric effects are much smaller. These results indicate that seismoelectric/electroseismic measurements may be used during reservoir hydrofracturing as an indicator that fracturing has occurred. We have not yet studied the relationship between the signals and the geometry or flow capacity of the fractures.

A second laboratory scale model was constructed to investigate the possibility of using crosswell seismoelectric data to identify and characterize fractures in the inter-well region of a reservoir. In this experiment we place a seismic source in one borehole and an electrode array in a second borehole. Our initial results indicate that when the seismic wave hits the fracture, fluid flow is initiated and a radiating electromagnetic wave is produced. This signal can provide information about the location and aperture of the fracture. Analysis of the results of these experiments show that the arrival time of the radiating EM wave can be used to determine the fracture location and dip angle in two dimensional models. Furthermore, the amplitude of the seismoelectric signal increases with increasing aperture.

NMR Experiments

The motion of fluid in the pore space of a rock due to seismic waves has not been directly observed. As a result, there are a number of different rock physics models that have been developed for relating the motion of fluids in pore space due to a passing seismic wave. These include the Biot model, squirt-flow models, and models that combine features of both. Theoretical models of fluid flow and the related seismoelectric conversion are based on somewhat simplistic assumptions about the nature of the pore space geometry. Geometric factors, such as the tortuosity, are conceptual representations of pore-scale fluid flow that play an important role in our theoretical models. Because of this, we have continued to pursue ways to use NMR methods to image the pore geometry and characterize the pore-scale fluid flow. During the past year David Cory's group has worked on the characterization of flow paths using variations of the Magic Angle Sample Spinning (MASS) methods to study pore fluid flow.

We are also working on a method to allow for a low frequency acoustic pulse to be input to a saturated, porous sample in an NMR system. We hope to be able to make measurements of the fluid velocity distribution within the pore space induced by the acoustic signal.

MINERALOGICAL SOCIETY OF AMERICA

1015 Eighteenth St NW Ste 601
Washington, DC 20036-5212

Grant: DE-FG02-01ER15127

Support of MSA and GS Short Courses and the Companion Reviews Volumes

J. Alex Speer, (202) 775-4344, fax (202) 775-0018, j_a_speer@minsocam.org

Objectives: The project is the support of six short course and the companion *Reviews in Mineralogy and Geochemistry* volumes proposed to and accepted by the Mineralogical Society of America (MSA) and Geochemical Society (GS) to be held in 2001, 2002, and 2003.

Project Description: The support has two purposes: (1) keeping student registration fees affordable; and (2) producing the *Reviews* volumes. Speaker travel costs have become the most significant MSA and GS short course expense. Student fees were kept low indirectly through reimbursing speaker travel (Molecular Modeling, Nanoparticles) or using speaker stipends (Stable Isotopes). A portion of the editorial work for each *Reviews* volume was covered, but the most significant production support was for printing of the *Reviews* volume on nanocrystals. This allowed MSA and GS to publish one additional short course volume in 2001 which they could not otherwise do and move the nanoparticles course up to 2001 from its originally 2003 scheduled time. The course could thus be offered when research into nanocrystals and nanotechnology is just beginning to be a significantly new field of investigation.

Results: There were three short courses during 2001, each with a companion *Reviews* volume:

[1] "Molecular Modeling Theory and Applications in the Geosciences" was held in Roanoke, Virginia on May 18-20, 2001, preceding the 2001 Goldschmidt Conference in Hot Springs, VA. The organizers of the course were Randall T. Cygan of Sandia National Laboratories and James D. Kubicki of Pennsylvania State University. 75 people (17 students, 58 professionals) attended the course with participants from the United States, United Kingdom, Germany, Switzerland, Australia, and Japan.

[2] "Stable Isotope Geochemistry" was held in Boston, Massachusetts on November 3-4, 2001, preceding the 2001 Annual Meeting of the Geological Society of America in Boston, MA. The organizers of the course were John W. Valley of the University of Wisconsin and David R. Cole of the Oak Ridge National Laboratory. 79 people (34 students, 32 professionals, and 13 speakers) attended the course with participants from the United States, Germany, Austria, New Zealand, Denmark, and Venezuela.

[3] "Nanoparticles and the Environment" was held at the University of California, Davis, on December 7-9, 2001 immediately prior to the AGU meeting in San Francisco. The organizers of the course were Jillian F. Banfield of the University of Wisconsin-Madison and Alexandra Navrotsky of the University of California Davis. 92 people (31 students, 53 professionals, and 8 speakers) attended.

The three companion volumes are:

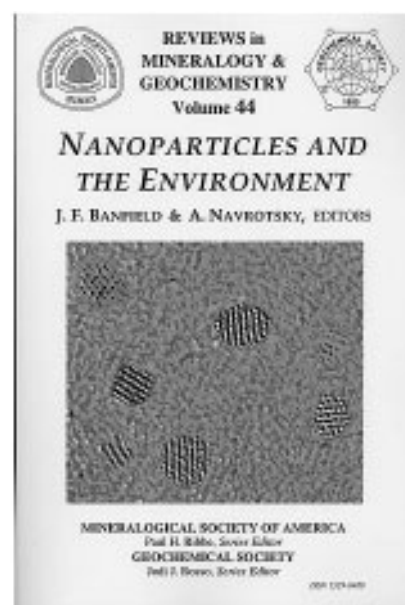
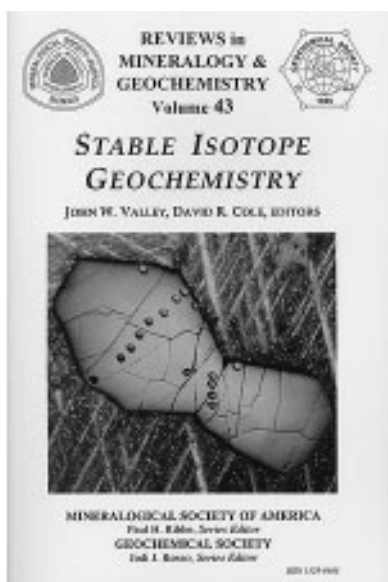
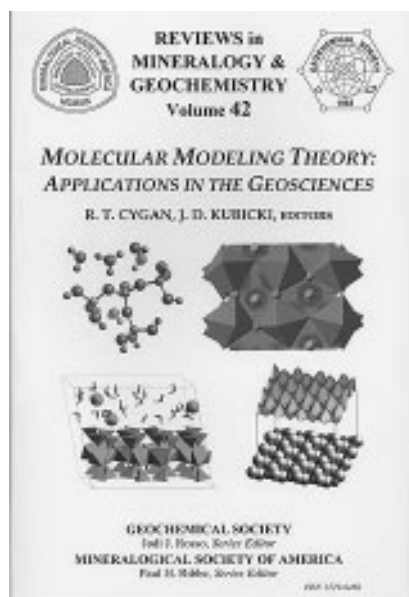
[1] "Molecular Modeling Theory: Applications in the Geosciences", edited by R. T. Cygan and J. D. Kubicki, *Reviews in Mineralogy and Geochemistry* volume 42, 14 chapters complete with references, 531 pages (ISBN 0-939950-54-5) \$32, \$24 for MSA, GSA and CMS members.

[2] "Stable Isotope Geochemistry", edited by J. W. Valley and D. R. Cole, *Reviews in Mineralogy and Geochemistry* volume 43, 13 chapters complete with references, 662 pages (ISBN 0-939950-55-3) \$32, \$24 for MSA, GSA and CMS members .

[3] "Nanoparticles and the Environment", edited by J.F. Banfield and A. Navrotsky, *Reviews in Mineralogy and Geochemistry* volume 43, 8 chapters complete with references, 349 pages (ISBN 0-939950-54-5) \$28, \$21 for MSA, GSA and CMS members

3,723 copies have been distributed thus far of the 3 volumes. Copies were distributed to all short course participants, 860 library subscribers to *American Mineralogist* (who are thought to include all library subscribers to *Geochemica et Cosmochimica Acta*), book reviewers, and by mail and meeting sales. The volumes have been on sale for differing lengths of time. That, and the fact that Volume 44 was unable to be included in the MSA membership renewals, account for the differing sales numbers. The breakdown:

Volume	number of volumes distributed to				total
	short course	reviewers	libraries	mail/meeting sales	
Volume 42	92	25	860	384 (since 5/10/01)	1361
Volume 43	79	35	860	340 (since 11/1/01)	1314
Volume 44	74	23	860	91 (since 12/7/01)	1048
				Total	3723



UNIVERSITY OF MINNESOTA, TWIN CITIES

Dept. of Geology and Geophysics and Minnesota
Supercomputer Institute
Minneapolis, MN, 55415-1227

Grant: DE-FG03-91ER14212

Magma Rheology, Mixing of Rheological Fluids, Molecular Dynamics Simulation , and Lithospheric Dynamics

D.A. Yuen, (612) 624-1868, fax (612) 624-8861, davey@krissy.mni.umn.edu; F. J. Spera, University of CA, Santa Cruz

Website: <http://banzai.msi.umn.edu>

Objectives: Mixing efficiency in complex rheology, molecular dynamics of complex fluids and micro-scale Rayleigh-Taylor instabilities, effects of complex rheology in lithospheric dynamics.

Project Description: This project will improve our understanding of the thermal, chemical, dynamical and mechanical state of the continental crust and subcrustal lithosphere with particular focus on the interactions between the various subsystems. The work plan includes: (1) rheological laboratory measurements on melts and magmatic suspensions; (2) Determination of the thermodynamical and transport properties of molten silicates by MD simulations; (3) Mixing processes of rheological fluids in convection and visualization of complex processes; (4) Coupling between mantle convection with temperature-dependent and non-Newtonian rheology and mantle diapirs on the thermal regime and subsidence curves of rift-related basins; (5) The dynamical influences of lithospheric phase transitions on the thermal-mechanical evolution of sedimentary basins; (6) The development of stress fields and criteria for faulting in the crust; (7) Modeling of heat and mass transport driven by thermal and compositional heterogeneities in porous media; and (8) Open system geochemical modeling of magmatic systems.

Results: The results described below are for the U of Minnesota part of this project. Additional results are given in the summary of activities can be found in the summary of activities by the University of California team led by F.J. Spera. We have studied with 2-D molecular dynamics the mixing phenomenon in the microscale, between 500 and 10 000 Å. We have employed up to 3 million particles interacting with a two-body potential and up to one million time-steps were integrated. We have focused on the temporal evolution of the mixing layer between two superimposed particle systems in a gravitational field directed from the heavier to the lighter particle ensemble. We have compared the micro properties with those observed in the macroworld. We found that the bubble-and spikes stage of mixing process is similar in both the micro (molecular-scale) and macro worlds. The mixing layer growth constant A , which can be obtained from molecular dynamics, is approximately the same as that obtained for 2-D simulations in the macroscale. The occurrence of Rayleigh-Taylor instability in the microscale, and its similarity to the same process in the macroscale, can also expand the concept of turbulence to microscaled flows on the nanoscale. This work has been published in *Physica D*, 137, 157-171, 2000.

We have studied the mixing properties and differences between Newtonian and non-Newtonian convection. Both the line and field methods were employed. The line-method is based on monitoring of passive particles linked into lines, while the field method relies on the advection of a passive scalar field by solving a partial differential equation with a hyperbolic character. Both visual and quantitative estimates revealed that the efficiency of the Newtonian mixing is greater than that for non-Newtonian (power-law) rheology. A chemical heterogeneity placed in the non-Newtonian convection forms preferentially horizontal structures, which may persist for at least 1 Ga in the upper-mantle. In addition, the non-Newtonian medium reveals a lesser amount of stretching of the lines than the Newtonian material. The rate of the Newtonian stretching fits well with an exponential time-dependence, while the non-Newtonian rheology shows the stretching rate close to a power-law dependence with time. Due to the non-linear character of the power-law rheology, the non-Newtonian fluid offers a natural scale-dependent resistance to deformation, which prevents efficient mixing at the intermediate length scales. This paper has several movies and can be found in *Electronic Geosciences*, 4:1, 1999.

We have studied the effects of low-temperature plasticity on the formation of shear zones. A thermal-mechanical model has been developed for describing the shear deformation of Maxwell viscoelastic material with a rheology close to dry olivine. In addition to diffusion and dislocation creep, we have included deformation by low-temperature plasticity, called the Peierls mechanism, which is significant at low temperatures and has a strong exponential dependence on the shear stress. When a sufficient magnitude of heat is produced by the rapid conversion of the elastically stored energy into viscous dissipation, thermal instability takes place and the deformation localizes in a narrow zone. For dry olivine and realistic values of the strain-rate, the effect of low-temperature plasticity is influential for temperatures between around 800 and 1000 K. This finding suggests that low-temperature plasticity may be crucial in regulating thermal-mechanical stability in the shallow portion of subducting slabs. This work has appeared in *Earth Planet Sci. Lett.*, 168, 159-172, 1999.

We have studied the effects of non-Newtonian rheology in producing ultra-fast plumes, which can spread out rapidly in horizontal direction upon impacting the lithosphere. These plumes can move at upward velocities in excess of meters / year and are considerably faster than the Newtonian plumes. These results show a direct separation of timescales between the rapidly rising non-Newtonian plumes and the ambient mantle circulation. This work has come out in *Tectonophysics*, Vol. 311, 31-43, 1999.

We have also studied mantled inclusions, commonly encountered in mylonites, which can record the deformation history. We have carried out two-dimensional numerical studies of time-dependent deformation behavior of inclusion and its dependence on rheology under simple shear. The inclusion is taken to be deformable and having its own intrinsic rheological properties. The results of numerical modeling shows that a key factor of structural appearance is the effective viscosity contrast between the inclusion and the matrix material. A high viscosity contrast from non-Newtonian rheology inhibits the stretching of the inclusion, preserving its round shape. This result is similar to our results in mixing. Wings or tails can only be developed in mineralogic systems with a high effective viscosity contrasts. This work has been published in *Earth Planet. Sci. Lett.*, 165, 25-35, 1999.

NATIONAL ACADEMY OF SCIENCES, BOARD ON EARTH SCIENCES AND RESOURCES

2101 Constitution Ave. NW
Washington D.C. 20418

Grant: DE-FG02-97ER14810

Board on Earth Sciences and Resources and Its Activities

Anthony R. de Souza, (202) 334-2744, fax (202) 334-1377, adesouza@nas.edu

Website: <http://www4.nationalacademies.org/cger/besr.nsf>

Objectives: The purpose of the Board on Earth Sciences and its committees is to provide a focal point for National Research Council activities related to earth science policy.

Project Description: The Board addresses the following strategic earth science issues: identifying the frontiers of basic and applied research in the Earth sciences; strengthening multidisciplinary programs and integrated approaches to research; assessing mineral and energy resources; investigating human interactions with the Earth; understanding environmental change; improving access to and use of scientific and geospatial data and information; evaluating breakthrough technologies for mitigating environmental problems; and enhancing Earth science education.

Results: During FY 2001, the Board on Earth Sciences and Resources produced 7 reports:

Review of EarthScope Integrated Science, 2001

Coal Waste Impoundments: Risk, Responses, and Alternatives, 2001

National Spatial Data Infrastructure Partnership Programs: Rethinking the Focus, 2001

Resolving Conflicts Arising From the Privatization of Environmental Data, 2001

Conceptual Models of Flow and Transport in the Fractured Vadose Zone, 2001

Evolutionary and Revolutionary Technologies for Mining, 2001

Future Roles and Opportunities for the U.S. Geological Survey, 2001

In addition to producing reports, the board and its standing committees in 2001 had about 40 projects under development or in the funding stage and 18 studies under way. During the year, the Board and its standing committees convened or facilitated meetings to exchange information among scientists, engineers, and policy makers from government, university, and industry. Most important, members of the Board visited with officials on the Hill and in various federal agencies, including staff members at the DOE BES. These informal, information exchange meetings have been so successful that they will continue in the coming fiscal year.

UNIVERSITY OF NEVADA, RENO

Department of Geological Sciences
Reno, NV 89512

Grant: DE-FG03-98ER14885

Growth of Faults, Scaling of Fault Structure, and Hydrogeologic Implications

Jane C. S. Long, University of Nevada, Reno, (702) 784-6987, fax (702) 784-1766, jcslong@mines.unr.edu; David Benson, Desert Research Institute; (775) 673-7496, fax (775) 673-7363, dbenson@dri.edu; Stephen Martel (808) 956-7797, fax (808) 956-3148, martel@soest.hawaii.edu; James P. Evans, Utah State University, (801) 797-2826, fax (801) 797-1588, jpevans@cc.usu.edu

Websites: www.hydro.unr.edu/homepages/benson/current/, www.hydro.unr.edu/homepages/schumerr.

Objectives: Our main objective is to find applicable equations of flow and transport in faulted and fractured zones based on their three-dimensional structure.

Project Description: We are developing an appropriate set of mathematical tools that can be used to evaluate the results of field tests in fractured and faulted rock. These governing equations will also be the appropriate models of transport across wide ranges of time and space scales. Previous hydraulic equations were based on a finite-sized representative elementary volume and small contrasts in media properties. Newer models that use fractional-order derivatives are based on very heterogeneous and scaling media. We are examining the relationship between these equations and the measurable properties of fully and partially water saturated media, particularly the distribution of very high and very low velocity regions. The probability and connectivity of these regions directly affects the order of the governing differential equation of flow and transport. In particular, solute transport in a highly variable velocity field may follow an equation with a fractional-order Laplacian dispersion term, and a time derivative of order $\gamma \leq 1$. The equation models the heavy-tailed transport that is characteristic of tracer tests in fractured media.

Results: In the year 2001, we made two key advances. The first was the discovery that the governing equation of large random motions (without a "characteristic" size) in 3-D contains a Laplacian operator of matrix-valued order. Compared to the classical Laplacian, which is of order $2I$, where I is the d -dimensional identity matrix, the new dispersion operator has eigenvectors aligned with principle plume growth directions, and eigenvalues $0 < \alpha_i \leq 2$ that correspond to the order of spatial fractional derivatives in the principle directions. While this sounds complicated, all one needs to do is determine the principle directions - the preferred fracture orientations, and the size of the largest particle motions. These two parameters give the entire governing equation. The equation is easy to solve, and provides analytic solutions of very complex plume behavior (see, e.g., www.hydro.unr.edu/homepages/schumerr).

Our other key discovery was the exact relationship between continuous time random walks and traditional mobile/immobile solute transport equations. For solute particles that move into an immobile

phase for random amounts of time that are heavy-tailed, a fractional time derivative of order $0 < \gamma \leq 1$ appears in the transport equation. When $\gamma = 1$, the classical equation with a linear retardation coefficient is recovered. The time-fractional equation describes solutes that move through media with a very heterogeneous distribution of immobile zones (i.e., matrix blocks). The power-law tail of breakthrough curves that is characteristic of fractional time is widely reported in tracer tests in all systems and all geometries. The tail is important, since it implies (for certain slopes) that the mean residence time is infinite. Unlike traditional methods, the fractional time derivative is "scaleless," which means that a test conducted at one scale can be used at any other scale. Solving the time-fractional equation uses subordination, which dictates that transforming a Brownian motion yields other stochastic processes. By extension, if we find that solutes are encountering random stoppages that are heavy-tailed, we can solve the traditional ADE without the fractional time derivative (using analytic or numerical solutions such as MT3D) and merely transform the solution.

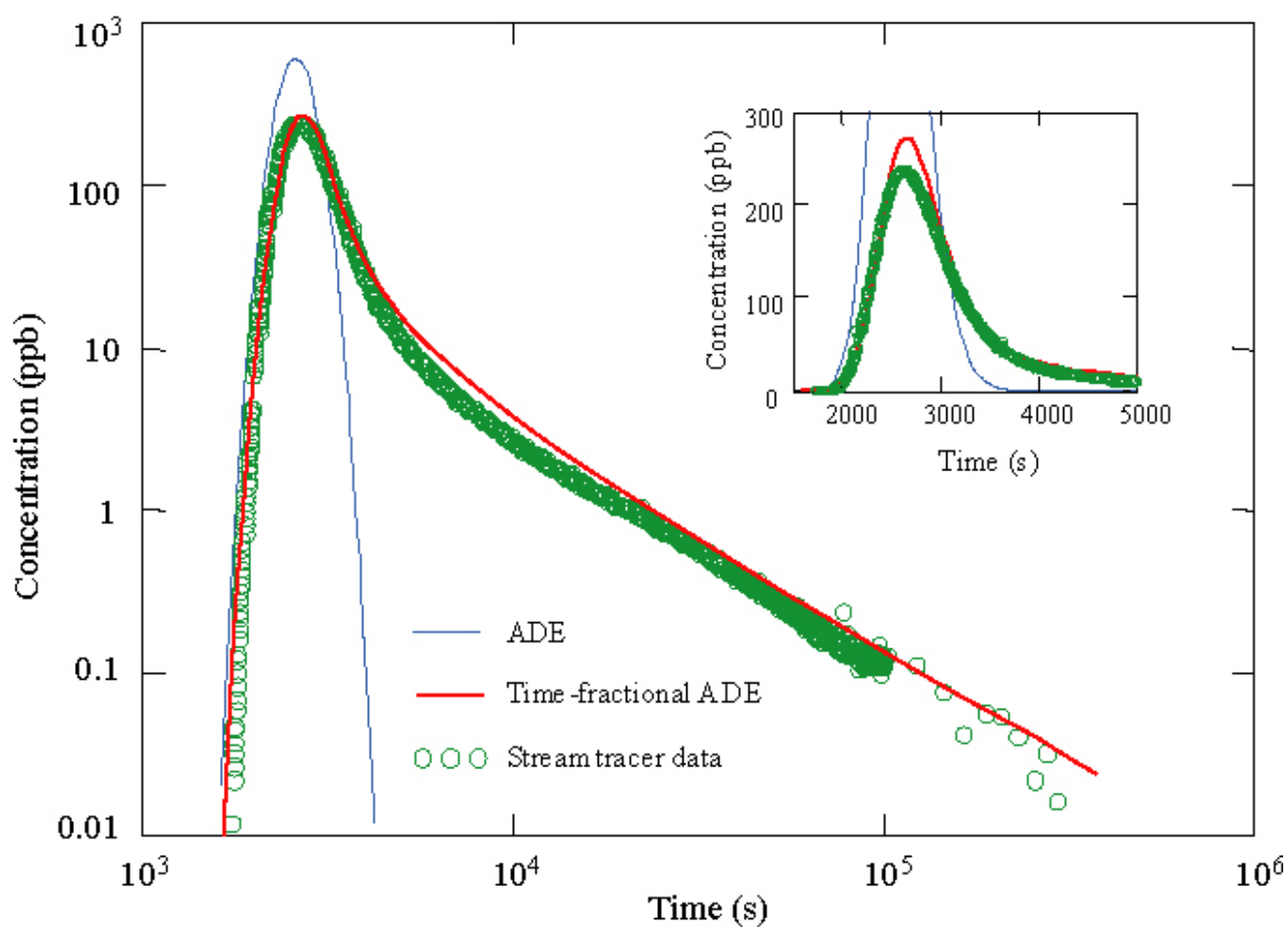


Figure 1. Breakthrough (arrival) of fluorescent dye 300 meters downstream of the injection point in a mountain stream. Order of fractional time derivative is 0.3, corresponding to late-time slope of -1.3.

NEW ENGLAND RESEARCH

331 Olcott Drive, Ste L1
White River Junction, Vermont 05001-9263

Grant: DE-FG02-98ER14906

The Role of Fracture Intersections in the Flow and Transport Properties of Rock

Stephen R. Brown, (802) 296-2401, fax (802) 296-8333, sbrown@ner.com; Harlan W. Stockman, Sandia National Laboratory, Arvind Caprihan, New Mexico Resonance

Objectives: Flow and solute-mixing behavior at fracture intersections is a complex function of surface roughness and channeling. The objective of this project is to gain a more complete understanding of flow channeling in fracture networks by physically modeling and analyzing several configurations of flow and transport through fracture intersections.

Project Description: We have addressed several problems concerning flow and transport through fracture intersections using a combination of numerical modeling, quantitative measurements, and visual observation of processes in real rough-walled fractures. Our observations included: channeling in single fractures, channeling within and through single fracture intersections, and channeling through fracture networks. These studies consider bulk flow and transport of solutes. For this work we used a combination of quantitative measurements, digital video imaging and magnetic resonance imaging (MRI) observations of flow through real rough-walled fractures, and numerical modeling via lattice Boltzmann (LB) methods.

Results: Several natural fracture intersections were replicated in transparent epoxy, while synthetic intersections were made from textured glass. Laboratory experiments of single-phase mixing of solutes were performed by flowing water and dye solutions through the specimens. We found that in intersecting natural fractures the degree of average mixing is greater than predicted by parallel plate streamline routing. Apertures at the intersection vary spatially, resulting in highly variable flow rates around the intersection. This leads to multiple pure fingers of each solution both bending around and crossing straight through an intersection. While the outlet fluids are heterogeneous (not uniformly mixed), the average degree of mixing is higher than expected for hydraulically equivalent parallel plates.

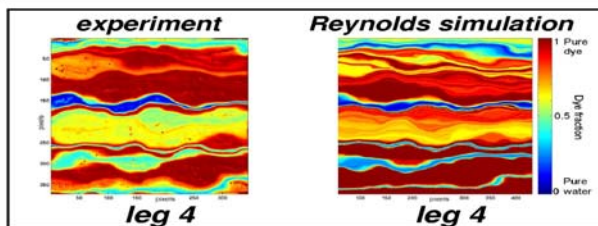
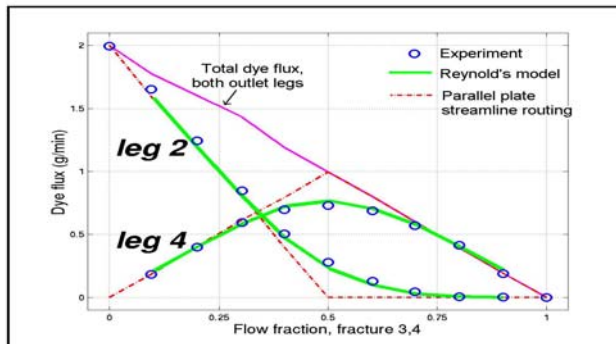
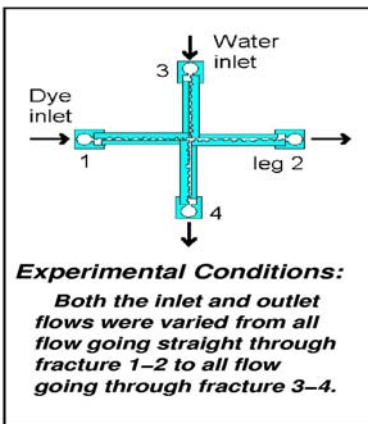
We have compared the experimental flow and mixing results to numerical methods using the experimentally-observed intersection geometry. The Reynolds equation for 2-dimensional flow was solved simultaneously for flow in both variable aperture fractures, with source and sink terms creating an intersection between the two. Numerical simulations for the textured glass laboratory specimen agree well with the laboratory experiments, both in the amount of average mixing and in the spatial distribution of dye streamlines.

We have also considered the effect of surface roughness on solute dispersion within large networks of fractures. A numerical model of a fracture network was created by taking the detailed properties and behaviors observed for the textured glass sample and replicating it many times to form a regular network

or lattice. Simulations of flow through this network results in dispersion which is intermediate between complete mixing and pure streamline routing. We found that identical network-wide dispersions can be obtained if we either (1) consider all details of flow and mixing in the rough fractures or (2) we simply assume that all components in a network of identical parallel-plate fractures each have the same effective mixing ratio as the rough-walled ones.

Using MRI we have attempted to obtain structural information, measure flow velocities, and quantify mixing in three dimensions. Beginning with a parallel plate specimen we developed techniques which we then applied to experiments on intersecting natural rock fractures. We found that it is possible to make accurate aperture measurements when there is no flow and to make adequate flow velocity measurements away from the intersection. However, with the available techniques and equipment we could not image flows near to or within the intersection, due to signal loss effects in small apertures typical of these natural specimens - especially when the liquid is flowing. Likewise, measurements of mixing processes were only possible in the parallel plate fracture specimen. Useful data could be gained in all cases, however, if we were to sacrifice spatial resolution and only measure properties in a statistical sense.

Can mixing be modeled as local streamline routing?
A laboratory test using textured glass



A laboratory experiment designed to test whether or not mixing can be modeled as a simple piece-wise application of local streamline routing along the intersection. Both images of dye flow patterns and quantitative analyses of the outlet fluids show that the assumptions are adequate.

UNIVERSITY OF NEW MEXICO

Department of Mechanical Engineering
Albuquerque, NM 87131

Grant: DE-FG03-97ER14778

Modeling of Mesoscale Phenomena During Sequestration of Carbon Dioxide in Porous Reservoirs

M. Ingber, (505) 277-6289, fax (505) 277-157 ingber@me.unm.edu; A. Graham, Texas Tech University, (806) 742-0451, fax (806) 742-355 agraham@coe.ttu.edu; L. Mondy, Sandia National Laboratories, (505) 844-1755, fax (505) 844-825 lamondy@sandia.gov

Objectives: The purpose of this program is to combine experiments, computations, and theory to make fundamental advances in our ability to predict transport phenomena in concentrated, multiphase, disperse systems, particularly when flowing through geologic media.

Project Description: Processes for the sequestration of carbon dioxide in porous reservoirs involve several components of multiphase flows. If hydraulic fracturing is used to develop local "sweet spots" (zones of high permeability), the flow and resulting distribution of the proppant can have a large impact on the subsequent sequestration process. Even without hydraulic fracturing, the creation of precipitates can drastically alter the characteristics of the porous formation itself. Furthermore, emulsions can form and fingering can take place at the supercritical CO₂/brine interface. In order to be of use in designing effective CO₂ sequestration processes, significant enhancements to currently available continuum-level suspension flow models are required. Both experimentation and high performance computing at the mesoscopic level are used to obtain microstructural information that is necessary for the development and refinement of the continuum models.

Results: The continuum models originally developed by Phillips et al. (1992) and Nott and Brady (1994) have been improved and implemented into a general-purpose finite element computer code. Results show good agreement with experimental measurements based on nuclear magnetic resonance (NMR) imaging in idealized three-dimensional flows (see Fig.) Normal stress contributions are modeled, which results in accurate predictions of suspended particle migration in curvilinear flows. The improved model also allows for non-neutrally buoyant particles and non-Newtonian suspending liquids.

Massively parallel computing has allowed particle level simulations, based on the boundary element method (BEM), with up to three thousand particles. Volume averaging of the stress tensor has been added to the codes to allow prediction of average macroscopically observed transport properties from particle scale simulations. These simulations lead to detailed information on individual particle and fluid motion that is unobtainable through experiments. For example, highly accurate transient calculations of collections of particles in nonlinear shear fields have demonstrated that particles in inhomogeneous shear fields migrate in the direction of the lower shear rate. This is, to our knowledge, the first explanation of this phenomenon from first principle physics. These very fundamental studies are elucidating the fundamental physics that govern the particle transport phenomena in multiphase systems.

This work is complemented by experimental work to provide insights and benchmarks. A study of apparent particle slip in confined geometries has been performed. Due to the finite size of the particles, suspensions of particles form a boundary layer near containing walls. The walls impose an ordering of the particles that extends several particle diameters into the bulk suspension. In constrained geometries such as the small channels in porous media, this boundary layer can extend over the entire channel. NMR imaging is used to determine the mesoscale structure and falling and rolling balls are used to investigate the mechanical properties at locations ranging from the centerline to the walls of the containing cylinder. It was found that there exists markedly non-Newtonian wall effects in concentrated suspensions in which the volume fraction of particles is greater than 0.2. At these higher concentrations, wall effects are much larger and extend further into the suspension than in Newtonian fluids.

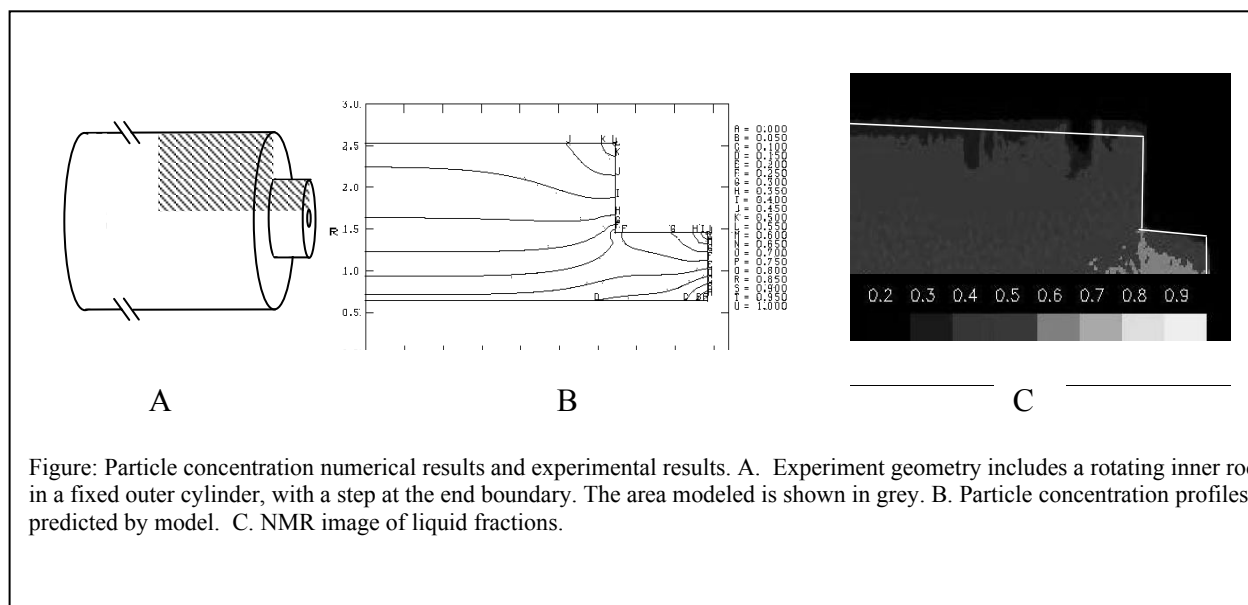


Figure: Particle concentration numerical results and experimental results. A. Experiment geometry includes a rotating inner rod in a fixed outer cylinder, with a step at the end boundary. The area modeled is shown in grey. B. Particle concentration profiles predicted by model. C. NMR image of liquid fractions.

NEW MEXICO INSTITUTE OF MINING AND TECHNOLOGY

Department of Earth & Environmental Science
Socorro, New Mexico 87801

Grant: DE-FG03-96ER14589

Investigation of Permeability Upscaling

John L. Wilson, (505) 835-5308, fax (505) 835-06436, jwilson@nmt.edu; Vincent C. Tidwell, Sandia National Laboratories, (505) 844-6025, fax (505) 844-6023, vctidwe@sandia.gov

Objectives: Experimentally investigate permeability upscaling for a variety of geologic materials, interpreting the measured permeability upscaling in light of the physical characteristics of the porous medium and the measurement characteristics of the sampling instrument. Specific objectives during this period are to (1) investigate and model the effects of non-uniform flow, local-scale anisotropy/heterogeneity, and non-Gaussian permeability distributions on permeability upscaling, (2) quantify measurement characteristics of the minipermeameter and incorporate them into models of permeability upscaling, and (3) extend physical investigations of permeability upscaling by testing rock types not well represented in current data base.

Project Description: Porous media flow and transport data are collected at a variety of scales, and then integrated into models at an even different and larger scale. Upscaling is used to translate the data to model effective media properties. A laboratory investigation of permeability upscaling is being conducted with the use of a novel minipermeameter test system. It allows precise, rapid, non-destructive measurement of permeability over a range of different sample supports (*i.e.*, sample volumes). By varying the size of the minipermeameter tip seal, measurements spanning five orders of magnitude on a per-volume basis are made subject to consistent boundary conditions and flow geometry. Thousands of measurements on multiple faces of meter-scale blocks of rock are collected with each of five different tip seals (0.31 - 5.08 cm ID) plus a single large tip seal (15.24 cm ID) designed to integrate over the entire sampling domain. This process is repeated on multiple rock samples, each of which exhibits different textural and structural characteristics. Key summary statistics are calculated from the data sets and analyzed with reference to their corresponding sample support. The measured data are then interpreted with the assistance of theory and simulation.

Results: Over 200,000 permeability measurements, associated with six different sample supports, have been collected from four rock samples: a planar bedded sandstone, a sandstone exhibiting nested scales of cross-stratification, a densely-welded tuff and a poorly-welded tuff. For each rock sample and each summary statistic investigated (*e.g.*, mean, semivariogram), distinct and consistent upscaling trends were measured. Rocks of similar genetic origin (*e.g.*, tuffs) were found to exhibit similar statistical and upscaling characteristics, while rocks of differing origin (*e.g.*, tuffs *vs.* sandstones) exhibited distinct differences. The noted differences can largely be attributed to variations in the physical attributes (*i.e.*, spatial patterns, correlation length scales) characterizing the individual rock samples. Quantitative interpretations were pursued through comparisons drawn with theoretical upscaling models, each differing according to key fundamental assumptions. Results indicate that the non-uniform flow geometry imposed by the minipermeameter and the local-scale (*i.e.*, at or below the smallest scale of

measurement) heterogeneity is a key process influencing the measured permeability upscaling. Using image analysis, we compared the permeability measurements and a wide variety of objective textural measures drawn from the corresponding digital (visual) images. There was no significant direct correlation despite the obvious resemblance of the permeability maps and visual images for each rock. This may have implications for geophysical characterization methods. Linear filter analysis was employed to characterize instrument sample support (*i.e.*, effective size of the sample support and the spatial weighting of heterogeneities comprising that support) associated with each measurement. We continue to collect and analyze additional data on new and old samples, including eolian sandstones and carbonates.

To better interpret upscaling results we studied the details of the gas minipermeameter measurement method using numerical and analytical mathematical models. We derived solutions for the flow field under various conditions of media heterogeneity, and developed an adjoint state method for theoretically determining the instrument's spatial filter function. The function shows great sensitivity to the permeability just below the inner tip seal radius, and a lower but still significant sensitivity to the permeability just below the outer tip seal radius. The function is proportional to the square of fluid velocity, a previously unreported observation for any instrument. In a recent collaboration with Fred Molz of Clemson University, we offer a simple explanation for this observation. We also calculated Green's Functions for the flow field, which are being used to derive stochastic perturbation solutions for minipermeameter flow in a stochastically heterogeneous rock sample.

We took a 30 by 30 by 2.5-cm thick slab of cross-stratified Massilon sandstone, characterized it with detailed permeability measurements with different tip seal sizes, x-ray measurements of porosity, and visual image analysis. We then saturated the slab with water and ran sodium-iodide tracer through the slab longitudinally. Break-through curves (BTCs) were constructed from effluent sampling, and two-dimensional digital images of the solute concentration fields at selected times during the tracer experiment were acquired using X-ray absorption. The tracer behavior was strongly influenced by the nested scales of heterogeneity in this rock sample, exhibiting even the influence of individual lamina in the cross-beds.

STATE UNIVERSITY OF NEW YORK AT STONY BROOK

Department of Geosciences
Stony Brook, New York 11794-2100

Grant: DE-FG02-94ER14449

High Precision Radiometric Dating of Sedimentary Materials

G.N. Hanson, (631) 632-8210, fax (631) 632 8240, gilbert.hanson@sunysb.edu; W.J. Meyers

Objectives: To develop field, petrographic and geochemical criteria to allow high precision U-Pb dating of sedimentary minerals within rapidly deposited sequences of carbonate and clastic rocks.

Project Description: The original goal was to obtain radiometric ages for sedimentary material with uncertainties of three million years or less to date the times of sedimentation. We have since shown that it is possible in some circumstances to obtain uncertainties of 1 Ma or less.

Results: While we have found it possible to provide precise ages for a number of key regions, our most daunting task has been to predict whether a sample will have high enough uranium concentrations to provide high precision ages. While still pursuing our dating we have placed more effort into finding better ways to evaluate the nature and siting of uranium in samples. This understanding should make it possible for us to better select field sites and samples for high precision dating. Our original model was that the uranium in the surface environment is U(VI). When uranium enters a reducing environment it becomes U(IV) and is incorporated into the Ca site of a carbonate or phosphate mineral. This is consistent with our observation that the samples with the highest uranium concentration are in organic-rich samples, *i.e.*, the organic material produces a reducing environment. To test this hypothesis we have begun collaborative research at Brookhaven National Laboratory's National Synchrotron Light Source (NSLS) using microbeam techniques including evaluation of major and trace element concentrations using synchrotron XRF, elemental speciation and coordination using x-ray absorption spectroscopy (XANES and EXAFS), and mineralogy using micro-XRD at resolutions of 10 microns or less. The results of these studies require us to rethink our model for U incorporation. In fact, there seem to be several pathways for U incorporation in sedimentary carbonates and phosphates and it is possible that none of them require reduction by organic matter.

Uranium incorporation in calcite

We have examined calcite from two samples that yielded our most precise U-Pb ages. One of these is a dark brown organic rich palesol calcite sample from the Permian Basin in West Texas that is dated at 298 ± 1 Ma. This sample has U concentrations that range from 2-20 ppm based on XRF mapping at NSLS. XANES analyses show that the U is in the oxidized state U(VI). The core sample is from a depth of 8700 feet so it has not been exposed to weathering since burial. Our working model for this sample is that the U is bound to organic matter. This complex may be in the calcite as an inclusion, or possibly could be incorporated in the crystal lattice. Information on the coordination environment of the U will be necessary to distinguish between possible mechanisms. The second sample is a tan colored tufa (spring) deposit from the Middle Miocene Barstow Formation of the Mojave Block, California that was dated at

16 ± 0.1 Ma. This sample has U concentrations that range from below detection limits to around 500 ppm based on XRF mapping at NSLS. XANES analyses show that the uranium is in the reduced state U(IV). This sample was likely formed in an oxidizing environment and is exposed at the surface today. Our working model for this sample is that U is incorporated in the Ca site. We surmise that bacteria may have been responsible for reducing the U and that it was quickly incorporated into the calcite as a reduced species.

Uranium and thorium incorporation in phosphate

Phosphate minerals have shown great potential to yield high-precision U-Pb ages, with uncertainties of 1 Ma or less. Jurassic fish coprolites from the Hartford Basin, Connecticut, are composed of authigenic phosphates and are U-enriched, up to 4000 ppm. These phosphates formed during early diagenesis in organic-rich muds, believed to precipitate within a sulfate-reducing environment at or just below the sediment surface, before the complete decay of organic material. Standard acid digestion of the nodules produces highly discordant U-Pb ages. After pyrolytizing, the samples yielded $^{207}\text{Pb}/^{235}\text{U}$ ages that are consistent with the depositional age of the sequence (ca. 200 Ma). The $^{206}\text{Pb}/^{238}\text{U}$ ages, however, are about 15 Ma too young, which we attribute to loss of ^{222}Rn or ^{226}Ra in the ^{238}U decay chain immediately after deposition. Microbeam analyses of the samples at NSLS shows that the uranium is U(VI) and is dominantly associated with organic compounds, not the apatite. These results suggest that reducing conditions are not what is important for uranium enrichment in these phosphatic nodules but that organic matter is sorbing the uranium.

We have initiated a study of phosphatized bones for U-Pb (and Th-Pb) dating. The analyses show dramatic differences in actinide behavior in fossil bones from three formations. A Pleistocene Gytosid shell bone has high concentrations of U and low Th within the francolite of the fossilized bone. XANES analyses on the francolite shows U in mixed oxidation states. The Cedar Mountain Fm bone (unidentified dinosaur species) is also francolite with high concentrations of U and low Th. XANES analyses of this bone shows solely U(IV). A francolite fish fossil from the Green River Fm has low U concentrations but is highly enriched in Th, up to 700 ppm. We do not have a working model to explain such high Th enrichment.

Phosphor Imaging Autoradiography

We have discovered that phosphor imaging, a radioactive tracer technique widely used in the biological sciences, is particularly valuable for analyzing polished slabs of rock samples for uranium and thorium abundances. We examined samples containing between 4 and >500 ppm U and ~700 ppm Th. Resolution of one mm or better was obtained even for low concentration (~10 ppm) samples. These high-resolution maps of U and Th allow us to effectively sample for geochronology.

STATE UNIVERSITY OF NEW YORK AT STONY BROOK

Department of Applied Mathematics and Statistics
Stony Brook, New York 11794-3600

Grant: DE-FG02 ER14261

Medial Axis Analysis of Porous Media

W. Brent Lindquist, (631) 631-8361, fax (631) 632-8490, lindquis@ams.sunysb.edu

Website: <http://www.ams.sunysb.edu/~lindquis>

Objectives: The goals of this program are to extract quantitative information on the geometry of pore structure in rock, the distribution of fluids in the pore spaces under two phase flow regimes at residual saturations, and the relationship between the pore structure and fluid distribution.

Project Description: High resolution (1 to 10 micron), three dimensional images of rock samples, either dry or containing fluids, are obtained using X-ray computed microtomography. For two-phase flow studies, fluid contrast is achieved by doping one phase with a high X-ray absorbing agent. For pore structure studies using dry or single phase flooded rock, the void space is segmented and its structure (coordination numbers, channel lengths, pore volumes, throat sizes) determined using computational geometry algorithms. For fluid distribution studies, images of two phase fluid distribution are differenced against single phase fluid distribution in the same rock volume to identify the position of individual fluids. Distributions of each phase are numerically mapped in the pore space and correlations with pore properties computed. The relationship between pore structure and fluid distribution is studied using network flow and lattice Boltzmann models.

Results: In collaboration with R. Seright (Petroleum Recovery Research Center, New Mexico Tech.) the fluid distributions at residual oil and water saturations have been studied in three suites of images: a berea core before and after injection of a water soluble gel; a berea core before and after injection of an oil soluble gel; and a polyethylene core before and after injection of a water soluble gel. At residual non-wetting fluid conditions, the average non-wetting fluid distribution is observed to be independent of pore body volume. Fluid distributions in the throat constrictions have been observed to mimic that in the pore bodies, discounting differential gel action on throats and pore bodies as a source of disproportionate permeability reduction.

The characterization of the void structure in a suite of vesiculated basalts (collaboration with S.-R. Song, Taiwan National Univ.) has been completed. Construction of a new throat detection algorithm was required to handle the extreme range of vesicle (and hence throat) sizes found in such vuggy materials.

A study of permeability prediction versus fracture aperture in fractured marbles (collaboration with B. Durham, LLNL) using lattice Boltzmann modeling has been completed. Good agreement with experimental permeability measurements is obtained.

STATE UNIVERSITY OF NEW YORK AT STONY BROOK

Department of Geosciences
Stony Brook, NY

Grant: DE-FG02-96ER14633

Surface Chemistry of Pyrite: An Interdisciplinary Approach

Martin A.A. Schoonen, (631) 632-8007, mschoonen@notes.cc.sunysb.edu; Daniel R. Strongin, (215) 204-7119, fax (215) 204-1532, dstrongi@nimbus.ocis.temple.edu

Website: <http://sbmp97.ess.sunysb.edu>

Objective: The primary goal of this research program is to understand the microscopic aspects of pyrite oxidation. Characterization of the reaction sites that control this chemistry is one of the immediate goals. Our continuing research strategy is to understand macroscopic observations of pyrite reactivity with an atomic/molecular level view. The results of this research will lead to a better understanding how pyrite reacts in a range of chemical environments.

Project Description: The reactivity of pyrite in anoxic and oxic environments is being investigated by integrating aqueous geochemical and modern surface science techniques. In addition the effect of visible light illumination of the pyrite surface during oxidation has been investigated (see below). The surface science techniques have generally operated in the ultra-high vacuum environment, but a recent emphasis has been to develop in-situ techniques to study the mineral surface on a microscopic level in the presence of an aqueous or gaseous phase. Research concentrates on well characterized and clean As-grown and powdered samples of pyrite. Electron spectroscopies in UHV and vibrational spectroscopy at real pressures are used to understand the atomic composition and the nature of the functional groups on pyrite after exposure to oxidizing aqueous and gaseous environments. In FY2000, two primary studies have investigated the effect of adsorbed phosphate and light on pyrite oxidation.

Results:

Modification of the pyrite surface with phosphate and the effect on oxidation

The effect of phosphate on the oxidation of crushed and {100} pyrite was investigated with aqueous geochemical and surface science techniques. Phosphate in solution significantly suppressed pyrite (crushed) oxidation for pH>4. At pH of 3 or less, phosphate expressed no experimentally discernable effect on pyrite oxidation. The use of surface science techniques, specifically, X-ray photoelectron spectroscopy (XPS), showed that at pH>4, phosphate became bound to Fe³⁺ sites on {100} pyrite during the oxidation process. Phosphate bound in this way showed a significant inhibition on pyrite oxidation (based on XPS determinations of sulfur and iron oxide product concentrations) under our experimental conditions. These results suggested that the rate of pyrite oxidation in the absence of phosphate was facilitated near or at Fe³⁺ bearing oxidation phases on the surface. Phosphate bound on Fe³⁺ oxide product either prevents O₂ adsorption on this phase or electronically modifies these surface regions, but in either case inhibits electron transfer from pyrite-Fe²⁺ sites to molecular O₂.

Thermal and photochemical oxidation of pyrite

The thermal and photon-induced (visible light) oxidation of pyrite in solutions between pH 2 and 6 with dissolved oxygen was investigated by integrating surface science experiments and both aqueous geochemical oxidation experiments. Pyrite oxidation was experimentally determined to be strongly dependent on temperature. Interestingly, however, it was not possible to cast the temperature dependence in a simple Arrhenius equation, since the activation energy measured depended on the progress variable. For example, activation energies based on proton release rate, sulfate release rate, and total iron release rate vary by as much as 40 kJ mol^{-1} . It was inferred from this data that sulfur and iron oxidation and their subsequent release into solution followed different pathways. Exposure of pyrite to visible light (provided by a Xenon lamp) led to an acceleration of the oxidation rate, but the increase was typically less than a factor of two. X-ray photoelectron spectroscopy experiments showed within our experimental resolution that the chemical composition of the pyrite surface was unaffected by visible light illumination. Batch sorption experiments, however, showed that the reaction stoichiometry of the oxidation process was altered, suggesting that there was a change in reaction mechanism due to the exposure to visible light.

STATE UNIVERSITY OF NEW YORK AT STONY BROOK

Department of Geosciences
Stony Brook, New York 11794-2100

Grant: DE-FG02-99ER14996

Micromechanical Processes in Porous Geomaterials

Teng-fong Wong, (631) 632-8212, fax (631) 632-8240, Teng-fong.Wong@sunysb.edu; Joanne T. Fredrich, Sandia National Laboratories

Objectives: This project focuses on the systematic investigation of the micro-scale characteristics of natural earth materials, and how these micro-scale characteristics control the macroscopic deformation and transport behavior. The research uses an integrated approach consisting of experimental rock mechanics testing, quantitative 2D and 3D microscopy and statistical microgeometric characterization, and theoretical and numerical analyses. The objective is to enhance fundamental understanding of failure and transport processes in geologic materials, and thereby strengthen the theoretical basis for the application of laboratory results to various technological operations of importance.

Project Description: Knowledge of the micro-scale characteristics and behavior of rocks is important for several energy-related applications, including global climate change and carbon management; oil field geoscience; geotechnical engineering efforts such as design and assessment of geologic nuclear waste repositories; and environmental remediation efforts at contaminated DOE and/or DoD installations. The experimental investigation provides a detailed understanding of the microstructure of geologic materials and how the micro-scale characteristics affect macro-scale behavior including brittle failure and fluid transport. Detailed and quantitative microstructural studies complement laboratory rock mechanics experiments. The results are used to formulate and evaluate theoretical and numerical models of rock deformation and fluid flow.

Results: (1) Investigation of water-weakening effect on the strength of porous sandstones. Our comprehensive data on the weakening effect of water on brittle strength and ductile compaction of several porous sandstones has allowed us to formulate a micromechanical model to consistently interpret the dilatant and compactive failure behaviors due to presence of water and initial damage in a fracture mechanics framework. Current research focuses on such behavior in carbonate rocks, including Solnhofen and Indiana limestones. (2) Triaxial compression experiments on 2 limestones (of initial porosities of ~3% and 14%) and detailed characterization of the failure envelopes in both the brittle and cataclastic flow regimes. The mechanical and microstructural data show that inelastic and failure behaviors in the Indiana limestone are qualitatively similar to those in porous clastic rocks. A manuscript describing this study is being prepared. We have also published a study on the relatively compact Solnhofen limestone. For the first time, a fairly complete set of data on porosity change and the brittle-ductile transition in the Solnhofen limestone have been acquired. The failure modes are associated with complex interplay of dilatancy, pore collapse and crystal plasticity processes, and several micromechanical models have successfully been employed to interpret the phenomena. (3) Quantitative characterization of the pore geometry of four Fontainebleau sandstone samples using

synchrotron x-ray tomography. The data elucidate the 3-dimensional geometry and connectivity of the pore space in a suite of Fontainebleau sandstone with porosities ranging from 7.5% to 22%. Algorithms were developed to quantify the distributions of coordination number, channel length, throat size and pore volume. This unique set of computed synchrotron X-ray tomographic data provide important constraints on geometric attributes of importance in the realistic modeling of permeability and fluid transport. (4) Damage evolution during the formation of a compaction band. Preliminary data show that localization mode in the form of compaction bands orthogonal to the maximum compressive stress is widely observed in porous sandstones in the transition from brittle faulting to cataclastic flow. We are systematically investigating the inelastic and compactive behaviors that promote such localization features. (5) Development of dilatancy and strength anisotropy in foliated rock. Mechanical tests were conducted on the Four-mile gneiss, and damage mechanics model was developed to analyze the anisotropic mechanical behavior in this and other foliated rocks, underscoring the critical role of mica in controlling the evolution of dilatancy and brittle failure.

NORTHWESTERN UNIVERSITY

Department of Civil Engineering,
Evanston, IL 60208-3109

Grant: DE-FG02-93ER14344

Interactions of Pore Fluid Pressure and Inelastic Deformation of Dilating and Compacting Rock

J.W.Rudnicki, (847) 491-3411, fax (847) 491-4011, jwrudn@northwestern.edu

Objectives: To obtain an improved understanding of the interactions of pore fluid pressure and inelastic deformation of dilating and compacting rock for applications to the technologically common problem of storing or recovering fluids from the earth's crust.

Project Description: One strategy that has been suggested for mitigating the possible adverse effects of greenhouse gases on global climate change is to sequester carbon dioxide in the earth's crust, for example, in depleted oil or gas reservoirs or deep saline aquifers. The implementation of this strategy safely and efficiently requires an improved understanding of the effects of coupling between changes in fluid flow with the inelastic deformation and failure of porous rock. Coupling of fluid with inelastic deformation can affect the evolution of failure and, depending on the rock response, either delay or accelerate localized failure. Formation of localized regions of failure, either shear bands or compaction bands, can cause barriers to fluid flow that adversely affect the ability to inject or withdraw fluids from the crust.

Results: Conditions have been derived for the onset of localized deformation for a transversely isotropic constitutive relation intended to model the response of geological materials in the axisymmetric compression test. Compaction bands, planar zones of localized pure compressive deformation (without shear) that form perpendicular to the direction of the maximum principal compressive stress, are predicted to occur when the incremental tangent modulus for uniaxial deformation vanishes. The expression for the critical tangent modulus for shear band formation is more complex and depends, in addition to material parameters available from axisymmetric compression geometry, on the shear moduli governing increments of shear in planes parallel and perpendicular to the axis of symmetry, respectively. Uncertainty about material parameters prevents a detailed comparison with observations but the results are consistent with observations of low angle shear bands (with normals less than 45° from the symmetry axis) for compressive volumetric strain.

The effects of heating caused by frictional slip have been examined for a weakening, fluid-saturated fault using an extension of the one-dimensional model of Rudnicki and Chen (JGR, 1988). Shear heating tends to increase pore pressure and decrease the effective compressive stress and the resistance to slip, and, consequently, promotes instability. Conversely, dilatancy tends to decrease pore pressure and inhibits instability. The analysis reveals that the interaction of the two effects complicates this simple picture. For fixed slip-weakening, an increase in the magnitude of dilatancy (within a certain range) can destabilize slip and, similarly, for a fixed magnitude of dilatancy (within a certain range), stronger slip-

weakening can stabilize fault slip. These counter-intuitive effects are due to the dependence of the shear heating on the total shear stress (not just its change).

UNIVERSITY OF NOTRE DAME

Dept. of Civil Engineering & Geological Sciences
South Bend, IN 46556

Grant : DE-FG02-96ER14668

Dissolution of Fe(III)(hydr)oxides by Aerobic Microorganisms

Patricia A. Maurice, (574) 631-9163, fax (574) 631-9236, patricia.a.maurice.3@nd.edu

Objectives: The overall objective of our research is to determine the rates and mechanisms whereby microbes dissolve Fe(III)(hydr)oxides in aerobic soil environments. Information about the rates and mechanisms of Fe(III)(hydr)oxide dissolution is fundamental for a wide range of hydrobiogeochemical processes, yet little is known about the mechanism of dissolution promoted by siderophore-producing microorganisms. Fe(III)(hydr)oxides sorb radionuclides and organic contaminants; thus their dissolution may cause remobilization of these sorbed pollutants. Our current studies focus on the effect of Al-for-Fe substitution in goethite on the adsorption of the hydroxamate siderophore, desferrioxamine-B (DFO), and the effect of a competing bioligand, oxalate.

Results: During this study year, we made significant progress on a study of microbially mediated dissolution of kaolinite. This research resulted in 2 invited papers, 1 published (*Geomicrobiology*) and 1 currently in press (*Chemical Geology*) and oral presentations at the 2000 Clay Minerals Society and meeting and the midwest Environmental Chemistry Workshop. A manuscript co-authored with L. Hersman on microbial dissolution of hematite, goethite, and ferrihydrite is currently under review in *Applied Environmental Microbiology*. Additionally, P. Maurice made significant progress on a review manuscript invited for publication in *Earth Science Reviews*. We also began a study of siderophore-promoted dissolution of kaolinite. Although the original proposal called for a postdoctoral associate to begin work in Spring 2000, we delayed this because of P. Maurice's 7/00 move to the University of Notre Dame. The new postdoctoral associate began work Sept. 1, 2000 and is focusing on microbial effects on mineral aggregation kinetics and clay mineral dissolution.

Microbially mediated kaolinite dissolution

Clay minerals are ubiquitous through terrestrial environments, and they represent important reactive surfaces in nature. Fe is an essential nutrient that is often limiting in aerobic environments. Previous research by our group showed that an aerobic *Pseudomonas mendocina* bacterium was able to dissolve Fe from Fe(III)(hydr)oxides for use as a nutrient under Fe-limited conditions. We hypothesized that the bacteria could also obtain Fe from Fe-bearing clays by enhancing the clay mineral dissolution. To test this hypothesis, we investigated the effects of an aerobic *Pseudomonas mendocina* bacterium on dissolution of well and poorly ordered Clay Minerals Society Source Clay kaolinites KGa-1b and KGa-2 under Fe-limited conditions. KGa-1b is a well ordered kaolinite with 0.04% Fe by weight. KGa-2 is a poorly ordered kaolinite with 0.94% Fe by weight. We also used a more Fe-rich kaolinite (1.96 % Fe) from a proprietary locality in South America. When the only source of Fe was uncleaned or weakly cleaned kaolinite, the bacteria were able to grow to population sizes greater than non-kaolinite-containing controls, indicating that they acquired Fe from the solid phase. Rates of Al release from

kaolinite were greatly enhanced in the presence of the bacteria; the mechanism(s) of this enhancement likely include pH increases and/or production of Al chelating agents such as siderophores. We could not measure rates of Fe release from the clays directly because of bacterial uptake of the Fe. However, comparison with microbial growth curves when Fe was added as FeEDTA suggested that geomicrobiologic processes resulted in micromolar concentrations of Fe release from the kaolinites.

Strong cleaning of the kaolinites in HCl at 85°C removed much of the surface Fe, as measured by X-ray photoelectron spectroscopy, and also resulted in a Si-enriched surface precipitate that could be observed by atomic force microscopy. Substantial etch pits were also observed on some particles. The bacteria were able to grow well on strongly cleaned KGa-2, which still retained a reasonable amount of accessible Fe, but not on strongly cleaned KGa-1b, whose Fe content was below detection.

Dissolution in 0.001 M oxalate was used as a means of comparing amounts of Fe that could be easily removed from the kaolinites by a complexing ligand. For the three kaolinites used in this study, including cleaned and uncleaned samples, we found an increase in microbial growth with increasing oxalate-accessible Fe. We therefore suggest that the bacteria are most able to access Fe present in the clays in a form that is readily available to complexation by organic ligands. Overall, our results demonstrate that clay minerals such as kaolinite may be important sources of Fe to microbial systems and also that bacteria may have significant effects on clay mineral dissolution in aerobic environments.

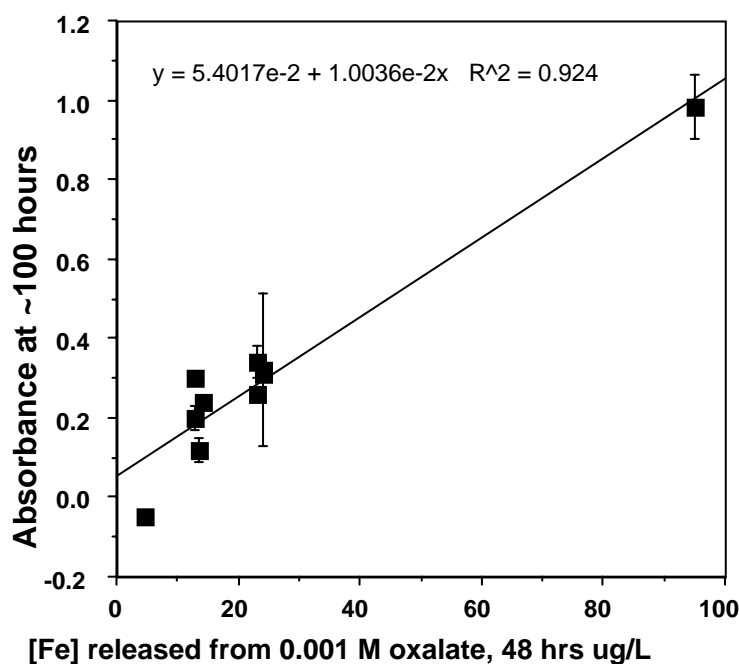


Figure 1. Fe released from 3 kaolinites (cleaned and uncleaned) during dissolution in 0.001 M oxalate versus microbial growth measured as absorbance. Microbial population sizes are greater on kaolinite samples with greater amounts of ligand-accessible Fe.

Siderophores are Fe complexing agents produced by bacteria. Preliminary measurements of siderophore production by the *p. mendocina* showed that the bacteria produce significant quantities of siderophore per unit cell in the presence of the kaolinites. The amount of siderophores produced per unit cell was found to decrease in the order: growth medium with no added Fe > growth medium with Fe added as kaolinite >> growth medium with Fe added as Fe(iii)(hydr)oxide > growth medium with Fe added as Fe-edta (dissolved form). Bacteria tend to produce greater quantities of siderophores per unit cell when they are Fe stressed. Hence, our results are consistent with the observation that the bacteria are capable of obtaining Fe from kaolinite, but that the Fe is not as abundant and/or not as easily accessible when presented in this form.

UNIVERSITY OF OKLAHOMA

School of Geology and Geophysics
Norman, Oklahoma 73019

Grant: DE-FG03-96ER14643

Development and Application of a Paleomagnetic/Geochemical Method for Constraining the Timing of Burial Diagenetic and Fluid Migration Events

R.D. Elmore, (405) 325-3253, fax (405) 325-3140, delmore@ou.edu; M.H. Engel

Objectives: The goal of this project is to develop paleomagnetic methods for dating diagenetic events in sedimentary rocks. Specific objectives include testing the hypotheses that fluid flow (e.g. basinal fluids, hydrocarbons), clay diagenesis and organic matter maturation are viable mechanisms for the occurrence of pervasive chemical remanent magnetizations (CRMs) that are commonly observed in sedimentary systems.

Project Description: Investigations of diagenetic processes such as fluid migration, clay diagenesis and the maturation of organic matter with burial commonly lack temporal control. The ability to constrain the time of events such as oil migration would be of significant benefit for exploration. Also, temporal controls for the various stages of the cycling of organic matter in the Earth's crust is important for our understanding of the carbon cycle and the development of predictive models with respect to carbon sequestration.

The paleomagnetic dating method is based on a genetic connection between diagenetic processes and the precipitation of authigenic magnetite. Isolation of the magnetization carried by the magnetite and comparison of the corresponding pole position to the apparent polar wander path allows the timing of diagenetic events to be determined. The research involves paleomagnetic field and laboratory tests to constrain appropriate chemical and physical conditions for magnetite authigenesis.

Results: We are continuing to build on our previous work in which we have documented the occurrence of chemical remanent magnetizations (CRMs) resulting from the precipitation of authigenic, magnetic minerals via rock/fluid interactions, clay diagenesis, and the maturation of organic matter.

Studies of Cambrian-Ordovician serpentinite in a tectonic terrane along the Highland Boundary Fault (HBF) in Scotland indicate that the HBF was a conduit for warm fluids in the Carboniferous that caused dolomitization, silicification, and hematite authigenesis. Preliminary paleomagnetic and geochemical results from a number of lithologies along the Moine thrust in northern Scotland also date a pulse of hot fluids in the Carboniferous-Permian. These results provide direct evidence for post-orogenic fluid activity and release of heat along faults.

We are testing clay diagenesis and maturation of hydrocarbons for the origin of numerous, widespread, pervasive CRMs in sedimentary systems that have not been altered by externally-derived fluids. We have completed a study on Jurassic sedimentary rocks on the Isle of Skye, Scotland, which are consistent with a connection between fluid-enhanced clay diagenesis and magnetite authigenesis/remagnetization.

Results from Mesozoic rocks in western North America where the timing of the smectite-to-illite conversion can be reliably inferred are encouraging. We are comparing results from Mesozoic strata in the disturbed belt of Montana where the rocks contain ordered illite/smectite that formed by moderate heating as a result of thrust loading, with equivalent strata on the adjacent Sweetgrass Arch which contain unaltered smectite-rich clay mineral assemblages. The results indicate that the magnetization in the rocks in the Sweetgrass Arch is weak and dominated by a modern viscous component. In contrast, the disturbed belt rocks have higher magnetic intensities and contain a pre-folding, reversed Tertiary magnetization that is interpreted to be a CRM residing in magnetite. A presence-absence test and the timing of acquisition for the CRM suggest that magnetite authigenesis is related to the smectite-to-illite conversion.

The results of laboratory simulation experiments indicate an increase in magnetitic susceptibility when smectites are heated at moderate temperatures (65°C, 97°C). Rock magnetic studies indicate that the increase in susceptibility is at least partly due to authigenesis of magnetite that is capable of carrying a stable magnetization. The magnetite authigenesis is not apparently associated with significant conversion of smectite to illite but to an earlier stage of clay diagenesis. The source of iron may be on the surface of the clay particles. The results suggest that smectite diagenesis triggered by temperatures equivalent to low burial could cause magnetite authigenesis and acquisition of a CRM.

We are also continuing to investigate maturation and migration of hydrocarbons into reservoirs as a mechanism to cause remagnetization by investigating the Mississippian Deseret Limestone and Permian White Rim Sandstone in Utah. The hydrocarbons in the Deseret are interpreted to have been generated in the Early Cretaceous during the Sevier Orogeny and to have migrated into the White Rim Sandstone in the Tertiary. Preliminary results indicate that the hydrocarbon-impregnated White Rim contains a magnetization in magnetite that is probably related to the hydrocarbons. The Deseret contains at least one CRM that appears to be Mesozoic in age.

OREGON STATE UNIVERSITY

Department of Geosciences,
104 Wilkinson Hall, Corvallis, OR 97331-5506

Grant: DE-FG03-00ER15030

Transport Visualization for Studying Mass Transfer and Solute Transport in Permeable Media

Roy Haggerty, (541) 737-1210, (541) 737-1200, haggertr@geo.orst.edu; Lucy C. Meigs, Sandia National Laboratories; Charles Harvey, Massachusetts Institute of Technology

Objectives: This research seeks: (1) to determine when small scale permeability structures cause solute spreading to be dominated by classical dispersion and when it causes solute spreading to be dominated by mass transfer; and (2) to develop models for predicting the effects of mass transfer over diverse time and length scales.

Project Description: Our approach is to conduct numerical simulations and laboratory experiments in heterogeneous media using conventional column techniques and novel transport visualization techniques. We are conducting numerical and laboratory experiments (1) to map transport regimes (conditions under which different equations adequately describe transport), (2) to apply mass transfer models developed at one time and space scale to larger scales, and (3) to investigate reactive transport with mass transfer.

Results: Numerical simulations and experimental work demonstrate that the upscaled solute transport behavior of a conservative solute is determined, not only by the standard spatial statistics of hydraulic conductivity, but also by the connectedness of the hydraulic conductivity field. Results demonstrate that hydraulic conductivity fields with the same standard spatial statistics may, or may not, produce mass-transfer behavior in a conservative solute depending on the connectedness characteristics of the media. Furthermore, mass transfer may be driven by both diffusion and advection.

We have developed a method, using tracer experiments conducted at different velocities, to construct a residence time distribution for the immobile domain that describes mass transfer by diffusion in heterogeneous media over a wide range of time scales. The scaling behavior of breakthrough curves can be predicted with this residence time distribution. For media with multiple rates of mass transfer, the use of the traditional single-rate model (i.e., exponential residence time distribution) gives poor predictions of transport when the scale of experiments and predictions differ. Our work has also shown that mass transfer driven by advection is important in some cases (see Figure). Building upon the diffusion work, we have begun to extend our residence-time methodology to fully capture both advective and diffusive mass transfer.

We have also developed a method using colorimetric chemical reactions to visualize reactive transport in porous media. Using this method we have demonstrated that commonly used models that assume perfect mixing between two reactants at the pores scale as they are transported through a porous media

can over predict the product formed. We have begun to make the first steps toward quantifying reactive transport in a highly heterogeneous medium, something that will have wide applicability to subsurface transport problems.

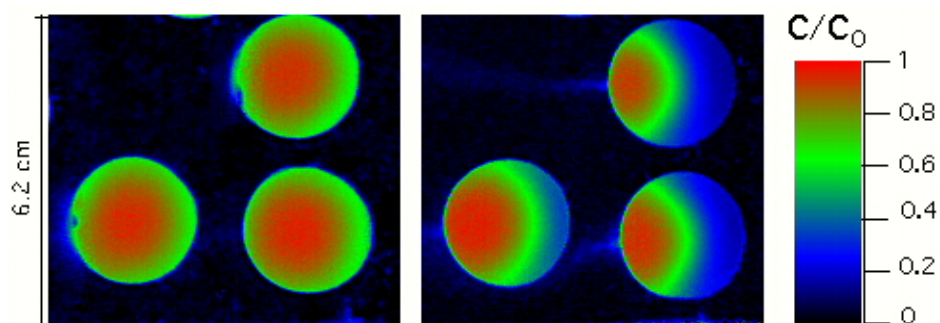


Figure: Comparison of solute concentration within low permeability regions for experiments conducted in two different transport regimes. The flow rate (1.32ml/min) and elapsed time (approx. 525 min.) are the same for both the diffusive mass transfer (left) and advective mass transfer (right) regime images. The right-hand figure, where solute is transported in and out of the bleb via advection, clearly shows the importance of advective mass transfer.

THE PENNSYLVANIA STATE UNIVERSITY

College of Earth and Mineral Sciences
Univ Pk, PA 16802

Grant: DE-FG02-01ER15209

Dissolution of Feldspar in the Field and Laboratory

Susan L. Brantley, (814) 863-1739 ph and fax, Brantley@geosc.psu.edu; Carlo G. Pantano (814) 863-2071, fax (814) 865-0016; pantano@ems.psu.edu

Objectives: Three questions are under investigation: 1) What are the structures of altered layers on dissolving crystalline and glassy feldspars? 2) What techniques can be used to investigate near-equilibrium dissolution of feldspar in the field or lab? 3) How is feldspar weathering affected by internal porosity and surface coatings?

Project Description: One of the most debated questions today in low-temperature geochemical kinetics centers upon the rate and mechanism of dissolution of feldspar, the most common mineral in the crust. In this project, the mechanisms of feldspar dissolution are investigated by emphasizing experiments with feldspar glass and crystal while comparing surface and solution chemistry. Surface sensitive analytical techniques (x-ray photoelectron spectroscopy, secondary ion mass spectrometry, NMR spectroscopy, atomic force microscopy) are used on samples reacted not only in the laboratory, but also in natural field settings. Specifically, laboratory work focuses on the structure of altered surface layers on feldspars, the rate of dissolution of feldspar crystal and glass in near-equilibrium and dilute solutions, and the presence of porosity and surface coatings on feldspars. In a complementary field project, the use of Sr concentrations and isotopic ratios are used to calculate feldspar dissolution rates.

Results: Fully polymerized glasses (albite, jadeite, and nepheline composition), two Na-aluminosilicate glasses containing non-bridging oxygens, and albite crystal were dissolved under ambient conditions. The fraction of octahedral aluminum with respect to total Al in the surface leached layer of glasses increases with increasing Al/Si ratio of the bulk glass (Figure 1). The NMR data also document repolymerization of the silicon network on the surface of nepheline glass, documenting alteration of the connectivity and coordination number of Al and Si during dissolution.

The effect of polymerization of the glass on the formation of a leached layer has also been investigated by dissolving fully polymerized aluminosilicate glasses with constant Al/Si and varying Ca/Na ratios. Secondary ion mass spectrometry, X-ray photoelectron spectroscopy, and Fourier-transform infrared reflection spectroscopy (FTIRRS) document surface layers on all glasses after dissolution. FTIRRS demonstrates that layer structures are independent of Ca/Na ratio.

Dissolution rates of plagioclase in two field settings (Cape Cod and Costa Rica) were also analyzed: rates in Cape Cod may be slower than laboratory rates at least in part because of surface coatings, while the Costa Rican samples are rate-limited by transport rather than interfacial dissolution.

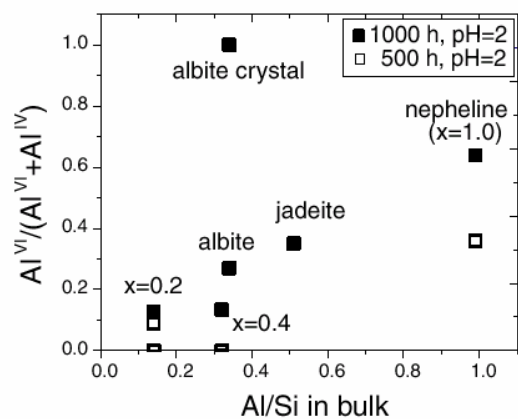


Figure 1. The relative amounts of six-fold coordinated Al in the hydrated glass surfaces, determined from CPMAS NMR spectra plotted as a function of Al/Si ratio in bulk glass and crystalline samples. The x notation refers to the composition in the join ($\text{Na}_2\text{O} : x \text{Al}_2\text{O}_3 : (3-x) \text{SiO}_2$).

THE PENNSYLVANIA STATE UNIVERSITY

Energy Institute
University Park, PA 16802

Grant: DE-FG02-00ER15111

Critical Chemical-Mechanical Couplings that Define Permeability Modification in Pressure-Sensitive Rock Fractures

Derek Elsworth, (814) 863-1643, fax (814) 865-3248, elsworth@psu.edu; Abraham S. Grader; Susan L. Brantley, Department of Geosciences

Objectives: This work is examining the controls on mineral dissolution, transport, and precipitation in rock fractures, and their influence on mechanical and transport properties. Laboratory flow-through tests, imaged by X-ray computerized tomography, are used as analogs to field-scale systems.

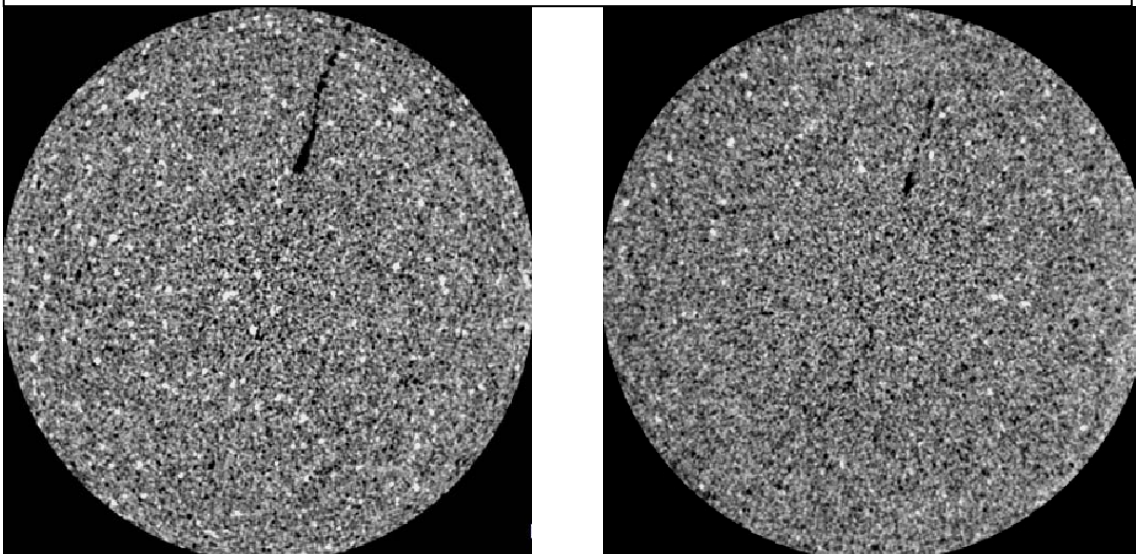
Project Description: Heated aqueous flow-through tests are being conducted on core samples containing through-going fractures. Effluent flow rates and chemical mass fluxes are recorded with changes in confining stress and temperature, while the sample is intermittently imaged by X-ray CT to monitor evolving spatial changes in porosity. Equilibrium and non-equilibrium models are applied to quantify the evolution of permeability, concurrent with changes in fracture porosity.

Results: Flow tests have been conducted on fractured Berea sandstone and novaculite at confining pressures to 6 MPa, and at temperatures to 150°C, using water as the permeant. The tests comprise through-flow in a core containing a single axial/diametral fracture, and are completed in an X-ray transparent pressure cell. Confining stress is applied to the core periphery through a flexible neoprene jacket. Axial pressure-drop is continuously monitored across the sample during the test, and is used as a proxy for permeability change with time. Sample scans, both dry and wet, and at various stages during the saturated flow-through cycle are used to link inferred changes in permeability with observed changes in fracture and matrix porosity. Scanner resolution is of the order of 50 microns, and is capable of identifying mass-loss through dissolution, as illustrated in the two successive scans of a fracture through the 5 cm diameter Berea core, in the figure. The figure illustrates the one o'clock to seven o'clock trending fracture both before fluid circulation (left) and after 4 days of constant circulation of water at 1 cc/min and 120°C, where a reduction in fracture porosity is tentatively apparent. Water chemistry is sampled during the test to define dissolution and precipitation processes, and to constrain mass balances.

Models have been developed to define and quantify key processes of pressure solution and free-face dissolution, and the influence of temperature, stress level, and chemistry on the rate of dissolution, its distribution in space and time, and its influence on the mechanical and transport properties of the fracture. Two approaches are used. The first involves the transformation of pressure solution data for clean quartz sands to represent behavior of a fracture in sandstone. Long-term closure is evaluated from a known fracture roughness profile and an evaluated equilibrium stress, defined from the prescribed surface activity of the asperity interface. The progress of fracture closure to this final equilibrium state is conditioned by rates of viscoelastic compression of the fracture asperities, in turn defined by pressure

solution or precipitation rates. Predicted dissolution rates and rates of porosity evolution are similar to laboratory results. The second approach involves the representation of pressure solution at the asperity contact as diffusion along a grain-boundary interface, accompanied by precipitation on the free face. The comparison of measured dissolution rates with results from the first method provide adequate agreement in rates of fracture healing, but rates predicted from the more physically consistent second method remain anomalously too fast. Further tests will examine component processes in further detail.

Figure 1: CT image of an artificial diametral fracture in Berea both before (left) and after (right) circulation of water for 4 days at 1 cc/min. The change in fracture volume is apparent. Sample diameter is 5 cm, and pixel resolution is of the order of 50 microns.



PRINCETON UNIVERSITY

Department of Geosciences, 151 Guyot Hall
Princeton, NJ 08544

Grant: DE-FG02-00ER15063

In-situ Evaluation of Soil Organic Molecules: Functional Group Chemistry, Aggregate Structures, Metal and Mineral Surface Complexation Using Soft X-rays

Satish C. B. Myneni, (609) 258-5848, fax (609) 258-1274, smyneni@princeton.edu

Website: <http://geoweb.princeton.edu/research/geochemistry/index.html>

Objectives: 1) The functional group chemistry and macromolecular structure of soil organic molecules, and their isolated humic substances
2) The influence of solution chemistry on the aggregate structures, protonation and metal complexation of model and natural organic molecules
3) The structure and chemistry of mineral adsorbed humic substances and soil organic molecules, and their role on ion-sorption as a function of solution chemistry and mineral surface structure.

Project Description: Humic substances, the biochemical alteration products of plant and biological material, are common in soils and natural waters and play a major role on mineral weathering, elemental cycling, C-storage in soils and sediments, and the fate and transport of contaminants in the environment. Although several investigators have examined their behavior in the environment, several of these studies are limited to humic substances isolated from soils and river water. This has been primarily due to the absence of *in-situ* spectroscopy, and microscopy methods for characterizing the chemistry of organic molecules in natural systems. However, the previous investigations have provided important clues on the functional group chemistry and macromolecular structures of these complex organic macromolecules. The aim of our research project is to: 1) develop synchrotron based soft x-ray instrumentation for studying these molecules in ambient conditions, 2) conduct experiments to understand the functional group chemistry and macromolecular structures of humic substances in soils and natural water, and their isolates, and 3) characterize the nature of humic interactions with mineral surfaces and their role in metal complexation.

Results:

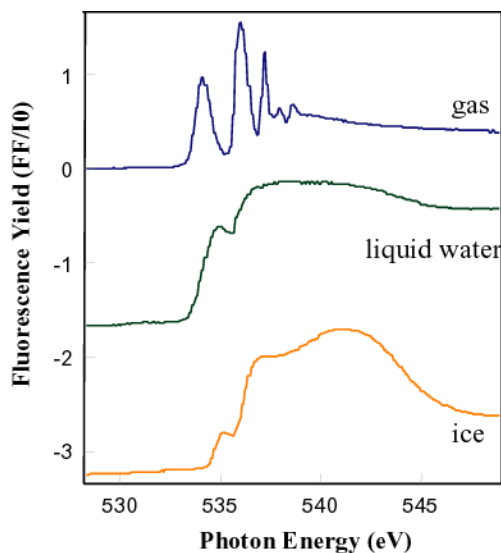
(a) Soft-X ray Endstation for Environmental Research (SXEER)

We built SXEER at the Advanced Light Source, Berkeley (ALS) to facilitate the X-ray spectroscopic studies of light elements (e.g., C, N, O) in aqueous solutions and at the interfaces. Using the prototype of this instrument we examined the H-bonding networks in liquid water, solvation of aqueous ions, and the nature of H_3O^+ and OH^- in liquid water, and the functional group chemistry of C-containing simple molecules (e.g. glycine, acetic acid, carbonate). This facility is optimized to collect the sample X-ray absorption spectra using sample fluorescence. With the bright and high flux synchrotron beams at the undulator beamlines at the ALS, it is possible to examine the molecular chemistry of dilute solutions (of the order of few millimolar in aqueous solutions and the detection limit varies significantly with the

absorption cross-section of different moieties in the organic molecule). Currently we are modifying this chamber to have a flow-through set up and facilities to examine reactions at the single crystal-water interfaces.

b) *X-rays Spectroscopic Investigation of H-bonding Environment in Liquid Water*

Since SXEER provides a unique opportunity to examine the electronic state of liquid water, our initial experiments were focused on the H-bonding environment in liquid water. These studies and the complementary electronic structure calculations on different forms of liquid water have been conducted in collaboration with Anders Nilsson at Uppsala University (currently at the Stanford Synchrotron Radiation Labs) and L.G.M Pettersson at Stockholm University. Our studies indicate that the X-ray absorption spectra of water at the O absorption edge are different for different forms of water (figure on the right). Our studies also suggest that the liquid water contain a significant number of broken H-bonds and



are

our

XAS studies provide the electronic state of different broken H-bonded species in liquid water. Currently we are conducting the molecular dynamics and DFT calculations to evaluate the structure and the electronic state of solvated water molecules around dissolved ions. Theoretical studies on H_3O^+ ions are just begun in collaboration with Roberto Car at the Princeton University.

c) *Functional Group Chemistry of Model Organics & Humic Substances in Aqueous Solutions and on Mineral Surfaces*

Using SXEER and other existing facilities at the synchrotrons, we are also examining the chemical state of different functional groups in organic molecules (e.g., $-\text{COOH}$, $-\text{SH}$) and their variation as a function of protonation and metal complexation in aqueous solutions. Our preliminary studies indicated that the $1s \rightarrow \pi^*$ and $1s \rightarrow \sigma^*$ transitions of different moieties are sensitive to their protonation state, and provide important clues to the nature of the organic molecule complexation patterns in solutions or on surfaces. We began investigations with simple and polymeric carboxylic acids, glycine, cysteine, acetohydroxamic acid, and siderophores. We are complementing these soft-XAS studies with vibrational spectroscopy studies. These model system studies are currently in progress. We are examining the functional group chemistry and metal complexation of isolated humic substances in aqueous solutions using the information obtained from the model systems discussed above. We are summarizing our results on the applications of XAS methods in the identification of functional groups of natural organics.

PURDUE UNIVERSITY

Department of Earth and Atmospheric Sciences
West Lafayette, Indiana 47907

Grant: DE-FG02-98ER14886

Mechanical Models of Fault-Related Folding

A.M. Johnson, (765) 494-0250, fax (765) 496-1210, gotesson@purdue.edu

Objectives The underlying goal of the research has been to provide a unified, mechanical infrastructure for studies of fault-related folding and to apply that infrastructure to studies of a wide range of field examples. The mechanical theory is being presented via programs that have graphical user's interfaces (GUI) so that structural geologists may model a wide variety of folds. The research is of value to many academic studies of fault-related folds, but it also provides practical methods of predicting forms of folds and other structural traps accessory to each type of fault-related fold and it provides explanations of kinds of ground deformation associated with ground deformation and rupture during during earthquakes.

Project Description: The research project can be divided into four parts. The first part is to investigate the geometric characteristics that identify fault-related folds of different types. In addition to exploring existing literature and seismic profiles, field mapping of fault-related folds in central Utah and along the southwest side of the Big Horn Basin in Wyoming will be combined with borehole data and seismic profiles of the structures. This combination of data will relate the folding observed in the field to the underlying faulting. The second part of the research is to derive mechanical analogs of idealized field examples of fault-related folds as well as various geometric models of fault-related folding. The combination of boundary conditions, rheological properties and mechanisms which produce fault-related folds of different types can be determined in these ways. The third component of the research is to explore what kinds of secondary structures occur together with primary structures, such as ramp anticlines and synclines, décollement folds, fault-arrest folds and fault-propagation folds, that would suggest new targets for petroleum exploration. The last component of the reaserch is to develop methods that will allow practitioners to generate their own examples of ideal fold forms, by specifying the conditions the practitioner suspects to be important in the tectonic environment.

Results: An analysis of deformation bands in San Rafael monocline, Utah by MS student Kaj Johnson shows that the stress state reflects local folding rather than a regional compression. His study also developed, based on beam and fracture theory, an explanation for flexural slip during folding and localization of layer-parallel faults in the limbs of the San Rafael Swell and other monoclines. The theory indicates that the layer-parallel faults should form along relatively weak layering where change of curvature, or coil, is maximized.

An MS study by Joe Durdella has provided a viable model for the formation of Pitchfork anticline in Bighorn Basin, Wyoming. He did this by describing the three-dimensional form of the structure, using a combination of surface, well log and seismic data, and applying the knowledge of fault-related folding

theory by way of mechanical models to determine the fold forming mechanisms. He showed that the Pitchfork anticline formed by a combination of two folding mechanisms, basement involvement through *Forced-Folding* and kinking through *Kink-Wedge* folding. The *Kink-Wedge* mechanism, newly developed for this study, produces a fold very similar in form to that of the Pitchfork anticline. It occurs in the sedimentary cover at the tip of a horizontal detachment as a result of uniform block translation, and is characterized by growth of the width and amplitude of the kink-wedge upward toward the ground surface. The *Forced-Fold* mechanism explains the translated and rotated basement block that truncates the kink-wedge downward in the Pitchfork anticline.

In addition to the field applications of fault-related folding, considerable progress has been made on mechanical theories of four structural processes of fault-related folding: *basement-cored-forced folding*, *sequential ramp folding*, *listric-fault folding*, and *gang-fault folding*. The analyses have been restricted to fault-arrest conditions so far but fault-propagation folding will be included in a more nearly general model, *faux pas* under development. Programs with graphical user's interfaces (GUIs) have been developed for each of these theoretical processes to calculate and display the fold forms produced by the various processes. Demonstration versions of the programs have been available for about a year at a Purdue website: www.eas.purdue.edu/fauxpli. The Forced Fold program and GUI (*FoFo FaRF*) simulate the deformation of sedimentary cover over displaced rigid basement blocks. This program models the folding of a sedimentary cover with a traction-free ground surface. The sedimentary cover may be homogeneous linear or nonlinear medium, or an anisotropic medium or a layered medium. The Gang Fault Fold program and GUI (*SeGaLi FaRF*) model 3D folds that form over blind faults. The faults may be listric or straight in profile and curved or straight in map view. The program Multiramp and Detachment and GUI (*SeDeRa FaRF*) model sequential ramp folding. The final program of the series, *Faux Pas FaRF*, is based on newly-developed, boundary element methods and will largely reproduce the classic types of fault-related fold illustrated in the Ph.D. dissertation by Wei Wei (1995).

PURDUE UNIVERSITY

Department of Physics
West Lafayette, Indiana 47907-1396

Grant: DE-F602-93ER14391

Seismic Monitoring of Time-Dependent Multi-Scale Heterogeneity in Fractured Rock

Laura J. Pyrak-Nolte, (765) 494-3027, fax (765) 494-0706, ljpn@physics.purdue.edu

Website : <http://www.physics.purdue.edu/rockphys>

Objectives: The objective of this proposal is to determine the effects of time-dependent multi-scale heterogeneity on seismic wave propagation through fractures and fractured rock. Specifically, we will address: the effects on the hydraulic -mechanical-seismic response caused by (1) heterogeneity within a fracture; (2) heterogeneity from multiple fractures and fracture networks; and (3) heterogeneity caused by geochemical interactions between pore fluids and rock, etc.

Project Description: A strategy for reducing carbon dioxide (CO₂) emissions into the atmosphere from power plants burning fossil fuel is to capture CO₂ and sequester the CO₂ in subsurface reservoirs. Candidates for geological sequestration include depleted oil and gas reservoirs, deep saline aquifers, and underground coal beds. Though these subsurface reservoirs often differ in lithology and structure, fractures are common to all. Fractures in rock are highly conductive rapid-flow paths that can connect otherwise hydraulically isolated rock formations. The principal focus of the work is to experimentally determine the link between the seismic properties of fractures and their hydraulic permeability. Furthermore, we will study how stress-distributions and invading fluids or gases alter the seismic signatures of fractures, with the goal of using these changes to actively monitor the changes in stress fields and the migration of fluids in a fractured reservoir. Achievement of the proposed research objective depends on the determination of the effect of micro-scale phenomena on macro-scale measurements through the combination of laboratory experiments and numerical analyses

Results: Experiments were performed to determine if laboratory seismic methods were sensitive to changes in a fracture induced by geochemical alteration. A seismic tomographic imaging experiment was performed on a limestone core containing a single fracture before and after reactive flow. The results indicated that geochemical alterations of the fracture as well as the fluid content in the fracture can be detected. However, from the reconstructed tomograms, the effect of gas saturation could not be separated from geochemical alteration.

Three separate experiments were designed to investigate the effect of partial gas saturation on seismic waves propagated across a fracture: (1) acoustic measurement during fluid invasion; (2) two-dimensional acoustic imaging of the fluid distribution; and (3) determination of the scaling nature of acoustic measurements. The magnitude and the relationship between fracture specific stiffness and frequency was observed to be a function of fluid saturation, i.e. the spatial and size distributions of each phase, as well as, static fluid patterns versus fluid invasion. The heterogeneous distribution of gas and

water played a stronger role in controlling the transmission of energy across the fracture than the underlying heterogeneity in fracture geometry (Figure 1).

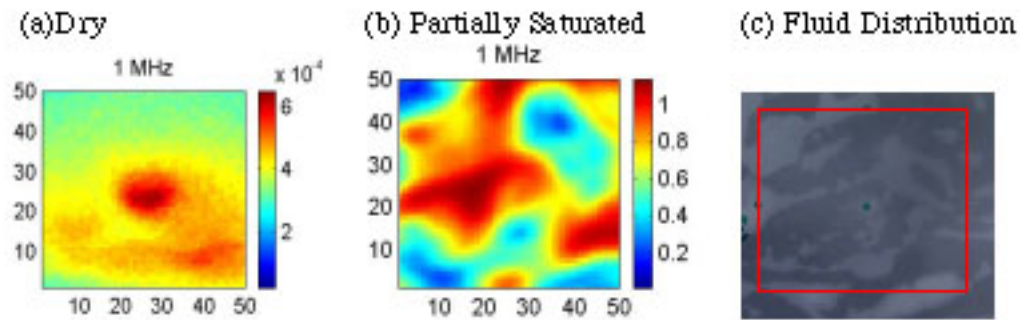


Figure 1. Two-dimensional maps of the maximum acoustic amplitude (at 1 MHz) for a single fracture in the (a) dry condition and (b) partially saturated condition. (c) The static fluid pattern of gas (light color) and water (dark color) distribution in the fracture for a 58 mm by 58 mm region. The red square represents the region of the fracture (50 mm by 50 mm) that was acoustically imaged in (b). The vertical and horizontal axes represent position in millimeters. The color scale in (a) and (b) represents the amplitude in Volts.

RENSELAER POLYTECHNIC INSTITUTE

Department of Earth & Environmental Sciences
Troy, New York 12180-3590

Grant: DE-FG02-94ER14432

Transport Phenomena in Fluid-Bearing Rocks

E.B. Watson, (518) 276-8838, fax (518) 276-6680, watsoe@rpi.edu

Objectives: The overall goal of this project is to provide insight into chemical transport processes in the Earth's crust and upper mantle that are accomplished by means of fluid flow, or that involve diffusive migration of fluid components (principally C, O, H).

Project Description: This is a multifaceted program of experimental research on the behavior and properties of C-O-H fluids and molecular species in rocks at depths exceeding ~20 kilometers in the Earth. The objectives are pursued using solid-media, high pressure-temperature techniques that have been in continuous development since the project began in 1994. Focus areas have included solute diffusion in supercritical fluids, permeability of rock analogs exhibiting equilibrium microstructure, and grain-boundary diffusion of molecular and atomic C-O-H species. These areas are viewed as complementary aspects of the same general problem of fluid-assisted mass transport: permeability controls the velocity of fluid flow; solute diffusion determines the efficacy of mass transport through a stationary fluid; and grain-boundary diffusion of C-O-H species controls communication between fluid-filled pores that are isolated from one another (as well as transport of fluid species in situations where no free fluid is present). Diffusion of C-O-H species may also determine whether and how a fluid phase develops during slow, progressive de-volatilization.

Results: Four specific short-term objectives have been pursued during the past year:

1) Direct characterization of the *3-D geometry of the fluid phase* in simple rock analogs. We have shown by serial sectioning of experimental charges that the mineral/fluid equilibrium microstructure of monomineralic rock analogs closely approximates an idealized geometry consisting of grain-edge tubules of roughly triangular cross-section.

2) Measurement of the *permeability of polyphase rock analogs* containing a minor phase of high aspect ratio. We have shown that the minor phase in fluid-bearing rocks resides principally in open pores at grain corners and has little effect on permeability.

3) *Spatial distribution of graphite and diffusion of elemental carbon* in grain boundaries under fluid-absent conditions. Our initial conclusion from high P-T annealing experiments on samples initially containing thin grain-boundary films is that graphite segregates into discrete microcrystals or clumps of microcrystals—i.e., the films are unstable and therefore cannot contribute to the high electrical conductivity of the deep crust (see Figure 1).

4) *Diffusion of CO₂ molecules* along grain boundaries in rocks. We are developing ¹⁴C radiotracer techniques designed to detect migration of CO₂ (and C) through the grain boundaries of rocks. Preliminary results indicate that the solubility of CO₂ in grain boundaries is very low and probably

undetectable in situ. Our current strategy involves development of CO₂ sinks to gauge the time-integrated grain-boundary flux.

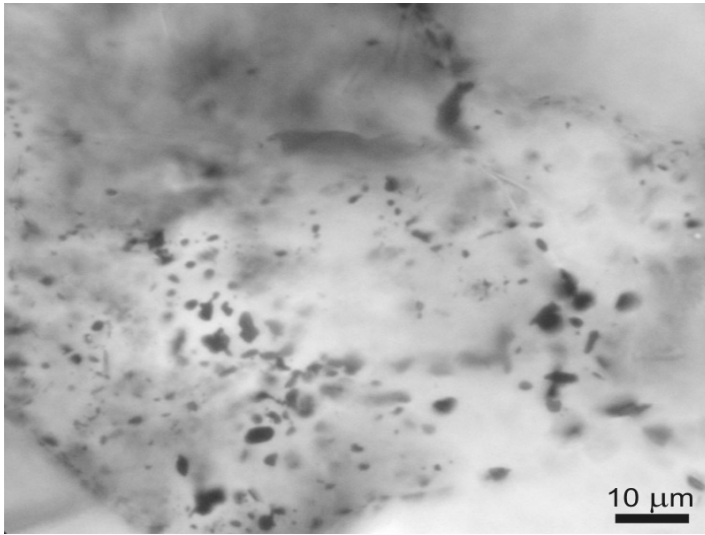


Figure 1. Transmitted-light optical micrograph of a 500-micron thick wafer of C-bearing quartzite annealed 5 days at 1300°C and 1 GPa. The quartz grains were initially coated with a ~50-nm film of amorphous carbon. The film has segregated into discrete patches along the grain boundaries.

NATIONAL MUSEUM OF NATURAL HISTORY, SMITHSONIAN INSTITUTION

Department of Mineral Sciences
Washington, DC 20560-0119

Grant : DE-FG02-00ER15070

Low-T, Fluid-Ashflow-Tuff Interactions: How Rock Textures, Chemistry, and Mineralogy Reflect reaction Pathways and Influence Rock Response to Heating

Sorena S. Sorensen, (202) 357-4010, fax (202) 357-2476, sorena@volcano.si.edu

Objectives: We aim to understand the textural, mineralogical and geochemical effects of low-T K-metasomatism of volcanic rocks and the fluid-flow mechanisms that cause them, and how subsequent metamorphism could alter such rocks. Results will yield information about the manifestations of fluid flow from the grain to regional scales, and provide insight into volcanic arc evolution.

Project Description: Near-surface, low-T, K-metasomatism of ashflow tuffs is a volumetrically and petrologically significant feature of the western United States. This project will (1) demonstrate how textures correlate with various mineralogical and geochemical effects of low-T K-metasomatism of Tertiary volcanic rocks in three settings in the western U.S.; (2) describe the fluid-flow mechanisms responsible for the alterations; (3) construct model reaction paths that predict how subsequent contact metamorphism could alter the compositions and/or textures of the rocks; and (4) test these predictions against case studies of variably metamorphosed arc-volcanic rocks that had previously been variably K-metasomatized at low-T conditions. The study will integrate cathodoluminescence (CL) textural analysis with major, minor, trace element and oxygen isotope geochemistry of rocks and minerals in order to discover grain-scale reaction mechanisms and to elucidate large-scale fluid-rock processes.

Field and Analytical Work During 2001 Fiscal Year:

During the last fiscal year, we have combined existing data for sample suites of K-metasomatized tuffs with new analyses and textural observations to build a database that links geochemical data with information about textures. The new geochemical data includes major, minor, and trace element whole-rock analyses of suites of metasomatized tuffs from Socorro, New Mexico, Creede, Colorado, and metasomatized, metamorphosed tuffs from the Duck Lake area near Mammoth Crest, eastern Sierra Nevada, California. Preliminary $\delta^{18}\text{O}$ data for mineral separates and whole rocks have been obtained for Creede and Socorro suites. Textural analysis focused on these suites and a suite from the Harcuvar Mountains of Arizona. Additional suites from the southern Inyo Mountains, and the Alabama Hills of eastern California were also investigated. Textures were examined with conventional and CL petrography, backscattered electron imaging (BSE), and elemental X-ray mapping, and augmented by mineral analysis with the electron microprobe.

Fieldwork was conducted in two separate trips. K-metasomatism is commonly associated with the upper plates of the detachment faults that define Tertiary metamorphic core complexes in Arizona, California and Nevada. During February, we collected a suite of samples of metasomatized volcanic rocks from the upper plate of the Bullard detachment fault in the Harcuvar Mountains of Arizona. We

supplemented this suite with samples from the Arizona Geological Survey. Additional detachment related samples were collected in the Picacho Peak area. In August, we collected a sample suite in the White Mountains of California. This suite of metavolcanic and metasedimentary rocks underwent alkali metasomatism that may be related to the emplacement of the Pellisier Flat Pluton. The rocks are contact metamorphosed to the biotite zone of the albite-epidote-hornfels facies. The suite was collected in order to characterize the alteration histories of this locality, including samples both distant from and adjacent to Jurassic and Cretaceous plutons.

Results:

Textural Features of K-metasomatism of Tertiary volcanic rocks.

Despite very different alteration environments, K-metasomatism in Creede, Colorado (related to caldera collapse and resurgence), Socorro, New Mexico (produced in an arid playa groundwater system in an extensional environment), and the Harcuvar Mountains, Arizona (in the upper plate of detachment fault), yielded strikingly similar chemical changes and mineral replacement mechanisms.

Low-temperature K-metasomatism at these localities proceeded by the replacement of original igneous feldspars by near-end-member orthoclase (var. adularia). Remnant igneous plagioclase phenocrysts are common in Socorro rocks, rare in Creede specimens, but have not been identified in Harcuvar samples. In less-altered rocks, green- to yellow-luminescent igneous plagioclase has been partially replaced by nonluminescent to faintly “brown”-luminescent $Or_{>97}$ feldspar. In more altered rocks, blue-luminescent Or_{40-70} sanidine phenocrysts have also been replaced. Some samples from Creede and Socorro contain fine-grained intergrowths of brown-luminescent illite/smectite and/or blue-luminescent kaolinite, with adularia. Replacement of igneous phenocrysts by albite is common (but geographically restricted) in both Creede and the Harcuvar Mountains. Textural analysis documents multiple generations or chemically distinct stages of metasomatism at each of these three localities.

CL Evidence for Reaction Mechanisms.

Feldspar replacement textures show dissolution of igneous feldspar and crystallization of metasomatic feldspar at grain to subgrain scales. Some replacement feldspar grew into open spaces produced by dissolution, and some altered feldspars contain pores that were filled with clay minerals and adularia. Replacement typically proceeded along cleavage, fracture, or grain-boundary surfaces. Plagioclase phenocrysts were typically the most susceptible to alteration, followed by sanidine phenocrysts; some groundmass feldspar was least susceptible to alteration. Thus, alteration proceeded from phases from the least to greatest Or contents.

Groundmass feldspar underwent different reaction mechanisms than phenocrysts that are replaced by end-member adularia. Samples that contain only a few modal percent feldspar phenocrysts, as well as samples in which feldspar phenocrysts have been replaced by albite display elevated K/Na ratios from 3 to 10. These rocks retain blue-luminescent groundmass feldspar grains, some of which have Or-enriched compositions. The heterogeneous alteration of groundmass likely reflects variations in pre-alteration compositions (with Or-poor grains more susceptible to alteration) and perhaps heterogeneous fluid access.

CL Evidence for Fluid Flow Mechanisms.

Fluid flow at the Creede, Socorro, and the Harcuvar Mountains localities evidently occurred primarily by grain-boundary flow through a highly permeable aggregate. Some fracture-controlled flow undoubtedly took place at each locality, as evidenced by quartz + adularia micro-veins and by the nucleation of adularia on igneous feldspars along preexisting fractures or veins. However, fractures would not be required for flow through the matrix of an inherently permeable and porous ash-flow tuff, and many altered samples lack evidence of fracturing.

Correlating CL with Chemistry

As with textural features, strikingly similar chemical trends are seen in these three settings. Variation in K_2O and Na_2O approximates a molar K:Na exchange ratio of 1, although some samples from Creede and Socorro (especially the Upper Lemitar Tuff) deviate from this ratio. These, and other features, differ from both igneous fractionation trends and the compositions of unaltered protoliths. CL images link whole-rock chemical data with replacement mechanisms. Modeling shows that whole-rock trends in K, Ca, Na, Rb, and Sr for most rocks can be accounted by the feldspar replacement: first plagioclase (Na, Ca, \rightarrow K; Sr \rightarrow Rb), then sanidine (Na \rightarrow K, Sr \rightarrow Rb).

The K/Na ratio of a particular sample reflects its original chemistry, its relative abundances of phenocryst types, and the composition and volume of the metasomatizing fluid. The K^+/Na^+ and K^+/H^+ ratios of the fluid will control adularia *versus* albite stability and feldspar *versus* clay stability. Because Al is probably immobile during low-temperature K-metasomatism, authigenic feldspar growth requires the breakdown of igneous feldspar, which will provide a local source of Al. Adularia replacement of alkali feldspar results in a 1:1 molar exchange of K for Na. Adularia replacement of An_{20} plagioclase (a typical An-content for Socorro tuffs) yields a K:Na exchange ratio of 1.5:1, assuming all of the Al in plagioclase is locally consumed to produce adularia. These feldspar exchange ratios encompass most of the alkali disturbance trends reflected by the compositions of these rocks. Replacement of feldspar by clay minerals (as described by Ennis et al., 2000) produces a variety of exchange vectors, including shallow slopes and alkali leaching. Some Creede and Socorro samples with underwent alkali leaching.

Metasomatism of Sierra Nevada arc volcanic rocks

Because both alteration chemistry and rock textures appear to survive later metamorphism of similar rocks, comparing the textures and geochemistry of rocks altered in different environments may discriminate between settings and shed light on the early alkali alteration histories of metamorphosed volcanic rocks in arc settings. Metavolcanic rocks from the southern Inyo Mountains, the Alabama Hills, and the Duck Lake area of the Mammoth Crest, eastern California, all share have geochemical (feldspar chemistry, whole-rock LIL enrichments, loss of Na, Ca, Sr) and CL textural features of the K-metasomatized Tertiary volcanic rocks from Creede, Socorro, and the Harcuvars.

In 2001, our work focused on rocks at Duck Lake, part of a lithotectonic assemblage exposed along the eastern front of the Sierra Nevada that likely represents the intra-caldera equivalent of outflow tuffs that were K-metasomatized in the nearby Ritter Range. Meta-rhyolite tuffs at Duck Lake show complex K, Na, and Ca systematics and disequilibrium feldspar phase relations that reflect a superposed history of contrasting metasomatic systems.

CL petrography shows igneous phenocryst and ground mass feldspar completely replaced by near-end-member orthoclase ($Or_{>95}$ after sanidine) and or albite ($Ab_{>95}$ after plagioclase). These textures resemble those of nearby meta-tuffs in the Ritter Range Pendent (on strike, 20 km NW), and of unmetamorphosed Tertiary tuffs (Creede, Socorro, Harcuvar Mountains) that have undergone low-temperature K- or K/Na-metasomatism. These early features are overprinted by Ca-metasomatism that is manifested by calcite veins and grossular + epidote veins with calcic plagioclase (An_{80-100}) vein envelopes. The early pseudomorphs of phenocrysts and groundmass feldspar are replaced by calcic plagioclase in this event. Whole-rock geochemistry shows concomitant gains of Ca and Sr and loss of Na. CaO/Na_2O for tuff samples ranges to 13, of value >6 times that of unaltered ashflow tuffs. K/Na, LIL, and REE values for Duck Lake tuffs are similar to those seen in the Ritter Range, Creede, and Socorro, but display distinct slopes on plots of K/Na versus Rb/Sr. Textures indicate that Ca was sourced by hydrothermal fluid derived from carbonates, probably locally. The Ca-rich silicate veins cut metamorphic fabrics that have been regionally attributed to batholith emplacement, indicating Ca-metasomatism occurred during retrograde phases of contact metamorphism.

UNIVERSITY OF SOUTHERN CALIFORNIA

Department of Aerospace and Mechanical Engineering
854 West 36th Place
RRB 101
Los Angeles, CA 90089

Grant: DE-FG03-00ER15092

Three-Dimensional Miscible Porous Media Flows with Viscosity Contrast and Gravity Override

Tony Maxworthy, (213) 740-5376, maxworth@usc.edu

Objectives: To perform a three-dimensional experimental investigation into the spatio-temporal dynamics of miscible porous media flows under the coupled effects of permeability heterogeneities, mobility contrast and gravitational segregation. Comparison with numerical simulations to be carried out at the University of California-Santa Barbara by collaborator Ekert Meiburg. .

Project Description: The role of heterogeneities, gravity override, and mobility contrast will be assessed in a three-dimensional, simulated porous medium in a 1/4-5 spot geometry . A rectangular parallelepiped will be filled with glass or plastic spheres and an interstitial, viscous fluid introduced to fill the box completely. The fluid will be partially displaced by pumping a less-viscous, dyed fluid, at a known flow-rate, into one corner of the box and removing interstitial fluid at the opposite corner. The displacement will be observed by traversing the box, at various levels, with a laser light sheet and video taping the movement of the dyed front. A close index-of-refraction matching between spheres and fluid is essential for the success of this technique. The results will be compared with detailed numerical computations being performed at the University of California-Santa Barbara by a group led by Professor Eckart Meiburg.

Results: Since the start of the project on 9/15/00 we have tried various combinations of fluid and sphere material to find a suitable refractive index match. So far this has been of limited success due to lack of manpower at this early stage of the project. We plan to hire a post-doctoral fellow by 3 or 4/01 to carry out this and the other experimental tasks on a full-time basis. To test other aspects of the experimental technique we have run a series of experiments in a Hele Shaw cell geometry. These results will be supplemented and presented at the annual meeting of the APS-DFD in the fall of 2001.

STANFORD UNIVERSITY

Department of Geological and Environmental Sciences
Stanford, California 94305-2115

Grant: DE-FG03-93ER14347

Metal Ion Sorption at Oxide Surfaces and Oxide-Water Interfaces: Spectroscopic Studies and Modelling

*Gordon E. Brown, Jr. and George A. Parks, (650) 723-9168, fax (650) 725-2199,
gordon@pangea.stanford.edu*

Objectives: This project concerns chemical interactions between metal ions in aqueous solution and oxide surfaces representative of those found in the Earth's crust. These “sorption” reactions partition the metal between fluid and solid phases and must be understood at a molecular level to develop both quantitative understanding of the geochemistry of mineral surfaces and the macroscopic models required to predict the fate of contaminants in earth surface environments. Our objectives are (1) to characterize sorption reactions by determining composition, molecular-scale structure, and bonding of the surface complexes produced using direct sorption measurements, synchrotron-based x-ray absorption fine structure (XAFS) spectroscopy and x-ray standing wave fluorescence spectroscopy, x-ray photoelectron spectroscopy (XPS), and UV/Vis/IR spectroscopy; (2) to investigate how these reactions are affected by the solid surface, the composition of the aqueous solution, the presence of simple organic ligands containing functional groups common in more complex humic and fulvic substances, the presence of microbial biofilms, and time; and (3) to develop molecular-level and macroscopic models of sorption processes. In FY 2000 we made good progress in each of these areas and continued our grazing-incidence XAFS and X-ray standing wave (XSW) studies of the interaction of heavy metals with mineral surfaces and with biofilm-coated alumina and goethite surfaces. In addition, we have used the results of our model system studies to help determine the speciation of heavy metals and metalloids in contaminated natural systems.

Project Description and Results: (1) *Pb(II) sorption on single crystal hematite surfaces:* We have continued our grazing-incidence (GI) XAFS studies of metal ions on single crystal metal oxide surfaces in order to provide more detailed information on sorption complexes than is possible using more conventional XAFS studies of sorbates on high surface area powdered sorbents. Pb(II) was found to adsorb on hematite (0001) and (1-102) surfaces as inner-sphere surface complexes. The predominant species at the experimental conditions used in this study is a multinuclear Pb adsorption complex. XANES and EXAFS analysis suggest the local structure of adsorbed Pb(II) to be a distorted trigonal pyramid of oxide and/or hydroxide ligands, some of which are part of the hematite surface. These results suggest that Fe₂O as well as FeOH, and Fe₃O surface sites can coordinate Pb(II), and in general support of the hematite surface bond-valence model proposed by our earlier work on Pb(II) sorption on iron hydroxide surfaces (Ostergren et al., 2000).

(2) *Long-Period XSW Studies of Pb(II) and Se(IV) in the Electrical Double Layer at Crystal Surfaces:* During the past year we completed an XSW study of Pb(II) and Se(IV) sorbed to single-crystal α -Al₂O₃

(0001) and (1-102) surfaces. Experimental XSW fluorescence yield data for Pb(II) and Pb(II)/Se(VI) adsorption on α -Al₂O₃ (0001) and (1 $\bar{1}$ 02) surfaces under *in situ* conditions were collected and analyzed. XSW results for Pb(II) uptake (at [Pb] = 6 to 600 μ M) on the (1-102) and (0001) surfaces of α -Al₂O₃ in the absence of Se(VI) confirm that the (1-102) surface has an overall higher affinity for Pb(II) uptake than the (0001) surface at pH = 4.5. The presence of Se(VI) at 600 μ M appears to result in a significant negative surface charge on the α -Al₂O₃ (1 $\bar{1}$ 02) surface, but only exerts a small influence at the (0001) surface. The observed reactivity differences are consistent with the differences in the surface structures of the hydrated α -Al₂O₃ substrates determined in separate crystal truncation rod diffraction experiments.

(3) *Grazing-Incidence XAFS Studies of Zn(II) Sorption on Alumina*: Grazing-incidence XAFS was used to study the sorption of Zn(II) on two crystallographically distinct surfaces of highly polished alumina single crystals as a simplified analog for metal ion sorption on natural aluminum-(hydr)oxides. Experiments were performed both *in-situ* (in contact with bulk solution) and *ex-situ* in a humidified N₂ atmosphere. The identification of an Al shell at roughly 3 Å in all samples indicates that Zn(II) binds as an inner-sphere complex on both the (0001) and (1-102) alumina surfaces. The first shell Zn-O distances suggest that Zn is in four-fold coordination with oxygen in the *in-situ* samples. However, sample drying appears to have induced the formation of polynuclear surface complexes with first shell Zn-O distances closer to values expected for six-fold coordination. These results are similar to those we obtained in an earlier DOE-supported study of Zn(II) sorption on high surface area alumina powder, but provide additional details about the most likely sorption site geometries.

(4) *EXAFS Determination of the Chemical Speciation and Sorption Processes of Zn in Natural Systems*: We have used XAFS spectroscopy, μ -XRF, SEM, Rietveld x-ray diffraction analysis, and selective chemical extractions to study the molecular-scale speciation of Zn in two smelter-impacted soils sampled near one of the largest Pb and Zn processing plants in Europe located in northern France about 50 km south of Lille. The tilled and wooded soils chosen for study differed in Zn concentration (\approx 600 and 1400 mg/kg, respectively), soil pH (7.5 and 5.5, respectively), and organic matter content (1.5 and 6.4 wt. % TOC, respectively). In both soils, the occurrence of Fe- and Zn-rich (up to 10 wt. % Zn) slag particles ranging in size from a few μ m to a few mm, was shown by μ -SXRF elemental mapping of soil thin sections as well as by SEM and chemical analysis of different soil size fractions. For both soils, XRD analysis of the dense coarse fraction, which contains up to 10 wt. % Zn, revealed the presence of a minor amount (1-1.5 wt. %) of crystalline ZnS (sphalerite and wurtzite). In this fraction, EXAFS data showed that Zn is mainly incorporated in tetrahedral sites of a magnetite-franklinite solid solution.

The clay fraction (< 2 μ m) represents the largest pool of Zn in both soils, with 77 and 62 % of the total Zn in the tilled and wooded soils, respectively. However, XRD was not able to detect any Zn-bearing phases in this fraction. Comparison of Zn K-EXAFS data of untreated and chemically treated samples from the bulk (< 2 mm) and the clay (< 2 μ m) soil fractions with Zn K-EXAFS data from more than 30 model compounds suggests that Zn is present in the following chemical forms: (i) Zn outer-sphere complexes, (ii) Zn-organic matter inner-sphere complexes, (iii) Zn/Al-hydrotalcite (Zn/Al-HTLC), (iv) phyllosilicates in which Zn is present in the dioctahedral layer at dilute levels, and (v) magnetite-franklinite solid solutions inherited from the smelting process. The presence of exchangeable Zn outer-sphere complexes and of Zn inner-sphere complexes on organic matter is indicated by the relative increase of second-neighbor contributions in the EXAFS RDFs after chemical treatments with 0.01 M

CaCl₂ and 0.1 M Na₄P₂O₇. The occurrence of Zn/Al-HTLC is demonstrated by the persistence of a Zn-Zn pair correlation at 3.10 ± 0.04 Å (i.e., edge sharing ZnO₆ octahedra in the trioctahedral layer structure) in EXAFS data of Na₄P₂O₇ treated soil samples and its disappearance after treatment with 0.45 M HNO₃. This latter treatment also revealed the occurrence of Zn-bearing phyllosilicates by two Zn-Mg/Al/Si pair correlations at 3.05 ± 0.04 Å and 3.26 ± 0.04 Å and of magnetite-franklinite solid solutions by a Zn-Mn/Fe/Zn pair correlation at 3.50 ± 0.04 Å. Significant changes in the relative proportions of the different forms of Zn between the two soils explain their different responses to chemical treatments and emphasize the relationships between solid state speciation and mobility of Zn in soils.

STANFORD UNIVERSITY

Geophysics Department
Stanford, California 94305-2215

Grant: DE-FG03-99ER14933

Inversion of multicomponent seismic data and rock physics interpretation for evaluating lithology, fracture and fluid distribution in heterogeneous anisotropic reservoirs

G. M. Mavko, (650) 723-9438, fax (650) 723-1188, mavko@stanford.edu; Francis Muir

Objectives: Conduct theoretical investigations into the effects of fluids and fractures on anisotropic elastic constants, and consequent constraints on lithology that may be obtained from seismic parameters.

Project Description: Seismic anisotropy, now widely recognized as a common feature of most subsurface formations, may lead to significant distortions in conventional seismic processing, such as errors in velocity analysis, mispositioning of reflectors, and misinterpretation of the amplitude variation with offset (AVO) response. Seismic anisotropy can arise from aligned fractures, stress-induced anisotropy, and intrinsic rock fabric anisotropy. Furthermore, geophysical characterization of fractured reservoirs via their elastic anisotropy is an extremely important economical problem, in particular for the continental United States. In tight formations, which can include sandstones, shales, carbonates, and coal, often the only practical means to extract fluids is by exploiting the increased drainage provided by fractures. The practical difficulties that must be overcome before effectively using these fractures include: Locating the fracture zones, determining the position, orientation, spatial density, and connectivity of fractures, and characterizing the spatial relationships of fractures to other reservoir heterogeneities which might enhance or inhibit the fluid flow. It is also important to understand the similarities and differences between fracture anisotropy and stress-induced anisotropy. Stress-induced anisotropy is especially important for less consolidated sediments. In this project, we are developing theoretical models to describe anisotropy in sediments and rocks. Fluids play an important role in the anisotropy. The presence of fluids is a key interpretation problem for the oil and gas industry, in amplitude-*versus*-offset analysis and in fluid substitution modeling using Gassmann's equations.

Results: A major portion of our activity this year was focused on laboratory measurements of the signatures of stress-induced velocity anisotropy. Details of the work are given in the attached paper. We give a brief summary of the results here.

Acoustic properties of rocks and soft sediments are commonly measured under hydrostatic pressure in the laboratory. However, the stress fields in the Earth are generally anisotropic. Moreover, the mechanical properties of sands are sensitive to the stress field and can drastically affect the borehole stability, and lead to shallow water flows, compaction, and subsidence. Despite these facts, there is a void in the literature about how to extrapolate acoustic measurements in sands under hydrostatic pressure to more realistic borehole and field stress conditions

As most of the acoustic measurements in rocks are measured in hydrostatic conditions and there is non-

studied equivalence of hydrostatic pressure and polyaxial stress experiments, one goal of our project is to compare compressional velocities in sand using hydrostatic and polyaxial apparatus. In order to find the equivalence between these apparatus, we simulate hydrostatic conditions in the polyaxial apparatus. For instance, we designed and implemented a quasi-hydrostatic stress test that consists in placing a sample under three orthogonal stresses of same magnitude.

We measured V_p under hydrostatic and quasi-hydrostatic stress conditions. We found that our sand samples had depositional fabric anisotropy that is evidenced in the velocities of a quasi-hydrostatic stress test. We attribute this effect to layering perpendicular to the direction of raining grains (sedimentation). In addition, we compare the results with a previous uniaxial strain test in the same sand. This comparison corroborates that the acoustic anisotropy (just mentioned) is not due entirely to stress. Moreover, we compare our measurements with hydrostatic data made in same sand at lower frequency, and also with other data made in finer sand at lower frequency. Our results indicate that velocities measured under hydrostatic pressure are faster than the velocities measured under polyaxial stress. Nevertheless, further study is needed.

Plans for next year: During the next year we will continue our laboratory work on the sources of anisotropy in soft sediments, with a series of experiments on uniaxial compaction under a variety of conditions. We will also use the results to theoretically explore the implications of fabric and stress-induced anisotropy on interpretation of seismic data. Most analysis at present is done assuming isotropic rock and sediment models. Preliminary results suggest that ignoring anisotropy can introduce systematic errors into interpretation of the seismic signatures of pore fluid and stress changes.

We will also continue with work on the rock physics signatures of fractured rock, and fluids, attempting to develop procedures for exploring the realistic range of conditions that might be encountered in a given field site.

STANFORD UNIVERSITY

Geophysics Department
Stanford, California 94305-2215

Grant: DE-FG03-86ER13601

Porous rocks with fluids: Seismic and transport properties

Amos Nur, (650) 723-9526, fax (650) 723-1188; anur@stanford.edu; Jack Dvorkin

Objectives: In this study we develop numerical methods for simulating physical experiments conducted in the lab on a rock sample. The experiments include fluid flow (for permeability determination); electrical flow (for resistivity determination); and elastic deformation (elastic-wave velocity and strength). The new algorithms are combined into a Virtual Rock Physics laboratory that also includes additional tools for image processing and statistical reconstruction of 3D pore topology. The main current emphasis is on permeability because it is one of the most important reservoir parameters and one of the most difficult to obtain in-situ. We also conduct laboratory measurements of the elastic-wave velocity as well as mechanical strength in methane hydrate and ice samples at varying temperature and stress.

Project Description: 1. Virtual Rock Physics Laboratory. We apply new optimized Lattice-Boltzmann algorithm to simulating viscous fluid flow in a realistic pore space. The detailed 3D pore space topology description comes from CT-scanned sandstone samples. We also use a statistical tool to recreate 3D topology from a 2D slice of the data. We explore how various microscale features (clay, diagenetic cement) affect permeability and how permeability varies due to diagenetic processes.

2. Measuring the mechanical properties of methane hydrate and ice. We synthesize methane hydrate from ice directly in the measurement cell by immersing the ice into a methane atmosphere. Simultaneous P- and S-wave velocity and mass measurements allow us to calculate the effective elastic moduli of the hydrate. Similar data are obtained on pure ice samples. We also record the samples' resistance to compaction which implies the strength of methane and ice. The results are important for mapping methane hydrate in situ from seismic profiling and assessing marine sediment stability.

Results: 1. Virtual Rock Physics Laboratory. We have combined a microscope, digital camera, and personal computer into a single setup to take a rock microimage, digitize and image-process it, statistically recreate 3D pore space, and simulate viscous fluid flow through the 3D pore space. We also obtained 3D pore space topology from a direct CT scan of a sandstone sample. Our calculations show that permeability directly calculated on a real 3D pore space topology matches the physically measured permeability. Also, the permeability of a statistically recreated sample is close to that calculated on the real 3D pore space. We have optimized the numerical calculator to drastically increase the speed of computations. It takes now only several minutes on a laptop PC. We have numerically altered the sample to introduce clay particles and contact cement. Dispersing clay particles in the pore space acts to drastically reduce permeability without significantly affecting porosity. We have also conducted numerical experiments on calculating the relative permeability by simulating a two-phase flow in a

realistic pore space. As a result, we have obtained realistic relative permeability curves.

2. Measuring the mechanical properties of methane hydrate and ice. Based on simultaneous compressional and shear wave speed measurements in ice and pure methane hydrate, we derive the pressure and temperature dependence of a suite of elastic properties for both materials. The temperature range is from -20 to -5 degrees Celsius for ice and from -15 to 15 degrees Celsius for the hydrate. The pressure range for ice is from 22 to 33 MPa and it is from 28 to 61 MPa for methane hydrate. The elastic-wave properties of ice and methane hydrate are very similar. However, there is a dramatic strength difference between the two materials. Whereas only 41 MPa applied for a few hours is required to fully compact granular ice, 103 MPa applied for several days is required to compact methane hydrate.

STANFORD UNIVERSITY

Department of Petroleum Engineering
Green Earth Sciences Building
367 Panama Street, Rm. 65
Stanford, CA 94305-2220

Grant: DE-FG03-99ER14983

Diffusion of CO₂ during Hydrate Formation and Dissolution

Franklin M. Orr, Jr., (650) 723-2750, (650) 725-6566, fmorr@pangea.stanford.edu

Objectives: The goal of this research is to understand what factors control hydrate formation and dissolution. Specific objectives are to: (1) determine mechanisms of hydrate film growth, (2) measure the rate of hydrate growth, (3) determine solute diffusivity through hydrate, and (4) measure hydrate dissolution rates.

Project Description: Mechanisms of hydrate formation and dissolution will play key roles if direct disposal of CO₂ in the oceans is undertaken. When CO₂ is released at depths below about 400 m, hydrate forms at the interface of the CO₂ and water. Formation of a hydrate film reduces the rate of dissolution of the liquid CO₂ in the surrounding seawater. Better definition of the mechanisms and rates of hydrate formation and dissolution is needed to determine transport of released CO₂ and to allow design of release facilities limit environmental impact of the CO₂.

Hydrate film growth was measured in a controlled setting in a 3 mm ID capillary tube. An interface between CO₂ and water was positioned in the capillary, and the temperature and pressure are adjusted to conditions at which hydrate forms. The thickness of a plug of hydrate that forms between the liquid CO₂ and water was then measured as a function of time.

Results: Significant difficulties were encountered in creating hydrate plugs repeatably. Simply cooling the capillary tube contents at the experimental pressure did not produce hydrates in a reasonable length of time, nor did starting with ice in the capillary and warming to the experimental temperature. In the method finally adopted, the capillary tube was filled with water, and CO₂ at the experimental pressure and temperature was introduced into the tube, displacing the water. A very thin film of hydrate formed where water wetted the capillary walls, and a plug of hydrate then formed and grew at the water/CO₂ interface in the center of the capillary. Fingers of hydrate sometimes formed along the edge of the capillary, an indication that growth of the hydrate film was not necessarily uniform in this geometry. Given the uncertainty in the uniformity of the hydrate film the diffusion coefficients reported below should be taken as upper bounds for the diffusion coefficient of CO₂ through hydrate. Given the difficulties in the creation of uniform hydrate plugs, it was not possible to measure dissolution rates reliably with this technique.

Experiments was performed at a temperature of 1° C and pressure of 5.9 MPa. Results of measurements of film growth were obtained. While there is some scatter, the measured film thickness is roughly linear

in the square root of time. In all the experiments film growth was observed only on the water side of the hydrate plug, an observation that is consistent with much faster transport of CO₂ molecules through hydrate cages than transport of water molecules through the hydrate lattice. Any formation of hydrate on the CO₂ side of the hydrate film (which would require water molecules to diffuse across the hydrate plug) was too slow to be observed on the time scale of the measurements. Thus, transport of CO₂ across the hydrate dominates the formation of new hydrate at in a water/hydrate/CO₂ system.

Diffusion coefficients for CO₂ through the hydrate were estimated to be 6×10^{-7} - 4×10^{-6} with most results in the range 2×10^{-6} - 4×10^{-6} cm²/s, about an order of magnitude lower than the diffusion coefficient for CO₂ through liquid water (2×10^{-6} cm²/s) but about four orders of magnitude bigger than typical values for diffusion through solids. These values indicate that formation of a hydrate film will reduce the rate of dissolution of liquid or vapor CO₂ into water below the rate observed when hydrate is absent. Thus, bubbles of CO₂ rising through the water column will survive longer if the CO₂ is released at depths for which the pressure is high enough and the temperature low enough that hydrate will form.

STANFORD UNIVERSITY

Department of Geological and Environmental Sciences
Stanford, CA 94305-2115

Grant: DE-FG03-94ER14462

Structural Heterogeneities and Paleo-Fluid Flow in an Analogue Sandstone Reservoir

D. D. Pollard, (650) 723-4679, fax (650) 725-0979, dpollard@pangea.stanford.edu

A. Aydin, (650) 725-8708, fax (650) 725-0979, aydin@pangea.stanford.edu

Website: <http://pangea.stanford.edu/geomech/index.html>

Objectives: To develop conceptual models and predictive tools for the spatial distribution of permeability in subsurface sandstone aquifers and reservoirs as determined by structural heterogeneities.

Project Description: We are carrying out an integrated research plan to map structural heterogeneities (deformation bands, compactive and dilatant deformation bands, joints, sheared joints, and faults) in the Aztec sandstone, at Valley of Fire (NV), to develop conceptual and mechanical models for their evolution, and to understand their effects upon groundwater and hydrocarbon flow in an analog reservoir. The goals of the present project are three fold: (1) Chemical characterization of colored alteration bands, the signature of the ancient chemically reactive flow systems, within the eolian sandstone. (2) Fault zone permeability upscaling based on the field data and fluid flow modeling and representation of fault permeability in reservoir simulation models. (3) Characterization and modeling of compaction bands in sandstone and their fluid flow properties.

Results: Three sub-projects are summarized below:

(1) Paleo-hydrologic and geochemical fieldwork at Valley of Fire State Park during the last year was focused on: 1) sampling across the diagenetic alteration zones for thin section and mineralogical analyses; 2) characterization of paleo-fluid flow indicators; and 3) preliminary mapping of paleo-fluid flow indicators. Based on thin section petrography, we distinguish thin hematite coatings on sand grains (uniform medium-red alteration colors) from coarser grained pore-filling hematite (purple and yellow striped alteration colors). We interpret the uniform red alteration as early diagenetic and the striped colors as the result of bleaching and partial remobilization of iron oxide under deep burial and late vadose conditions. Paleo-fluid flow indicators include oxidation/reduction haloes around concretions and adjacent to deformation bands, and the lobate/cuspate shape of reduction and oxidation fronts. Based on oxidation/reduction patterns we determined the paleo-flow direction for an approximately 100 m² area within the “layered orange and white” unit. Interpreting these patterns as the result of reducing brines, we obtained a SW-directed up dip paleo-flow direction. The regional distribution of striped colored and partly bleached units between structurally lower and upper homogeneous red units is consistent with regional-scale up dip migration of reducing hydrocarbon-related brines through the Aztec Formation.

(2) Representation of fault zone permeability and their representation in reservoir flow models

Due to limitations in the numerical code, earlier work used a multi-step approach to solve for block-equivalent permeability: Consequently we calculated the permeability of the domain of interest through a series of coarsening grids. Using a new and better-suited numerical code, we solve for the bulk permeability in one step, thereby improving the accuracy and efficiency of the calculations. We have determined that the use of periodic boundary conditions is inappropriate for modeling rock with fractures that are continuous over length scales greater than the domain of interest. The use of no-flow boundary conditions retains fracture-flow continuity and better reflects the field observation. We have extended this work by applying the calculated block-equivalent permeability to faults in reservoir-scale flow simulations. By analyzing faults with different slip magnitudes, we were able to produce a relationship between up-scaled fault permeability and fault slip. We have compared three simulation scenarios with that used in standard oil-field practice in which faults are represented as tunable, single-permeability features. In the simplest model scenario, we find no significant difference in flow response between the two methodologies. The two more complex cases, however, displayed significant differences with regard to breakthrough time and liquid production rates. These differences are attributed to the representation of faults with variable slip and the corresponding variable fault -normal and -parallel permeability.

(3) Compactive deformation bands in sandstone: mechanics of compressive failure in porous, granular materials

This new research initiative has grown out of the results of several projects conducted previously under this grant that demonstrated the potential for low permeability deformation bands (DBs) to substantially impede fluid flow through an otherwise porous rock. In particular, the technique we developed to calculate effective permeability tensors for use in reservoir and aquifer flow simulations based on any given repetitive DB pattern led naturally to two fundamental questions: (1) How do these DB patterns develop? and (2) Can they be predicted in the subsurface?

Over the past year, we have focused on compactive deformation bands (CDBs), which exhibit limited primary shearing and constitute the volumetrically dominant DB type in the Valley of Fire. We have collected highly targeted data from field observations, measurements and thin-section analyses of CDBs in order to determine the fundamental mechanics governing their propagation and pattern development. Based on the results to date, we believe that CDBs initiate in response to localized compressive stress concentrations and then propagate as brittle “anti-cracks” in a nominally linear elastic medium. The inelastic, grain-scale processes of compaction, pore loss and strain hardening that occur in the wake of a propagating tip result in the stiff, relatively impermeable “inclusion-like” feature recognized in the field as a CDB. Thus, we hypothesize that the systematic arrays of CDBs seen in the field developed as a consequence of the mechanical interactions of their propagating tips with each other and with their surroundings in response to a tectonically derived ambient stress field. We are encouraged that pursuing this line of research will greatly enhance our ability to interpret CDB arrays in the subsurface as functions of measurable mechanical parameters and realistic regional stress histories.

STANFORD UNIVERSITY

Department of Geophysics
Stanford, California 94305-2215

Grant: DE-FG03-99ER14962

Coupled Fluid Deformation Effects in Earthquakes and Energy Extraction

P. Segall, (650) 725-7241, fax (650) 725-7344, segall@stanford.edu

Website: <http://kilauea.stanford.edu>

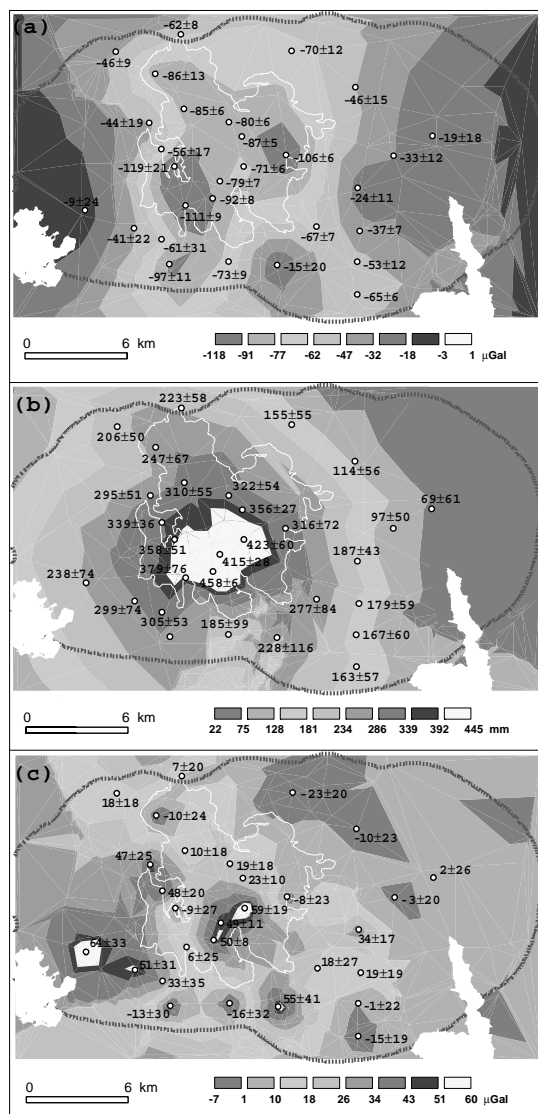
Objectives: To better understand the effects of coupled deformation and fluid flow in geologic systems.

Project Description: The focus of current research has been to determine whether recent uplift and seismicity in the Long Valley volcanic/geothermal area can be demonstrated to result from magmatic as opposed to hydrothermal processes. Long Valley has experienced nearly 1 meter of uplift and several tens of thousands of earthquakes in the last two decades. Repeated micro-gravity measurements combined with vertical displacement data can discriminate between magmatic intrusion, and thermal expansion or pressurization of the caldera hydrothermal system.

Results: We analyzed the source of inflation of Long Valley caldera by combining geodetic and micro-gravity data. Uplift from GPS and leveling, two-color EDM measurements, and residual gravity change determinations were used to estimate the intrusion geometry, assuming a vertical prolate ellipsoidal source. We surveyed 44 existing leveling monuments in Long Valley caldera in July 1999, using dual frequency GPS receivers. We found that the resurgent dome stood 74 ± 7 cm higher today than in 1975. To constrain the inflation source, we inverted two-color EDM and uplift data from the 1985-99 unrest period using spherical or ellipsoidal sources. We find that the ellipsoidal source satisfies both the vertical and horizontal deformation data, whereas the spherical point source cannot. The main source of deformation is a prolate ellipsoid located beneath the resurgent dome at a depth of 5.9 km (95% bounds of 4.9 to 7.5 km). This body is vertically elongated, has an aspect ratio of 0.475 (95% bounds are 0.25 to 0.65) and a volume change of 0.086 km³ (95% bounds are 0.06 to 0.13 km³). Importantly, we found that failure to account for the ellipsoidal nature of the source biases the estimated source depth by 2.1 km (35%), and the source volume by 0.038 km³ (44%).

We reoccupied the Long Valley gravity network twice, in the summer of 1998 (33 stations), and the summer of 1999 (37 stations). Before gravity data can be used to estimate the density of the intrusion, they must be corrected for the effect of vertical deformation (the free-air effect) and changes in the water table. We use geostatistical techniques to interpolate uplift and water table changes at the gravity stations. We find a volume change from 1982 to 1999 of 0.136 km³ and a density of around 1700 kg/m³. 95% confidence bounds of 0.105 to 0.187 km³ for the volume, and 1180 to 2330 kg/m³ for the density were determined using the bootstrap. Our results do not support hydrothermal fluid intrusion as the primary cause of unrest, and confirm the intrusion of silicic magma beneath Long Valley caldera. Failure to account for the ellipsoidal nature of the source biased the estimated source depth by 2.9 km (a

33% increase), the volume change by 0.019 km^3 (a 14% increase) and the density by about 1200 kg/m^3 (a 40% increase).



A) Gravity changes from 1982 to 1999 corrected for water table fluctuations, values in mgal, error is one standard deviation. B) Uplift at gravity stations between 1982 to 1999 estimated from GPS and leveling data. C) Residual gravity correcting for the free-air effect.

TEMPLE UNIVERSITY

Department of Chemistry
Philadelphia, Pennsylvania

Grant: DE-FG02 ER14644

Surface Chemistry of Pyrite: An Interdisciplinary Approach

*Daniel R. Strongin, (215) 204-7119, fax (215) 204-1532, dstrongi@nimbus.ocis.temple.edu;
Martin A.A. Schoonen, Department of Geosciences, State University of New York, Stony Brook,
NY; (516) 632-8007, schoonen@sbmpo4.ess.sunysb.edu*

Objective: The primary goal of this research program is to understand the microscopic aspects of pyrite oxidation. Our continuing research strategy is to understand macroscopic observations of pyrite reactivity with an atomic/molecular level view. The results of this research will lead to a better understanding how pyrite reacts in a range of chemical environments.

Project Description: The reactivity of pyrite in anoxic and oxic environments is being investigated by integrating aqueous geochemical and modern surface science techniques. The surface science techniques have generally operated in the ultra-high vacuum environment, but a recent emphasis has been to develop in-situ techniques to study the mineral surface on a microscopic level in the presence of an aqueous or gaseous phase.

Results:

Mechanism of Pyrite Oxidation

A remarkable finding in FY01 was that pyrite upon contact with O₂-free water produces hydrogen peroxide in solution. Trivalent Fe [i.e., Fe(III)], which is associated with the defect, is capable of oxidizing the water into a hydroxyl radical and a proton. This reaction and the subsequent formation of hydrogen peroxide can be represented by the following reactions: (1) $\text{H}_2\text{O} + \text{Fe(III)-FeS}_2 \rightarrow \text{OH}^\bullet + \text{Fe(II)-FeS}_2 + \text{H}^+$ and (2) $2\text{OH}^\bullet \rightarrow \text{H}_2\text{O}_2$

In subsequent experiments the existence of OH[•] directly after pyrite is immersed in water has been experimentally demonstrated. The formation of OH[•] through the interaction of pyrite with water provides a mechanism for the rapid oxidation of the S(-II) species associated with the defect and explains the instantaneous production of sulfate in XPS studies and in batch oxidation experiments from this laboratory. Research has also shown that the hydrogen peroxide concentration increases upon illumination of the pyrite slurry. This could be a result of a separate process in which a photoelectron/hole pair generated by capture of a photon reacts with water to form OH[•]. The hole, h⁺, can react with water and produce the OH radical (i.e., $\text{h}^+ + \text{H}_2\text{O} \rightarrow \text{H}^+ + \text{OH}^\bullet$)

Synthesis and reactivity of FeS₂ thin films

A major recent objective in this research program has been to synthesize atomically pure FeS₂ thin films. Natural pyrite or its pseudomorph marcasite are never pure FeS₂ due to substitution of iron and sulfur by related elements (Fe: Cu, Zn, Ni ; S: As, Se, Te); furthermore, many crystals contain mineral inclusions. A continued research effort has been in the area of thin film synthesis. These films make excellent model surfaces so that structure and reactivity correlations, a major goal of our entire research effort, can be established. In FY01 the reactivity of marcasite thin films were investigated in well-controlled gaseous mixtures of O₂ and H₂O and thin films of marcasite were deposited directly on to a ZnSe attenuated total reflection crystal so that in-situ studies of the marcasite-water interface could be studied.

Bi-layer forming lipids as oxidation suppressant

In FY01, the molecular level understanding developed from this research project was used to design an effective method to inhibit pyrite oxidation. Most suppression strategies to date have concentrated on encapsulating the pyrite surface with a mineral layer to prevent oxidants to interact with it or ligands have been added that combine with *aqueous* Fe³⁺ so that it does not adsorb onto the pyrite surface. These strategies typically often fail at low pH or they pose environmental problems themselves. In light of this concern, bilayer-forming lipids containing functional groups that we know bond strongly to the active sites on pyrite were investigated. Formation of the bilayers excluded water from the surface and protected the surface-lipid bonding. Hence, bonding of the lipid to the Fe(III) site (1) inhibited electron transfer between oxidant and pyrite surface and (2) excluded low pH water from interacting with the surface-lipid bond.

Streaming potential measurements on pyrite

In FY2001 a streaming potential apparatus was developed that allows the determination of the zeta potential, which is related to surface charge, on mm-size pyrite particles. Streaming potentials are the result of the displacement of charge in the diffuse double layer adjacent to a charged surface. The displacement of charge creates a potential that sets up a ionic return current through the solution. Pyrite, or any conducting material, represents a problem in that the return current can also pass through the bulk of the material. To derive meaningful streaming potential measurement, it is necessary to also determine the electrical conductivity of the pyrite and pyrite surface (surface conductance). Electrical conductivity measurements on clean pyrite and oxidized pyrite show a drastic increase in electrical conductivity after oxidation of the pyrite. This result is not only important for the interpretation of the streaming potential measurement, but it is also of interest to geophysicists working on the electrical properties of geomaterials.

THE UNIVERSITY OF TENNESSEE

Center for Environmental Biotechnology
Institute for Rare Isotope Measurements
10521 Research Drive, Suite 300
Knoxville, TN 37932

Grant: DE-FG02-01ER15159

Completion of Kr-81 and Kr-85 Analysis Development for Hydrogeology and Testing its Validity by Assessing Aquifer Recharge Rates.

N. Thonnard, (865) 974-9702, fax (865) 974-8289, nthonnar@utk.edu; L.D. McKay

Website: <http://web.utk.edu/~irim>

Objectives: (1) Implement system improvements identified earlier to Kr-85 RIMS analyses for hydrogeology, (2) validate the technique with standards of known Kr-85 activity, (3) measure Kr-85 in samples from a hydrogeologically simple, but well-characterized aquifer, and (4) apply Kr-85 to measure recharge in the outcrop region of a major confined aquifer serving a large metropolitan area.

Project Description: The development of the mass spectrometric-based analytical technique utilizing multiple isotopic enrichments and laser-based resonance ionization to measure the concentration of the rare Kr-81 and Kr-85 isotopes in hydrogeologic samples is being completed.

The analytical process consists of (1) collecting a groundwater sample, (2) degassing the water sample, (3) separating Kr from the recovered gases, (4) isotopic enrichment to reduce interfering isotopes by 10^5 , (5) a second isotopic enrichment of 10^4 , and (6) detection of the rare krypton isotope in a resonance ionization time-of-flight mass spectrometer. Modifications to the equipment and procedures, identified during a previous program, are being implemented to improve reliability, efficiency and accuracy.

A staged testing program of the complete system starts by verifying the analytical method with analyses of krypton samples of known Kr-85 activity. Analysis of Kr-85 concentration in samples collected from a very simple, well-studied aquifer, whose age/depth relationship is well-known, verify that reliable age-determinations are possible with this technique. Finally, samples are to be collected from the unconfined recharge region of a major confined aquifer for Kr-85 analysis to demonstrate that this isotope can be used to answer an important hydrogeologic question, the magnitude of recharge in a heterogeneous aquifer, which is a question that has been difficult to assess with current techniques.

Results: This project has only recently been initiated.

TEXAS A&M UNIVERSITY

Department of Petroleum Engineering, 3116 TAMU
College Station TX 77843-3116

Grant: DE-FG03-00ER15034

Time-Lapse Seismic Monitoring and Performance Assessment of CO₂ Sequestration in Hydrocarbon Reservoirs

Akhil Datta-Gupta, (979) 847-9030, fax (979) 845-1307; datta-gupta@tamu.edu), Richard L. Gibson, gibson@geo.tamu.edu); Bruce Herbert herbert@geo.tamu.edu

Objectives: The goal this project is to assess the feasibility of time-lapse seismic monitoring of CO₂ sequestration using coupled fluid flow, geochemical and seismic modeling. Concurrently we want to develop a formalism for the assimilation of static and dynamic data sources in the reservoir and quantification of uncertainty in performance predictions.

Project Description: We apply numerical modeling of both fluid flow (CO₂) and seismic wave propagation in a representative model of a sequestration site to quantify the changes in seismic reflections that might be observed in realistic applications. The very fast, but approximate, ray-Born seismic modeling algorithm facilitates rapid comparisons of model scenarios, including analysis of different phases of CO₂ and different formation rock properties. Changes in rock velocities caused by the variations in pore fluids are computed using the Gassmann's equation, and empirical equations based on laboratory data are used to model the dependence of velocities on pressure. Our approach combines rapid streamline-based fluid flow simulations with the high speed, three-dimensional seismic modeling. A critical component of performance assessment of a CO₂ sequestration project will be accurate characterization of reservoir properties such as porosity and permeability by integrating a wide variety of data sources. A second component of our research is to systematically incorporate all the static and dynamic data sources into reservoir models and characterize the uncertainty about physical parameters, in particular, porosity and permeability that control the performance predictions of fluid flow simulation models.

Results: We performed flow simulation followed by seismic modeling for both the liquid and supercritical fluid (SCF) phases of CO₂ to compare their influence on seismic data. These results show that the SCF will generally produce a larger change in seismic properties than liquid CO₂ because it has the larger contrast between its density and compressional wave velocity and the corresponding properties of brine. We have also examined the time-lapse amplitude variation with offset for both phases of CO₂, and the results show that this examination of the dependence of reflection amplitude on angle of incidence will also help to distinguish between the different phases of CO₂ in situ. For subsurface characterization, we have developed a hierarchical Bayesian approach to multiscale data integration using Markov Random Fields (MRF). Our method is computationally efficient and well suited to reconstruct fine scale spatial fields from coarser, multi-scale samples (e.g., based on seismic and production data) and sparse fine scale conditioning data (e.g., well data). We have applied our

approach to a field example that utilizes seismic amplitudes and well log data to reconstruct 3-D distribution of porosity conditioned to well and seismic data as shown below.

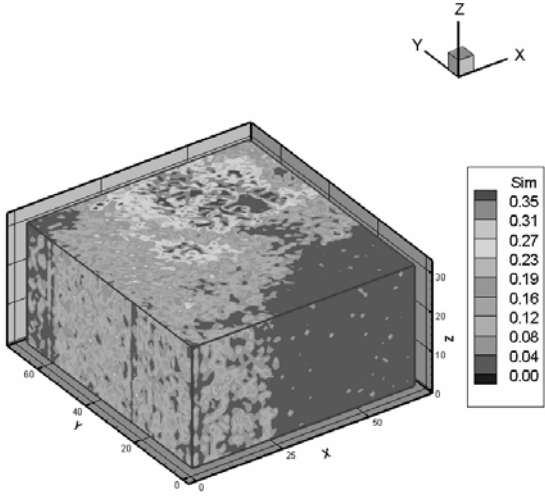
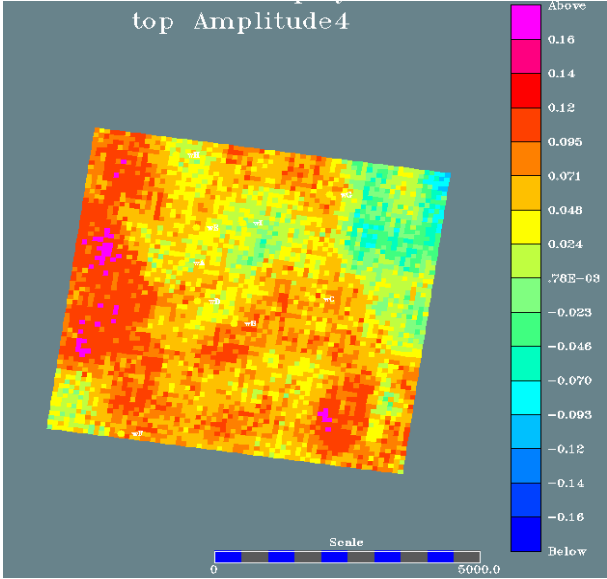


Fig. 1: A field application of fine-scale spatial modeling using Markov Random Field conditioned to well and seismic data: (a) seismic amplitude from the top of the reservoir (b) 3-D porosity distribution using Markov Random Field

TEXAS A&M UNIVERSITY

Center for Tectonophysics
Geology & Geophysics Dept.
College Station, TX 77843-3115

Grant: DE-FG03-ER14887

Fluid-Assisted Compaction and Deformation of Reservoir Lithologies

A.K. Kronenberg, F.M. Chester, J.S. Chester, and A. Hajash, (979) 845-0132, fax (979) 845 – 616, a-kronenberg@tamu.edu

Objectives: This research addresses the volumetric creep compaction, chemical reaction processes, and distortional deformation of quartz aggregates subjected to aqueous fluids at temperatures, effective pressures and stress states representative of diagenetic conditions. Specific goals include 1) determination of the transition from isochemical brittle deformation to fluid-assisted solution-transfer creep, 2) identification of the mechanisms of solution-transfer creep, and 3) evaluation of mechanical and chemical rate laws for clastic reservoir lithologies.

Project Description: The compaction and diagenesis of sandstones that form reservoirs to hydrocarbons depend on mechanical compaction processes, fluid flow at local and regional scales, and chemical processes of dissolution, precipitation and diffusional solution transport. Using an experimental approach, the rates of compaction and distortional deformation of quartz aggregates exposed to reactive aqueous fluids at varying stress states are under investigation. Pore fluid compositions and reaction rates during deformation are measured and compared with creep rates, and acoustic emissions and microstructures of specimens are used to determine the contributions of mechanical and chemical processes to deformation and pore structure evolution.

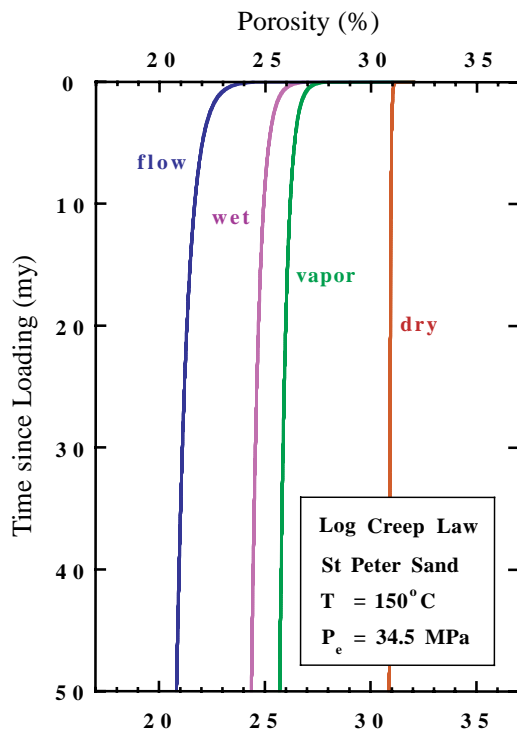
Results: During this year, we have brought to completion a number of studies of fluid-assisted compaction and deformation of porous, fluid-saturated quartz aggregates, based on short and long-term compaction and triaxial shortening experiments, acoustic emissions monitoring, and microstructural observations by backscattered SEM imaging. Through short-term hydrostatic and triaxial loading experiments, we have determined the critical envelope that defines those conditions of rate-insensitive grain crushing of quartz aggregates. In long-term hydrostatic experiments at effective pressures well below critical conditions, we have measured the compaction creep of quartz aggregates under dry and wet conditions with initial volumetric strain rates of $> 10^{-8} \text{ s}^{-1}$ falling off logarithmically with time, with the lowest rates measured at $3 \times 10^{-10} \text{ s}^{-1}$.

Microstructural SEM observations and statistical measures of grain cracking combined with acoustic emission rates suggest that the principal deformation mechanism is fluid-assisted cracking rather than diffusive mass transfer processes over all conditions tested. Volumetric creep rates and acoustic emission rates correlate extremely well at low effective pressures and temperatures and both follow logarithmic transient laws over a wide range of time scales, from 10^2 to 10^7 sec. At higher effective pressures and temperatures, a secondary creep mechanism, which does not correlate with the occurrence

of acoustic emissions, begins to become important. This process could either be mass transport of silica from loaded grain contacts to free quartz-fluid interfaces or slow quasi-static crack growth, both of which are enhanced by the presence of a reactive fluid.

The creep compaction laws we have determined for fluid-saturated quartz aggregates at diagenetic temperatures and pressures have important implications for porosity reduction of natural sands during burial and the quality of hydrocarbon reservoirs. Assuming that the transient laws we have determined in the laboratory extend to longer, geologic times and lower strain rates, we predict that reactive fluids during burial have profound effects on brittle mechanical processes of porosity reduction (Fig. 1A). Little or no porosity reduction is predicted for dry sand, while porosity reduction by fluid-assisted cracking reaches ~11% when coarse quartz sands are subjected to percolating fluids over times of 50 my. According to our logarithmic creep laws, we predict rapid early rates of compaction followed by progressively slower compaction at constant temperature and load. However, as sediments are subjected to increasing temperatures and loads during burial, actual compaction curves will be influenced both by the transient creep laws and their sensitivity to these environmental parameters. If we assume a burial rate of 100m/my a geothermal gradient of 20°C/km, a simple, linear $\beta - P_e$ relationship, and an activation enthalpy for creep compaction of 70kJ/mol (that for subcritical, fluid-assisted cracking), we predict porosity-depth curves that resemble empirical relations observed for sandstone reservoirs (Fig. 1B).

A)



B)

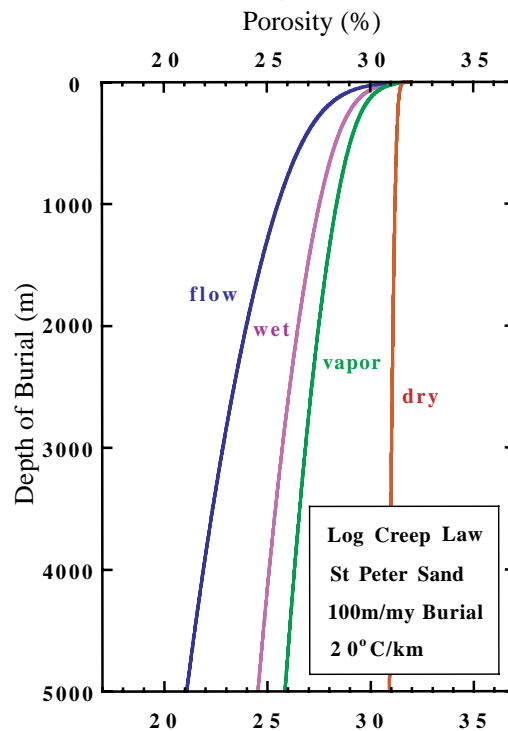


Figure 1: Predicted porosity reduction based on experimentally determined logarithmic creep law for fluid-saturated quartz aggregates (A) extrapolating to geologic times at the experimental temperature and pressure, and (B) extrapolating assuming a linear $\beta - P_e$ relation, an activation enthalpy H^* of 70 kJ/mol, and a natural depositional loading rate and geothermal gradient.

TEXAS A&M UNIVERSITY

Texas Engineering Experiment Station
College Station, TX

Grant: DE-FG03-00ER15033

Experimental and analytic studies to model reaction kinetics and mass transport of carbon dioxide sequestration in depleted carbonate reservoirs

John W. Morse, (979) 845-9630, fax (979) 845-9631, morse@ocean.tamu.edu ; Daulat Mamora

Objectives: 1) to determine and model the reaction kinetics of dissolution of carbonate minerals in saline waters under temperature and pressure conditions approximating those in gas-bearing carbonate reservoirs; 2) study the displacement of natural gas by supercritical carbon dioxide, and 3) develop an integrated model for the sequestration of carbon dioxide in carbonate gas reservoirs.

Project Description: Sequestration of carbon dioxide in depleted gas reservoirs appears to be a viable option, with a possible economic spin-off from the recovery of significant gas reserves. At the elevated temperatures and pressures encountered in reservoirs, carbon dioxide behaves as a supercritical fluid. Under these conditions, little is known regarding the kinetics of calcite dissolution by carbon dioxide, diffusion of carbon dioxide in natural gas, and displacement of natural gas by carbon dioxide. This project is conducting research to better understand these phenomena through experimental determination of the reaction kinetics for calcite dissolution, coefficient of dispersion, and displacement mechanisms in respect to supercritical carbon dioxide at temperatures and pressures typically found in reservoirs. The requisite data will be used to develop a model for mass transport and reaction kinetics for the injection and storage of carbon dioxide in carbonate or carbonate-bearing depleted gas reservoirs.

Results: More than seventy "free-drift" experimental runs have been conducted that examine the influences composition, carbon dioxide partial pressure and temperature exert on the rate constant and reaction order of calcite dissolution in simulated brines. The dissolution is followed in an open-system by measurement of pH at fixed carbon dioxide partial pressure as a function of time where the carbon dioxide partial pressure is fixed by continually bubbling a carbon dioxide-nitrogen gas mixture into the reaction chamber. The reaction is allowed to proceed from extreme undersaturation to near equilibrium. Calibration of the pH electrode is accomplished by measuring the total alkalinity and total dissolved carbon at two points during the experiment while noting the reporting mV value at the time of sampling. Typically, samples were drawn before the addition of calcium carbonate and again at the completion of the run. The measured alkalinity and total carbon dioxide are then used to calculate pH values using the Pitzer model allowing for a two-point calibration of the electrode. The actual carbon dioxide partial pressure in the chamber can also be confirmed from these alkalinity and total carbon dioxide measurements. The rate of dissolution can be obtained by relating the change in pH to a change in total carbon dioxide that is then equivalent to a change in the calcium carbonate content of the solution. The various matrixes used in initial experiments have focused on three compositions of different calcium to sodium ratios and total dissolved solid content. These open-system "free-drift"

experiments have proved successful at 25.0 C at high carbon dioxide partial pressure (e.g., carbon dioxide partial pressure greater than 0.05 bar). Results have been interpreted using a general reaction rate equation in which a plot of the log of the reaction rate versus the log of one minus the saturation state yield a rate constant and reaction order. These in turn can be modeled as functions of the previously described physical and compositional variables.

Supercritical carbon dioxide displacement experimental runs were conducted at pressures ranging from 1000 to 3000 psig (7.0-20.8 MPa). Results show the stable displacement of methane by carbon dioxide, with relatively insignificant carbon dioxide dispersion (dispersion coefficient averages 0.01 cmsquared per minute). Probably the most important result is that methane recoveries at carbon dioxide breakthrough are very high, 73%-96% of initial methane volume in the cell. In the field this would mean that carbon dioxide sequestration in depleted gas fields would not only sequester carbon dioxide but also recover a significant amount of hitherto unrecoverable gas reserves that would help defray the cost of carbon dioxide sequestration.

UNIVERSITY OF TEXAS

Department of Geological Sciences
P.O. Box 7726, Austin, TX 78713-7726

Grant: DE-FG03-97ER14812

High-resolution temporal variations in groundwater chemistry: Tracing the links between climate, hydrology, and element mobility in the vadose zone

Jay L. Banner, (512) 471-5016, fax (512) 471-9425, banner@mail.utexas.edu

Website: <http://www.geo.utexas.edu/faculty/banner/>

Objectives: To evaluate the extent to which radiogenic and stable isotopic and trace element variations in speleothems and modern groundwater from the same aquifer provide a means to reconstruct temporal changes in groundwater geochemistry, flow routes, and corresponding climatic controlling processes.

Project Description: This study is using cave calcite deposits (speleothems) and modern groundwater samples to develop a new approach, integrating Sr, Nd, C, O, H and U-series isotope variations with other geochemical and hydrologic tracing tools, to provide 1) improved sensitivity in reconstructing temporal records of groundwater evolution, and 2) a new perspective on the links between climate variability, hydrology, soil evolution, and groundwater chemistry. An understanding of controls on the modern hydrologic system provides a framework within which to interpret the speleothem record. Groundwater, soils, rainfall, speleothem and aquifer rocks are sampled in selected catchments using low-contamination procedures, and analyzed by mass spectrometry. Two karst aquifers were selected for intensive study to achieve the aims of this project. Results presented below highlight our study of the Edwards aquifer.

Results: A comprehensive chronology for cave deposits (speleothems) from widely-separated caves across central Texas provides a 71,000-year record of temporal changes in hydrology and climate. Concordant ages were determined by the independent uranium-238/thorium-230 and uranium-235/protactinium-231 dating schemes. The growth rates of these deposits vary over nearly three orders-of-magnitude, with three periods of rapid growth from 71-60 ka, 39-33 ka, and 24-12 ka. These growth rate shifts correspond in part with global glacial-interglacial climatic shifts, and reflect the regional response of this hydrologic system to regional and global climate variability on orbital-forcing time scales. Within the modern Edwards aquifer system, we examine short-term variability in recharge water chemistry. Mass-balance modeling of Sr isotope and trace element (Mg/Ca and Sr/Ca ratios) variations indicate that variations in fluid compositions are predominantly controlled by: 1) vadose groundwater residence times, and 2) water-rock interaction with overlying soils and host aquifer carbonate rocks. The results indicate the fundamental control on recharge water chemistry by local compositional variations in soils.

THE UNIVERSITY OF TEXAS

Department of Geological Sciences
Austin, Texas 78712-1101 U.S.A.

Grant: DE-FG03-97ER14772

Thermohaline Convection in the Gulf of Mexico Sedimentary Basin, South Texas

*John M. Sharp, Jr., (512) 471-3317 or (512) 471-5172, fax (512) 471-9425,
sharp@mail.utexas.edu; Craig T. Simmons, School of Chemistry, Physics, and Earth Sciences,
Flinders University, Adelaide, South Australia, Craig.Simmons@es.flinders.edu.au*

Objectives: To evaluate thermohaline convection in the Gulf of Mexico Basin and other sedimentary basins as a mechanism for mass transport in geologic settings

Project Description: The research tasks were: 1) the selection and development of models of thermohaline convection and cross-formational diffusion; 2) evaluation of the evolution thermohaline convection above and within the overpressured zone; 3) modeling the effects of the hydrostratigraphic framework of the Gulf of Mexico Basin and its effects on thermohaline convection scenarios; and 4) evaluation of the effects of sediment heterogeneity, including fractures on free convection.

Results:

1. We selected the U. S. Geological Survey code SUTRA as the primary model and created simplified pre- and post-processors for the system and extensions for the graphics. We evaluated several models. SUTRA was found to be the most robust and also allowed us full access to the code. The initial set of simulations was completed by the end of November 1998.
2. These simulations documented the appropriate ranges of parameters for the processes that create the salinity inversions in the Gulf of Mexico Basin. This upwelling of brines into the permeable rocks creates lateral salinity variations and observed density inversions. These are largely responsible for the instability that creates thermohaline convection. In the Gulf of Mexico Basin, we infer that:
 - 2.1. Shale permeabilities below the top of overpressures, on geological time and spatial scales, are greater by an order of magnitude or more than above the overpressures. This is created by natural hydraulic fracturing.
 - 2.2. Salinity inversions do not appear to be maintainable for long ($>10^4$ years) in the extremely overpressured or the hydropressured zones.
 - 2.3. There exists a transition between diffusion and convection dominated solute transport. Free convection, at least in this setting, is not a simple "on off" process.
 - 2.4. The transition zone, between over pressures and hydrostatic pressures, is sufficient to arrest thermohaline convection in Gulf Coast sediments.
 - 2.5. The results demonstrate the process by which sedimentary basins become density stratified with geologic time.

3. The gathering of data on the hydrostratigraphic framework proved unexpectedly difficult. All existing stratigraphic interpretations are far too large in scale to be meaningful in modeling efforts and salinity data spatial distributions were both spotty and sparse. Shale permeability variations have never been documented, although petrographic and seismic data show significant heterogeneity. We resorted to numerical simulations of high permeability zones caused either by zones of microfractures or by facies changes. We recommend a detailed program of data gathering be attempted to provide the requisite details.

4. The model simulations show several significant results. These are, perhaps, the most interesting and intriguing results of this research:

4.1. Traditional Rayleigh Number criteria, commonly used to estimate whether or not a system will freely convect, are of questionable validity in this or similar settings.

4.2. The effects of permeability and salinity field heterogeneities can dominate the determination of a system's stability or instability. Hitherto, this has been rarely addressed. The onset and subsequent growth or decay of convective instabilities is intimately related to the style or structure of the heterogeneous porous media under consideration. Heterogeneity is important for two principle, but opposing reasons. Heterogeneity (*i*) serves as the triggering mechanism for the onset of instabilities, and (*ii*) is the most important factor controlling whether instabilities, once generated, will grow or decay.

4.3 Vertically continuous high permeability regions enhance growth conditions (e.g., vertical fracturing or conduits, sinusoidal horizontal conductivity distributions). The effects of fractures on thermohaline convection were evaluated, and we prepared a closed form analytical solution on this process. These calculations demonstrate that fracture sets with even minimal aperture are enough to dissipate salinity inversions. However, intermediate low permeability regions provide resistance to horizontal dispersive mixing. In lenticular or layered structures (e.g., stochastic distributions) increased variance and increased horizontal correlation in the permeability field create laterally extensive low permeability barriers to the vertical upflow and downflow necessary to maintain convective flow.

THE UNIVERSITY OF TEXAS at DALLAS

Center for Lithospheric Studies
P.O. Box 830688 (FA31)
Richardson, TX 75083-0688

Grant: DE-FG03-01ER15166

3-D sedimentological and geophysical studies of clastic reservoir analogs: Facies architecture, reservoir properties, and flow behavior within delta front facies elements of the Cretaceous Wall Creek Member, Frontier Formation, Wyoming

Janok P. Bhattacharya, (972) 883-2449, fax (972) 883-2537, janokb@utdallas.edu, George A. McMechan, (972) 883-2419, fax (972) 883-2829, mcmec@utdallas.edu

Objectives: The research will integrate outcrop, core, shallow subsurface Ground Penetrating Radar (GPR), Global Positioning System (GPS), and Laser Range Finding technologies in 3-D reservoir characterization of an ancient delta deposit, followed by modeling and flow simulation. We focus on deltaic sandstone because very few studies investigate the bed-scale facies architecture of deltaic depositional systems in outcrop, despite the economic importance of deltas in hydrocarbon production worldwide.

Project Description: In this study, we integrate outcrop sedimentology and shallow subsurface Ground Penetrating Radar (GPR) to image and map the 3D facies architecture of dipping, river-dominated delta front sandstones and mudstones in the Turonian Wall Creek Member of the Frontier Formation, in Wyoming. Regionally, the Wall Creek Member shows a mixture of different upward coarsening facies successions associated with distinctly different overlapping sandstone bodies separated by prodelta mudstones that form in different delta lobes. The southern lobe, which is the focus of our study, is about 15 m thick. It grades upward from burrowed to current rippled sandstones, interbedded with oyster-bearing mudstones, into structureless to flat stratified and ripple cross-laminated sandstones interpreted as delta front turbidites. Photomontages along depositional dip show inclined beds dipping southeast, in the same direction as paleocurrents, suggesting that they are delta front clinofolds.

We focus on sedimentology, core description and analysis, collection of multifrequency GPR, and construction of 3D petrophysical models. This research will establish the 3-D shape and extent of dipping delta front sandstones and mudstone interbeds that are potential flow barriers. This project is being completed in conjunction with a separately-funded research effort at LSU. Researchers there will take the 3-D models built by UTD to generate 3-D models of permeability and simulate the effects of geologic variability on fluid flow. This component of the investigation will examine correlation of radar and fluid transport properties, and gridding methods for geologically and geometrically complex delta-front strata, and "designed" sets of flow simulations.

Results: The focus of activity in this first project year was on initiating GPR acquisition and determining optimum GPR collection parameters. During a 10 days field season, 3 line-kilometers of 50 MHz GPR data were acquired and processed on a coarsely-spaced 2D grid of lines lying parallel and

perpendicular to depositional dip. Dip lines show offlapping clinoform beds with tangential bottomsets that match those observed in the outcrop. Strike-lines show mounded, lens-shaped geometries, and suggest that individual delta front bodies are about 0.5 km wide. This 2D grid is the basis for quantifying large-scale facies architecture typically not imaged by the relatively low resolution of 40Hz seismic data and will be used to site the 3D studies planned in summer of 2002. We also collected additional photographs of some newly-discovered delta front clinoform strata in the Wall Creek south of our initially proposed area. These have been scanned and digitally spliced together as photomosaics and will be the focus of additional effort in 2002.

TEXAS TECH UNIVERSITY

Department of Chemical Engineering
Lubbock, TX 79409

Grant: DE-FG03-99ER14932

Modeling of Mesoscale Phenomena During Sequestration of Carbon Dioxide in Porous Reservoirs

A. Graham, Texas Tech University, (806) 742-0451, fax (806) 742-355, agraham@coe.ttu.edu
M. Ingber, University of New Mexico, (505) 277-6289, fax (505) 277-157, ingber@me.unm.edu;
L. Mondy, Sandia National Laboratories, (505) 844-1755, fax (505) 844-825,
lamondy@sandia.gov

Objectives: The purpose of this program is to combine experiments, computations, and theory to make fundamental advances in our ability to predict transport phenomena in concentrated, multiphase, disperse systems, particularly when flowing through geologic media.

Project Description: Processes for the sequestration of carbon dioxide in porous reservoirs involve several components of multiphase flows. If hydraulic fracturing is used to develop local "sweet spots" (zones of high permeability), the flow and resulting distribution of the proppant can have a large impact on the subsequent sequestration process. Even without hydraulic fracturing, the creation of precipitates can drastically alter the characteristics of the porous formation itself. Furthermore, emulsions can form and fingering can take place at the supercritical CO₂/brine interface. In order to be of use in designing effective CO₂ sequestration processes, significant enhancements to currently available continuum-level suspension flow models are required. Both experimentation and high performance computing at the mesoscopic level are used to obtain microstructural information that is necessary for the development and refinement of the continuum models.

Results: The continuum models originally developed by Phillips et al. (1992) and Nott and Brady (1994) have been improved and implemented into a general-purpose finite element computer code. Results show good agreement with experimental measurements based on nuclear magnetic resonance (NMR) imaging in idealized three-dimensional flows (see Fig.) Normal stress contributions are modeled, which results in accurate predictions of suspended particle migration in curvilinear flows. The improved model also allows for non-neutrally buoyant particles and non-Newtonian suspending liquids.

Massively parallel computing has allowed particle level simulations, based on the boundary element method (BEM), with up to three thousand particles. Volume averaging of the stress tensor has been added to the codes to allow prediction of average macroscopically observed transport properties from particle scale simulations. These simulations lead to detailed information on individual particle and fluid motion that is unobtainable through experiments. For example, highly accurate transient calculations of collections of particles in nonlinear shear fields have demonstrated that particles in inhomogeneous shear fields migrate in the direction of the lower shear rate. This is, to our knowledge, the first explanation of this phenomenon from first principle physics. These very fundamental studies

are elucidating the fundamental physics that govern the particle transport phenomena in multiphase systems.

This work is complemented by experimental work to provide insights and benchmarks. A study of apparent particle slip in confined geometries has been performed. Due to the finite size of the particles, suspensions of particles form a boundary layer near containing walls. The walls impose an ordering of the particles that extends several particle diameters into the bulk suspension. In constrained geometries such as the small channels in porous media, this boundary layer can extend over the entire channel. NMR imaging is used to determine the mesoscale structure and falling and rolling balls are used to investigate the mechanical properties at locations ranging from the centerline to the walls of the containing cylinder. It was found that there exists markedly non-Newtonian wall effects in concentrated suspensions in which the volume fraction of particles is greater than 0.2. At these higher concentrations, wall effects are much larger and extend further into the suspension than in Newtonian fluids.

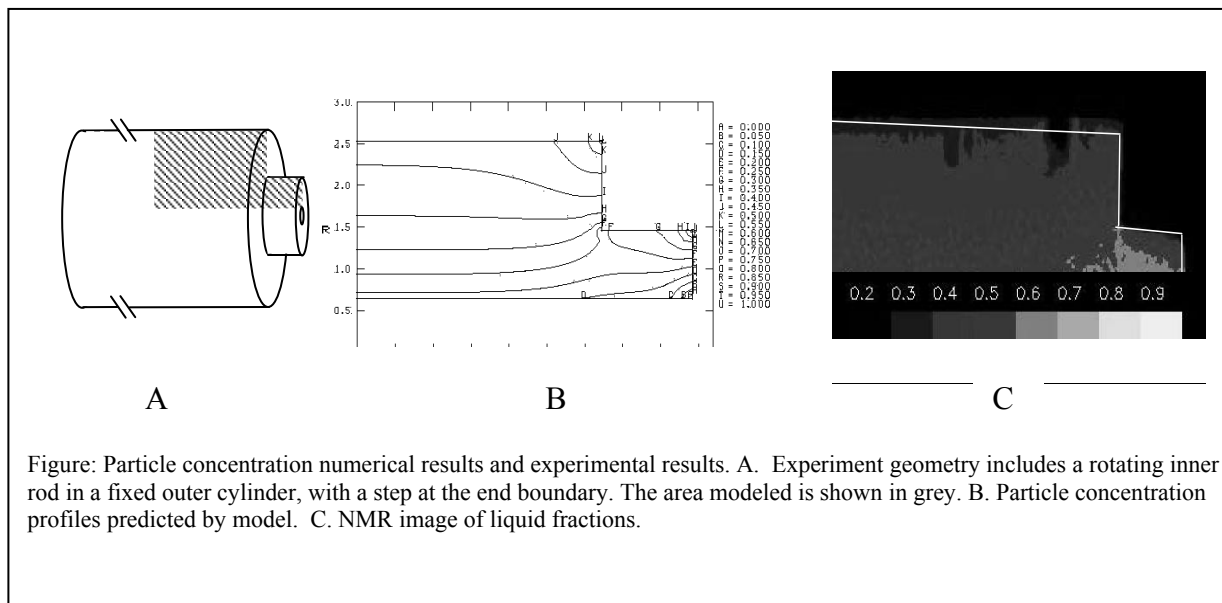


Figure: Particle concentration numerical results and experimental results. A. Experiment geometry includes a rotating inner rod in a fixed outer cylinder, with a step at the end boundary. The area modeled is shown in grey. B. Particle concentration profiles predicted by model. C. NMR image of liquid fractions.

UNIVERSITY OF UTAH

Department of Geology and Geophysics
135 S. 1460 S.
Salt Lake City, Utah 84112-0101

Grant: DE-FG03-00ER15043

A Comparative Study of the Feasibility for CO₂ Sequestration in Faulted and Fractured Sandstones in Eolian and Fluvial Deltaic Deposits

*Craig Forster, (801) 581-7162, (801) 581-7065, cforster@geofluid.esri.utah.edu; J. P. Evans
Utah State Univ, jpevans@cc.usu.edu*

Objectives: The goals of this integrated project are to complete a reservoir characterization of faulted Aeolian Jurassic Navajo Sandstone, and the Ferron Sandstone in Central Utah, in order to determine its feasibility as a long-term sequestration site for CO₂-charged fluids. This project is a collaboration between Utah State University and the University of Utah, and the following is a summary of the entire project work performed to date. The Utah State group is working on reservoir characterization issues, while the University of Utah group is examining the geochemistry of the system and will perform flow models of the candidate sites. In addition, we examine faults of the Colorado Plateau along which CO₂-charged springs, geysers, and travertine deposits are common, in order to evaluate how a CO₂ storage site might fail.

Project Description: We have used a multi-scale, multifaceted approach to determine the hydraulic structure of a fault zone in aeolian sandstone. We have shown that identifying the fault zone components and their properties are important in determining the bulk hydraulic properties of the fault zone. In this section, we summarise the key results from the Big Hole fault drilling project.

Results: By careful observations of core, minipermeameter tests, permeability tests at confining pressures, and an analysis of the bulk permeability of the faulted volume, we show that a four-component system best represents the structure of the Big Hole fault.

The host rock exhibits considerable variability in properties, despite being within one unit of aeolian sandstone. We have characterised four main sub-facies within the Navajo Sandstone, each with distinct petrophysical properties.

Deformation bands are zones of cataclasis, rarely more than a few mm's wide that accommodate mm's to cm's of slip.

Slip-surfaces are planes upon which the majority of the slip (strain) has been taken up within zones of deformation bands. At the surface, they are usually planes of parting; within our core samples, they may be planes of parting or mated surfaces. Thus, the permeability significance is poorly understood. They have previously been modelled as high permeability features.

The fault core consists of tightly packed deformation bands and highly crushed rock with a very low overall porosity (down to 1%, Shipton, 1999; Shipton and Cowie, in press). The width of the fault core

is highly variable both along strike and down dip, and cannot be correlated with the displacement on the main fault.

We estimate the transverse bulk permeability of the fault zone to be 7-57 md for the faults sampled by our boreholes. Sensitivity analyses shows that bulk fault zone permeability is most dependant on the thickness of the amalgamated deformation bands and slip surfaces that make up the fault core, suggesting that where present, such fault cores should be identified and thicknesses estimated for use in reservoir simulators. Our data also indicate that thicknesses of the fault core may vary *in situ*, and do not correlate with the amount of slip.

The fault core and fault zone cluster thickness exhibit no correlation with the amount of slip on the fault. However damage zone thickness, as determined from the first deformation band recognized in the hanging wall through the ends of the drill holes varies from 10 to 24 m, does correlate with the amount of displacement. For our data set, this relationship would predict that the fault should be about 4.7 cm thick at site 2 where the fault has 8 m of slip; and at site 1 with approximately 3 m of slip, the fault should be only 1.8 cm thick. Clearly, caution should be used when applying “global” data sets to specific cases, and it may be more accurate to restrict the use of such relationships to the specific rock types and geologic settings under consideration (Evans, 1990). We do not examine the effects of changes in continuity of the fault structure (*cf.*, Antonellini and Aydin, 1994; Hesthammer and Fossen, 2000). However, we do recognize the importance of variations in fault architecture parallel to the fault plane. The *in situ* flow tests show that such variations may significantly alter the macroscopic hydrologic properties of the fault zone.

We examine evidence for long-term leakage from natural CO₂ reservoirs in southeastern Utah. CO₂-charged springs and geysers are localised along fault zones throughout the region, and have deposited travertines, some of which may be as old as 200,000 years. These are either natural springs or springs that were induced by recent drilling. The faults cut siltstones, shales, and sandstones, and their outcrop appearance suggests they should be effective barriers to cross-fault flow (fine grained, clay-rich fault gouge). Abundant large calcite veins cut the faults, suggesting that fluid pressures in the past were high enough to rupture the faults. The spring waters are highly saline and high in Na, Cl, Ca, and dissolved CO₂. Modelling of the water chemistry indicates that the water is either saturated or supersaturated in aragonite, calcite, dolomite, fluorite and gypsum, all of which are observed in the veins along the faults, and that the water from both areas is likely to have come from organic decomposition of a sequence of marine evaporates at depth. Preliminary isotopic data from calcite veins show that the veins are highly enriched in ¹³C. This can only be explained if the veins have a fluid source in Palaeozoic marine rocks. The heavy δ¹³C values provide further evidence for thermal decomposition of organic material or development of methane. Structural analyses of the system show that the faults sole into Pennsylvanian salt beds 2-3 km deep. This suggests that the spring waters are sourced in Palaeozoic rocks and flow along the faults to the surface. Past evidence for rupture of the fault seals indicates that reservoir pressures may exceed lithostatic pressure, causing the reservoir to leak repeatedly over time. These data indicate that injection of CO₂ -rich fluids into geologic reservoirs must be carefully designed and monitored to avoid slow seepage or fast rupture to the biosphere.

UTAH STATE UNIVERSITY

Department of Geology
Logan, UT 84322-4505

Grant: DE-FG03-00ER15042

A Comparative Study of the Feasibility for CO₂ Sequestration in Faulted and Fractured Sandstones in Eolian and Fluvial Deltaic Deposits

J. P. Evans, (801) 797-2826, fax (801) 797-1588, jpevans@cc.usu.edu; Craig Forster, Univ. of Utah; cforster@geofluid.esri.utah.edu

Objectives: The goals of this integrated project are to complete a reservoir characterization of faulted Aeolian Jurassic Navajo Sandstone, and the Ferron Sandstone in Central Utah, in order to determine its feasibility as a long-term sequestration site for CO₂-charged fluids. This project is a collaboration between Utah State University and the University of Utah, and the following is a summary of the entire project work performed to date. The Utah State group is working on reservoir characterization issues, while the University of Utah group is examining the geochemistry of the system and will perform flow models of the candidate sites. In addition, we examine faults of the Colorado Plateau along which CO₂-charged springs, geysers, and travertine deposits are common, in order to evaluate how a CO₂ storage site might fail.

Project Description: We have used a multi-scale, multifaceted approach to determine the hydraulic structure of a fault zone in aeolian sandstone. We have shown that identifying the fault zone components and their properties are important in determining the bulk hydraulic properties of the fault zone. In this section we summarise the key results from the Big Hole fault drilling project.

Results: By careful observations of core, minipermeameter tests, permeability tests at confining pressures, and an analysis of the bulk permeability of the faulted volume, we show that a four-component system best represents the structure of the Big Hole fault.

The host rock exhibits considerable variability in properties, despite being within one unit of aeolian sandstone. We have characterised four main sub-facies within the Navajo Sandstone, each with distinct petrophysical properties.

Deformation bands are zones of cataclasis, rarely more than a few mm's wide that accommodate mm's to cm's of slip.

Slip-surfaces are planes upon which the majority of the slip (strain) has been taken up within zones of deformation bands. At the surface, they are usually planes of parting; within our core samples, they may be planes of parting or mated surfaces. Thus, the permeability significance is poorly understood. They have previously been modelled as high permeability features.

The fault core consists of tightly packed deformation bands and highly crushed rock with a very low overall porosity (down to 1%, Shipton, 1999; Shipton and Cowie, in press). The width of the fault core is highly variable both along strike and down dip, and cannot be correlated with the displacement on the main fault.

We estimate the transverse bulk permeability of the fault zone to be 7-57 md for the faults sampled by our boreholes. Sensitivity analyses shows that bulk fault zone permeability is most dependant on the thickness of the amalgamated deformation bands and slip surfaces that make up the fault core, suggesting that where present, such fault cores should be identified and thicknesses estimated for use in reservoir simulators. Our data also indicate that thicknesses of the fault core may vary *in situ*, and do not correlate with the amount of slip.

The fault core and fault zone cluster thickness exhibit no correlation with the amount of slip on the fault. However damage zone thickness, as determined from the first deformation band recognized in the hanging wall through the ends of the drill holes varies from 10 to 24 m, does correlate with the amount of displacement. For our data set, this relationship would predict that the fault should be about 4.7 cm thick at site 2 where the fault has 8 m of slip; and at site 1 with approximately 3 m of slip, the fault should be only 1.8 cm thick. Clearly, caution should be used when applying “global” data sets to specific cases, and it may be more accurate to restrict the use of such relationships to the specific rock types and geologic settings under consideration (Evans, 1990). We do not examine the effects of changes in continuity of the fault structure (*cf.*, Antonellini and Aydin, 1994; Hesthammer and Fossen, 2000). However, we do recognize the importance of variations in fault architecture parallel to the fault plane . The *in situ* flow tests (section 6) show that such variations may significantly alter the macroscopic hydrologic properties of the fault zone.

We examine evidence for long-term leakage from natural CO₂ reservoirs in southeastern Utah. CO₂-charged springs and geysers are localised along fault zones throughout the region, and have deposited travertines, some of which may be as old as 200,000 years. These are either natural springs or springs that were induced by recent drilling. The faults cut siltstones, shales, and sandstones, and their outcrop appearance suggests they should be effective barriers to cross-fault flow (fine grained, clay-rich fault gouge). Abundant large calcite veins cut the faults, suggesting that fluid pressures in the past were high enough to rupture the faults. The spring waters are highly saline and high in Na, Cl, Ca, and dissolved CO₂. Modelling of the water chemistry indicates that the water is either saturated or supersaturated in aragonite, calcite, dolomite, fluorite and gypsum, all of which are observed in the veins along the faults, and that the water from both areas is likely to have come from organic decomposition of a sequence of marine evaporates at depth. Preliminary isotopic data from calcite veins show that the veins are highly enriched in ¹³C. This can only be explained if the veins have a fluid source in Palaeozoic marine rocks. The heavy $\delta^{13}\text{C}$ values provide further evidence for thermal decomposition of organic material or development of methane. Structural analyses of the system show that the faults sole into Pennsylvanian salt beds 2-3 km deep. This suggests that the spring waters are sourced in Palaeozoic rocks and flow along the faults to the surface. Past evidence for rupture of the fault seals indicates that reservoir pressures may exceed lithostatic pressure, causing the reservoir to leak repeatedly over time. These data indicate that injection of CO₂ -rich fluids into geologic reservoirs must be carefully designed and monitored to avoid slow seepage or fast rupture to the biosphere.

UTAH STATE UNIVERSITY

Department of Mathematics and Statistics, and
Department of Geology
Logan, UT 84322-4505

Grant : DE-FG03-95ER14526

Growth of Faults and Scaling of Fault Structure

J. P. Evans, (801) 797-2826, fax (801) 797-1588, jpevans@cc.usu.edu; K. Hestir (801) 797-2826, fax (801) 797-1822, hestir@sunfs.math.usu.edu; S. Martel, University of Hawaii, (808) 956-7797, fax (808) 956-5512, martel@soest.hawaii.edu; J.C.S. Long, University of Nevada at Reno, (702) 784-6987, fax (702) 784-1766, jcslong@mines.unr.edu

Objectives: We examine faults up to 10 km long in two localities to determine how fault structure scales, and develop a mechanically based stochastic model of fault growth that appears to represent the structure of faults, when conditioned by the field data and understanding of the three-dimensional mechanics of the faults.

Project description: Left-lateral strike slip faults in the central Sierra Nevada have long been used as a natural laboratory for the study of fault mechanics (Segall and Pollard, 1983; Martel et al., 1988, Martel, 1990. We examined faults that have 10's cm of slip and have trace lengths of 10's m to faults up to 10 km long and that have over 100 m of slip in order to determine the processes of fault growth near the base of the seismogenic zone. We also develop methods to invert structural data in order to infer the three-dimensional structure of the faults.

Results: *Small fault data:* Field mapping of small-displacement, well-exposed faults in granitic rocks of the Sierra Nevada, California, provide data on the three-dimensional structure of faults. The faults have up to 1 m of slip, formed at depths of 8-15 km, and represent brittle faults that formed at the earliest stages of development. The small faults are characterized by quartz-epidote-chlorite mineralization on narrow slip surfaces with numerous faults and fractures at fault tips. Splays in the tip regions have abundant quartz-epidote-chlorite mineralization. Data on the length, shape, orientation, and density of the splay faults show that the splays are planar fractures whose trace lengths do not exceed 10 – 20 % of the starting fault trace. Angles between the splays and the starting fault range between 35-45°. Inversion of the data using a stochastic method of conditional coding which creates models based on field data and mechanics indicates that the small faults can be modeled as a circular starting crack with an annular ring of cohesion that is 5-10% of the diameter of the fault. Splay faults within the cohesive zone are best represented as planar faults whose length is a function of the position along the tip line of the fault. This cohesive zone may represent the cohesive or breakdown zone on faults that slip seismically, and thus, these faults reflect the geometry and composition of dynamic crack propagation and arrest.

Large faults: Field-based structural analysis of the exhumed, 10 km-long Gemini and Glacier lakes strike-slip fault zones elucidates processes of growth, linkage, and termination for moderately sized strike-slip fault zones in granitic rocks. The Gemini fault zone is a 9.3 km-long left-lateral fault system that was active at depths of 8-11 km within the transpressive Late-Cretaceous Sierran magmatic arc.

The fault zone cuts four granitic plutons and is composed of three steeply dipping northeast- and southwest-striking noncoplanar segments that nucleated and grew along preexisting cooling joints. The fault core is bounded by sub-parallel fault planes that separate highly fractured epidote-, chlorite-, and quartz-breccias from undeformed protolith. The displacement-distance profile shows that the Gemini fault zone is segmented into three 2-3 km-long segments by two zones of displacement minima. Displacement is highest (131 m) on the western third of the fault zone and tapers to zero at the eastern termination. Slip vectors plunge shallowly west-southwest and show significant variability along strike and across segment boundaries. Four types of microstructures reflect thermal and compositional changes along strike, and show that deformation was concentrated on narrow slip surfaces at, or below, greenschist facies conditions. Taken together, we interpret the fault zone to be a segmented, hard-linked fault zone in which geometrical complexities of the faults and compositional variations of protolith and host rock resulted in non-uniform slip orientations, complex fault segment interactions, and asymmetric displacement-distance profiles.

Slip Localization: Our examination of small individual faults reveal that, similar to other workers, the fault surfaces are marked by foliated chlorite-epidote-quartz zones. In detail, the microstructures of the small faults reveal the evolution from brittle Mode I fracture filled by chlorite, epidote, and quartz to brittle fracture and cataclastically deformed rocks to the development of very fine-grained cataclasites and ultracataclasites. The initial shear-induced microstructures are developed on faults with as little as several mm of slip, and the transition to the foliated textures may occur for as little as 10-20 cm of slip. Fault surfaces with chlorite-epidote-quartz assemblages display a strongly developed foliation foliated texture and what appear to be thin dark regions that represent a narrow slip zone.

We have also conducted whole-rock geochemical analyses of these small faults, and the data show that these small faults exhibit subdued, but notable changes similar to those observed in much larger faults. The small faults exhibit a 1-3 wt % reduction in SiO_2 , small increases in MgO, CaO, and TiO_2 . Similar, but much larger, changes have been documented for faults of the SAF system (Evans and Chester, 1995) and are interpreted to be the result of reactions that take place in the fault zone while it is active. These reactions are reaction-softening reactions that transform feldspars to micas and hornblende and biotite to chlorite.

These microstructures are remarkably similar to the much larger faults, such as those seen on the San Gabriel and Punchbowl faults, where displacements are up to 44 km. With only 1 m of slip, the Sierran faults exhibit very fine-grained dark cataclasite fault rocks with opaque matrix, and often develop the thin slip surfaces several mm thick. We draw an analogy with the direct shear experiments in which well developed shear fabrics form with only mm of displacement, and subsequent slip is often accommodated by the development of stable microstructures that include foliated cataclasites and ultracataclasites, and the creation of a narrow slip zone, typically at the margin of the small fault. Experiments of shearing of phyllosilicate-rich gouge in an environment where slip in phyllosilicates and pressure solution is promoted also show that slip may localize very early in the history of the system, and leads to a strain weakening response. We suggest that slip in faults that form at depths of 4-13 km, in a wet environment, seems to localize **very** early, and strain-softening mechanisms associated with hydrothermal and reactive fluids may be activated in the earliest stages of faulting.

VIRGINIA POLYTECHNIC INSTITUTE AND STATE UNIVERSITY

Department of Geological Sciences
Blacksburg, Virginia 24061

Grant: DE-FG05-89ER14065

Experimental studies in the system H₂O-CH₄-“petroleum”-salt using synthetic fluid inclusions

R. J. Bodnar, (540) 231-7455, fax (540) 231-3386, bubbles@vt.edu

Objectives: The major objective of this project is to experimentally determine the pressure-volume-temperature-composition (PVTX) relationships of fluids in the C-O-H-NaCl system over the complete range of PTX conditions encountered in crustal energy, resource and hazardous waste-related environments.

Project Description: Volumetric (PVT) data provide the fundamental information needed to understand the physical and chemical behavior of fluids in shallow crustal environments. These data represent the basis for developing empirical or theoretical equations of state to predict the thermodynamic properties of fluids over crustal PTX conditions. In this study the PVTX properties of fluids in the C-O-H-NaCl system are being experimentally determined using the synthetic fluid inclusion technique as well as a newly designed high-pressure cell for use on the Raman microprobe. These combined techniques permit determination of phase equilibria and PVT properties of fluids over a wide range of PTX conditions.

Results: A technique has been developed that allows the methane concentration, salinity, and pressure of H₂O-salt-CH₄ fluid inclusions to be determined using Raman spectroscopy. With this technique it is now possible to determine the composition and pressure at trapping of natural fluid inclusions in hydrocarbon basins. Pressure (depth) is one of the most poorly constrained variables in developing models for hydrocarbon generation and migration. This technique can now be used to determine formation pressures, which can then be incorporated into burial history models for use in hydrocarbon exploration. This technique has been patented with ExxonMobil and Virginia Tech as joint owners of the patent.

Experimental and analytical studies to determine the PVTX properties of H₂O-CH₄ fluids over the range of conditions found in crustal hydrocarbon reservoirs have been completed. These data have been used to generate an empirical model that predicts the solvus (methane solubility) and the isochores (lines of constant volume) in the methane-water system. This model can be used to predict formation conditions for methane-bearing fluid inclusions in hydrocarbon basins which, in turn, provides constraints on basin evolution as related to hydrocarbon generation and migration.

Preliminary studies have been conducted to develop a technique to determine the P-T stability limits of methane hydrate in submarine and permafrost environments. The technique combines results of conventional microthermometric analysis of fluid inclusions to determine the temperature at which the hydrate phase disassociates, with Raman analysis of the fluid inclusion at that same temperature to determine the methane pressure in the inclusion. This research builds on earlier work that developed an empirical relationship between the methane pressure and the position of the dominant Raman peak for methane. This study is being extended to examine the effects of salt and other volatile species on the stability of the methane hydrate phase.

VIRGINIA POLYTECHNIC INSTITUTE AND STATE UNIVERSITY

Department of Geosciences
Blacksburg, VA 24061

Grant: DE-FG02-00ER15112

Investigation of the Physical Basis of Biomineralization

P. M. Dove, (540) 231-2444, fax (540) 231-3386, dove@vt.edu

Objectives: To determine principles of mineral assembly that govern interactions of simple protein analogs and key inorganic impurities with carbonate minerals and the resulting structures/polymorphs that form. A long-term goal is to establish the physical basis for biomineralization and accompanying roles of solutes in natural and engineered Earth systems.

Project Description: Primary biominerals form through biologically mediated activities of marine and freshwater organisms. They result from organic-directed crystal nucleation and growth processes acting in concert to yield chemically and morphologically complex structures. When combined with a macromolecular matrix of proteins, polysaccharides, and lipids, these structures fulfill specific physiological functions such as providing stiffness and strength to mineralized skeletal tissues. An understanding of organic-mineral surface interactions also has applications for 1) developing avoidance strategies for cementation/scaling in oil/gas fields; 2) understanding the long-term behavior of carbonates in waste repositories; 3) developing new biomaterial technologies in the synthesis of lightweight mineral composites. This project combines in situ Atomic Force Microscopy (AFM) investigations of kinetic and thermodynamic calcite surface properties with surface chemical modeling to determine the mechanisms by which amino acids and inorganic impurities modify the assembly of calcium carbonate minerals.

Results:

Resolving the Controversial Role of Mg^{2+} in Calcite Biomineral Formation.

Magnesium is a key determinant in $CaCO_3$ biomineral formation and has emerged as an important paleotemperature proxy. However, macroscopic observations have failed to provide a clear physical understanding of how Mg^{2+} modifies carbonate growth. Atomic force microscopy was used to directly resolve the controversial mechanism of calcite inhibition by Mg^{2+} through molecular-scale determination of the thermodynamic and kinetic controls of Mg^{2+} on calcite morphology and growth. Comparison of directly observed monomolecular step velocities to standard impurity models demonstrated that calcite growth inhibition was due to enhanced mineral solubility through Mg^{2+} incorporation. Terrace width measurements on calcite growth spirals showed that step-edge energies were unaffected by Mg^{2+} incorporation according to the Gibbs-Thomson relation. Finally, solubilities determined from microscopic observations of step dynamics are linked to macroscopic measurements of the $Ca_{1-x}Mg_xCO_3$ system.

Selective Binding of Amino Acids to Atomic Steps of Calcite Creates Chiral Structures. The conventional paradigm that defines current views on biomineralization is commonly described by the term “stereochemical recognition”, a concept that emphasizes geometrical and chemical incentives to binding. However, this view of the organic-inorganic interactions at the mineral surface seems

incompatible with the mechanistic picture of crystallization given by the terrace-step-kink model of Burton, Cabrera and Frank. Indeed, this traditional model of growth emphasizes the inhibiting effect of modifiers on step motion through step pinning at kink sites, rather than stereochemical matching to newly expressed facets. We reconcile these two divergent views. By using the chiral structure of the amino acids as a probe, we show both qualitatively and quantitatively that macroscopic shape modification results from changes to the calcite step-edge free energies in response to enantiomer-specific binding of the amino acids to individual step risers. In essence, the amino acid acts like a surfactant, and the concept of stereochemical recognition merges smoothly with that of the terrace-step-kink model.

Morphological consequences for intrasectoral impurity zoning: A plausible molecular-scale mechanism for elongated calcite Magnesium is considered the principal modifier of calcite morphology in many natural environments. However, the physical mechanism by which magnesium alters the external form of calcite has remained controversial due to a lack of direct experimental insight. Here we use *in situ* molecular-scale observations of step dynamics and growth hillock morphology to directly resolve the role of Mg^{2+} in governing calcite surface morphologies. We show that Mg^{2+} directly modifies the surface morphology of calcite as a consequence of intrasectoral zoning into vicinal faces on growth hillocks. These step-specific interactions are especially evident at low Mg/Ca ratios in solution, where steps with acute step-edge geometries are observed to be rough while obtuse steps remain smooth. Higher Mg/Ca solution ratios cause the edges of both step-types to become rough and the growth spiral to approach a more isotropic form. Coincidentally, new step-directions are generated by decreased growth velocities parallel to the *c*-glide plane. Calculations indicated that these new step directions are likely the result of strain at the intersection of nonequivalent step-types, resulting from differential Mg^{2+} incorporation across the boundary of those steps. This hypothesis was validated by observations of growth hillock recovery from impurity poisoning which demonstrated the presence of ‘remembered’ strain at the boundary of the non-equivalent step-types. The results of this study offer a plausible molecular-scale explanation for the elongated calcite crystals that are commonly observed in sedimentary environments.

VIRGINIA POLYTECHNIC INSTITUTE AND STATE UNIVERSITY

NanoGeoscience and Technology Laboratory
Department of Geological Sciences
Blacksburg, VA 24061

Grant: DE-FG02-99ER15002

Microbial Community Acquisition of Nutrients from Mineral Surfaces

Michael F. Hochella, Jr., (540) 231-6227, fax (540) 231-3386 hochella@vt.edu; Duane Berry and Matthew Eick, Dept. of Crop and Soil Environmental Sciences; John Little, Dept. of Civil and Environmental Engineering; Malcolm Potts, Dept. of Biochemistry; Chris Tadanier, Dept. of Geological Sciences

Objectives: Minerals and microbes undergo complex interactions in nature that impact broad aspects of near-surface Earth chemistry. Our primary objective in this project is to gain insight into how microbial species and communities acquire critical but tightly held nutrients residing on or within minerals common in rocks and soils, and to quantitatively study related microbe-mineral interactions.

Project Description: The overall purpose of this project is to search for and delineate fundamental physiological strategies and/or environmental conditions by which microbial species or consortia interact with minerals and mediate release of strongly bound nutrients/contaminants from mineral surfaces. The underlying hypothesis is that microbes employ specific physiological strategies and/or take advantage of specific environmental circumstances that result in release of chemical components tightly bound to mineral surfaces. This is being studied in various ways, including 1) using a model nutrient-mineral system of orthophosphate sorbed to goethite in the presence of a soil derived microbial consortium, 2) using biological force microscopy (BFM) techniques to characterize interactions of metal reducing bacteria with iron oxyhydroxide minerals, and 3) using chemical force microscopy (CFM) to study the interaction of bacteria-produced siderophores on iron oxyhydroxide minerals.

Results: In FY2001, we focused on the ability of various surface complexation models to adequately describe nutrient adsorption and surface charging phenomena. Our results demonstrate that commonly used surface complexation models are unable to adequately describe orthophosphate-goethite adsorption behavior over a wide range of surface coverage nor adequately describe surface charging behavior. We therefore implemented the thermodynamically, electrostatically, and crystallographically more robust Charge-Distribution Multi-Site Complexation model in FITEQL 4.0, which allowed both the adsorption and surface charge data to be satisfactorily modeled.

In FY2001, we also used BFM to study the nanomechanical properties of biomolecules that bridge the interface between *Shewanella* and goethite when they are in contact. The force curves collected by BFM suggests the presence of an outer membrane protein produced by the bacterium that may play a role in mediating electron transfer to the mineral. The results of these studies provide direct evidence that microorganisms actively recognize minerals and produce or localize biomolecules at the interface with the mineral.

We have also successfully isolated the siderophore azotobactin (1.3 kDa) from *Azotobacter vinelandii* (a nitrogen-fixing soil aerobe), and selectively attached it to hydrazide-terminated AFM tips using protein-coupling techniques. Using this CFM approach, we have shown that azotobactin has a much greater affinity for iron oxyhydroxide mineral surfaces compared to isostructural aluminum minerals. This result supports our working hypothesis that siderophore-mediated acquisition of iron involves direct interaction between the siderophore molecule and the mineral surface in aqueous Fe-limited environments.

UNIVERSITY OF WASHINGTON

Department of Earth and Space Science
Box 351650
Seattle WA 98195

Grant: DE-FG03-99ER14976

Two and Three-dimensional Magnetotelluric and Controlled Source Electromagnetic Inversion

John Booker, (206) 543-9492, fax (206) 543-0489 booker@geophys.washington.edu

Objectives: Develop practical algorithms for imaging multi-dimensional underground structure using natural or controlled source very low frequency electromagnetic energy. Emphasis is on implementations suitable for computer resources widely available.

Project description: Electrical conductivity in the sub-surface depends primarily on the presence of ionic fluids and metallic films or objects. Imaging electrical conductivity structure has applications in the exploration for water, where it is particularly sensitive to quality, temperature and permeability, for minerals, where it is directly sensitive to the target and for petroleum, where conductivity (or its lack) is diagnostic of trapping structure such as salt, volcanics and limestone that are often difficult to penetrate with seismic energy. Electrical conductivity is particularly useful in a wide variety of waste remediation targets and in the determination of permeability in reservoir rocks. Determining conductivity in the subsurface is a problem in electromagnetic (EM) remote sensing with deeper targets requiring lower frequency. The EM signal can be natural, or in noisy industrial situations, may be artificial. If both electric and magnetic fields are measured, the data are termed magnetotelluric (MT). Modern understanding of sub-surface structure has made evident its fundamental three-dimensional (3D) character. Recent developments in equipment make it possible to collect MT data on dense surface grids. However, the inverse problem of extracting 3D structure from such data is computationally formidable even with the largest and fastest modern computers. Such resources are not often available to industrial contractors and certainly not appropriate in the field, where imaging can result in important feedback to the data collection process. This has led to the search for algorithms that can fully invert the data, but require very small fractions of the computer resources that standard approaches entail. Our basic approach involves approximate iterative schemes that have the property that their error goes to zero as convergence is approached.

Results: The departure of Martyn Unsworth from the University of Washington Faculty to take up a position at the University of Alberta resulted in a significant reorganization of our effort. A major result has been joining forces with Randall Mackie of GSY_International who has been working on a non-linear conjugate gradient algorithm for 3D MT inversion. In the past year, we have carefully examined convergence properties of a two-dimensional (2D) version of the non-linear conjugate gradient algorithm. This has led to a variety of improvements, particularly to the structure penalty side-condition necessary for uniqueness. These lessons are being transferred to the 3D algorithm. A major goal of our work, to include controlled sources in our 3D algorithms is just beginning, but should be completed prior to expenditure of our currently granted funds. We have also been examining an

important parallel issue: conversion of 2D data sets contaminated by the response of local 3D structure to 2D data sets. We have concluded, in contrast to standard practice, that the distortion of the magnetic field can rarely be ignored and have developed an interactive program to determine strike of the regional 2D structure and the coefficients of the electric and magnetic distortion operators. A novel feature of this work is constraining the off-diagonal elements of the magnetic distortion operator (which have generally been ignored because no one knew how to determine them) by the requirement that the MT impedance have a premissable relationship between magnitude and phase as a function of frequency. This constraint demonstrates that these off-diagonal elements are indeed small in most cases.

UNIVERSITY OF WASHINGTON

Department of Earth and Space Science
Box 351650
Seattle WA 98195

Grant: DE-FG03-97ER14781

Electromagnetic Imaging of Fluids in the San Andreas Fault

M. Unsworth, (206) 543-4980, unsworth@geophys.washington.edu

Objectives: To obtain high-resolution images of the electrical resistivity of the San Andreas fault (SAF) zone. This will permit the fault zone architecture and fluid distribution to be constrained.

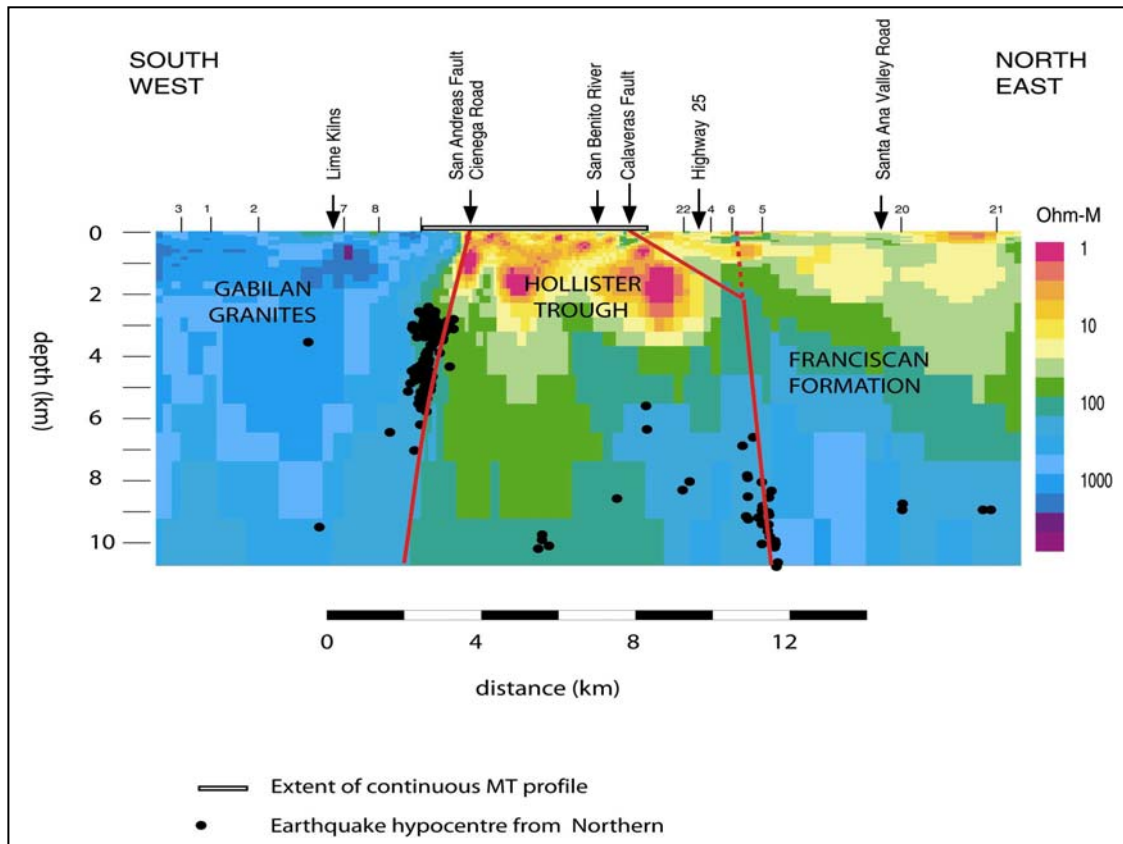
Project description: There is increasing evidence that fluids may play a significant role in the earthquake rupture process. However, the difficulty of directly observing fluids in active fault zones currently limits progress in understanding these processes. Magnetotelluric (MT) data collected in 1994 at Parkfield and Carrizo Plain showed that the fault zone at these locations has very different electrical structure.

To further examine how these differences might be related to fault zone seismicity, a two-phase program of MT data acquisition and interpretation is being undertaken. In the first phase, data will be collected on additional profiles across the SAF at Middle Mountain, Parkfield to obtain a three-dimensional image of the electrical resistivity in this area. In the second phase, a three-dimensional survey of the central creeping section of the SAF near Hollister will be undertaken.

Results: During this period the second phase of data acquisition took place. Magnetotelluric data were collected on two profiles that crossed the creeping section of the San Andreas Fault south of Hollister. After careful analysis to remove the effects of cultural noise, the electrical resistivity model shown in the figure on the following page was produced by inversion of the data. The following features can be observed in the model

1. The San Andreas Fault forms a steeply dipping boundary between the granites of the Gabilan Range and the lower resistivity rocks of Franciscan formation. The earthquake hypocenters are coincident with the electrically imaged fault.
2. Low resistivity units are found between the San Andreas and Calaveras Fault, extending to a depth of around 4 km. The lowest resistivities (and by inference, the highest fluid contents) are associated with the San Andreas and Calaveras Faults. As at Parkfield, the active fault trace is found on the edge of the low resistivity fault zone in the upper 3 km.
3. As at Parkfield, the conductive feature in the shallow structure is probably due to a zone of fractured rock, permeated with saline groundwater. This appears to be common to all locations at which the fault is creeping. The origin of the groundwater is uncertain. It may have an origin in the deep crust, or could be due to infiltration from the surface.

4. A zone of low resistivity is located between the San Andreas and Calaveras faults. The precise location of the surface trace of the Calaveras Fault, and its relationship to the resistivity anomaly is being investigated.



UNIVERSITY OF WISCONSIN

Department of Civil and Environmental Engineering
Geological Engineering Program/ 1415 Engineering Drive, Madison, WI 53705

Grant: DE-FG02-99ER14995

Three-Dimensional Transient Electromagnetic Inversion

David L. Alumbaugh, (608) 262-3835, fax (608) 263-2453, alumbaugh@engr.wisc.edu; Gregory Newman, Sandia National Laboratory

Objective: To develop, implement, and test three-dimensional (3D) transient electromagnetic (TEM) forward modeling and inversion algorithms for geophysical characterization of the subsurface. The codes then will be used to assess the TEM geophysical technique for characterizing hazardous waste and contaminated sites, and for monitoring CO₂ sequestration processes in subsurface reservoirs.

Project Description: State of the practice TEM data analysis employs layered (1D) inversion of individual 'soundings', and then 'stitching' the results together to provide a 2D or 3D interpretations. This can result in artifacts and misinterpretation in areas of complex subsurface structure. Code development occurring at Sandia National Laboratories under this project is providing forward and inversion algorithms that can properly account for complex 3D geometries. Simulations at the University of Wisconsin are employing the new schemes to analyze problems important to the DOE. Specific topics being addressed include crosswell and singlewell monitoring of CO₂ sequestration processes, and identifying where standard TEM processing breaks down when inverting data collected over dipping structures. The various analyses involve; 1) visualizing the current systems that are induced by a rapidly terminating current source in or over a 3D model; 2) analyzing and comparing the data that would be measured by different source-receiver configurations and offsets; 3) using linear inversion theory to define how the spatial sensitivity of the different source-receiver configurations to the 3D model changes over time; 4) 1D inversion of simulated profile data over various 3D structures to determine artifacts that develop in the resulting images.

Results: The forward modeling scheme has been employed to simulate measurements made before and after a CO₂ flood in the Maljamar Oil Field of New Mexico; the reservoir model was provided by scientists at Lawrence Livermore National Laboratories. Preliminary modeling using simulation of measured fields at receiver positions and current visualization has shown that a CO₂ injection may be detectable as long as it is injected into a region that is relatively conductive compared to the injection zone itself. A second important finding is that quick ($1e^{-6}$ seconds) current termination in the transmitter can provide enhanced sensitivity to resistive units at very early times. If the termination time is $1e^{-5}$ seconds this sensitivity is lost.

The 'geologic dip' study has shown that if the geology consists of a resistor over a conductor, stitched 1D inversions of central loop sounding data can provide realistic estimates of the true structure up to dips of approximately 27 degrees. In addition, even though artifacts appear for dips that are greater than this value, the artifacts become more focused near the center of the dipping interface; for a 90 degree dip only those stations immediately adjacent to the dipping interface are affected. However, when a conductor overlies a resistor, then the method is very insensitive to the dip-angle. In fact the profile data resulting over a structure that dips at 27 degrees is almost identical to that collected over a vertical-contact.

UNIVERSITY OF WISCONSIN

Department of Geology and Geophysics
Madison, Wisconsin 53706

Grant: DE-FG02-93ER14328

Precipitation at the Microbe-Mineral Interface

Jillian F. Banfield, (608) 265-9528, fax (608) 262-0693, jill@geology.wisc.edu

Objectives: Microbial biomineralization can dramatically modify the distribution of metals in the environment. The goals of this research are to determine the mechanisms by which cell surfaces, enzymatic activity, and microbial byproducts impact metal speciation and induce mineral precipitation.

Project description: Work focuses on biogeochemical processes in metal-contaminated environments associated with two abandoned mines. Field work has been carried out in Washington, where uranium contamination of soils and sediments has occurred, and in a flooded underground mine tunnel in SW Wisconsin, where Zn, Pb, and U contaminants are cycled across a redox boundary. We are analyzing how microbial activity in oxic and anoxic zones results in formation of metal oxide, metal sulfide, and phosphate biominerals in proximity to, and within, cells. These precipitation reactions occur as the result of enzymatic reactions involved in energy generation, sequestration of toxic ions, and adsorption onto cell polymers. In the later project period we have concentrated on uranium contaminated water and sediments, focusing on the mechanism of uranium reduction and determination of the organisms responsible.

Results: Microbial impact on the form and distribution of uranium near the Earth's surface was investigated through combination of molecular biological characterization of the microbial communities, experiments involving cultured microorganisms, and high-resolution mineralogical and geochemical analyses. Research focused on uranium transformations that occur in anaerobic, microaerobic and aerobic sediments associated with the Midnite Mine field site in WA. The goals of the work were to determine which microorganisms impact uranium cycling in the natural environment, the mechanisms by which organisms are resistant to the chemical toxicity of uranium, and the nature of the solid products of biological uranium resistance pathways and metabolic activity. Attention has been given to the form and size-dependent structure and reactivity of uranium mineral products because these factors impact uranium bioavailability and transport.

Uranium mobility in aqueous systems is significantly controlled by its redox state. Microbial U(VI) reduction in nature was studied in experiments where growth of indigenous microbial populations was stimulated in field-collected sediment and water by addition of organic substrates. We have shown that soluble hexavalent uranium, U(VI), is converted to insoluble tetravalent uranium, U(IV), leading to the precipitation of abundant uraninite (UO₂) nanoparticles that develop within the periplasm and in solutions surrounding cells, and that coat cell surfaces and form colloidal aggregates in proximity to cells. Uraninite formed as the result of microbial activity has a particle size that spans the range from molecules up to ~3 nm. Both TEM and EXAFS data indicate that these nanoparticles retain the basic

uraninite structure. However, detailed analyses demonstrated structural distortion due to predominance of surface ions. Calculations using the measured surface stress predict a change in solubility that is consistent with that measured previously for “amorphous” or “poorly crystalline” materials. TEM data indicate that UO_2 nanoparticles grow via aggregation-based routes, in some cases mediated by organic polymers. This leads to formation of distinctive particle morphologies (rods), and microstructures, including dislocations at grain boundaries and twins. Preliminary experiments suggest that, despite its reduced form, uranium may be dispersed in the environment by aqueous transport of these tiny particles. By combining data from molecular biological, geochemical, and mineralogical studies, we inferred that *Desulfosporosinus* spp. reduced U(VI) in field-collected sediment and water. The capability of enzymatic U(VI) reduction by our isolate and a commercially available strain of *Desulfosporosinus* spp. was confirmed in pure culture. Results suggest that these microbes possess a periplasmic hydrogenase that is involved in uranyl reduction. *Desulfosporosinus* spp. are relatively wide spread in near surface and subsurface environments. Thus, these organisms may be important in natural uranium cycling. Because of their metabolic capabilities, they also have considerable potential for bioremediation.

In situ observations of shallow, natural, surface sediments underneath oxic water showed that uranium is largely in reduced form. Results from molecular biological studies revealed that the sediments were colonized by microbial populations that consist of aerobic, microaerophilic and strictly anaerobic bacteria, including known U(VI)-reducing bacteria. Direct observations indicate cells concentrate uranium; geochemical data indicate that reduction occurs via a direct microbial pathway and not via an indirect route mediated by sulfide mineral surfaces or dissolved sulfide species. Uranium bioreduction in the sediment leads to zones as enriched in uranium as U(IV) as economically important uranium deposits. These sediments differ from adjacent, oxidized zones, which contain little uranium. Data indicate uranium cycling between minerals and pore fluids in association with seasonal groundwater fluctuations.

In summary, the concept that microbes reduce uranium in nature has been based on laboratory evidence for this transformation. We demonstrated biological uranium reduction in the natural environment for the first time and confirmed that, at our field site, the transformation occurs via a direct, enzymatic pathway. Our results prove enzymatic uranium reduction by gram positive *Desulfosporosinus* spp. isolates, increasing the number of taxa known to carry out this important transformation. We have shown that uranium remains reduced in microaerobic zones of active nitrogen cycling. The size and size-dependent morphology, structure, and crystal growth pathways of biogenic uraninite have been determined. This work, much of it part of the Ph.D. thesis of Yohey Suzuki (2001), enhances our understanding of the geomicrobiology of uranium in the natural environment. The data have relevance to understanding of biogeochemical uranium cycles in the past, as well in modern environments. The data also have relevance to environmental cleanup of uranium-contaminated sites.

UNIVERSITY OF WISCONSIN

Department of Materials Science and Engineering
Madison, WI 53706

Grant: DE-FG02-98ER14850

Deformation and Fracture of Poorly Consolidated Media

Bezalel C. Haimson, (608) 262-2563, fax (608) 262-8353, haimson@enr.wisc.edu

Objectives: We investigate failure mechanisms around boreholes and the formation of borehole breakouts in high-porosity sandstone and artificial rock. We are particularly interested in the grain-scale micromechanics of failure leading to borehole breakouts in poorly consolidated granular materials, and aim at assessing whether these phenomena could be put to use for in situ stress evaluation and for borehole stability prediction.

Project description: For borehole stability studies we employ a specially fabricated biaxial loading cell mounted inside a compression loading machine, which allow us to carry out drilling of axial boreholes (diameters of 14-40 mm) in rock blocks (150x150x230 mm) already subjected to a state of true triaxial in situ stress. This procedure closely simulates field conditions. Berea sandstone of 24-26% porosity, St. Peter sandstone, Tablerock and other sandstones, and artificial granular material of similarly high porosity are tested. After drilling specimens are cut into several cross sectional slices and the condition of the borehole is carefully inspected. If breakouts are visible, their dimensions are recorded. Thin sections are prepared of critical cross sections and later studied under an optical microscope.

Results: The emphasis in our testing program this year has been on St. Peter sandstone, which is abundant in Minnesota and Wisconsin. St. Peter sandstone is composed of 100% quartz grains cemented together by sutured contacts. The porosity is within 11-19%. A first major finding here was that beyond a certain threshold of far-field stresses, the borehole breakouts that develop in St. Peter sandstone are invariably very narrow (6-10 grain diameters) and long (several borehole diameters), and have the appearance of fractures. The fracture-like breakouts are counterintuitively oriented perpendicular to the maximum horizontal stress.

Two types of St. Peter sandstone mechanical behavior have been observed. In the higher porosity variety of St. Peter sandstone (16-19%) there is very little intragranular microcracking behind the breakout tip, and the intergranular failure there consists mainly of broken grain sutures. There is an apparent zone of reduced porosity near the breakout tip. Using a digital imaging software package, we determined that void space occupies a smaller percentage of the area in front of the tip of the breakout than in the areas on either side of the breakout. This reinforces our earlier finding in high porosity Berea sandstone that these breakouts are potentially emptied compaction bands in which debonded and compacted grains are removed and flushed out by the circulating drilling fluid. In addition, the length of the breakouts was found to vary directly with the ratio of maximum to minimum horizontal principal stress, raising the possibility of using measured breakout depth in wellbores to estimate the in situ state of stress.

In the lower porosity (11-14%) St. Peter sandstone a narrow compaction band zone of crushed grains ahead of the breakout tip is clearly evident, caused by extensive failure of both sutured grain contacts and the grains themselves. The explanation for this micromechanical behavior lies in the additional observation that in the higher porosity Berea and St. Peter sandstones sutured contacts are limited to relatively small areas of the grain surface. Such contacts are readily severed at stress levels lower than quartz-grain strength, yielding debonded but intact grains within the compaction bands. On the other hand, sutured contacts in the 12% St. Peter are considerably more extensive, covering most of the grain surfaces, and rendering the strength of the matrix equal to that of individual grains. Hence, the compaction band here contains both debonded and crushed grains.

UNIVERSITY OF WISCONSIN

Department of Geology and Geophysics
Madison, Wisconsin 53706

Grant: DE-FG02-93ER14389

Microanalysis of Stable Isotope Ratios in Low Temperature Rocks

John W. Valley, (608) 263-5659, fax (608) 262-0693, valley@geology.wisc.edu

Website: <http://www.geology.wisc.edu/zircon>

Objectives: To further develop microanalytical techniques for stable isotope analysis and to employ them to decipher the complex effects of superimposed hydrothermal events in modern and fossil geothermal systems (Long Valley, Yellowstone, BTIP/Skye, Timber/Yucca Mtn.).

Project Description: This study focuses on samples of altered volcanic rocks from the Long Valley caldera, Timber Mountain caldera complex, Yellowstone, and on hydrothermally altered granites from related rocks from the British Tertiary Igneous Province (BTIP). New techniques allow analysis of stable isotope ratios in ultra-small samples of refractory and of highly reactive samples; and oxygen isotope ratio can now be contoured across single crystals. Mineral zonation patterns provide new insights into the process of water/rock interaction: mechanisms of exchange, timing, degree of equilibration, variability of fluid fluxes, and fluid sources. Enhanced understanding of these processes is essential for improving computer models of fluid flow through hot rocks.

Results: At the Long Valley and Yellowstone, these results provide information on the nature of magma chambers at depth, the size of the modern geothermal resource, and the volcanic hazards. At Timber Mountain, the results restrict theories of ancient vs. on-going hydrothermal activity. On the Isle of Skye, Scotland, samples of granite from beneath an ancient, deeply eroded caldera provide further insights for active systems. In a new, application of these techniques last year, we studied 3.1 to 4.4 Ga detrital zircons and inferred that the first geothermal systems on Earth were formed within 170 m.y. of the formation of the Earth itself.

Long Valley. We submitted a paper on Long Valley to "Contributions to Mineralogy and Petrology" in 2001:

Yellowstone. We have published 3 papers describing our research at Yellowstone.

British Tertiary Igneous Province We published a paper summarizing 6 years of research in the British Tertiary Igneous Province.

Timber Mountain/ Oasis Valley caldera complex. We submitted a paper in 2001, which includes our results for Trench 14 at Yucca Mountain:

Archean Zircons. We have published two papers describing oxygen isotope compositions of detrital zircons from Western Australia, including one that we dated at 4.404 Ga, which is the oldest known

sample of the Earth. Surprisingly, this zircon has a high $\delta^{18}\text{O}$ value, evolved REE chemistry, and inclusions of quartz, which we interpret to mean that it came from a granitic magma formed by melting material that was hydrothermally altered at the surface of the Earth before 4.4 Ga. This is the earliest suggestion of liquid water on the surface of the Earth and has implications for the origin of life as well as being the first geothermal system.

UNIVERSITY OF WISCONSIN

Department of Geology and Geophysics
Madison, Wisconsin 53706

Grant: DE-FG02-98ER14852

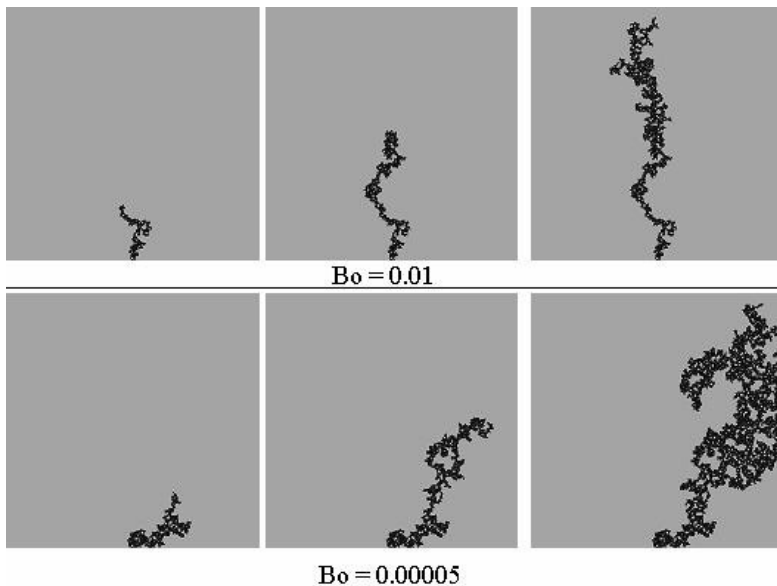
Pore-Scale Simulations of Rock Deformation, Fracture, and Fluid Flow in Three Dimensions

H. F. Wang, (608) 262-5932, fax (608) 262-0693, wang@geology.wisc.edu

Objectives: The objective is to develop a numerical, percolation model on the geologic scale for two-phase, immiscible fluid displacement in a porous medium.

Project Description: Two-phase displacement in a porous medium occurs in many geologic processes. Although pore scale mechanics can be readily understood in terms of the relevant viscous, capillary, and buoyancy forces, geologic scale, multiphase flows (large and slow) remain beyond the capabilities of current models. Conceptual and computational methods are being developed to separate a geologic-scale percolation model into a series of simulations that capture appropriately the dominant percolation behavior. The product of our research will be an understanding of the controls on the spatial distribution of the non-wetting fluid clusters.

Results: The Invasion-Percolation-in-a-Gradient (IPG) model is capable of incorporating all forces --- viscous, buoyancy, and capillary forces --- relevant to geologic problems of two-phase flow in a porous medium. Our calibration of the IPG model to a data set of two-phase flow experiments on glass bead packs showed that the characteristic throat radius is about 10% of the site radius, assuming that the site radius is approximately the grain size. Two-dimensional model results of the fractal dimension and the invasion probability of a throat on the interface are in excellent agreement with predictions for limiting cases of Capillary number and Bond number. In moving from two to three-dimensional media, trapped wetting clusters do not scale with the extent of the invading cluster, remaining under 5 to 8 pores in size.



WOODS HOLE OCEANOGRAPHIC INSTITUTION

Department of Marine Chemistry and Geochemistry
Woods Hole, MA 02543

Grant: DE-FG02-97ER14746

Laboratory Constraints on the Stability of Petroleum at Elevated Temperatures: Implications for the Origin of Natural Gas

Jeffrey Seewald, (508) 289-2966, fax (508) 457-2164, jseewald@whoi.edu

Objectives: Constrain the role of water and minerals during organic transformations responsible for the conversion of oil to natural gas at elevated temperatures and pressures

Project Description: Factors that regulate the generation and composition of natural gas during the thermal maturation of petroleum are poorly understood. The origin of natural gas is being investigated by conducting a series of laboratory heating experiments to constrain the stability of petroleum and its degradation products in the presence and absence of water and minerals at elevated temperatures and pressures. These experiments will assess carbon isotope fractionation and the catalytic activity of minerals, aqueous species, and water during oxidative decomposition of hydrocarbons and organic acids. Theoretical modeling is being used to evaluate thermodynamic and mass balance constraints on the production of carboxylic acids and dry natural gas.

Results: Experiments conducted in the absence of added minerals are characterized by high aqueous hydrogen concentrations indicative of extremely reducing conditions. Oil decomposition produced a methane-poor assemblage of low molecular weight hydrocarbons consistent with thermal cracking of longer-chain hydrocarbons. Despite the presence of water as an oxygen source, relatively minor amounts of carbon dioxide were produced. Low molecular weight products generated from oil dissolved in water were enriched in branched compounds relative to products generated in an oil phase.

In the presence of a suitable oxidizing agent such as a hematite-magnetite-pyrite mineral buffer, oil decomposition produced substantial amounts of carbon dioxide in addition to a methane-rich assemblage of low molecular weight hydrocarbons. Formation of alteration products that are both oxidized and reduced relative to the original oil is consistent with a reaction pathway involving stepwise oxidation of *n*-alkanes to produce alkenes, alcohols, ketones, and carboxylic acid reaction intermediaries. Depending on the oxidation state of the chemical system, carboxylic acids may either decarboxylate to produce *n*-alkanes and carbon dioxide or undergo complete oxidation to carbon dioxide. In general, these results are consistent with observations from natural environments where oxidative oil degradation associated with thermochemical sulfate reduction is occurring.

Decomposition of short-chain *n*-alkanes by stepwise oxidation is significantly faster than thermal cracking and produces a more methane-rich assemblage of low molecular weight products. These data suggest that water and redox reactive minerals facilitate reaction pathways that are not available in a pure oil system. The presence of numerous oxidizing agents in sedimentary basins suggests oxidative degradation of low-molecular weight *n*-alkanes may play a key role in the formation of “dry” natural gas.

WOODS HOLE OCEANOGRAPHIC INSTITUTION

Department of Marine Chemistry and Geochemistry
Woods Hole, Massachusetts 02543

Grant: DE-FG02-89ER13466

Organic Geochemistry of Outer Continental Margins and Deep Water Sediments

J.K. Whelan, (508) 289-2819, fax (508) 457-2164; jwhelan@whoi.edu

Website: <http://dynatog.whoi.edu/>

Objectives: The objective of this program is to develop a better understanding of processes of hydrocarbon generation and migration in coastal and offshore sedimentary basins as an aid in predicting favorable exploration areas and strategies for oil and gas production.

Project Description: Current research focuses on utilization of organic compounds in elucidating mechanisms, rates, and consequences of subsurface fluid flow. A particular interest is understanding the role of gas in driving fluid movement in sedimentary basin processes in collaboration with scientists at Cornell University, Louisiana State University and oil companies; and the Geochemical and Environmental Research Group (GERG) at Texas A&M.

Results: Previous work provided evidence for on-going oil and gas injection (termed dynamic migration) into reservoirs of Eugene Island Block 330 (EI330) and areas to the south along the Louisiana Gulf Coast shelf edge and slope. Research this year completed an extensive organic geochemical data set of a larger north south transect in the same area extending from South Marsh Island 9 in the North to Green Canyon 184 in the south. Working with scientists at Cornell, the data was then placed into its correct 3-D geological context. This approach has proven to be very powerful in helping us to better understand how on-going upward gas flow has affected oil and gas accumulations within the transect. Some preliminary results are:

- a) the "gas washing" previously observed for EI330 in which reservoired oils are "washed" with multiple volumes of upward migrating gas has occurred over recent geologic time throughout the transect. In the past, the effect has been strongest in SMI9 to the North and is just beginning now in GC184 to the south. At GC184, the present day upward migrating gas produces dramatic features at the seafloor including gas hydrates and a prolific biological community using methane as the primary food source.
- b) biomarkers indicate that the oil throughout the transect is probably derived primarily from Jurassic and early Cretaceous rocks which were trapped below a subsurface salt layer until recent salt movement allowed upward hydrocarbon migration into shallower modern reservoirs;
- c) the timing of oil migration is strongly influenced by faults and the timing of salt movement;

d) petroleum migration is very recent and primarily vertical. Minor changes in oil biomarkers over the transect are consistent with localized vertical migration through holes in the salt;

e) the biomarkers and maturity markers are consistent with edges of modern day salt domes acting as migration conduits from deeper reservoirs;

f) the organic indices show the degree of oil biodegradation which is related to the rate and timing of oil charging of reservoirs. If the reservoir was charged slowly in the past in shallower reservoirs, then the oil will be heavier and of lower quality than if the reservoir was charged more rapidly and recently.

Use of organic geochemical indicators together with basin modeling and 3D visualization allows a better understanding of the interaction of oil source, degree of oil biodegradation, the timing and rate of reservoir filling for a specific oil accumulation, and the quality (and profitability) of the oil expected. Determination of oil type is a particular problem in this Gulf of Mexico transect, where gas-oil ratios and subtle oil source changes occur over very short distances, even though the overall oil biomarker compositions remain relatively constant.

WOODS HOLE OCEANOGRAPHIC INSTITUTION

Department of Geology and Geophysics
Woods Hole, MA 02543

Grant: DE-FG02-00ER15058

Evolution of Pore Structure and Permeability of Rocks under Hydrothermal Conditions

Wen-lu Zhu, (508) 289-3355, fax (508) 457-2183, wzhu@whoi.edu; J. Brian Evans, Massachusetts Institute of Technology

Objectives: The pore structure and transport properties of rocks, including fluid permeability and electrical conductivity, can be altered by a wide variety of diagenetic, metamorphic, and tectonic processes. We are studying the interrelationships among permeability, mechanical properties, and the pore shape, under hydrothermal conditions, in mineral aggregates, with and without reactions.

Project Description: A better understanding of the processes that change porosity in the Earth is important for improving resource recovery, predicting rates of metamorphism, understanding fault mechanics and fault stability, and estimating rates of deformation by pressure solution. Laboratory results indicate that the measurements of macroscopic transport properties can be rationalized by considering the evolution of the pore space. As the mineral aggregates react and lithify, a larger fraction of porosity becomes ineffective for fluid or electrical transport. In this study, we use an integrated approach consisting of experimental testing, quantitative microscopy, and theoretical and numerical analyses to quantify changes in surface roughness, porosity, and pore dimensions. Detailed microstructure study will be made using standard optical, scanning electron, and laser confocal scanning optical microscopes. The image data will then be used in network models to predict the permeability.

Results:

1. Shear localization in Solnhofen limestone at elevated temperature

We conducted a suite of deformation tests on Solnhofen limestone, a fine-grained carbonate rock with initial porosity of ~4%. The experiments were conducted at confining pressures ranging from 70 to 400 MPa. Distilled water was used as the pore fluid at a constant pore pressure of 50 MPa. To investigate the temperature effects on deformation mechanisms and failure modes, we deformed these samples 298, 323, 373, and 473 K respectively. Our experimental data show that the failure process is sensitive to both pressure and temperature conditions. The stress required for the inception of dilatancy and localization increases with increasing pressure and decreasing temperature. At low pressures and temperatures, significant amount of strain softening and an abrupt stress drop were observed during localization. However, at higher pressure and temperature, the localization process became rather progressive, with strain softening and dilatancy accumulating over large amount of axial strain (up to 6%).

2. Network modeling for permeability in partially molten rocks

We developed a 3D network model to calculate permeability as a function of distributions of the dihedral angle and melt fraction. In our model, each channel is treated as a prism with a length of the

grain boundary. The cross-sectional area of each prism is determined by a given dihedral angle and a melt fraction. By incorporating different wetting angles into a network model, we are able to predict the permeability of partially molten rocks, taking the grain-scale heterogeneity of melt distribution into account. Our results show that the permeability of an anisotropic system can be significantly different from the calculated permeability of an isotropic system with the same median dihedral angle using the power law relationship described above. Using quantitative microstructural data of melt distribution, our network model provides better estimation of permeability in partially molten systems.

UNIVERSITY OF WYOMING

Department of Geology and Geophysics
Laramie, WY 82071-3006

Grant: DE-FG03-96ER14623

Mineral Dissolution and Precipitation Kinetics: A Combined Atomic-Scale and Macro-Scale Investigation Targeted Towards CO₂-Sequestration Data Needs

Carrick M. Eggleston, (307) 766-6769, fax (307) 766-6679, carrick@uwyo.edu, Steven R. Higgins (307) 766-3318, fax (307) 766-6679, shiggins@uwyo.edu; Kevin G. Knauss (510) 422-1372, fax (510) 422-0209, knauss@s19.es.llnl.gov

Objectives: The objectives of this research are 1) to improve the hydrothermal atomic force microscope as a research tool, 2) to improve our understanding of carbonate mineral dissolution and growth through extensive experimentation at both microscopic and macroscopic size-scales, and 3) to study simultaneous dissolution and growth.

Project Description: This project is a combined atomic-scale and macro-scale study designed to improve our understanding of mineral dissolution and precipitation processes specifically affecting coupled silicate mineral dissolution and carbonate mineral growth expected as part of a CO₂ sequestration strategy of injection into deep aquifers. Our atomic-scale studies utilize a Hydrothermal Atomic Force Microscope (HAFM), of our design, for molecular-level experiments on the kinetics of nucleation, step motion and other phenomena on mineral surfaces under conditions relevant to CO₂-sequestration. The same conditions used in HAFM experiments are also investigated with macroscopic hydrothermal reactors (for stoichiometric rate data) and geochemical reactive transport codes. This approach allows us to address many still-open questions concerning the exact forms for rate laws near and far from equilibrium, the microscopic interpretation of these rate laws, the activation energies and formation energies for key microscopic surface structures (*e.g.*, steps, kinks), and the impact of specific aquifer solute catalysts and inhibitors.

Results: During work on an enhanced HAFM, the importance of knowing solution composition *at the HAFM imaging location on the mineral surface* has come into stark focus. We therefore designed and implemented a fluid cell inlet jet for which hydrodynamics are well known over a range of flow velocities (Fig. 1). Recent tests following system improvements show that the current maximum operating conditions in the HAFM are 70 bars and 170 °C. We have studied the dissolution of magnesite and calcite (104) surfaces under a wide variety of conditions. For magnesite, step density, rather than step velocity, is a strong function of pH near the surface and that the step orientation is sensitive to pH (Figure 1). Mass transport is only important at very low fluid velocities for magnesite, but calcite dissolution generally occurs within the mixed transport-kinetics controlled regime where quantitative information can only be obtained by accounting for the transport components. Alkaline earth carbonate secondary precipitate formation on calcite surfaces significantly alters the net flux of Ca²⁺ and may passivate the CaCO₃ surface from further reaction. Macroscopic experiments designed to investigate the

simultaneous dissolution of labradorite and the precipitation of secondary carbonate minerals have been underway since December, 2001.

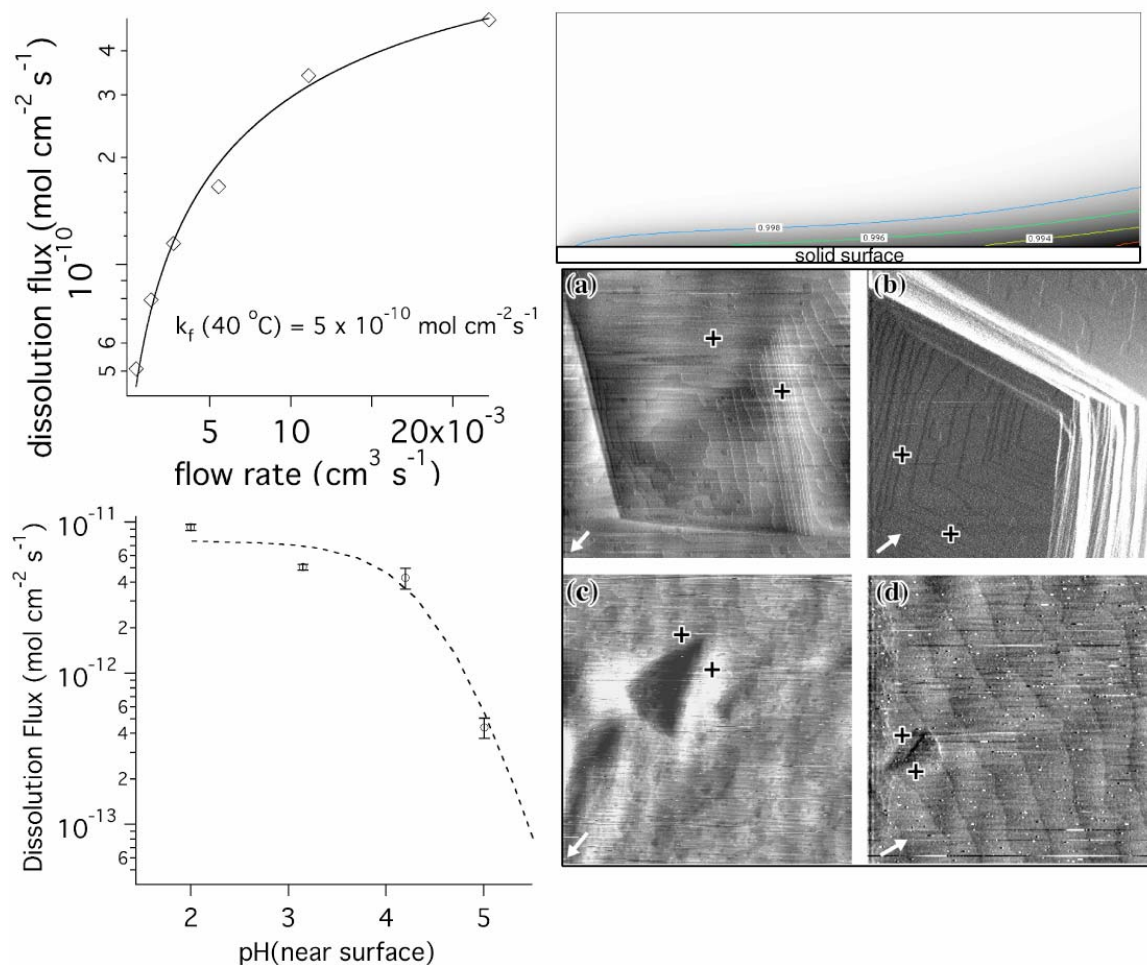


Figure. Clockwise from upper left (1) Dissolution rate of calcite versus fluid flow rate in the HAFM at 40 °C with an inlet pH = 7. The solid line is a theoretical model fit with one experimental parameter. (2) Two-dimensional concentration map (1.0 mm x 0.4 mm) in the HAFM fluid cell calculated for magnesite dissolution with a flow rate of $1.4 \times 10^{-3} \text{ cm}^3 \text{ s}^{-1}$ at pH = $-\log[\text{H}^+] = 4.2$ at 60 °C. The AFM tip scans the solid surface near the lower right corner of this map. Contours indicate the ratio of the spatially varying proton concentration to the inlet proton concentration, $[\text{H}^+]_{x,y}/[\text{H}^+]_{\text{inlet}}$. (3) HAFM images of magnesite during dissolution at 60 °C with inlet pH = (a) 5.0 (image size: 6.7 μm x 6.7 μm), (b) 4.2 (image size: 2.0 μm x 2.0 μm), (c) 3.2 (image size: 7.0 μm x 7.0 μm), (d) 2.0 (image size: 6.6 μm x 6.6 μm). Arrows indicate absolute sample orientation, showing rotational relationship among images. (4) Surface reaction limiting dissolution rate of magnesite as a function of pH at 60 °C. The dashed line is a theoretical fit to a model based on proton adsorption as a pre-equilibrium step.

YALE UNIVERSITY

Department of Geology and Geophysics
New Haven, Connecticut 06520-8109

Grant: DE-FG02-95ER14522

A Field Experiment on Plants and Weathering

Robert A. Berner, (203) 432-3183, fax (203) 432-3134, robert.berner@yale.edu

Objectives: For the year 2001 objectives were to: (1) submit a final paper concluding our study of the effects on geochemical cycling resulting from experimental deforestation, (2) continue our theoretical calculations of long-term carbon cycling and atmospheric CO₂, (3) conclude our study of the stomatal density of fossil leaves as an indicator of past levels of atmospheric CO₂ and (4) continue our study of the effects of varying O₂/CO₂ on the fractionation of carbon isotopes during photosynthesis and how results can be applied to theoretical calculations of the evolution of atmospheric oxygen.

Project Description: (1) A report on the drainage water chemistry, subsequent to the cutdown of pine trees from experimental plots at the Hubbard Brook Experimental Forest Station, has been submitted for publication (for a description of this research see the Report for 2000). (2) A revised GEOCARB model for the evolution of atmospheric CO₂ over Phanerozoic time has been published, (3) Ginkgo and Metasequoia leaves from herbarium collections have been studied to calibrate the paleo-CO₂ stomatal method and fossil Ginkgo and Metasequoia leaves from rocks have been measured. (4) In collaboration with Dr. David Beerling (Univ. Sheffield, UK), we have completed a first series of plant growth experiments under varying O₂/CO₂ and combined results with the determination at Yale of the carbon isotopic composition of fossil plants in order to make deductions about ancient O₂ levels.

Results: (1) Our revised GEOCARB calculations indicate that past levels of CO₂ probably varied more (but with the same overall pattern) than thought previously, with generally higher levels during the Mesozoic era. (2) The stomatal density for Ginkgo leaves collected over the past 140 years correlates very closely, in an inverse manner, with known atmospheric CO₂ levels. Using the calibration, values of paleo-CO₂ have been determined for portions of the Cretaceous, Paleocene and Eocene periods (70-45 Ma) and the results published in Science and Earth Science Reviews (3) In a new paper we show that changes in atmospheric O₂/CO₂ affect the fractionation of carbon isotopes during photosynthesis for a variety of land plants. These results have enabled the theoretical calculation of O₂/CO₂ levels over the Phanerozoic that show results for the Permo-Carboniferous that agree with our independent studies based carbon cycle modeling and the carbon isotopic analysis for fossil plants.

YALE UNIVERSITY

Department of Geology and Geophysics
New Haven, Connecticut 06520-8109

Grant: DE-FG02-01ER15173

Plants, Weathering, and the Evolution of Atmospheric Carbon Dioxide and Oxygen

Robert A. Berner, (203) 432-3183, fax (203) 432-3134, robert.berner@ yale.edu

Objectives: This grant was initiated August 15, 2001 so that the period covered is short. The objectives are a continuation of several of those from the preceding grant DE-FG02-95ER14522. (1) continue our theoretical calculations of long-term carbon cycling and atmospheric O₂ and CO₂, (2) continue our study of the stomatal density of fossil leaves as an indicator of past levels of atmospheric CO₂ and (3) continue our study of the effects of varying O₂/CO₂ on the fractionation of carbon isotopes during photosynthesis and how results can be applied to calculations of the evolution of atmospheric oxygen.

Project description: (1) The stomatal index of Ginkgo and Metasequoia leaves from herbarium collections were calibrated against CO₂ for the past 120 years and the stomatal method applied to the deduction of Miocene, Cretaceous, and Eocene paleo-CO₂ levels (2) In collaboration with Dr. David Beerling (Univ. Sheffield, UK), we completed measurements at Yale of the carbon isotopic composition of fossil plants, to help make deductions about ancient O₂ levels.

Results: (1) The stomatal index method has enabled estimation of CO₂ levels for portions of the Cretaceous, Paleocene and Eocene periods (70-45 Ma, (2) In a new paper (Beerling et al, 2002, Geochim. Cosmochim. Acta-in press) we show that changes in atmospheric O₂/CO₂ affected the fractionation of carbon isotopes during photosynthesis for a variety of land plants over Phanerozoic time. The results for the Permo-Carboniferous agree with our independent studies based on carbon cycle modeling.

YALE UNIVERSITY

Department of Geology and Geophysics
P.O. Box 208109
New Haven, Connecticut 06520-8109

Grant: DE-FG02-90ER14153

Reactive Fluid Flow and Applications to Diagenesis, Mineral Deposits, and Crustal Rocks

D. M. Rye, (203) 432-3174, fax (203) 432-3134, danny.rye@yale.edu) E. W. Bolton (203) 342-3149, edward.bolton@yale.edu)

Website: <http://www.geology.yale.edu/crustal-fluids>

Objectives: To initiate new: modeling of coupled fluid flow and chemical reactions of geologic environments; experimental and theoretical studies of water-rock reactions; collection and interpretation of stable isotopic and geochemical field data at many spatial and temporal scales on systems ranging from soils to metamorphic rocks.

Project Description: Theoretical modeling of coupled fluid flow and chemical reactions, involving kinetics, has been employed to understand the differences between equilibrium, steady-state, and non-steady-state behavior of the chemical evolution of open fluid-rock systems. The numerical codes developed in this project treat multi-component, finite-rate reactions combined with advective and dispersive transport in multi-dimensions. The code incorporates heat, mass, and isotopic transfer in both porous and fractured media. Experimental work has obtained the kinetic rate laws of pertinent silicate-water reactions and the rates of Sr release during chemical weathering. *Ab initio* quantum mechanical techniques were employed to obtain the kinetics and mechanisms of silicate surface reactions. Geochemical field-based studies were carried out on the mineralization and potential source rocks of the Irish base-metal sediment-hosted ore system, in veins and wall rocks of the Dalradian metamorphic complex in Scotland, and on weathering in the Columbia River flood basalts. The geochemical and isotopic field data, and the experimental and theoretical rate data, were used as constraints on the numerical models and to determine the length and time scales relevant to each of the field areas.

Results: Analytical and numerical models were extended for metamorphic processes in the presence of mixed volatiles (CO₂ and water). Depending on the rates of heating and fluid flow, these open-system, kinetic models can exhibit reaction histories with significant departures from equilibrium and can produce quite different fluid flux estimates from those based on the equilibrium approach. Although such flux estimates are typically within an order of magnitude of correctly modeled flow and reaction models, we have presented a more consistent model, and have shown the dangers of blindly applying the typically used flux calculations. These results should have major impact on how fluid/rock interaction is interpreted and the dominant role of open system behavior. Besides underscoring the central role of kinetic control, our models also illustrate the importance of metastable reactions. Our two-dimensional models were extended to include full dispersion of the binary fluid as well as matrix compaction following reactions, which create voids upon volatile release. Localized heating can drive fluid flows by

either reaction induced volatile production, or by buoyancy driven convection, depending on the permeability of the matrix.

Grain-scale oxygen isotope exchange modeling underscores the significance of a kinetic approach in open systems. Our results of detailed modeling of diffusion in grains indicate that the standard method of utilizing a $k_{\text{effective}}$ for the rate of exchange is only useful for slow flow rates and/or very fast diffusion rates, and can break down for systems composed of grains with differing diffusion rates. Complex zoning patterns within grains may be common. Dissolution and precipitation, along with simple models of Ostwald ripening, show profound influences on the isotopic evolution of the system.

A white light interferometric system directly measured dissolution rates of both dolomite and anorthite. These measurements revealed strong spatial variations of dissolution on crystal surfaces. Etch pits retreat at separate characteristic rates compared to the retreat of the rest of the surface. The observations have led to a new "stepwave" theory of dissolution kinetics.

Ab initio method calculations were performed to extract rate constants for hydrogen isotope exchange for the aqueous (7 water) orthosilicic acid system. These computations were computed using high-level *ab initio* vibrational frequencies. The rate constants computed suggest that the equilibration occurs less than a second at room temperature, indicating that the exchange rate between species in solution and the water are so fast that any reaction between species in solution and solid phases are likely to directly reflect the hydrogen isotopic composition of the fluid. Vibrational frequency calculations have also been performed for the oxygen isotope exchange reaction for the aqueous (7 water) orthosilicic acid system for rate constant calculations.

Biotite dissolution was characterized as a function of saturation state and pH. Strontium isotopic ratios of the biotite and the solution were also measured. Field studies, of the Columbia River basalt and surrounding rocks, found that weathering rates of basalt were about three times those of either diorite or granite. Strontium fluxes were approximately equal in all three rock-types, with Sr isotopic ratios similar to the parent rock. A coupled flow and mass transfer model showed that weathering of large volumes of fresh flood basalts will tend to lower the strontium isotopic composition of seawater, and at the same time tend to draw down the CO₂ concentration of the atmosphere.

Pb isotopic results from all possible source rocks in the Irish Midlands demonstrate unequivocally that the Pb in these world class ore bodies was largely derived from the underlying basement rocks and delivered to the ore deposition site by fluid flow in nearly vertical fractures. By implication, the low temperature fluid flow in the ore-formation part of the basin was profoundly affected by injection of fluid and heat of deep origin.

Light stable isotopic studies of the Dalradian Complex indicate large local fluid fluxes and mass transport were important processes throughout the complex.

Subject Index

- Acids, 16, 44, 47, 50, 67, 72, 101, 139, 140, 141, 144, 161, 162, 216, 241, 255
 organic, 66, 241, 255
- Actinides, 249
- Activity coefficients, 44, 153
- Age dating, 28, 45, 58, 59, 100, 109, 179, 180, 189, 218, 225
- Age dating
 exposure ages, 100
- Air-water interface, 27
- Aluminum, 31, 44, 45, 46, 47, 101, 102, 103, 112, 146, 156, 157, 162, 175, 192, 193, 197
- Amphiboles, 64, 68, 105
- Aqueous, 12, 26, 31, 33, 44, 45, 48, 50, 65, 66, 67, 69, 70, 72, 74, 103, 116, 121, 136, 139, 140, 146, 147, 153, 154, 159, 161, 162, 182, 195, 199, 200, 206, 216, 220, 222, 239, 240, 241, 255, 260
- Aqueous geochemistry, 241
- Aquifer, 26, 31, 32, 33, 47, 48, 97, 101, 131, 192, 214, 225, 259
- Atomic Force Microscopy, 12, 32, 49, 50, 60, 69, 70, 71, 72, 75, 76, 106, 127, 143, 156, 157, 158, 192, 194, 241
- Bacteria, 60, 65, 74, 75, 101, 156, 157, 158, 206, 248, 249
- Basalt, 14, 19, 24, 94, 116, 145, 172, 181, 262, 263
- Basalts
 MORB, 58, 116
- Beamlines, 117
- Biofilms, 206, 207, 249
- Biomineralization, 49, 75, 143, 144, 161, 248
- Birnessite, 16
- Bonding, chemical, 69, 80, 89, 120, 146, 153, 162, 206
- Borehole, 17, 18, 19, 43, 53, 77, 78, 90, 168, 196, 246, 250, 251
 stability, 250
- Boron, 91, 92
- Brines, 26, 44, 67, 118, 208, 209, 220, 224, 226, 239, 255
- Brucite, 62
- Calorimetry, 105
- Capillarity, 24, 86, 87, 128, 129, 148, 168, 187, 188, 211, 254
- Carbon, 29, 33, 34, 35, 40, 43, 46, 49, 53, 58, 65, 67, 70, 79, 84, 90, 99, 100, 108, 109, 118, 131, 136, 146, 150, 151, 184, 197, 201, 224, 255, 261
- Carbon
 carbon cycle, 58, 261
- Carbon 14, 45
- Carbon dioxide, 17, 19, 22, 26, 29, 33, 40, 41, 42, 43, 45, 46, 47, 48, 51, 61, 62, 65, 66, 67, 70, 78, 84, 86, 94, 95, 98, 99, 100, 106, 127, 128, 131, 146, 147, 168, 187, 197, 199, 206, 211, 220, 224, 232, 233, 235, 236, 246, 255, 259, 261, 262, 263
- Carbon dioxide sequestration, 17, 26, 33, 41, 46, 47, 48, 86, 106, 127, 128, 187, 220, 259
- Carbonates, 14, 22, 29, 47, 48, 49, 51, 65, 70, 72, 86, 105, 106, 108, 110, 118, 121, 122, 127, 143, 144, 146, 147, 152, 178, 179, 184, 189, 206, 208, 224, 253, 259
 minerals
 calcite, 43, 48, 49, 50, 53, 63, 65, 66, 67, 70, 71, 72, 89, 90, 106, 108, 121, 127, 142, 143, 144, 179, 180, 224, 225, 233, 236, 258, 259, 260
- Carbonates
 minerals, 47, 49, 65, 70, 108, 143, 224
 minerals
 dolomite, 65, 89, 106, 108, 120, 233, 236
- Catalysis, 16
- Cesium, 154, 159
- Chemical potential, 139, 140
- Chromatography, 16, 201, 202
- Chromium, 15, 35, 117, 121, 154, 159, 207, 241
- Clays, 17, 27, 30, 35, 43, 53, 66, 88, 90, 91, 105, 121, 158, 189, 190, 210, 222, 233, 236
 kaolinite, 27, 89, 121, 156, 157, 158
 smectite, 89, 91, 110, 152, 189
- Clays
 illite, 27, 91, 110, 152, 189
 montmorillonite, 27, 30, 31, 66, 89

Climate, 11, 28, 49, 64, 79, 96, 109, 131, 134, 184, 225, 240
 Climate Change, 28, 49, 79, 109, 184
 Colloid transport, 27, 69
 Colloids, 27, 69, 96
 Compaction, 20, 80, 84, 119, 164, 184, 186, 210, 220, 222, 223, 250, 251
 Conductivity
 electrical, 17, 41, 43, 53, 90, 164, 210, 242, 258
 hydraulic, 83, 166, 191
 Constitutive relationships, 87, 129, 188
 Convection, 112, 141, 169, 226, 252, 262
 thermohaline, 112, 226, 227
 Cosmic rays, 45, 57
 Creep, 170, 222, 223, 244
 Crust, 35, 43, 53, 55, 63, 90, 112, 138, 169, 186, 199, 206, 244, 253
 Crystallography, 117
 deep saline aquifer, 51, 197
 Defects, 64, 70, 75, 76, 143, 155, 160, 192, 216
 Deforestation, 261
 Diagenesis, 16, 91, 110, 127, 148, 152, 153, 189, 190, 201, 222
 Diamond anvil, 117
 Diffusion, 28, 35, 44, 45, 63, 64, 67, 68, 83, 113, 116, 118, 121, 125, 141, 146, 147, 166, 170, 191, 199, 211, 224, 226, 262
 Diffusion
 coefficients, 44, 64, 68, 116, 121, 125, 147, 211
 Dissolution, 12, 26, 28, 29, 42, 44, 46, 47, 48, 59, 60, 66, 70, 71, 72, 75, 76, 87, 88, 95, 101, 102, 116, 121, 129, 141, 153, 154, 155, 156, 157, 158, 159, 160, 161, 188, 192, 194, 199, 211, 222, 224, 249, 259, 260, 262
 Earth materials, 54, 79, 120, 184
 Earthquakes, 19, 39, 54, 93, 124, 244
 Elastic Properties, 209, 210
 Electric double layers, 72
 Electrical properties, 41, 42, 203
 Electrolytes, 44, 72, 139, 140, 153
 Electron transfer, 75, 76, 182
 Energetic particles, 57
 Energy transport, 125
 Enthalpy, 26, 112, 161
 Entropy, 113
 Environment, 19, 28, 49, 56, 57, 58, 74, 75, 96, 120, 121, 125, 127, 182, 195, 196, 203, 216, 218, 238, 248, 249
 Epidote, 64, 68, 237, 238
 Equation of state, 44, 140
 Erosion, 37, 59, 141, 142, 167, 261
 rates, 59
 Fault, 110, 152, 196, 214, 237, 238, 244
 faults, 26, 93, 110, 124, 125, 145, 152, 172, 196, 213, 214, 232, 233, 235, 236, 237, 238, 244
 Faults and faulting, 28, 93, 110, 112, 124, 145, 148, 152, 164, 169, 172, 185, 196, 213, 214, 232, 233, 235, 236, 237, 238, 244, 253, 258
 gouge, 214, 233, 236, 253
 mechanics, 164, 237, 258
 San Andreas Fault, 244
 Feldspars, 63, 68, 127, 164, 192, 210, 238, 253
 albite, 68, 192, 193
 anorthite, 262
 orthoclase, 12, 127
 Feldspars
 plagioclase, 68, 110, 152, 192
 Ferric iron oxides, 75
 Fingering, 87, 111, 129, 188
 Fluid conductivity, 18
 Fluid flow, 14, 15, 33, 37, 55, 79, 84, 86, 88, 110, 118, 123, 125, 127, 128, 129, 130, 136, 141, 152, 168, 181, 184, 186, 187, 188, 189, 199, 208, 210, 213, 220, 222, 250, 252, 256, 262, 263
 fast flow, 39, 125, 194
 multiphase, 26, 82, 86, 128, 148, 175, 181, 187, 230, 254
 porous media, 111, 205
 reactive, 42, 213
 unsaturated, 24, 87, 129, 188
 Fluid inclusions, 63, 118, 120, 239, 240
 Fluid migration, 29, 33, 64, 84, 189, 213
 Fluid-rock interactions, x, 14, 62, 63, 68, 108
 Fluorescence, 14, 32, 117, 120, 206
 Fractional derivatives, 55

Fractionation, 62, 63, 65, 67, 91, 94, 108, 116, 121, 261
 Fractures, 14, 20, 24, 26, 29, 37, 39, 42, 43, 80, 81, 86, 87, 88, 123, 125, 128, 129, 132, 133, 141, 142, 148, 173, 174, 184, 187, 188, 194, 196, 197, 208, 213, 214, 216, 227, 238, 250, 251
 aperture, 24, 42, 43, 88, 125, 129, 188, 194, 214
 mechanics, 26, 184
 systems, 123, 132
 Friction, 93, 123, 124
 Gas
 hydrates, 210, 256
 Hydrates, 147, 240
 natural, 34, 95, 137, 201, 224, 239, 255
 noble, 29, 33, 34, 45, 51, 100, 136, 137, 138
 Gassmann technique, 39, 40, 208, 209, 220
 Geochemical transport, x, 12, 199
 Geochemistry low temperature geochemistry, x, 45, 58, 62, 94, 108, 117, 204, 206, 220, 225, 232, 235
 Geomorphology, 45, 134
 Geophysics, x, 17, 19
 Geothermal, 28, 42, 61, 62, 65, 66, 108, 109, 110, 152, 215, 252
 GIXAS, 32
 Glaciation, 134
 Glass, 24, 64, 80, 81, 83, 94, 112, 161, 162, 164, 165, 166, 168, 173, 191, 192, 193, 205, 254
 Glasses
 aluminosilicate, 30, 161, 162, 192
 Gold, 64, 118, 162
 Grain boundaries, 43, 53, 90, 154, 155, 159, 160, 199
 Granite, 54, 145, 168, 172, 244, 250, 252, 253, 263
 Granular flow, 123
 Gravity, 17, 26, 49, 82, 87, 111, 123, 128, 129, 175, 187, 188, 205, 215, 230
 Ground-penetrating radar, 228, 229
 Groundwater, 17, 28, 29, 33, 34, 65, 110, 125, 136, 137, 152, 168, 218, 225, 244, 249
 hydrocarbon movement, 35, 91, 138
 Hydrocarbon source, 33, 34, 98, 136, 137
 Hydrocarbons, 33, 34, 35, 39, 66, 84, 91, 98, 108, 136, 137, 138, 140, 168, 220, 228, 239, 256
 Hydrology, x, 29, 213, 225
 Hydrolysis, 66, 192, 193
 Hydrothermal, 42, 48, 62, 63, 64, 65, 67, 96, 108, 109, 117, 118, 120, 164, 189, 215, 238, 252, 253, 258, 259
 fluids, 96, 117, 120, 189
 systems, 42, 108, 109, 215
 hydroxyl, 30, 103, 116, 192
 Imaging, x, 19, 22, 33, 40, 42, 78, 82, 114, 118, 119, 122, 154, 155, 157, 159, 160, 168, 173, 175, 194, 197, 228, 230, 242, 246
 seismic, 19, 78, 246
 subsurface, x
 subsurface geophysical imaging, x
 Instability, 56, 109, 111, 169, 170, 226, 227
 Inverse methods, 17, 18, 19, 77, 78, 132, 203, 242, 244, 246
 Iron, 15, 31, 32, 59, 60, 64, 65, 73, 74, 75, 76, 101, 102, 105, 106, 120, 121, 154, 156, 157, 158, 159, 216, 249
 oxides, 16, 59, 117, 182
 goethite, 32, 60, 72, 75, 101, 102, 121, 156, 206, 241
 hematite, 32, 59, 60, 72, 75, 76, 106, 117, 121, 156
 magnetite, 66, 72, 73, 75, 121, 189
 Iron
 oxides, 32, 60, 121
 oxides
 hematite, 107
 magnetite, 66
 isotope partitioning, 63, 65, 66, 94
 Isotopes, 29, 33, 34, 51, 62, 91, 94, 96, 108, 109, 131, 136, 137, 192, 204, 218, 253
 argon, 108
 carbon, 65, 66, 94, 109, 146, 233, 236
 chlorine, 51, 100
 cosmogenic, 45, 59, 100
 fractionation, 62, 63, 65, 67, 91, 94, 116, 252, 255
 helium, 29, 137

hydrogen, 62, 68, 116, 150, 151, 263
 Iodine, 51
 oxygen, 63, 64, 65, 66, 94, 108, 109, 204, 252, 253, 262
 stable isotopes, 62, 67, 94, 108, 151, 252
 Isotopes
 carbon, 108, 109, 131, 261
 cosmogenic, 34, 51, 138
 exchange, 67, 150
 osmium, 96
 uranium, 29, 51
 Joint inversion, 17, 18, 132, 203
 Kerogen, 16, 98, 99, 150, 255
 Kinetics, 12, 35, 47, 48, 49, 50, 64, 65, 66, 70, 75, 101, 116, 118, 127, 142, 143, 144, 153, 156, 164, 223, 224, 259, 260, 262, 263
 Krypton, 34, 136, 137, 218, 219
 Lattice-Boltzman models, 79, 123, 141, 173
 Lead, 28, 105, 108, 109, 121, 122, 162, 179, 180, 206, 207, 248, 249, 253, 263
 Lithology, 17, 38, 114, 197, 208
 Magmatism, 28, 29, 58, 94, 109, 112, 113, 169, 215, 237, 252, 253
 Magnetosphere, 56, 57
 Manganese oxide, 105, 121
 Mantle, 39, 40, 43, 53, 80, 90, 96, 98, 112, 117, 137, 169, 170, 199
 Marble, 43, 141
 Mass spectrometry, 16, 43, 45, 51, 53, 90, 94, 108, 192, 225
 accelerator mass spectrometry, 45, 46, 51
 inductively coupled plasma, 101
 ion microprobes, 63, 67, 68, 91, 108, 109, 192, 252
 resonance ionization, 218
 time-of-flight, 218, 219
 time-of-flight Seismic crosswell tomography, 43, 53, 90, 218
 Mass transfer, 35, 63, 83, 87, 88, 98, 99, 110, 128, 129, 152, 166, 187, 188, 191, 263
 Mechanics
 damage, 185
 micromechanics, 55, 80
 Melts, 94, 112, 121, 169
 Mercury, 162
 Metamorphism, 29, 43, 53, 90, 91, 164, 204, 258
 Methane, 33, 61, 131, 201, 210, 233, 236, 239, 240, 255, 257
 Micas, 105, 127, 154, 159, 185, 238
 biotite, 64, 154, 155, 159, 160, 238
 Micas
 muscovite, 13, 127
 Microorganisms, 16, 59, 60, 65, 74, 76, 118, 156, 157, 158, 206, 241, 248, 249
 Microorganisms
 microbes, 241
 Microstructure, 15, 40, 54, 79, 184, 199, 258
 Mineral-fluid interface, 12, 154, 159
 Minerals
 dissolution, 28, 47, 66, 156, 157, 158, 259
 growth, 48, 50, 259
 solubility, 144
 surface chemistry, 12, 35, 48, 66, 67, 70, 74, 106, 117, 121, 143, 144, 146, 153, 156, 161, 182, 195, 206, 207, 241, 259, 263
 Molecular dynamics, 72, 74, 88, 140, 146, 169
 Molecular modeling, 88, 161
 NaCl, 26, 44, 45, 63, 67, 68, 146, 147, 239
 Nanoscale, 55, 169
 Neodymium, 28, 29, 225
 Nitrogen, 29, 150
 Nonlinear, 54
 nonlinear behavior, 54
 Nuclear Magnetic Resonance (NMR), 82, 103, 146, 150, 162, 168, 175, 192, 230
 Numerical simulation numerical modeling, 26, 42, 59, 80, 83, 86, 87, 111, 123, 128, 166, 168, 187, 191, 205, 227
 Oceans, 29, 42, 49, 58, 95, 96, 116, 118, 211, 218, 224, 256
 Olivine, 94, 100, 170
 Organic sulfur, 16
 Oxidation state, 35, 120, 121
 Paleoclimate, 58, 108, 109
 Paleomagnetism, 189
 Peclet number, 111, 125
 Permeability, 14, 15, 17, 24, 37, 38, 39, 42, 47, 55, 80, 83, 84, 85, 86, 108, 110, 111, 118, 123, 125, 148, 152, 164, 166, 168, 177, 178,

185, 186, 191, 194, 197, 199, 205, 210, 213,
 214, 220, 226, 227, 228, 232, 233, 235, 242,
 258
 measurement, 85, 86, 177, 178, 232, 235
 Petroleum, 16, 17, 34, 52, 82, 86, 98, 108, 110,
 128, 136, 151, 152, 175, 187, 196, 201, 230,
 239, 242, 255
 migration, 110, 152
 pH, 12, 27, 29, 31, 47, 65, 66, 67, 68, 69, 70,
 75, 101, 154, 158, 159, 162, 182, 192, 207,
 248, 255
 Phase
 relationships, 61
 Plasma instabilities, 56
 Platinum, 64
 Pore structure, 118, 119, 164, 168, 181, 184,
 258
 Poroelastic properties, 38, 39
 Porosity, 14, 17, 18, 20, 34, 39, 40, 42, 47, 80,
 84, 86, 113, 119, 137, 164, 165, 178, 181,
 184, 194, 209, 210, 213, 220, 228, 232, 235,
 250, 251, 258
 Porous media, 27, 41, 55, 87, 111, 112, 123,
 127, 128, 168, 169, 187, 205, 214, 227
 Precipitation, 12, 26, 28, 29, 42, 44, 46, 47, 48,
 58, 65, 66, 71, 118, 134, 143, 146, 189, 199,
 206, 222, 223, 248, 249, 259
 pressure-volume-temperature, 239
 Protonation, 48, 66, 153, 195, 260
 Pyrite, 120, 182, 216
 Pyrolysis, 98, 150
 hydrous, 150
 Quantum mechanics, 139, 161, 162, 262
 Quartz, 31, 32, 45, 46, 63, 66, 100, 118, 127,
 153, 164, 199, 210, 222, 223, 237, 238, 250,
 252, 253
 Reactive transport, 35, 36, 48, 259
 Reduction, 12, 35, 37, 46, 60, 74, 75, 76, 80,
 98, 111, 118, 119, 154, 159, 164, 206, 209,
 214, 238, 249, 250
 Remediation, 17, 28, 42, 79, 86, 106, 117, 128,
 184, 187, 242
 Reservoirs
 characterization, 39, 232, 235
 dynamics, 62
 Resolution, 12, 14, 15, 22, 35, 40, 41, 42, 63,
 72, 75, 78, 79, 80, 86, 87, 108, 109, 118,
 120, 127, 128, 132, 141, 142, 154, 155, 159,
 160, 168, 181, 183, 187, 194, 201, 203, 218,
 219, 221, 225, 228, 234, 244, 246, 248
 Retrograde metamorphism, 43, 53, 90
 Reynolds
 equation, 173
 number, 80, 125
 Rheology, 112, 169, 170
 Richard's equation, 87, 129, 188
 Rivers, 167, 256
 Rock mechanics, x
 Rock mechanics, x, 79, 184
 Rock physics, 22, 38
 Sandstone, 14, 20, 21, 22, 54, 80, 84, 85, 86,
 164, 165, 168, 177, 178, 181, 184, 194, 213,
 214, 232, 235, 250, 251
 scanning probe microscopy, 70
 Sedimentology, 15, 29, 35, 110, 122, 127, 152,
 226, 256, 262
 Sediments, 14, 15, 16, 29, 31, 34, 49, 60, 64,
 117, 120, 122, 134, 137, 179, 201, 207, 226,
 248
 Seepage, 233, 236
 seismic absorption, 22
 Seismic velocity, 17, 39, 119
 Seismic wave propagation, 20, 52, 54, 77, 197
 Seismology, 19
 computational, 19
 seismic anisotropy, 197
 Selenium, 35
 Shale, 91, 120, 164, 214
 Shear localization, 186
 Silica, 20, 31, 47, 116, 153, 161, 162, 263
 Silicates, 20, 21, 29, 47, 91, 94, 105, 112, 116,
 153, 154, 155, 159, 160, 199, 215, 259, 262
 Soils, 16, 35, 106, 117, 121, 195, 207, 225,
 241, 248, 262
 Solar wind, 56
 Solid solutions, 105, 106, 108, 122, 249
 Solubility, 34, 44, 66, 67, 118, 136, 137, 144,
 147, 161, 239

Sorption, 12, 13, 31, 32, 35, 66, 69, 71, 74, 88,
 117, 120, 121, 146, 147, 153, 154, 159, 168,
 182, 183, 195, 206, 207, 248
 Space plasmas, 56
 Speciation, 16, 26, 35, 67, 72, 112, 118, 120,
 122, 153, 206, 207, 248
 Spectrometry
 infrared, 94
 Mössbauer, 75
 Spectroscopy, 12, 14, 16, 31, 43, 53, 90, 94,
 103, 117, 127, 146, 154, 158, 159, 182, 183,
 192, 195, 206, 207, 216, 218, 239, 240
 electron spectroscopy
 electron energy loss spectroscopy (EELS),
 154, 159
 XANES, 16, 35, 122, 162
 X-ray, 195
 X-ray photoelectron spectroscopy, 154, 158,
 159, 182, 183
 Speleothems, 109, 225
 Strontium, 28, 29, 69, 96, 105, 118, 189, 192,
 207, 225, 253, 262, 263
 Sulfates, 16, 44, 45, 67, 105, 139, 183, 206,
 249
 Sulfides, 118, 120, 248, 249
 Sulfur, 16, 182, 183, 216
 Surface
 charge, 72, 127, 153, 206
 chemistry, 31, 70, 121, 130
 Synchrotron, 12, 14, 16, 31, 35, 71, 75, 89,
 117, 120, 184, 195, 206, 216, 249
 Synchrotron radiation, 12, 117
 Tectonics, 28, 84, 110, 148, 152, 164, 196, 258
 Thermochronometry, 108
 Thermodynamics, 44, 49, 50, 61, 62, 74, 75,
 98, 105, 106, 112, 139, 144, 147, 153, 202,
 239, 255
 Thorium, 51, 64, 96, 97
 Tomography, 14, 15, 40, 41, 132, 181, 184
 Trace elements, 35, 113, 120, 204, 225
 Transmission Electron Microscopy (TEM), 32,
 154, 159
 Transport coefficients, 44, 123
 Transport properties, 41, 112, 154, 159, 164,
 169, 194, 210, 258
 TRXRF, 32
 Tuff, 85, 177
 Uranium series, 58, 109, 225
 vadose, 24, 27, 28, 97, 225
 Vertical-scanning interferometry, 72
 Viscoelasticity, 39, 170
 Volcanoes, 14, 28, 58, 100, 109, 204, 215, 252
 Water, 61, 62, 94, 95, 98, 99, 107, 116, 146,
 147, 199, 216, 222, 223, 239
 Water-rock interaction, 239
 Wave equation one way wave equation, 52,
 114
 Wave propagation, 19, 20, 40, 52, 53, 54, 77,
 197, 209
 Weathering, 29, 47, 96, 97, 120, 121, 127, 153,
 197, 261, 262, 263
 rock varnish, 134
 Xenon, 28, 34, 136, 137
 X-ray diffraction, 71, 207
 X-ray scattering, 12
 Zeolites, 105

Author Index

<u>Contributor</u>	<u>Organization</u>	<u>Page</u>
Aldridge, David. F.	Sandia National Laboratories	73
Alumbaugh, David. L.	University of Wisconsin	252
Amonette, J. E.	Pacific Northwest National Laboratory	65
Anovitz, L. M.	Oak Ridge National Laboratory	55
Aydin, A.	Stanford University	217
Baer, D. R.	Pacific Northwest National Laboratory	65
Banfield, J. F.	University of Wisconsin	254
Banner, J. L.	University of Texas	230
Bedzyk, Michael. J.	Northwestern University	2
Bénézeth, P.	Oak Ridge National Laboratory	60,63
Benson, D.	Desert Research Institute	132
Berge, P. A.	Lawrence Livermore National Laboratory	30,211
Bernabé, Yves	Université Louie Pasteur, France	164
Berner, R. A.	Yale University	267
Berry, D.	Virginia Polytechnic Institute & State University	247
Berryman, James. G.	Lawrence Livermore National Laboratory	30,31
Beveridge, T.	University of Guelph	71
Bhattacharya, Janok	University of Texas	233
Birn, J.	Los Alamos National Laboratory	49
Blair, S. C.	Lawrence Livermore National Laboratory	29
Blencoe, J. G.	Oak Ridge National Laboratory	55
Bodnar, R. J.	Virginia Polytechnic Inst. & State Univ.	245
Boles, James. R.	University of California at Santa Barbara	107,150
Bolton, E. W.	Yale University	268
Booker, J. R.	University of Washington	248
Bourcier, W. L.	Lawrence Livermore National Laboratory	34,
Brantley, Susan. L.	The Pennsylvania State University	194,196
Broecker, Wallace. S.	Columbia University	132
Brown Jr., Gordon. E.	Stanford University	209
Brown, Stephen.R.	New England Research	77,175
Burns, Daniel R.	Massachusetts Institute of Technology	169
Burton, E.A.	Lawrence Livermore National Laboratory	34
Caffee, M.	Lawrence Livermore National Laboratory	37,43,52,97
Caprihan, Arvind.	New Mexico Resonance	77
Carroll, Susan. A.	Lawrence Livermore National Laboratory	39,
Casey, William.H.	University of California at Davis	100,103
Chester, F. M.	Texas A&M University	227
Chester, J. S.	Texas A&M University	227
Chialvo, A.A.	Oak Ridge National Laboratory	63
Cole, D. R.	Oak Ridge National Laboratory	56,57,59,62
Constable, Steven	Scripps Institute of Oceanography, UCSD	206

Cygan, R. T.	Sandia National Laboratories	85
Daily, William D.	Lawrence Livermore National Laboratory	32
Datta-Gupta, Akhil	Texas A & M University	225
Davis, James.A.	U. S. Geological Survey	23
de Groot-Hedlin, Cathrine	Scripps Institute of Oceanography, UCSD	206
DePaolo, Donald. J.	Lawrence Berkeley National Laboratory	19
de Souza, Anthony R.	National Academy of Sciences	173
De Yoreo, Jim	Lawrence Livermore National Laboratory	41
Dietrich, W. E.	University of California, Berkeley	52,97
Dixon, D. A.	Pacific Northwest National Laboratory	67,70
Dove, Patricia. M.	Georgia Institute of Technology	41,141
Duba, A. G.	Lawrence Livermore National Laboratory	35,46,87
Dupuis, M.	Pacific Northwest National Laboratory	67
Durham, W. B.	Lawrence Livermore National Laboratory	34
Dvorkin, Jack.	Stanford University	214
Eggleston, Carrick M.	University of Wyoming	40,265
Eick, M.	Virginia Polytechnic Institute & State University	247
Elmore, R. D.	University of Oklahoma	191
Elsworth, Derek	The Pennsylvania State University	196
Engel, M. H.	University of Oklahoma	191
Epstein, S.	California Institute of Technology	91
Evans, J. Brian	Massachusetts Institute of Technology	164,264
Evans, James. P.	Utah State University	143,174,237,241,243
Fehler, Michael.	Los Alamos National Laboratory	45,
Felmy, A. R.	Pacific Northwest National Laboratory	70
Fenter, Paul.	Argonne National Laboratory	2
Finkel, R.C.	Lawrence Livermore National Laboratory	37,52,97
Forster, Craig.	University of Utah	233,237,241
Fredrich, Joanne T.	Sandia National Laboratories	76,186
Fredrickson, J. K.	Pacific Northwest National Laboratory	71
Garven, Grant T.	Johns Hopkins University	107,150
Gary, S. P.	Los Alamos National Laboratory	49
Ge, Shemin.	University of Colorado	122
Gibson, Richard L.	Texas A & M University	225
Glass, R. J.	Sandia National Laboratories	84,125,189
Goldstein, S. J.	Los Alamos National Laboratory	51
Gorby, Y.	Pacific Northwest National Laboratory	71
Grader, Abraham S.	The Pennsylvania State University	196
Graham, A.	Texas Tech University	79,177,235
Grechka, Vladimir.	University of Colorado	130
Guyer, R. A.	Los Alamos National Laboratory	47,
Haggerty, Roy	Oregon State University	80,166,193
Haimson, B. C.	University of Wisconsin	256
Hajash, A.	Texas A&M University	227
Hamilton, W.	Oak Ridge National Laboratory	63

Hanson, G. N.	State University of New York, Stony Brook	181,
Harrison, T. M.	University of California at Los Angeles	105
Harvey, Charles	Massachusetts Institute of Technology	80,166,193
Helgerud, M.	Stanford University	163
Helgeson, Harold C.	University of California, Berkeley	95
Herbert, Bruce	Texas A & M University	225
Hersman, Larry E.	Los Alamos National Laboratory	53,98,155
Hervig, Richard. L.	Arizona State University	68
Hestir, Kevin.	Utah State University	143,174,243
Higgins, Steven. R.	University of Wyoming	40,265
Hochella Jr., M.F.	Virginia Polytechnic Institute & State University	247
Holcomb, D. J.	Sandia National Laboratories	81
Horita, J.	Oak Ridge National Laboratory	56,59,62
Hoversten, G. Michael	Lawrence Berkeley National Laboratory	8
Hudson, G.B.	Lawrence Livermore National Laboratory	43
Ilton, Eugene S.	Lehigh University	153,159
Ingber, M.	University of New Mexico	79,177,235
Johnson, A.M.	Purdue University	198
Johnson, L. R.	Lawrence Berkeley National Laboratory	10
Johnson, Paul A.	Los Alamos National Laboratory	46
Jones, K. W.	Brookhaven National Laboratory	4
Kennedy, B. Mack	Lawrence Berkeley National Laboratory	19,25,134
Kirkpatrick, R.James	University of Illinois at Urbana-Champaign	144
Klein, W.	Boston University	90,121
Klusman, Ronald W.	Colorado School of Mines	128
Knauss, Kevin G.	Lawrence Livermore National Laboratory	39,40,265
Koplik, Joel	City College of the City University of NY	120
Kronenberg, A. K.	Texas A&M University	227
Labotka, T. C.	University of Tennessee	223
Ladd, Anthony, JC	University of Florida	29,139
Larner, Kenneth L.	Colorado School of Mines	130
Lay, T.	University of California at Santa Cruz	111
Lee, Ki Ha	Lawrence Berkeley National Laboratory	8
Lindquist, W.Brent	State University of New York, Stony Brook	183
Lins Neto, R. D.	Pacific Northwest National Laboratory	70
Little, J.	Virginia Polytechnic Institute & State University	247
Liu, Tanzhuo.	Columbia University	132
Liyang, L.	Oak Ridge National Laboratory	63
Long, Jane. C. S.	University of Nevada at Reno	143,174,243
Majer, E. L.	Lawrence Berkeley National Laboratory	10
Mamora, Daulat	Texas A & M University	229
Martel, Stephen	University of Hawaii	143,174,243
Mastalerz, M.	Indiana University	148
Mathez, E. A.	American Museum of Natural History	35,46,87
Maurice, Patricia A.	Kent State University	53,98,155

Mavko, G. M.	Stanford University	211
Maxworthy, Tony	University of Southern California	208
McEvelly, Thomas V.	Lawrence Berkeley National Laboratory	10
McKay, L. D.	University of Tennessee	223
McMechan, George. A.	University of Texas at Dallas	233
Meiburg, Eckart	University of California at Santa Barbara	108
Meigs, Lucy	Sandia National Laboratories	80,166,193
Meyers, W. J.	State University of New York, Stony Brook	181,
Miller, Donald.G.	Lawrence Livermore National Laboratory	36
Mok, Ulrich	Massachusetts Institute of Technology	164
Mondy, L.	Sandia National Laboratories	79,177,235
Morris, J.P.	Lawrence Livermore National Laboratory	29
Morrison, H. Frank	Lawrence Berkeley National Laboratory	8
Morse, John W.	Texas A & M University	229
Muir, Francis	Stanford University	211
Murrell, M. T.	Los Alamos National Laboratory	51
Myer, Larry R.	Lawrence Berkeley National Laboratory	11,13
Myneni, Satish, C.B.	Princeton University	197
Nagy, Kathryn, L.	University of Colorado	124
Naney, M.T.	Oak Ridge National Laboratory	55
Navrotsky, Alexandra	University of California at Davis	102
Newman, Gregory A.	Sandia National Laboratories	74,252
Newmark, Robin L.	Lawrence Livermore National Laboratory	32,
Nicholl, M. J.	Oklahoma State University	84,125,189
Nihei, Kurt. T.	Lawrence Berkeley National Laboratory	13
Nimz, G.J.	Lawrence Livermore National Laboratory	43
Nishiizumi, K.	University of California at Berkeley	52,97
Nur, Amos.	Stanford University	214
Olsson, W. A.	Sandia National Laboratories	81
Orr, Franklin.M.	Stanford University	215
Ortoleva, Peter J.	Indiana University	146
Palmer, D.A.	Oak Ridge National Laboratory	63
Pantano, Carlo.	The Pennsylvania State University	194
Parks, G. A.	Stanford University	209
Phillips, Brian L.	University of California at Davis	100
Pollard, D. D.	Stanford University	217
Potts, M.	Virginia Polytechnic Institute & State University	247
Pruess, Karsten	Lawrence Berkeley National Laboratory	17
Pyrak-Nolte, Laura J.	Purdue University	200
Rajaram, H.	University of Colorado	84,125,189
Ramirez, A.L.	Lawrence Livermore National Laboratory	32
Rard, Joseph. A.	Lawrence Livermore National Laboratory	36
Reedy, Robert	Los Alamos National Laboratory	52,97
Reeves, G. D.	Los Alamos National Laboratory	50
Reitmeyer, Rebecca	U. S. Geological Survey	23

Richter, Frank M.	University of Chicago	113
Riciputi, L. R.	Oak Ridge National Laboratory	57,62
Rivers, Mark L.	University of Chicago	114
Roberts, J. J.	Lawrence Livermore National Laboratory	33
Rock, Peter A.	University of California at Davis	103
Rothman, Daniel H.	Massachusetts Institute of Technology	167
Rudnicki, J. W.	Northwestern University	188
Rundle, John. B.	University of Colorado	90,121
Rustad, J. R.	Pacific Northwest National Laboratory	67,70
Rye, D. M.	Yale University	268
Schimmelmann, A.	Indiana University	148
Schoonen, Martin A. A.	State University of New York, Stony Brook	184,221
Seewald, Jeffrey.	Woods Hole Oceanographic Institution	261
Segall, P.	Stanford University	220
Shankland, T. J.	Los Alamos National Laboratory	35,46,47,87
Sharp, John M.	University of Texas	231
Shock, Everett. L.	Washington University	137
Silver, E.	University of California at Santa Cruz	111
Simmons, Craig T.	Flinders University, South Australia	231
Smith, E.	Los Alamos National Laboratory	47,
Sorensen, Sorena S.	Smithsonian Institution	207
Spera, F. J.	University of California at Santa Barbara	109,171
Spetzler, Hartmut	University of Colorado	122,127
Sposito, Garrison	Lawrence Berkeley National Laboratory	22,53,98,155
Stockman, Harlan W.	Sandia National Laboratories	77,175
Stolper, E.	California Institute of Technology	91
Straatsma, T. P.	Pacific Northwest National Laboratory	70
Strongin, Daniel R.	Temple University	184,221
Sturchio, Neil C.	Argonne National Laboratory	12
Sutton, Stephen R.	University of Chicago	114,117
Sverjensky, Dimitri A.	Johns Hopkins University	151
Symons, N.P.	Sandia National Laboratories	73
Tadanier, C.	Virginia Polytechnic Institute & State University	247
TenCate, J. A.	Los Alamos National Laboratory	47,
Thonnard, N.	University of Tennessee	223
Tidwell, Vincent C.	Sandia National Laboratories	82,179
Toksöz, M. N.	Massachusetts Institute of Technology	45,169
Tokunaga, T. K.	Lawrence Berkeley National Laboratory	15,27
Torgerson, Thomas	University of Connecticut	25,134
Tossell, J. A.	University of Maryland	161
Travis, B. J.	Los Alamos National Laboratory	48
Tripp, Alan C.	University of Utah	239
Tsang, Chin-Fu	Lawrence Berkeley National Laboratories	17
Tsvankin, Ilya	Colorado School of Mines	130,211
Unsworth, M.	University of Washington	248,250

Vairavamurthy, Murthy A.	Brookhaven National Laboratory	6
Valley, J. W.	University of Wisconsin	258
Vasco, D.	Lawrence Berkeley National Laboratory	8
Veblen, David R.	Johns Hopkins University	153,159
Wan, Jiamin	Lawrence Berkeley National Laboratory	18
Wang, H. F.	University of Wisconsin	29,260
Wasserburg, G. J.	California Institute of Technology	93
Watson, E. B.	Rensselaer Polytechnic Institute	202
Waychunas, Glenn A.	Lawrence Berkeley National Laboratory	23
Wesolowski, D. J.	Oak Ridge National Laboratory	60,63
Whelan, J. K.	Woods Hole Oceanographic Institution	262
Williams, Lynda	Arizona State University	68
Wilson, John L.	New Mexico Institute of Mining and Technology	82,179
Wong, Teng-fong	State University of New York at Stony Brook	76,
Wood, R. H.	University of Delaware	137
Wu, Ru-Shan	University of California at Santa Cruz	111,
Wu, X. Y.	University of California at Santa Cruz	111
Xie, X. B.	University of California at Santa Cruz	111
Yuen, David A.	University of Minnesota	48,171
Zachara, J. M.	Pacific Northwest National Laboratory	71
Zhu, Wenlu	Woods Hole Oceanographic Institution	164,264

DOE/OBES Geosciences Research: Historical Budget Summary

(Thousands of dollars)

ON-SITE INSTITUTION	FY 96	FY 97	FY 98	FY 99	FY00
Argonne National Laboratory	600	620	620	740	438
Brookhaven National Laboratory	528	350	425	595	870
Idaho National Laboratory	65	40	40	0	0
Los Alamos National Laboratory	1960	2096	1509	1260	1235
Lawrence Berkeley National Laboratory	2197	2170	2320	2160	2332
Lawrence Livermore National Laboratory	1940	1915	1421	1445	1736
Oak Ridge Inst for Sci and Ed			85	110	155
Oak Ridge National Laboratory	1251	1195	1228	1235	1145
Pacific Northwest Laboratory	684	600	770	760	815
Sandia National Laboratory	1616	1725	1845	1635	1324
total, on-site published	10865	10826	10263	9940	10050
total, off-site published	8815 0	9705 0	11226	12851	10649
total, operating published	19680	20521	21489	22791	20699
total, equipment	1258	1450	1256	1235	1340
Total GEOSCIENCES-published	20938	21971	22745	24026	22039
OFF-SITE INSTITUTION					
AM. Mus. NY (Mathez)	69	85	98	87	
Arizona (Harpalani - Conf)					10
Arizona St. (Buseck)	132	139			
Arizona St. (Hervig/Williams)	59	74	83	70	
Boston Univ. (Klein)	74	77	123	129	116
Brown U (Yund)	152				

Cal Tech. (Stolper)	140	142	146	150	135
Cal Tech. (Wasserburg)	400	400	465	400	325
Calif, Univ. of Berkeley (Helgeson)	185	192	195	197	190
Calif, Univ. of Berkeley (Nishiizumi)		160	164	160	144
Calif, Univ of Berkeley (Sposito)		67	70	73	74
Calif. Univ. of Davis (Casey)	110	108	104	121	108
Calif, Univ of Davis (Navrotsky)		150		169	160
Calif, Univ. of Davis (Rock)	151	134	138		
Calif, Univ. of LA (Harrison)	111	119	123	124	126
Calif, Univ. of LA (McKeegan)	44				
Calif. Univ. of SB (Boles)	20	31	16		70
Calif. Univ of SM (Meiburg)					69
Calif. Univ. of SB (Spera)	75	76	89	92	82
Calif, Univ of Santa Cruz (Wu)			278	267	251
Calif, Univ of San Diego (DeGroot-Hedlin)		49	58		
Carnegie Inst of Wash (Hemley)			37		
Chicago, Univ. of (Richter)		183	141		
Chicago, Univ. of (Sutton/Rivers)	341	418	429	440	475
Chicago, Univ. of (Sutton)	159	131	137	299	
Colo, Univ. of (Ge)	13	86		120	101
Colo, Univ of (Nagy)				99	128
Colo, Univ. of (Rajaram)	79	124		60	54
--					
Colo, Univ. of (Rundle)	114	120	130	136	122
Colo, Univ. of (Spetzler)	132	152	161	168	
Col. Sch of Mines (Klusman)					159
Col Sch of Mines (Tsvankin)			230	240	216
Columbia Univ. (Broecker)	137	134	154	130	

Conn. Univ. of (Torgersen)	65	68	79	188	
Delaware, Univ. of (Wood)	109	111	124	236	
Desert Res. Inst. (Tyler)	80	148			
Duke Univ (Malin)			44		
Florida, Univ. of (Ladd)			85	70	63
Georgia Tech (Dove)	91	39	86	145	
Hawaii, Univ. of (Martel)	79	84	130		117
Illinois, Univ of (T. Johnson)		138			
Illinois, Univ. of (Kirkpatrick)					395
I.R.I.S. (Simpson)	211				
Indiana, Univ. of (Ortoleva)	102	108	141	124	112
John Hopkins Univ.(Garven)	67	70	77		77
Johns Hopkins Univ.(Sverjenski)	118	105	108	110	100
Johns Hopkins Univ.(Veblen)	156	163	110	110	99
Kent State Univ (Maurice)		33	34	69	
Lehigh Univ. (Ilton)	44	37	115	115	104
Lehigh Univ. (Moses)	123				
Maine Science & Tech (Shehata)		340			
Maryland, Univ. of (Tossell)	28	56	47	48	63
Michigan, Univ. of (Ballentine)	69	71	69		
Michigan, Univ. of (Halliday)	207	226	200		
Minn. Univ of (Yuen)	78	76	91	100	90
MIT (B. Evans)		185	188	198	185
MIT (Harvey)					35
MIT (Rothman)				134	135
MIT (Toksoz)			150	160	144
MIT (Toksoz)					240
NASA (Blankston)	113	95	113		

NAS/NRC (Schiffries/DeSouza)	100	100	100	100	90
Nevada, Univ of (Long)			106	106	96
New England Res (S. Brown)			211	372	
New Mexico Inst. Min. Tech.(Wilson)	30	64		72	65
New Mexico, Univ of (Ingber)			76	80	71
New Mexico, Univ. of (Miller)	100				
NY, City Univ. of CC (Koplik)	98	98	100	99	89
NY, State Univ. of SB (Hanson)	131		155	164	155
NY, State Univ. of SB (Lindquist)	33	35	50	95	
NY, State Univ. of SB (Schoonen)	48	51	54	65	60
NY, State Univ. of SB (Wong)	71	99	100	106	95
Northwestern Univ. (Rudnicki)		88	148	91	89
Notre-Dame, Univ. of (Maurice)					70
Notre Dame Univ (Pyrak-Nolte)	78	81	83		
Ohio St. Univ (Adler)	43				
Okla, Univ. of (Elmore)	158		219	131	127
Okla Sate (Nicholl)				40	36
Oregon St. Univ (Egbert)	41				
Oregon State Univ (Haggerty)					76
Penn St. Univ. (Barnes)	81	87	93		
Penn St. Univ. (Brantley)	117	107	200	142	110
Penn St. Univ. (Brantley) conf.	10				
Penn St. Univ. (Elsworth)					109
Princeton (Myneni)					102
Princeton Univ (Navrotsky)	150				
Purdue Univ. of (Johnson)			130	238	

Purdue Univ. (Pyrak-Nolte)					180
Rensselaer Polytech. Inst. (Watson)	146		181	179	161
Rice Univ. (Mango)	105	109	111	213	
Rust Geotech, Inc. (Fukui)	87	35			
Rutger Univ (Cheney)		75	75		
Smithsonian Institution (Sorensen)					88
Southern Calif. Univ. of (Aki)	112				
Southern Calif. Univ of (Maxworthy)					85
Stanford Univ. (Brown)		247	259	268	
Stanford Univ. (Harris)	120	125			
Stanford Univ (Mavko)				115	104
Stanford Univ. (Nur)	193	196	211	219	200
Stanford Univ. (Nur)			150	150	135
Stanford Univ (Orr)				136	
Standard Univ. (Pollard)	232	250	195	199	179
Stanford Univ. (Segall)				93	97
Temple Univ. (Strongin)	76	49	52	60	60
Tennessee Univ. of (Thonnard)	82	69			
Texas, Univ of (Banner)			152	152	
Texas, Univ. of (Hardage)	175	175			
Texas, Univ of (Sharp)		61	58	59	
Texas, Univ of Dallas (McMechan/Bhattacharya)	164	124	162	137	124
Texas, A&M Univ. (Kronenberg)			184	350	
Texas A & M Univ (Datta-Gupta)					304
Texas A&M Univ (Morse)					259
Texas Tech Univ (Graham)				100	90
Utah, Univ. of (Forster)					25

Utah, Univ. of (Tripp)	55	57	60	80	73
Utah St. (Hestir)	160	157	73	84	
Utah St (Evans)			129	147	85
VPI & SU (Bodnar)	100	104	122	118	108
VPI & SU (Dove)					202
VPI & SU (Hochella)				161	159
Washington, Univ. of (Booker)	116				
Washington, Univ of (Booker-conf)			8		
Wasington, Univ. of (Unsworth/Booker)		96	97	205	
Washington Univ, St. Louis (Shock)	75	80	106	201	
Wisconsin (Alumbaugh)				52	50
Wisconsin (Alumbaugh - conf)					10
Wisconsin, Univ of (Banfield)	104	139	149	114	103
Wisconsin, Univ of (Haimson)			125	127	115
Wisconsin, Univ. of (Valley)		148	153	147	336
Wisconsin, Univ of (Wang)			50	95	
WHOI (Chave)	55				
WHOI (Eglinton)	135				
WHOI (Seewald)		130	79	134	120
WHOI (Whelan)	195	200	205	377	
WHOI (Zhu)					41
Wyoming, Univ. of (Eggleston)	81	56	56		95
Yale Univ. (Berner)	91	92	177	197	
Yale Univ. (Lasaga/Rye)	290	295	240	247	222
Other	90	244	222	316	505
OFF-SITE TOTALS	8815	9705	11226	12851	10649